

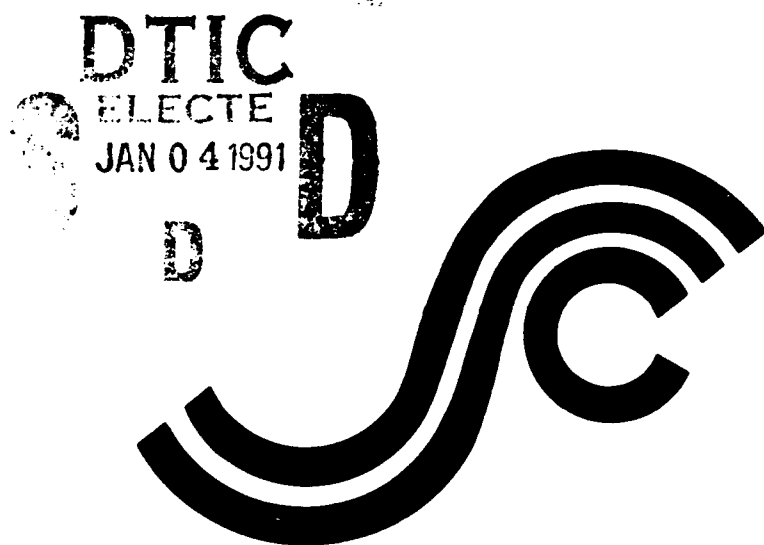
AD-A230 198

DUPLICATE COPY

1

SSC-335

# PERFORMANCE OF UNDERWATER WELDMENTS



This document has been approved  
for public release and sale; its  
distribution is unlimited

SHIP STRUCTURE COMMITTEE

1990

91 1 3 205

## SHIP STRUCTURE COMMITTEE

THE SHIP STRUCTURE COMMITTEE is constituted to prosecute a research program to improve the hull structure of ships and other marine structures by an extension of knowledge pertaining to design, materials and methods of construction.

RADM J. D. Sipes, USCG, (Chairman)  
Chief, Office of Marine Safety, Security  
and Environmental Protection  
U. S. Coast Guard

Mr. Alexander Malakhoff  
Director, Structural Integrity  
Subgroup (SEA 55Y)  
Naval Sea Systems Command

Dr. Donald Liu  
Senior Vice President  
American Bureau of Shipping

Mr. H. T. Haller  
Associate Administrator for Ship-  
building and Ship Operations  
Maritime Administration

Mr. Thomas W. Allen  
Engineering Officer (N7)  
Military Sealift Command

CDR Michael K. Parmelee, USCG,  
Secretary, Ship Structure Committee  
U. S. Coast Guard

## CONTRACTING OFFICER TECHNICAL REPRESENTATIVES

Mr. William J. Siekierka  
SEA 55Y3  
Naval Sea Systems Command

Mr. Greg D. Woods  
SEA 55Y3  
Naval Sea Systems Command

## SHIP STRUCTURE SUBCOMMITTEE

THE SHIP STRUCTURE SUBCOMMITTEE acts for the Ship Structure Committee on technical matters by providing technical coordinating for the determination of goals and objectives of the program, and by evaluating and interpreting the results in terms of structural design, construction and operation.

### U. S. COAST GUARD

Dr. John S. Spencer (Chairman)  
CAPT T. E. Thompson  
CAPT Donald S. Jensen  
CDR Mark E. Noll

### NAVAL SEA SYSTEMS COMMAND

Mr. Robert A. Sielski  
Mr. Charles L. Null  
Mr. W. Thomas Packard  
Mr. Allen H. Engle

### MARITIME ADMINISTRATION

Mr. Frederick Seibold  
Mr. Norman O. Hammer  
Mr. Chao H. Lin  
Dr. Walter M. Maclean

### MILITARY SEALIFT COMMAND

Mr. Glenn M. Ashe  
Mr. Michael W. Touma  
Mr. Albert J. Attermeyer  
Mr. Jeffery E. Beach

### AMERICAN BUREAU OF SHIPPING

Mr. John F. Conlon  
Mr. Stephen G. Arntson  
Mr. William M. Hanzalek  
Mr. Philip G. Rynn

## SHIP STRUCTURE SUBCOMMITTEE LIAISON MEMBERS

### U. S. COAST GUARD ACADEMY

LT Bruce Mustain

### U. S. MERCHANT MARINE ACADEMY

Dr. C. B. Kim

### U. S. NAVAL ACADEMY

Dr. Ramswar Bhattacharyya

### STATE UNIVERSITY OF NEW YORK MARITIME COLLEGE

Dr. W. R. Porter

### WELDING RESEARCH COUNCIL

Dr. Martin Prager

### NATIONAL ACADEMY OF SCIENCES MARINE BOARD

Mr. Alexander B. Stavovy

### NATIONAL ACADEMY OF SCIENCES COMMITTEE ON MARINE STRUCTURES

Mr. Stanley G. Stiansen

### SOCIETY OF NAVAL ARCHITECTS AND MARINE ENGINEERS- HYDRODYNAMICS COMMITTEE

Dr. William Sandberg

### AMERICAN IRON AND STEEL INSTITUTE

Mr. Alexander D. Wilson

Member Agencies:

United States Coast Guard  
Naval Sea Systems Command  
Maritime Administration  
American Bureau of Shipping  
Military Sealift Command



## Ship Structure Committee

An Interagency Advisory Committee  
Dedicated to the Improvement of Marine Structures

September 5, 1990

Address Correspondence to:

Secretary, Ship Structure Committee  
U.S. Coast Guard (G-MTH)  
2100 Second Street S.W.  
Washington, D.C. 20593-0001  
PH: (202) 267-0003  
FAX: (202) 267-0025

SSC-335  
SR-1283

### PERFORMANCE OF UNDERWATER WELDMENTS

For many years we have been developing the technology needed to produce sound, high quality welds in an underwater environment. Virtually every facet of the marine industry can benefit from this research as it continues. In sponsoring this project, it was not the intention of the Ship Structure Committee to develop an all-inclusive document on wet welding. We did, however, strive to provide additional important data that will be an informative and valuable contribution to the literature. This report indicates that wet welds produced using the shielded metal arc process may be suitable for some structural applications. The information found in this report should be useful as we move toward accepting wet welds with the same confidence that we accept those made in a dry environment.

  
J. O. SIPES  
Rear Admiral, U. S. Coast Guard  
Chairman, Ship Structure Committee

Accession For	
NTIS CRA&I	
DTIC TAB	
Unannounced	
Justification:	
By _____	
Distribution /	
Availability Date:	
Dist	Available or Special
A-1	

**Technical Report Documentation Page**

1. Report No. SSC-335	2. Government Accession No.	3. Recipient's Catalog No.	
4. Title and Subtitle <b>Performance of Underwater Weldments</b>		5. Report Date <b>September 1986</b>	6. Performing Organization Code <b>SHIP STRUCTURE COMMITTEE</b>
7. Author(s) <b>R. J. Dexter, E. B. Norris, W. R. Schick, P. D. Watson</b>		8. Performing Organization Report No. <b>SR 1283</b>	
9. Performing Organization Name and Address Southwest Research Institute P.O. Drawer 28510 San Antonio, TX 78284		10. Work Unit No. (TRAILS)	11. Contract or Grant No. <b>DTCG23-82-C-20017</b>
12. Sponsoring Agency Name and Address Ship Structure Committee c/o U.S. Coast Guard (G-M) 2100 Second Street, SW Washington, D.C. 20593		13. Type of Report and Period Covered <b>FINAL REPORT</b>	
14. Sponsoring Agency Code <b>G-M</b>			
15. Supplementary Notes			
16. Abstract Data reported herein indicate that the wet and wet-backed metal arc welding (SMAW) process can produce welds suitable for structural applications provided certain limitations of the welds are considered in design. Welding procedure qualification tests and fracture toughness (J <sub>C</sub> ) tests were performed on wet, wet-backed, and dry fillet and groove welds made with 1) A-36 steel and E6013 electrodes, and 2) A-516 steel and nickel alloy electrodes. Despite hardness measurement exceeding 300 HV1.0 in ferritic welds and 400 HV1.0 in austenitic welds, no hydrogen cracking or brittle fracture behavior was observed. Generally, the Charpy tests indicated upper-shelf behavior at 28°F and the HAZ was found to be tougher than the weld metal. Statistical analysis reveals the effect and interaction of water depth, plate thickness, restraint material, and location of notch in the weld. A correlation between the toughness and Charpy impact energy was developed. Design guidelines are formulated and illustrated by examples for the use of these welds in structural applications. The fracture toughness of the welds is sufficient to be tolerant of flaws much larger than those allowed under AWS specifications.			
17. Key Words Underwater Weld(s), Wet Weld(s), Repair, Wet-Backed Weld(s), Fracture Toughness, Mechanical Properties, Qualification Test, Design, Design Guidelines, Fracture, Fracture Mechanics, Flaws, Defects, Crack Porosity, (74)		18. Distribution Statement Available from: National Technical Information Service Springfield, VA 22151 or Marine Technical Information Facility National Maritime Research Center Kings Point, NY 10024-1699	
19. Security Classif. (of this report) <b>UNCLASSIFIED</b>	20. Security Classif. (of this page) <b>UNCLASSIFIED</b>	21. No. of Pages <b>248</b>	22. Price

METRIC CONVERSION FACTORS

Approximate Conversions to Metric Measures

Approximate Conversions from Metric Measures								
Symbol	When You Know	Multiply by	To Find	Symbol	When You Know	Multiply by	To Find	
<u>LENGTH</u>				<u>LENGTH</u>				
in	inches feet yards miles	'2.5 30 0.9 1.6	centimeters centimeters meters kilometers	mm cm m km	millimeters centimeters meters meters kilometers	0.04 0.4 3.3 1.1 0.6	inches inches feet yards miles	
ft	<u>AREA</u>				<u>AREA</u>			
yd <sup>2</sup>	square inches	6.5	square centimeters	cm <sup>2</sup>	square centimeters	0.16	square inches	
m <sup>2</sup>	square feet	0.09	square meters	m <sup>2</sup>	square meters	1.2	square yards	
yd <sup>2</sup>	square yards	0.8	square meters	km <sup>2</sup>	square kilometers	0.4	square miles	
m <sup>2</sup>	square miles	2.6	square kilometers	ha	hectares (10,000 m <sup>2</sup> )	2.5	acres	
ac	acres	0.4	hectares	ha	hectares	13	MASS (weight)	
<u>MASS (weight)</u>				<u>MASS (weight)</u>				
oz	ounces	28	grams	g	grams	0.036	fluid ounces	
lb	pounds	0.46	kilograms	kg	kilograms	2.2	pints	
ton	short tons (2000 lb)	0.9	tonnes	t	tonnes (1000 kg)	1.1	quarts	
<u>VOLUME</u>				<u>VOLUME</u>				
ml	teaspoons	6	milliliters	ml	milliliters	0.03	gallons	
Tbsp	tablespoons	16	milliliters	ml	liters	2.1	fluid ounces	
fl oz	fluid ounces	30	milliliters	ml	liters	1.06	pints	
c	cup	0.24	liters	l	liters	0.26	quarts	
pt	pint	0.47	liters	l	cubic meters	36	gallons	
qt	quart	0.96	liters	l	cubic meters	1.3	cubic feet	
gal	gallons	3.8	liters	l	cubic meters	1	cubic yards	
yd <sup>3</sup>	cubic feet	0.03	cubic meters	m <sup>3</sup>	m <sup>3</sup>			
m <sup>3</sup>	cubic yards	0.76	cubic meters	m <sup>3</sup>	m <sup>3</sup>			
<u>TEMPERATURE (exact)</u>				<u>TEMPERATURE (exact)</u>				
°F	Fahrenheit temperature	5/9 (after subtracting 32)	Celsius temperature	°C	Celsius temperature	9/5 (then add 32)	Fahrenheit temperature	
°C	°C			°C	°C		°F	
<u>TEMPERATURE (approx.)</u>				<u>TEMPERATURE (approx.)</u>				
°F	-40	32	40	1	32	40	212	
°C	-40	0	20	1	0	20	100	
inches	cm	2	2	1	1	2	1	
°C	0	10	20	30	40	50	60	
°F	32	50	60	70	80	90	100	

1 in. = 2.54 cm (exactly). For other exact conversions and more detail tables see NBS Misc. Publ. 284, Units of Weight and Measure. Price \$2.25 SD Catalog No. C13 10 284.

## TABLE OF CONTENTS

	PAGE
1.0 Introduction.....	1
2.0 Discussion and Analysis of Available Data.....	4
2.1 Discussion of the Quality of Underwater Welds.....	4
2.1.1 Metallurgical Considerations.....	4
2.1.2 Hydrogen Damage.....	6
2.1.3 Influence of Porosity on Fatigue Resistance and Fracture Toughness.....	8
2.1.4 Material Thickness.....	12
2.1.5 Water Depth.....	12
2.1.6 Electrode Selection and Welding Position...	13
2.2 Analysis of Underwater Welding Data Available from the Literature and from Industry.....	16
2.2.1 Peak HAZ Hardness.....	18
2.2.2 Weld Metal Tensile Strength.....	20
2.2.3 Radiographic and Visual Test (RT/VT) Acceptability.....	23
2.2.4 Bend Test Acceptability.....	25
2.3 Conclusions: Factors Chosen for the Test Matrix...	27
2.4 References.....	31
3.0 Experimental Program.....	35
3.1 The Test Matrix.....	35
3.2 Discussion of Test Results.....	39
3.2.1 Visual and Radiographic Examination.....	40
3.2.2 Side Bend Tests.....	42
3.2.3 Transverse-Weld Tension Test.....	45
3.2.4 Hardness Traverse.....	45
3.2.5 Fillet Weld Tests.....	46
3.2.6 All-Weld-Metal Tensile Test.....	46
3.2.7 Charpy Tests.....	47
3.2.8 $J_{Ic}$ Fracture Toughness Tests.....	50
3.2.9 Chemical Analyses.....	61
3.3 References.....	63
4.0 Statistical Analysis of Test Data.....	64
4.1 Decomposition of the Test Matrix.....	64
4.2 Grouping and Analysis of Variance.....	67
4.3 Results of Regression Analysis.....	67
4.3.1 $K_{Ic}$ .....	68
4.3.2 CVN.....	79
4.3.3 Bendscore.....	81
4.3.4 All-Weld-Metal Test Results.....	82

TABLE OF CONTENTS (Cont'd.)

	PAGE
4.4 Summary.....	83
5.0 Design Guidelines for Underwater Wet and Wet-Backed Welds .....	87
5.1 Introduction and Overview.....	87
5.1.1 Residual Stresses.....	87
5.1.2 Tensile Strength.....	87
5.1.3 Ductility.....	88
5.1.4 Susceptibility to Cracking and Other Discontinuities.....	90
5.1.5 Resistance to Fracture.....	90
5.1.6 Resistance to Subcritical Crack Growth.....	91
5.1.7 Statement of Design Guidelines.....	91
5.2 Design Procedures to Assure Ductility of Wet and Wet-Backed Welded Connections.....	98
5.3 Design Details to Limit Impact of Cracking.....	100
5.3.1 Details to Provide Redundancy.....	100
5.3.2 Details to Limit Crack Size.....	101
5.4 Fracture Control Guidelines.....	102
5.5 Guidelines for Limiting Cyclic Stress to Control Fatigue Crack Propagation.....	106
5.6 References.....	108
6.0 Summary, Conclusions, and Recommendations.....	109
6.1 Use of Wet and Wet-Backed Welds.....	109
6.2 Effect of Variables on Weld Quality.....	112
6.3 Material Property Data and Correlations.....	114
6.4 Summary of Design Guidelines.....	119
6.5 Conclusions.....	122
6.6 Recommendations.....	126
Appendix A .....	128
A.1 Documentation of Welding Parameters.....	128
A.2 Visual and Radiographic Examination.....	128
A.3 Side Bend Tests.....	134
A.4 Transverse-Weld Tension Test.....	147
A.5 Hardness Traverse.....	151
A.6 Fillet Weld Breakover Bend Test.....	155
A.7 Fillet Weld Tensile Test.....	157
A.8 All-Weld-Metal Tension Test.....	160
A.9 Charpy V-Notch Impact Tests.....	162
A.10 J <sub>Ic</sub> Tests.....	171

TABLE OF CONTENTS (Cont'd.)

	PAGE
Appendix B .....	181
B.1 Variables in the Analysis.....	181
B.1.1 Grouping Variables.....	181
B.1.2 Results of Tests.....	183
B.2 Results of Grouping and Analysis of Variance.....	187
B.2.1 Results Within the Weld Type Subgroup.....	191
B.2.2 Results Within the Restraint Subgroup.....	199
B.2.3 Results Within the Wet-Ferritic Subgroup...	199
B.2.4 Results for All Data.....	218
Appendix C .....	228
Bibliography.....	239

## LIST OF FIGURES

FIGURE NO.	PAGE
2.1 Sigmoidal Shape of Crack Growth Rate Curve for Underwater Weld with Porosity.....	10
2.2 Macroscopic Examination Specimens Showing Increased Porosity with Depth.....	11
2.3 Effect of Carbon Equivalent and Wet vs Wet-Backed Welding on HAZ Hardness.....	21
2.4 Effect of Plate Thickness and Welding Depth on Weld Metal Tensile Strength.....	24
3.1 Test Matrix.....	36
3.2 Example of Load vs Load Line Displacement for $J_{Ic}$ /CTOD Test.....	51
3.3 Example of $J$ Resistance Curve.....	52
3.4 Example of CTOD Resistance Curve.....	54
3.5 Example of Relationship Between $J$ and CTOD.....	56
3.6 $J_{Ic}$ Shown According to Weld Type.....	57
3.7 Procedure and Location of Hardness Impressions....	59
4.1 Total Test Matrix of Groove Welds.....	65
4.2 Subgroups Within Total Test Matrix.....	66
4.3 Display of $K_{Ic}$ Vs CVN For Wet-Ferritic Subgroup of Underwater Welds.....	71
4.4 Regression Analysis: $K_{Ic}$ vs $K_{Ic}$ Predicted by Relation ( $\epsilon$ ) as a Function of CVN and Zone For Underwater Welds in Wet Ferritic Subgroup.....	73
4.5 Histograms of $K_{Ic}$ Grouped by Weld Type for Weld Type Subgroup of Underwater Welds.....	74
4.6 Results of Regression Analysis: $K_{Ic}$ vs Predicted by Relation ( $g$ ) as a Function of Material, Thickness, Depth, Zone, and Restraint For All Test Data on Underwater Welds.....	76
4.7 Display of $K_{Ic}$ vs CVN For All Test Data on Underwater Welds.....	77
4.8 Results of Regression Analysis: $K_{Ic}$ vs $K_{Ic}$ Predicted by Relation ( $h$ ) Which Includes CVN as well as Material, Depth Zone, and Restraint For All Test Data on Underwater Welds.....	78
4.9 Histograms of $K_{Ic}$ Grouped by Material Combination For All Data in Weld Type Subgroup.....	80
5.1 Typical Brace Replacement.....	93
5.2 Attachment of Cofferdam to Steel Place Structure..	95
5.3 Details to Limit Crack Size.....	96
5.4 Strip Patch Repair of Sheet Piling.....	97
A-1 Macroscopic Examination Specimens Showing Increased Porosity with Depth.....	133

LIST OF FIGURES (Cont'd.)

FIGURE NO.	PAGE
A-2 Layout of Test Plate for Qualification Tests.....	135
A-3 Side Bend Test Specimen.....	136
A-4 Side Bend Test Procedure.....	137
A-5 Transverse-Weld Reduced-Section Tensile Test Specimen.....	149
A-6 Procedure and Location of Hardness Impressions....	152
A-7 Procedure and Location of Hardness Traverse.....	153
A-8 Hardness Traverse: Specimen 41-3.....	154
A-9 Fillet Weld Break-Over Bend Test Specimen.....	158
A-10 Fillet Weld Tensile Test Specimen.....	159
A-11 Location and Drawing of All-Weld-Metal Tensile Test Specimen.....	161
A-12 Layout of Test Plate for Charpy Impact Test Specimens.....	163
A-13 Charpy V-Notch Impact Test Specimen.....	164
A-14 Layout and Preliminary Preparation of $J_{Ic}$ Test Compact Tension Specimen.....	173
A-15 $J_{Ic}$ Compact Tension Specimen.....	174
A-16 Full Range J-Resistance Curve: Specimen 41-1-2H...	179
A-17 J-Resistance Curve: Specimen 41-1-2H.....	180
B.1 .....	189
B.2 .....	194
B.3 .....	195
B.4 .....	197
B.5 .....	198
B.6 .....	199
B.7 .....	201
B.8 .....	202
B.9 .....	203
B.10 .....	205
B.11 .....	206
B.12 .....	207
B.13 .....	208
B.14 .....	209
B.15 .....	211
B.16 .....	212
B.17 .....	213
B.18 .....	215
B.19 .....	216
B.20 .....	217
B.21 .....	218
B.22 .....	220
B.23 .....	221
B.24 .....	222

LIST OF FIGURES

FIGURE NO.	PAGE
B.25 .....	224
B.26 .....	225
B.27 .....	226

## LIST OF TABLES

TABLE NO.	PAGE
2.1 Sigmoidal Shape of Crack Growth Rate Curve for Underwater Weld with Porosity [Ref. 2.10].....	10
2.2 Macroscopic Examination Specimens Showing Increased Porosity with Depth.....	11
2.3 Effect of Carbon Equivalent and Wet vs Wet-Backed Welding on HAZ Hardness.....	26
2.4 Effect of Plate Thickness and Welding Depth on Weld Metal Tensile Strength.....	28
3.1 Test Matrix.....	43
3.2 Macroscopic Examination Specimens Showing Increased Porosity with Depth.....	48
3.3 Layout of Test Plate for Qualification Tests.....	62
4.1 Total Test Matrix of Groove Welds.....	65
4.2 Subgroups Within Total Test Matrix.....	66
5.1 Typical Brace Replacement.....	104
A.1 .....	129
A.2 Bend Test Results.....	138
A.3 Transverse-Weld Tensile Test Data.....	150
A.4 Weld Crown Hardness Range - HV.....	156
A.5 Charpy Data Data for 25.4 mm (1/2 in.) Thick 0.36 CE with Ferritic Filler.....	164
A.6 Compiled Results of $J_{IC}$ Tests.....	174

## 1.0 INTRODUCTION

Wet welds are made with the pieces to be joined, the welder/diver, and the arc surrounded by water. The wet and wet-backed shielded metal arc welding (SMAW) process offers greater versatility, speed, and economy over underwater welding techniques involving chambers or minihabitats. However, the welds can rarely achieve the same quality as dry welds. The welds are quenched very rapidly often resulting in a very hard weld and heat-affected zone (HAZ). Evolved gases trapped in the weld metal manifest as porosity. Hydrogen (evolved as water is dissociated) may cause cracking in the welds. Arc stability in water may be inferior to that in air resulting in other discontinuities. Wet-backed welds are performed with water behind the pieces to be joined only, but are subject to some of the same problems. This report addresses the quality of underwater wet and wet-backed SMAW welds and presents preliminary design guidelines that facilitate the use of these welds for structurally-critical connections despite limited ductility and toughness and susceptibility to discontinuities.

The American Welding Society (AWS) has published rules (AWS D3.6, "Specification for Underwater Welding") for qualifying the welder/diver and welding procedure for underwater welding. AWS D3.6 Specification defines three types of underwater welds including hyperbaric and dry chamber welds) according to some mechanical and examination requirements. In descending order of quality level are: Type A, intended for structural applications; Type B, intended for limited structural applications; and Type C, for application where structural quality is not critical. A fourth category apart from these three, Type O, is intended to have qualities equivalent to those normally specified by a code or standard applicable to the particular type of work (e.g., ANSI/AWS D1.1, "Structural Welding Code - Steel").

Data reported in the literature and those reported herein indicate that the wet and wet-backed SMAW process can produce the Type B quality level for most structural steels. AWS D3.6 Specification states that Type B welds must be evaluated for fitness and purpose but gives no guidelines for making this evaluation. The purpose of this study is to supplement AWS D3.6 Specification by providing some data on the toughness and mechanical properties of these welds as well as rational design guidelines for the use of Type B wet and wet-backed welds in structural applications. The guidelines focus on avoiding yielding of the wet welds\* avoiding continuous lengths of structurally-critical welds, and limiting the alternating stress.

As a basis for these guidelines, an effort was made to gather data on the properties of wet and wet-backed welds. Data were gathered from the literature and from industry. Statistical analysis of this available data was used to identify important variables for the design of an experimental program to supplement the available data.

Welding procedure qualification tests were performed on fillet and groove welds prepared by dry, wet-backed, and wet SMAW processes. These tests included visual (general and transverse macrosection) and radiographic examinations, transverse weld tensile tests, bend tests, all-weld-metal tensile tests, Charpy impact tests, hardness tests, fillet weld break tests, and fillet weld tensile tests. In addition, the fracture toughness of the welds was characterized by the J resistance curve and  $J_{Ic}$ . For some of these tests the crack tip opening displacement (CTOD) was

---

\*Throughout this report, the term "wet weld" will be used for convenience to include both wet and wet-backed underwater welds prepared with the SMAW process.

measured and related to J and crack extension. Charpy and  $J_{IC}$  tests were performed with the notch both in the weld metal and in the heat-affected zone. The experiments and subsequent statistical analysis reveal the effect and interaction of weld type (dry, wet-backed, or wet), water depth, plate thickness, restraint, and material.

Two base metal/filler metal combinations were used in the experiments: a 0.36 carbon-equivalent (CE)\* A-36 steel with an E6013 electrode and a 0.46 CE A-516 steel with a nickel alloy electrode.

The scope of this study is limited to the mechanical properties of wet and wet-backed welds, excluding the development of electrodes and welding techniques. Extensive research of these subjects has been reported elsewhere in the literature.

The following section of this report presents background on the underwater wet and wet-backed SMAW process, including discussion of data gathered from the literature and from industry sources and how these data led to the choice of major variables in the experiments. Section 3.0 presents details of the experimental program. A statistical analysis of the test data is in Section 4.0. Section 5.0 presents the design guidelines. Example problems using the design guidelines are contained in Appendix C. Section 6.0 is a summary which includes relevant conclusions and recommendations.

---

\*  $CE = C + \frac{M_n}{6} + \frac{Cr + M_O + V}{5} + \frac{N_i + C_{II}}{15}$  (see Page 5)

## 2.0 DISCUSSION AND ANALYSIS OF AVAILABLE DATA

### 2.1 Discussion of the Quality of Underwater Welds

A review of the literature disclosed that a number of effects contribute to significant differences between wet welds and welds made in air. These effects can be grouped into several specific categories:

- Metallurgical considerations
- Hydrogen damage
- Porosity
- Material thickness
- Water depth
- Electrode selection and welding position.

Each of these categories is discussed separately below.

#### 2.1.1 Metallurgical Considerations

The major problem with wet welding is the inherent rapid quench that the weldment receives due to the water environment. The quenching effect has been reported to be primarily due to conduction into the base plate [2.1] and not heat transfer directly to the water. This rapid conductive heat loss is dependent on the moving water generated by the rising bubble column caused by the welding arc [2.2]. Cooling rates of wet welds are 10 to 15 times more rapid than those welds made in air [2.3].

This rapid quench causes a significantly different microstructure in the weld metal and the adjacent heat-affected zone (HAZ) when compared with normal atmospheric welds. It has been reported [2.1] that the width of the HAZ is up to 50 percent

smaller in wet welds compared to dry welds. Martensite and other brittle transformation structures form in the grain coarsened region of the HAZ. These very hard microstructures have very limited ductility and are much more susceptible to hydrogen damage. Peak hardness of the HAZ is controlled by the hardenability of the base material. The most common method of classifying a materials hardenability is by its carbon equivalent (CE), i.e.,

$$CE = C + Mn/6 + \frac{Cr + Mo + V}{5} + \frac{Ni + Cu}{15} .$$

Recent work by Sea-Con Services [2.21] suggests that Silicon affects the weldability of underwater welds and that a factor of Si/6 should be included in the expression for CE. Cottrell [2.24] has developed a formula for predicting heat affected zone hardness and weldability which include other factors, especially cooling rate. It is widely accepted that the higher the CE a material has, the more hardenable it becomes. Data in this study (Section 3.6) show higher hardness for the 0.46 CE material than the 0.36 CE material (a different filler metal was also used). However, data provided by Gooch [2.3] suggests that the character of the microstructure and the peak HAZ hardness was not affected by carbon equivalent over the range 0.28 to 0.47.

Recent work by Olson and Ibarra [2.20] shows that Manganese and Oxygen decrease as the depth of the underwater weld increases. The decrease in Manganese in turn changes the microstructure obtained at a given cooling rate.

Even with the knowledge that excessive cooling rates will exist in wet welding, it is not possible to accurately predict the character of the microstructure nor the peak hardness. Other factors have a direct impact on the hardness. Arc energy and

welding travel speed control the heat input of a weld. The higher heat inputs, i.e., larger electrodes, wider weld beads and slower travel speed, tend to produce less hardening in the weld metal and HAZ due to slower cooling rates [2.1]. Further, the effect of increasing arc energy does not affect the cooling rate for thin plates as significantly as it does for thicker sections [2.2]. Local dry spot techniques have been developed which exclude the water in the immediate area of the arc. Such devices must protect a certain minimum area around the welding arc or increased cooling rates can be experienced [2.2]. Cooling rates and peak hardnesses can be lowered significantly by the application of preheat to the weld seam but this requires additional equipment, time and expense.

#### 2.1.2 Hydrogen Damage

Underwater wet welding has experienced mixed results with regard to hydrogen induced ( $H_2$ ) cracking. The literature contains reports of hydrogen cracking in both the weld metal and HAZ in low CE materials when using ferritic electrodes, however, there are a large number of reports as well as practical experience that conclude most structural steels can be welded with ferritic filler materials. Interestingly and for reasons not well understood, a relatively high hydrogen electrode, E6013, is widely used with the underwater wet SMAW process with very good results. The E7018 electrode is commonly used with the wet-backed SMAW process. In this study (Sections 3.3 and 3.4), crack-free ferritic wet welds were made with the E6013 electrode. However, wet-backed welds prepared from 12.7 mm (1/2 in.) plates with the E6013 electrode contained large cracks, but this would not be the electrode of choice for the wet-backed welds.

The source of hydrogen is the boiling and dissociation of the water at the welding arc. An investigation at MIT studied the

arc bubble dynamics and heat transfer mechanisms of underwater welding and this is covered thoroughly in Reference [2.4]. The water dissociates into hydrogen and oxygen and the bubble is made up of these and decomposition products of the electrode. Dadian [2.5] reported that the bubbles contain 70 percent hydrogen, 1 percent oxygen, 27 percent CO<sub>2</sub>/CO and it has been estimated [2.6] that the arc column may be 90 percent hydrogen.

This abundance of hydrogen is available to the weld pool, dissolves into the molten metal and diffuses to the HAZ. Upon solidification, the hydrogen can manifest as porosity or HAZ cracking. The cracking can occur when a sufficient quantity of diffused hydrogen is present in a suitably stressed and sensitive microstructure. The hardenability (CE) of the base material and the cooling rate are thought to have a direct bearing upon crack susceptibility.

The use of austenitic or nickel alloy electrodes is believed to reduce the amount of diffusible hydrogen available to the HAZ. This is due to the higher solubility of hydrogen in austenite and the lower diffusibility. It was found in Reference [2.7] that successful welds can be made on relatively high CE materials using austenitic electrodes. (In Section 3.3, it is reported that crack-free wet-backed welds and wet welds at a depth of 10 m (33 ft) were obtained for this study on a 0.46 CE A-516 steel with a proprietary nickel alloy electrode.)

There still exists a problem with HAZ and fusion zone cracking when many of the stainless steel electrodes are used under restrained conditions. In addition, some fully austenitic electrodes can be poor performers in bend testing if contamination in the weld pool causes hot cracking or liquified grain boundaries. Based upon a rather large number of tests and

practical experience [2.7] it is believed that mild steel with  $CE \leq 0.40$  can be successfully welded with ferritic electrodes and  $0.40 < CE < 0.60$  can be welded with austenitic (high nickel or nickel base) electrodes. However, this rule of thumb does not necessarily apply to higher yield strength steels, and procedure qualification tests should be performed under high restraint to assure the materials weldability.

Methods to reduce the amount of hydrogen available to the weld pool have included shrouding the arc with a small container or stream of gas. Properly applied shrouding can reduce the quench effect and reduce the HAZ and weld metal hardness. Note that waterproofing of the electrodes is a very important variable, yet most of the waterproofing techniques and compounds remain proprietary information.

#### 2.1.3 Influence of Porosity on Fatigue Resistance and Fracture Toughness

Changes in fatigue lives and fracture toughness caused by porosity in dry SMAW welds have been indicated in the literature [2.11-2.17]. Carter et al. [2.18] investigated double-vee butt welds with varying degrees of porosity in 19 mm (3/4 in.) steel plates with yield strengths of 345 MPa (50 ksi) and concluded that the lives of welds with fine, medium, and large porosity (as defined in the ASME Boiler and Pressure Vessel Code) were reduced by 16, 24, and 6 percent, respectively, when compared to clear welds. Harrison [2.19] has compiled data available in the literature prior to 1972 in the form of quality levels divided by S-N curves for 0, 3, 8, 20 and 20+ percent porosity in as-welded C-Mn steel weldments.

Matlock et al. [2.10] have obtained crack growth rate data on surface, habitat, and wet underwater welds from several suppliers (Figure 2.1). Surface and habitat welds (free from porosity) had growth rates slower than or equal to growth rates of comparable steel base plate, but underwater wet ferritic welds prepared at a depth of 10 m (33 ft) (affected by porosity) exhibited a  $da/dN$  curve with an unusually high slope which, for  $\Delta K$  less than  $30 \text{ MPa}\sqrt{\text{m}}$ , ( $27 \text{ ksi}\sqrt{\text{in}}$ ) (which would be near the end of the fatigue life) indicated growth rates much less than surface or habitat welds and comparable steel plate. They found that the slope of the  $da/dN$  curve monotonically increased according to the porosity level. Interestingly, wet welds prepared by a different supplier at a depth of only 3 m (10 ft) did not have much porosity and behaved just like the surface welds, which indicates that the effect of the crack growth rate is due mainly to porosity rather than microstructural changes from the rapid quench. Examination of fracture surfaces revealed that for small crack extensions (low  $\Delta K$ ), pores act to "pin" the crack front and retard crack growth. Hence for low  $\Delta K$ , increasing porosity led to a decrease in crack growth rate. At high  $\Delta K$ , the size of the pores was comparable to the plastic zone width and increments of crack extension, and the pinning mechanism was no longer active, but the pores acted to reduce cross-sectional area and increase the local stress at the crack tip. This same mechanism was attributed to a reduction in plastic limit load at fracture with increasing porosity.

For underwater wet welds in this study (as shown in Figure 2.2), the porosity increased markedly with increasing depth, and the mean  $K_{Ic}$  (as determined from  $J_{Ic}$ ) decreased from  $195 \text{ MPa}\sqrt{\text{m}}$  ( $177 \text{ ksi}\sqrt{\text{in}}$ .) for dry welds to range from 120 to  $85 \text{ MPa}\sqrt{\text{m}}$  ( $109$  to  $77 \text{ ksi}\sqrt{\text{in}}$ ) for wet welds prepared at 10 m (33 ft) and 60 m (198 ft,) respectively. Ibarra and Olson [2.20] have noted changes in weld

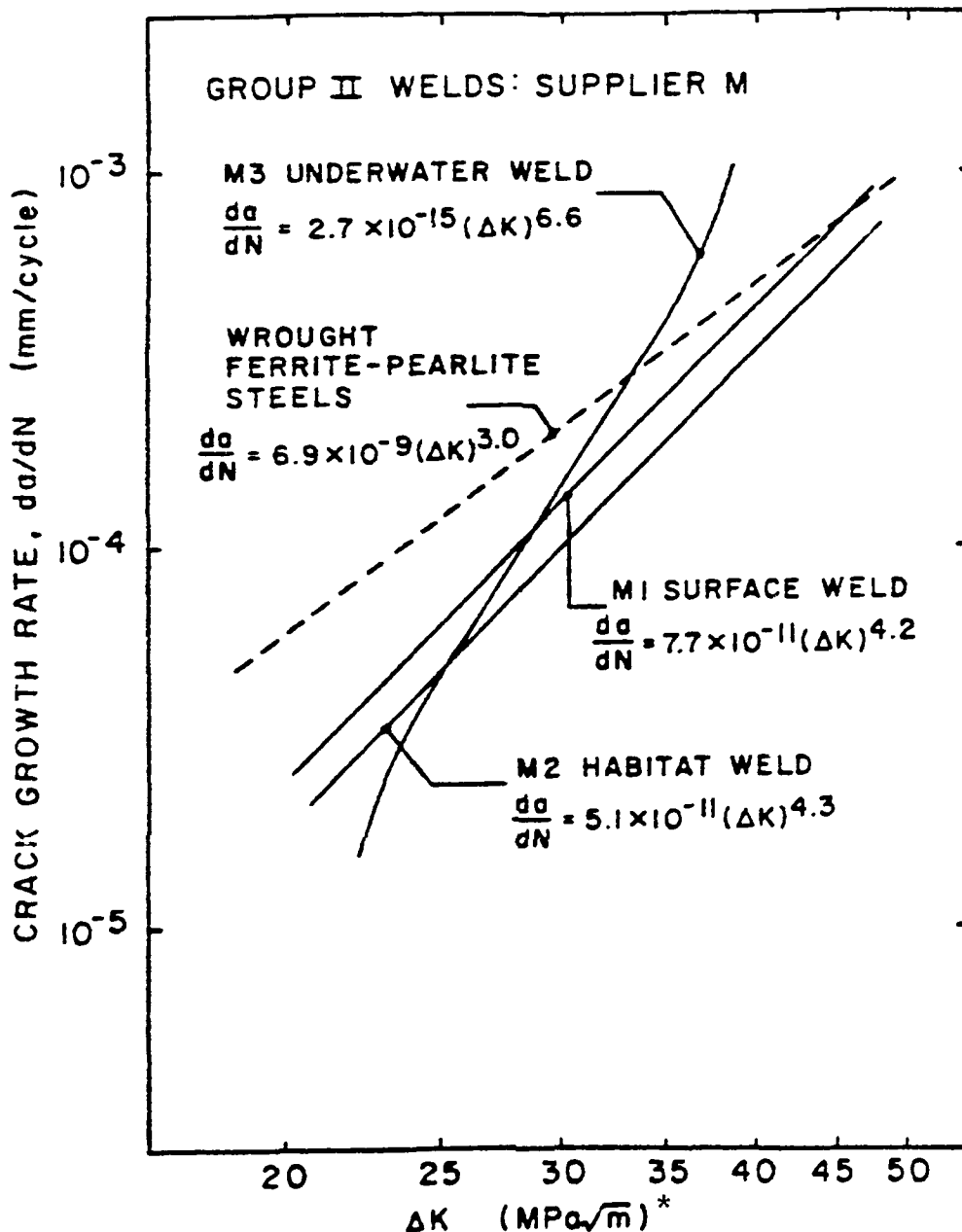
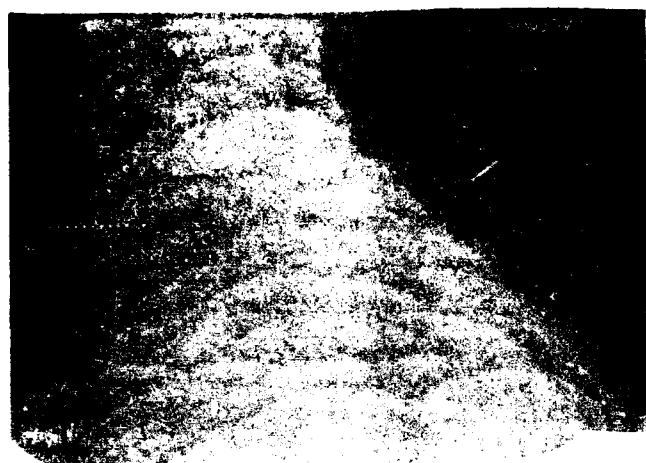
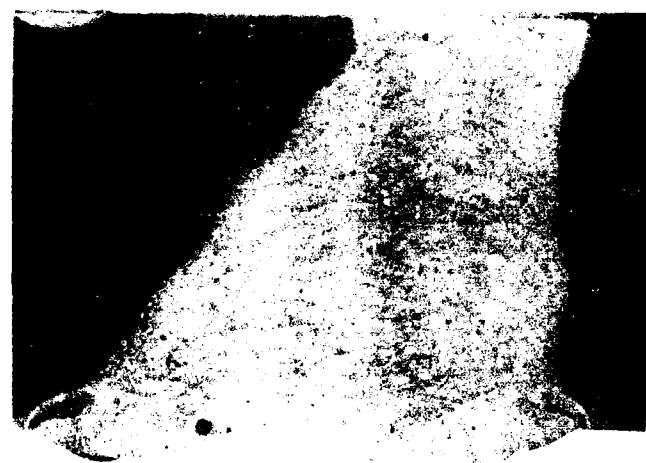


FIGURE 2.1. SIGMOIDAL SHAPE OF CRACK GROWTH RATE CURVE FOR UNDERWATER WELD WITH POROSITY [REF. 2.10].

\*English Equivalent Units:  $\Delta K(\text{ksi}\sqrt{\text{in.}}) = (\text{MPa}\sqrt{\text{m}})/1.10$   
 $\frac{da}{dN}$  (in./cycle) = (mm/cycle)/25.4



20-2  
Dry Weld



21R-1  
Wet Weld  
at 10 m  
(33 Ft)



23R-1  
Wet Weld  
at 60 m  
(198 Ft)

FIGURE 2.2. MACROSCOPIC EXAMINATION SPECIMENS SHOWING INCREASED POROSITY WITH DEPTH.

chemistry and microstructure with depth which also contribute to changes in toughness.

#### 2.1.4 Material Thickness

As conduction to the base metal is the primary cooling mechanism [2.1] and the plate surfaces are cooled by moving water [2.2] caused by the rising bubbles, thinner plates have more rapid cooling rates in the through thickness direction.

Data reported herein suggest that plate thickness does not significantly affect hardness test and bend test results. Material thickness affected the results of Charpy (CVN) and  $J_{Ic}$  fracture toughness tests. Specimens from 25.4 mm (1 in.) plates showed about the same toughness in the HAZ and weld metal, which was about the same as the toughness of weld metal in the 12.7 mm (1/2 in.) plate specimens. However, unlike the 25.4 mm (1 in.) plates, the specimens taken from 12.7 mm (1/2 in.) plates showed higher toughness in the HAZ than in the weld metal.

Results of controlled thermal sensitivity (CTS) and Y-groove cracking tests [2.23] indicate that the occurrence of cracking increases as plate thickness decreases, the opposite of the trend in drywelds. The previously mentioned cracking which occurred in the wet-backed welds prepared with the E6013 electrode occurred only in the 12.7 mm (1/2 in.) plate.

#### 2.1.5 Water Depth

It is generally accepted that porosity increases as the water depth and pressure increases. This increase in porosity with depth was also observed in this study (Section 3.3, e.g., Figure 2.2). Toughness data (CVN and  $J_{Ic}$ ) showed that depth affected the

weld metal toughness, but HAZ toughness showed inconsistent results. Bend test results were clearly poorer with increasing depth.

Tests were made in the Gulf of Mexico to determine the effects of seawater at increasing depths as reported by Grubs and Seth [2.7]. Four welds were made down to 51 m (166 ft) using E6013 electrodes and the appearance and tensile results were good. Tensile strength of specimens made from butt welds all exceeded the minimum for the plate material. Porosity was the only reported defect. Porosity was rated excessive in the 10 m (33 ft) and 31 m (102 ft) depth welds and it was noted that the 51 m (166 ft) weld had an even greater amount of porosity. Porosity was attributed to the wet electrode coating or waterproofing method used.

#### 2.1.6 Electrode Selection and Welding Position

A wide range of electrodes, both ferritic and austenitic, have been investigated for metallurgical properties and performance in underwater welding. Testing has included a variety of coatings and flux coverings, e.g., cellulose, rutile, oxidizing, and acid iron oxide and basic types. The rutile ferritic AWS type E6013 is the most widely applied underwater electrode and is also sold specifically for underwater welding.

One study [2.8] found that coatings with iron powder additions gave the best arc stability where the current and voltage fluctuations were minimal. A stable cup was provided on the end of the electrode which appears to provide some degree of mechanical protection from the water environment. A coating based on iron oxide gave better resistance to hydrogen cracking which was attributed to a combination of low-strength weld metal and beneficial effects of high FeO content on weld metal and HAZ hydrogen concentrations.

The only other alternative found in the study [2.8] to reduce hydrogen cracking susceptibility was high nickel or nickel base deposits. However, austenitic welds contained bands of hard martensite along the fusion boundaries. High nickel austenitic welds produced for this same study [2.8] were found to have low bend test ductility, attributed to grain boundary segregates. Results reported herein (Section 3.4) show the austenitic wet welds had poorer bend test results than the ferritic welds.

In other tests [2.7], E6013 electrodes were selected because of better weldability in all positions when used underwater. Based on the dry weld metal properties E6013 electrodes would not be first choice because of less ductility and lower radiographic quality than low hydrogen electrodes. However, low hydrogen electrodes had very poor weldability underwater. Observations made [2.7] using restraint welding conditions indicated that the maximum carbon equivalent (CE) without underbead cracking was 0.392 while the minimum carbon equivalent with underbead cracking was 0.445. From this study, a "rule of thumb" was established to use mild steel electrodes for a CE of 0.40 and lower and for material with a CE of 0.40 and greater austenitic electrodes should be used. Values recorded for the maximum heat-affected zone hardness on restrained tests that did not have underbead cracking were Vickers 30Kg 408 (Rockwell C34). The minimum heat-affected zone hardness with cracking was Vickers 30Kg 439 (Rockwell C42).

Good tensile test results were reported by Grubbs and Seth [2.7] for the E6013 electrodes in spite of the porosity level which was rated from good to excessive. (The tensile test results reported herein, Section 3.5, were all greater than the minimum specified for the base material also despite excessive porosity.) Porosity was the only discontinuity present in the mild steel welds

[2.7] except for the underbead cracking on the higher CE materials. Impact tests conducted on underwater welds compared to dry welds indicated the impact strength of the underwater welds is about half of the strength of the dry weld. However, reasonable toughness for the underwater weld was reported at -1°C (+30°F) with an average of 30 J (22 ft-lbs) [2.7]. Results of the present study reported in Section 3.10 show an average impact energy of 43 J (32 ft-lbs) for ferritic wet welds compared to 56 J (41 ft-lbs) for dry welds made with the same electrode.

Testing of austenitic electrodes was made to find suitable all position welding characteristics that also produce crack-free welds in the high carbon equivalent materials [2.7]. Tests made with the same restraint as for mild steel electrodes on 0.597 CE material (A-517 25.4 mm (1 in.) plate) demonstrated that high carbon equivalent material could be successfully wet welded with high nickel or nickel base electrodes. Results of this study (Section 3.10) show an average impact energy of 72 J (53 ft-lbs) for austenitic wet welds compared to 94 J (69 ft-lbs) for dry welds made with the same electrode.

Development of a nickel base or austenitic electrode was conducted for the Naval Facilities Engineering Command [2.9] which would give deposits having a greater tolerance for hydrogen for steels of all carbon equivalents. Based on the results obtained in these tests and other work, the 112 nickel-based electrode and the R142 stainless steel electrode were recommended. Observations made on these results included comments that: welds were free of undercut and underbead cracking, bead appearance improved and porosity increased with increasing current, optimum coating thickness varied with each electrode, depth of cup increased with increasing coating thickness, proper waterproofing was necessary for satisfactory operation, and excessive heating damages the

waterproof coating even though the coating is not burned completely by the arc.

## 2.2 Analysis of Underwater Welding Data Available from the Literature and from Industry

A statistical analysis was performed of available test data reported in the literature and gathered for this study from industry sources. The objectives of this study was to create a basis for the design of the test matrix. The data were very sparse (e.g., no  $J_{Ic}$  or  $K_{Ic}$  fracture toughness data was available, only limited CTOD data was available [2.3] and the only known crack growth rate data was only recently reported [2.10]). Industry sources were generally reluctant to release data. Very little data is available on the long-term performance of underwater wet welded repairs, because the wet welding technique is widely used only in the Gulf of Mexico, where inspection requirements are less stringent, hence many of the repairs have never been reinspected following completion and acceptance of the work.

A statistical analysis of the experimental data generated in this program was performed separately and is reported in Section 4. Comparison of the results of these separate analyses is mostly reserved for Section 4.4. The nature of the test data analyzed in this section is different than that analyzed in Section 4. The data in this section includes a wide variety of materials, test methods, and test results reported. This data shows only general effects but is useful because it shows the variability expected for a wider population of test data. The data analyzed in Section 4 is for two specific heats of base metal/filler metal combinations, and tests were conducted under similar and controlled conditions. Therefore, more significant conclusions can be drawn about the effect of the variables on these materials, but the results are

limited to these materials and cannot therefore be proven to be generally applicable.

The underwater welding data were analyzed using a forward stepwise regression routine. In this procedure, independent variables are added one-by-one to a prediction equation on a dependent variable. The criterion for entering a variable into the above equation was based on the significance of the partial F test for the entering variable. If the variable was significant at the 0.25 level, it was included and the stepping procedure continued. The significance of the estimated coefficients also was determined using a 0.10 significance level. This was done in order to discover which variables contributed most to the regression equation.

The independent variables utilized in the statistical analyses were:

- Wet or wet-backed welding
- Carbon or low-alloy steel base plate
- Carbon equivalent
- Base plate thickness
- Carbon steel, stainless, or nickel-base weld metal
- DCRP or DCSP (Direct Current Reversed or Standard Polarity)
- Flat, vertical, horizontal, or overhead position
- Fresh water or salt water
- Water temperature
- Water depth
- Rod or wire diameter.

The dependent variables which were used to examine the effects of these independent variables were weld metal tensile

strength, peak heat-affected zone (HAZ) hardness, bend test (pass or fail), and nondestructive examination by radiographic (RT) and/or visual (VT) tests (pass or fail).

Most of the welds in the data base were made by the shielded metal arc weld (SMAW) process, but a limited amount of data reported for flux core arc welds (FCAW) and metal inert gas welds (MIG) were also analyzed.

The contributions of all applicable independent variables were examined against each of the dependent variables. Subsets were then selected to eliminate any independent variables which severely restricted the number of observations because of blanks in the data base. The evaluations by each dependent variable are discussed separately in the following paragraphs.

#### 2.2.1 Peak HAZ Hardness

Five independent variables which significantly (90 percent confidence) explained HAZ hardness were defined as shown in Table 2.1A. The physical effects of two of these, plate steel grade and water temperature, were rather small (<40 HVN). On the other hand, wet welding tended to increase the peak HAZ hardness more than 100 HVN compared to water-backed welding, and base metal carbon equivalent was indicated to increase the peak HAZ hardness approximately 5 HVN per point (0.01 percent). The prediction equations for peak Vickers HAZ hardness are:

$$\text{HVN} = 157 + 566(\text{C.E.}) \text{ for wet-backed welds}$$

and

$$\text{HVN} = 282 + 566(\text{C.E.}) \text{ for wet welds}$$

TABLE 2.1. EFFECT OF WELDING VARIABLES ON HAZ HARDNESS

A. SMAW Only, All Coatings --190 Observations

<u>Variables Added</u>	<u>Range (min/max)</u>	<u>F to Remove<sup>(a)</sup></u>	<u>Mult. R<sup>2</sup> ( percent)</u>	<u>Reg. Coeff.</u>
-	-	-	-	157 <sup>(b)</sup>
C.E. ( perc. )	.109/.597	55.55	47.57	566
Wet	0/1	7.32	51.35	125
A-36	0/1	9.29	53.04	-42
Thickness (in.)*	.375/1.000	2.20	54.21	-45
Water temp. (°F)*	44/80	3.16	55.13	-1
Vertical position	0/1	0.10	55.44	-10
Fresh water	0/1	0.67	55.55	19
Water depth (ft)*	1/293	0.35	55.63	<1
Electrode dia. (in.)*	.125/.188	0.25	55.69	282
Horizontal position	0/1	0.76	55.71	-30
Flat position	0/1	0.72	55.88	-26
C.S. weld metal	-1/1	0.05	55.89	-1
DCRP	0/1	0.02	55.90	-2

B. FCAW/MIG Only --44 Observations

(All were wet welds using C.S. weld metal in the flat position and in fresh water.)

<u>Variables Added</u>	<u>Range (min/max)</u>	<u>F to Remove<sup>(c)</sup></u>	<u>Mult. R<sup>2</sup> ( percent)</u>	<u>Reg. Coeff.</u>
-	-	-	-	760 <sup>(b)</sup>
C.E. ( percent )	.180/.499	64.04	46.10	1638
Water temp. (°F)*	60/80	64.71	65.71	14
Water depth (ft)*	1/33	26.87	84.16	-7
Thickness (in.)*	.500/.875	35.68	86.84	-657
A-36	0/1	26.28	92.55	195
Electrode dia. (in.)*	.045/.094	0.18	92.58	95

(a) 90 percent confidence level, F = 2.75

(b) Intercept value

(c) 90 percent confidence level, F = 2.84

\* 1.0 in. = 25.4 mm, 1.0 ft = 3048 m, (°F-32) 5/9 = °C

where (C.E.) = carbon equivalent in percent. The magnitudes of the contributions of carbon equivalent for wet and wet-backed welds are illustrated by Figure 2.3.

When two reduced subsets (the top five variables with and without coating) were evaluated, no other significant variables were discovered. However, an analysis of the FCAW and MIG data selected 44 observations, and water temperature, plate thickness, water depth, and base plate material were indicated to be additional significant variables for these welding processes (see Table 2.1-B). It should be pointed out that the 44 observations were all obtained on wet welds, therefore, no comparative evaluation could be made between wet and water-backed welds in this data set.

### 2.2.2 Weld Metal Tensile Strength

The statistically significant (>90 percent confidence level) independent variables affecting weld metal tensile strength were determined to be plate thickness and water depth. The analysis was repeated using the top five entering variables (plate thickness, water depth, flat position, base plate material, and carbon equivalent), both with and without electrode coating as a sixth variable, to evaluate the latter's contribution. However, the number of observations in the six-variable analysis was too small to provide significant results.

The analysis based on the 13 independent variables applicable to SMAW welds provided the most useful subset, and the results are summarized in Table 2.2-A. Again, all of these data applied to wet welds, so the wet versus water-backed parameter could not be evaluated. The prediction equation utilizing the two significant (90 percent confidence) independent variables is:

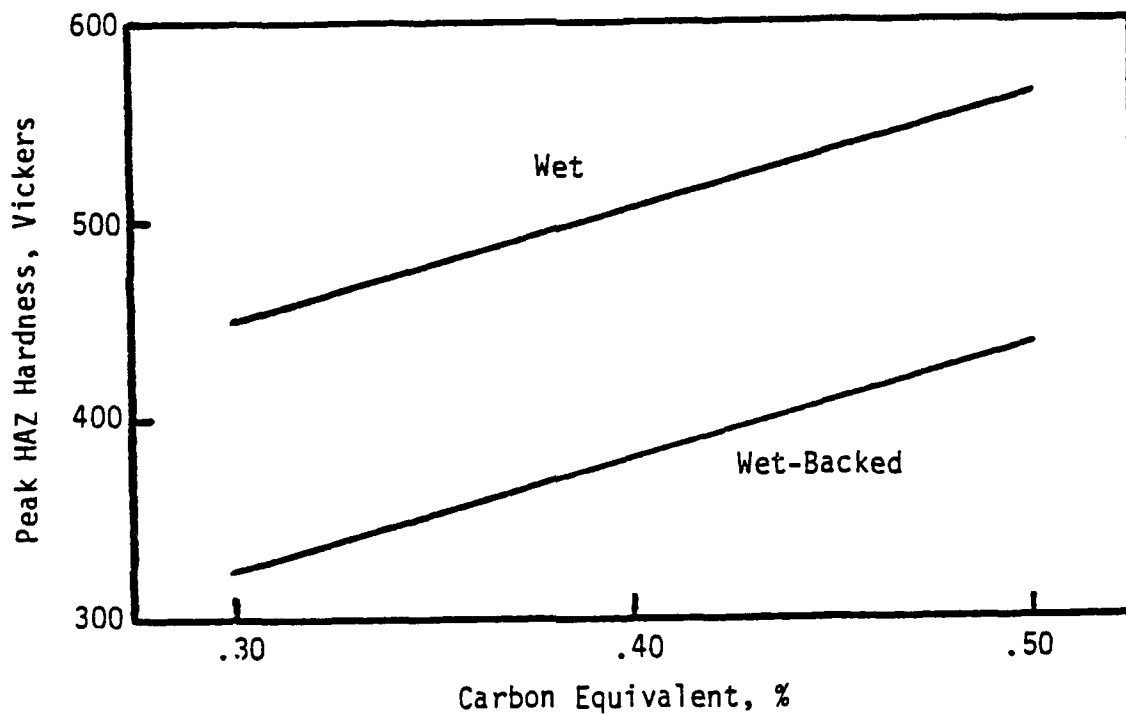


FIGURE 2.3. EFFECT OF CARBON EQUIVALENT AND WET VS WET-BACKED WELDING ON HAZ HARDNESS.

TABLE 2.2. EFFECT OF WELDING VARIABLES ON WELD  
METAL TENSILE STRENGTH

A. SMAW Only, All Coatings --95 Observations

(All were wet welds.)

<u>Variables Added</u>	<u>Range (min/max)</u>	<u>F to Remove<sup>(a)</sup></u>	<u>Mult. R<sup>2</sup> ( percent)</u>	<u>Reg. Coeff.</u>
-	-	-	-	54.2 <sup>(b)</sup>
Thickness (in.)*	.375/1.000	24.01	34.50	41.9
Flat position	0/1	0.36	45.32	7.2
Water depth (ft)*	1/295	2.85	46.61	-0.037
A-36	0/1	2.33	47.35	-5.7
C.E. ( percent)	.109/.597	1.50	48.44	-26.2
Water temp. (°F)*	46/85	0.96	48.87	0.2
Electrode dia. (in.)*	.125/.188	0.74	49.26	-123.0
DCRP	0/1	0.69	49.66	-3.0
Horizontal position	0/1	0.07	49.71	-3.2
Vertical position	0/1	0.02	49.72	-1.9

B. FCAW/MIG Only -- 38 Observations

(All were wet welds using C.S. weld metal in the flat position and in fresh water.)

<u>Variables Added</u>	<u>Range (min/max)</u>	<u>F to Remove<sup>(c)</sup></u>	<u>Mult. R<sup>2</sup> ( percent)</u>	<u>Reg. Coeff.</u>
-	-	-	-	34.1
Electrode dia. (in.)*	.045/.094	2.32	4.62	176.1
C.E. ( percent)	.270/.499	1.60	8.61	78.2
Thickness (in.)*	.625/.875	0.47	9.76	28.5
Water temp. (°F)*	60/80	0.58	10.51	-0.5
Water depth (ft)*	1/33	0.34	11.42	0.3
DCRP	0/1	0.02	11.47	0.6

(a) 90 percent confidence level, F = 2.79

(b) Intercept value

(c) 90 percent confidence level, F = 2.88

\* 1.0 in. = 25.4 mm, 1.0 ft = .3048 m, (°F-32) 5/9=°C

$$\text{Weld Metal UTS} = 54.2 + 41.9(t) - 0.037(d)$$

where  $t$  is the plate thickness in inches; and  $d$  is the welding depth in feet. This prediction equation, illustrated in Figure 2-4, indicates that the contributions to weld metal tensile strength by plate thickness and welding depth are significant. Thus, these were chosen as primary variables in the experimental program. However, results reported herein show little variance in the tensile test results because the failure was usually in the base metal which, of course, gave results independent of thickness and depth.

The analysis was repeated using the 13 independent variables applicable to FCAW and MIG welds. Only 38 observations were obtained and no significant contributions by any of the independent variables to weld metal tensile strength were discovered (see Table 2.2-B). Not only was this data set limited to wet welds in the flat position and in fresh water, the thickness range was small 16 mm to 22.4 mm (5/8 in. to 7/8 in.), and the wet welding depth was quite limited 10 m (33 ft). Therefore, the contribution of plate thickness and welding depth would be difficult to discover.

### 2.2.3 Radiographic and Visual Test (RT/VT) Acceptability

An analysis employing all 14 independent variables applicable to SMAW defined five significant (90 percent confidence) variables which contribute to the acceptance rate by RT and/or VT. Although the analysis explained about half of the variability of RT/VT acceptability, it was based on only 80 observations. Therefore, the analysis was repeated with electrode coating removed as an independent variable. The number of observations were

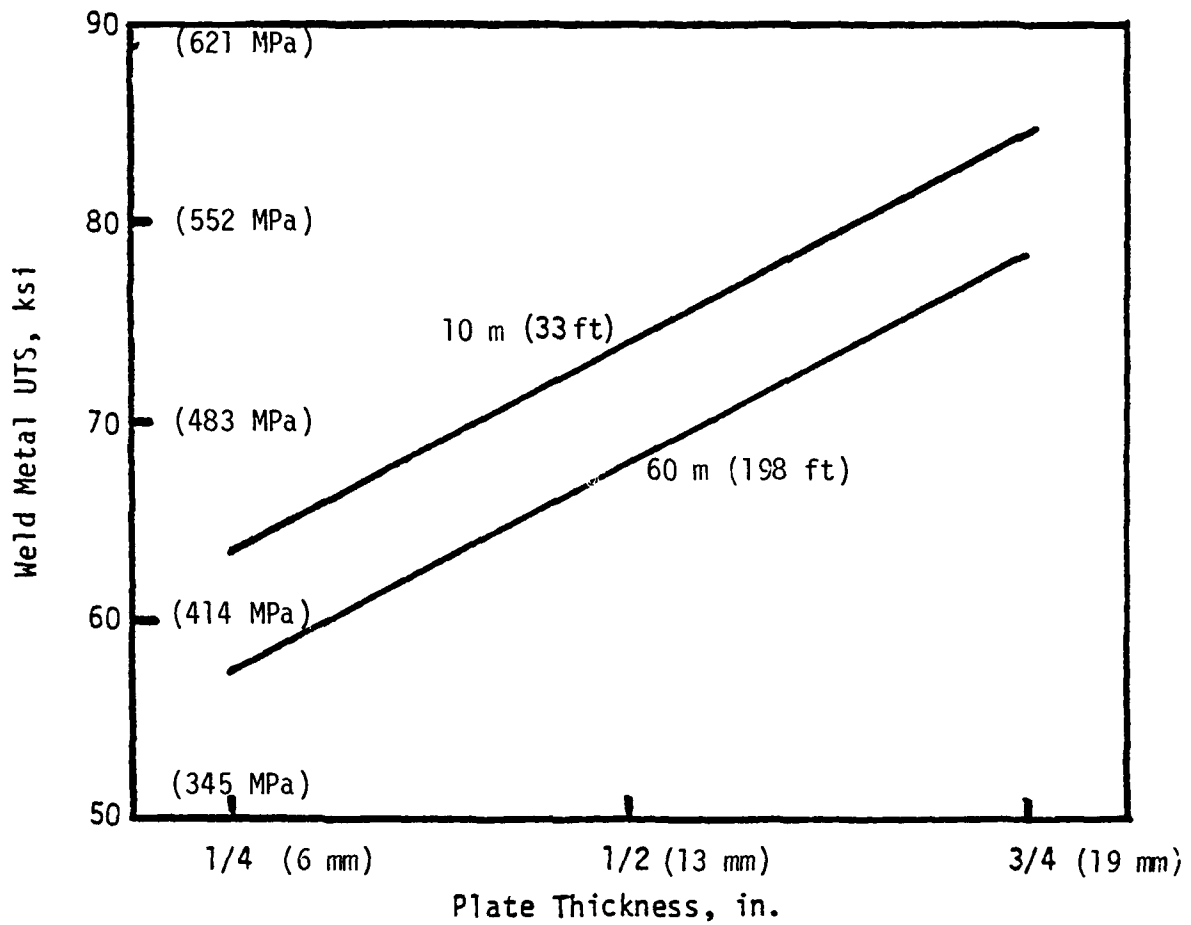


FIGURE 2.4. EFFECT OF PLATE THICKNESS AND WELDING DEPTH ON WELD METAL TENSILE STRENGTH.

increased to 184, but only one-fourth of the variability was explained, see Table 2.3. Both analyses indicate that:

- Welds made on A-36 steel base plate tend to produce less rejects than welds made on low-alloy base plate.
- Increasing carbon equivalent tends to increase the acceptance rate. This may be confounded by the electrode selection that could not be included in the analysis.
- Warmer water reduces the number of defective welds.
- Sounder welds may be produced in thicker plates.

In addition, the 80-observation data set analysis indicates that increasing the welding depth may decrease the acceptance rate. Alternately, the 184-observation data set analysis indicates that fresh water welds may produce less rejects than salt water welds. Analysis of another subset indicates that less rejects may be produced when welding in the flat position.

#### 2.2.4 Bend Test Acceptability

When all 14 independent variables applicable to SMAW were evaluated against all bend test results, six of the variables were discovered to be a statistically significant (90 percent confidence) contributor based on 74 observations, see Table 2.4-A. Three subsets were evaluated, but the overall fit appeared to be worse even though more observations were included. However, since the bend radii varied by nearly an order of magnitude (1.5t to 10t), the data base was divided into three groups and reanalyzed.

TABLE 2.3. EFFECT OF WELDING VARIABLES ON ACCEPTANCE BY RT/VT

A. SMAW Only--80 Observations

<u>Variables Added</u>	<u>Range (min/max)</u>	<u>F to Remove<sup>(a)</sup></u>	<u>Mult. R<sup>2</sup> ( percent)</u>	<u>Reg. Coeff.</u>
-	-	-	-	-1.48 <sup>(b)</sup>
A-36	0/1	20.80	20.23	0.63
C.E. ( percent)	.237/.510	8.00	33.89	2.3
Thickness (in.)*	.375/1.000	3.25	40.47	0.60
Water depth (ft)*	1/295	6.90	44.03	-0.002
Water temp. (°F)*	46/85	6.54	46.89	0.012
Flat position	0/1	0.89	48.97	-0.17
Rutile coating	0/1	0.58	49.52	0.20
Wet	0/1	0.33	49.89	-0.16
Vertical position	0/1	0.25	50.08	-0.097
Fresh water	0/1	0.19	50.26	0.046
Horizontal position	0/1	0.05	50.29	-0.041
Electrode dia. (in.)	.125/.188	0.01	50.30	-0.46

B. SMAW Only, All Coatings--184 Observations

<u>Variables Added</u>	<u>Range (min/max)</u>	<u>F to Remove<sup>(a)</sup></u>	<u>Mult. R<sup>2</sup> ( percent)</u>	<u>Reg. Coeff.</u>
-	-	-	-	0.90 <sup>(b)</sup>
Water temp. (°F)*	44/85	5.04	7.31	-0.008
Fresh water	0/1	9.33	13.78	0.31
A-36	0/1	15.86	17.67	0.34
Thickness (in.)*	.375/1.000	11.69	21.62	-0.70
C.E. ( percent)	.109/.597	5.91	23.15	1.3
Flat position	0/1	2.41	25.73	-0.15
C.S. weld metal	-1/1	1.16	26.50	-0.04
Water depth (ft)*	1/295	0.59	26.75	-0.001
Wet	0/1	0.32	26.90	0.15
Horizontal position	0/1	0.18	26.98	0.05
Electrode dia. (in.)*	.125/.188	0.02	26.99	-0.40

(a) 90 percent confidence level, F = 2.75

(b) Intercept value

(c) 90 percent confidence level, F = 2.79

\*1.0 in. = 25.4 mm, 1.0 ft = .3048 m, (°F-32) 5/9=°C

As an additional independent variable, bend radius was discovered to be a significant factor, as would be expected, along with polarity (DCSP is better) and plate thickness (thinner material is better).

Separate analyses were carried out on welds that were subjected to 2t bend tests and 3t bend tests. The analysis of the 2t bend test group is summarized in Table 2.4-B; the 3t bend test group is summarized in Table 2.4-C.

When 2t bend test data were considered separately, weld metal composition, base metal composition, and water depth emerged as significant variables, based on 56 observations. An analysis of the 3t data (79 observations) defined polarity, carbon equivalent (lower is better) and base plate material (low-alloy steel is better) as significant variables.

### 2.3 Conclusions: Factors Chosen for the Test Matrix

Based on the review of the literature and statistical analysis of available data, the following conclusions were reached:

Weld Type: There is an obvious difference between wet and wet-backed welds, and since the scope of the project was to include both types of welds, they were both included in the test matrix. Dry welds were also included as a basis for comparison. To achieve consistency, wet, wet-backed welds are normally made with a different electrode (E7018) than the wet welds (E6013) and the results for the wet-backed welds made with the E6013 electrode are not representative of ferritic wet-backed welds in general.

Base Plate Carbon Equivalent and Filler Metal: The weldability of base plate is related to the amount of carbon and

TABLE 2.4. EFFECT OF WELDING VARIABLES ON ACCEPTANCE BY TEND TEST

A. SMAW Only, All Bend Test Diameters -- 74 Observations

<u>Variables Added</u>	<u>Range</u> <u>(min/max)</u>	<u>R to Remove<sup>(a)</sup></u>	<u>Mult. R<sup>2</sup></u> <u>(percent)</u>	<u>Reg Coeff.</u>
-	-	-		--3.59 <sup>(b)</sup>
Water temp. (°F)*	50/85	4.24	9.48	0.018
Flat position	0/1	4.05	13.71	0.44
DCRP	0/1	15.13	18.47	1.6
Rutile Coating	0/1	11.90	31.56	1.2
A-36	0/1	6.58	34.39	1.0
Fresh water	0/1	3.05	38.11	-0.61
Thickness (in.)*	.375/.1000	0.57	39.93	0.37
Electrode dia. (in.)*	.125/.156	0.64	40.45	6.3
C.E. ( percent)	.139/.446	0.50	40.96	0.72
Horizontal position	0/1	0.29	41.30	0.13
Vertical position	0/1	0.03	41.33	0.040
Water depth	8/295	0.02	41.35	nil

B. SMAW Only, Bend Test Diameter < 2t -- 56 Observations

(All fresh water, no vertical welds.)

<u>Significant Variables Added</u>	<u>Range</u> <u>(min/max)</u>	<u>T to Remove<sup>(c)</sup></u>	<u>Multi. R<sup>2</sup></u> <u>( percent)</u>	<u>Reg. Coeff.</u>
-	-	-		-1.37 <sup>(b)</sup>
C.S. weld metal	-1/1	14.82	13.30	-0.52
Water depth	1/293	12.83	22.63	-0.007
A-36	0/1	19.74	44.21	0.88

C. SMAW Only, Bend Test Diameter = 3t -- 79 Observations

(All wet welds.)

<u>Significant Variables Added</u>	<u>Range</u> <u>(min/max)</u>	<u>F to Remove<sup>(a)</sup></u>	<u>Multi. R<sup>2</sup></u> <u>( percent)</u>	<u>Reg. Coeff.</u>
-	-	-		-2.16 <sup>(b)</sup>
Water temp. (°F)*	50/80	1.18	13.26	-0.010
DCRP	0/1	6.68	19.32	-0.39
C.E. ( percent)	.180/.597	6.13	24.93	-2.5
A-36	0/1	4.15	30.71	-0.38
Fresh water	0/1	2.61	34.52	0.64

(a) 90 percent confidence level, F = 2.79

(b) Intercept value

(c) 90 percent confidence level, F = 2.84

\*1.0 in. = 25.4 mm, 1.0 ft = .3048 m, (°F-32) 5/9 = °C

other elements in the steel. Presently mild steels with a CE less than 0.40 can be readily welded underwater. Higher CE material usually requires an austenitic filler metal to prevent hydrogen cracking. The CE influences the hardness of the HAZ. Statistical analysis showed that increasing the CE decreased the likelihood of rejection based on NDE, but this is likely to be due to the use of the austenitic electrodes with these higher CE base plates. Lower CE base plates performed better in the bend test, but this is also likely to be influenced by electrode selection.

Small variation of the carbon equivalent within the range where ferritic electrodes can be used did not significantly affect the mechanical properties of test welds [2.3]. Therefore, it was decided to use a high CE base plate and austenitic filler metal as well as a mild steel base plate with CE less than 0.40 and a ferritic filler metal to gather data on these two unique types of welds. Actual comparison to determine the effect of CE will, of course, be confounded by the differing filler metal.

Welding Depth: Welding depth influences bead shape and arc stability as well as the chemistry, microstructure, and porosity of the weld. It has been shown to affect the occurrence of cracking (especially under restraint), weld metal tensile strength, bend test acceptability, and RT/VT acceptability. Therefore, depth was included in the test matrix. At the time the test matrix was planned, ferritic wet welds were made down to 60 m (198 ft), although this capability was recently extended down to below 100 m (330 ft). Ferritic welds were therefore planned in the range of 10 m to 60 m (33 to 198 ft) or one to six atmospheres. Austenitic welds on higher CE base plate are limited to a depth of about 10 m (33 ft). Originally, the capability to make these welds down to 60 m (198 ft) was thought to be within reach. However, attempts to weld at deeper depths failed and the test matrix was revised to include more ferritic welds instead.

Plate Thickness: Plate thickness directly affects the cooling rate, and hence the hardness and crack susceptibility of welds. Statistical analysis revealed a possible influence on weld strength, therefore 12.7 mm and 25.4 mm (1/2 in. and 1 in.) plates were included in the test matrix.

Other Variables: The above variables were thought to be the primary factors influencing underwater wet and wet-backed weld performance. Other variables considered were:

- Polarity: Straight polarity is normally used and seems to yield better results.
- Water Temperature: Small variations in water temperature in the range 0 to 21°C (32 to 70°F) cannot be shown to contribute significantly to weld performance.
- Electrode Diameter and Type: Only a few electrode types and diameters are successfully being used in wet welding. We chose to use two of the most commonly used. For one condition in the test matrix, a weld was made with a larger diameter 4.1 mm (5/32 in.) electrode as well as the 3.3 mm (1/8 in.) electrode to examine this effect.
- Welding Position: Although the difficulty of welding is affected by welding position, it could not be shown to significantly affect hardness, RT/VT acceptability, weld strength, or bend test performance, and was therefore not included in the test matrix.

- Salinity: The performance of welds made in salt water has been shown to be better than those made in fresh water [2.22]. Therefore, as a worst case and for convenience, the test welds were prepared in fresh water.

#### 2.4 References

- 2.1 Brown, R.T., and Masubuchi, K., "Fundamental Research on Under Water Welding," Welding Journal, Vol. 54, No. 6, June 1975.
- 2.2 Tsai, C.L., and Masubuchi, K., "Mechanisms of Rapid Cooling and Their Design Considerations in Underwater Welding," Proceedings Offshore Technology Conference, Houston, Texas, OTC 3469, April 30 May 3, 1979.
- 2.3 Gooch, T.G., "Properties of Underwater Welds, Part 1 Procedural Trials and Part 2 Mechanical Properties," Metal Construction, March 1983.
- 2.4 Tsai, C.L., and Masubuchi, K., "Interpretive Report on Underwater Welding," Welding Research Council, Bulletin No. 224, February 1977.
- 2.5 Dadian, M., "Review of Literature on the Weldability Underwater of Steels," Welding In The World, Vol. 14, No. 3/4, 1976.
- 2.6 Brown, A.J., Staub, J.A., and Masubuchi, K., "Fundamental Study of Underwater Welding," 4th Annual Offshore Technology Conference OTC 1621, April 30 - May 3, 1972.

2.7 Grubbs, C.E., and Seth, O.W., "Underwater Wet Welding with Manual Arc Electrodes," Published in Underwater Welding for Offshore Installations, The Welding Institute, Abington Hall, Abington, Cambridge, 1977.

2.8 Stalker, A.W., Hart, P.H.M., and Salter, G.R., "An Assessment of Shielded Metal Arc Electrodes for the Underwater Welding of Carbon Manganese Structural Steels," Offshore Technology Conference, OTC 2301, Houston, Texas, May 5-8, 1975.

2.9 Sadowski, E.P., "Underwater Wet Welding Mild Steel with Nickel Base and Stainless Steel Electrodes," Welding Journal, July 30, 1980, pp. 30-38.

2.10 Matlock, D.K., Edwards, G.R., Olson, D.L., and Ibarra, S., "An Evaluation of the Fatigue Behavior in Surface, Habitat, and Underwater Wet Welds," Underwater Welding Soudage Sous L'Eau, Proceedings of the International Conference held at Trondheim, Norway, 27-28 June 1983 under the auspices of the International Institute of Welding, Pergamon Press, Oxford, England, p. 303, 1983.

2.11 Kobayash, K., "Quality Control in Shipbuilding," in Proceedings of the International Conference held in London, England, November 19-20, 1975, Vol. 1, The Welding Institute, Cambridge, p. 28, 1976.

2.12 Newman, R.P., "Effect on Fatigue Strength of Internal Defects in Welded Joints--A Survey of the Literature," BWRA Report D2/2/58, Weld. Res. Abroad, Vol. V, No. 5, 1959.

2.13 Burdekin, F.M., Harrison, J.D., and Young, J.G., "The Effect of Weld Defects with Special Reference to BWRA Research," Weld. Res. Abroad, Vol. 14, No. 7, pp. 58-67, August-September 1968.

2.14 Clough, R., "Application of Weld Performance Data," Br. Weld. J., Vol. 15, No. 7, pp. 319-325, July 1968.

2.15 Pollard, B. and Cover, R.J., "Fatigue of Steel Weldments," Weld. J., Vol. 51, No. 11, pp. 544s-554s, 1972.

2.16 Honig, E.M., "Effects of Cluster Porosity on the Tensile Properties of Butt-Weldments in T-1 Steel," CERL Report M-109, November 1974.

2.17 de Kazinczy, F., "Fatigue Properties of Repair Welded Cast Steel," Br. Weld. J., Vol. 15, No. 9, pp. 447-450, September 1968.

2.18 Carter, C.J., et al., "Ultrasonic Inspection and Fatigue Evaluation of Critical Pore Size in Welds," Technical Report AMMRC TR-80-35, International Harvester Company, Hinsdale, IL, AMMRC Contract DAAG46-76-C-0058, September 1982.

2.19 Harrison, J.D., "Basis for a Proposed Acceptance-Standard for Weld Defects", Metal Construction, Vol. 4, No. 3, pp. 99-107, March 1972.

2.20 Olson, D.L. and Ibarra, S., "Underwater Welding Metallurgy" presented at Underwater Welding Workshop, November 13 and 14, 1985, Colorado School of Mines, Golden, CO.

2.21 Personal communication with J. Dally of Sea-Con Services.

2.22 Grubbs, C.E., "Qualification of Underwater Wet Weld Procedures at Water Depths Down to 325 Feet" presented at ADC Diving Symposium, Houston, TX, 1986.

2.23 Masumoto, I., Matsuda, K. and H. Masayoshi "Study on the Crack Sensitivity of Mild Steel Welded Joint by Underwater Welding", Trans. of the Japan Welding Society, Vol. 14, No. 2, October, 1983.

2.24 Cottrell, C.L.M., "Hardness Equivalent May Lead to a More Critical Measure of Weldability," Metal Construction December, 1984.

### 3.0 EXPERIMENTAL PROGRAM

#### 3.1 The Test Matrix

An experimental program was conducted as part of an effort to quantify the changes in strength, ductility, and toughness of wet and wet-backed underwater fillet and groove welds. The test matrix is shown in Figure 3.1. The experiment was primarily designed to examine the effect on these properties of:

- Material: A-36 steel with a carbon equivalent of  $0.36 \pm 0.03$  was used with a ferritic filler metal; and A-516 Grade 70 steel with a carbon equivalent of  $0.46 \pm 0.03$  was used with a nickel alloy filler metal.
- Plate thickness: For each material combination above, single bevel groove weld specimens were prepared from 12.7 mm (1/2 in.) and 25.4 mm (1 in.) plate thicknesses.
- Depth: Ferritic wet welds of 12.7 mm (1/2 in.) and 25.4 mm (1 in.) thickness were prepared at 60, 35, and 10 m (198, 115, and 33 ft); as well as dry welds prepared at the surface. 25.4 mm (1 in.) thick ferritic welds were also made at 20 and 30 m (66 and 99 ft). Wet-backed welds are prepared only at 10 m (33 ft). Austenitic wet and wet backed welds were also prepared at a depth of 10 m (33 ft) as well as dry welds.

		0.36 ± .03 CE, Ferritic Filler				0.46 ± .03 CE, Nickel Alloy Filler	
	Fillet (1/2-in.) -Plate	Weld Tensile (1 in.) Plate	Restraint (1 in.) Plate	Groove (1/2 in.) Plate	Groove (1 in.) Plate	Groove (1/2 in.) Plate	Groove (1 in.) Plate
Wet	60 m (198 ft)	$\frac{1}{2}$ (13F)	$\frac{1}{2}$ (23T)	$\frac{1}{2}$ (23R)	$\frac{1}{2}$ (13)	$\frac{1}{2}$ (23)	$\frac{1}{2}$ (33)
	35 m (115 ft)	$\frac{1}{2}$ (12F)	$\frac{1}{2}$ (22T)	$\frac{1}{2}$ (22R)	$\frac{1}{2}$ (12)	$\frac{1}{2}$ (22)	$\frac{1}{2}$ (32)
	10 m (33 ft)	$\frac{1}{2}$ (11F)	$\frac{1}{2}$ (21T)	$\frac{1}{2}$ (21R)	$\frac{1}{2}$ (11)	30 m 1) 20 m 1) 10 m 3) (21, 218, 21D)	99 ft (299) (66 ft (266) (33 ft (31) (218, 21D)
	Wet-Backed 10 m (33 ft)				$\frac{1}{2}$ (11B)	$\frac{1}{2}$ (21B)	$\frac{1}{2}$ (31B)
Dry					$\frac{1}{2}$ (10)	$\frac{1}{2}$ (20)	$\frac{1}{2}$ (30)

FIGURE 3.1. TEST MATRIX

Note: 1/2 in. = 12.7 mm  
 1 in. = 25.4 mm  
 1 ft = .3048 m

Other plates were prepared to examine:

- Restraint: A series of 25.4 mm (1 in.) thick A-36 groove weld plate specimens were prepared from plates pre-welded to a very stiff frame, simulating restrained structural joints.
- Weld Preparation: A double bevel weld was prepared at 10 m (33 ft) for the 25.4 mm (1 in.) ferritic weld. All other welds in the study were single bevel preparations.
- Procedure Variation: An additional 25.4 mm (1 in.) ferritic single bevel weld was made with a procedure variation, specifically a 4.1 mm (5/32 in.) electrode was used rather than the standard 3.3 mm (1/8 in.) electrode.
- Fillet welds: A set of fillet weld tensile tests and fillet weld break-over tests will be conducted on ferritic fillet welds prepared at three depths from 12.7 mm (1/2 in.) material.
- Weld metal tensile strength: Extra width 25.4 mm (1 in.) thick groove welds are prepared to extract all-weld-metal tensile test specimens.

The austenitic welds at 35 and 60 m (115 and 198 ft) depth were originally planned, however, these welds could not be made and were dropped from the test matrix. In Figure 3.1 these sectors of the matrix are hatched. Instead of the deeper austenitic welds, the additional 25.4 mm (1 in.) ferritic welds were made; welds at 20 and 30 m (66 and 99 ft) and welds at 10 m (33 ft) using a procedure and preparation variation. With these additions, better information about the variation of weld quality and toughness can be obtained by concentrating tests at 10 m (33 ft). Also the

variation with depth at these more common shallow depths can be better ascertained.

The meaning of the specimen identification code numbers in Figure 3.1 is:

First digit - Material:      1 = 12.7 mm (1/2 in.) A-36  
                                  2 = 25.4 mm (1 in.) A-36  
                                  3 = 12.7 mm (1/2 in.) A-516  
                                  4 = 25.4 mm (1 in.) A-516

Second digit(s) - Depth:     0 = surface  
                                  1 = 10 m (33 ft))  
                                  2 = 35 m (115 ft)  
                                  3 = 60 m (198 ft)  
                                  66 = 20 m (66 ft)  
                                  99 = 30 m (99 ft)

Letters:                        F = fillet weld  
                                  T = all-weld-metal tensile  
                                  R = restrained  
                                  B = wet-backed weld  
                                  S = weld with procedure variation 4.1 mm (5/32 in.) electrode  
                                  D = double bevel weld preparation

This code will be used throughout this report when referring to a particular test plate. Actually, most sectors of the test matrix represent three test plates prepared under identical conditions. (One plate is used to provide Charpy specimens, another for  $J_{Ic}$  compact tension specimens, and the other for side bend, tensile, and macro examination and hardness traverse specimens). The welding procedure used for each plate is documented in Appendix A, Table A.1.

The following typical welder/diver qualification tests were conducted on each groove weld:

1. Visual examination
2. Radiographic examinations
3. Bend tests at 57.2 mm (2.25 in.) radius, 25.4 mm (1 in.) radius, and 19.0 mm (0.75 in.) radius
4. Reduced section (transverse weld) tensile tests
5. Metallographic macro examination
6. Hardness traverse

All-weld-metal tensile tests were performed on specially prepared ferritic groove welds at 10, 35 and 60 m (33, 115, and 60 m (198 ft). Chemical analysis of the base metal and filler metals was also performed. Charpy V-notch impact tests and  $J_{Ic}$ -CTOD fracture mechanics tests were conducted for both the weld metal and heat affected zone locations of all the welds. The purpose of the  $J_{Ic}$  tests is to make comparisons of fracture toughness among the welds and to establish the ability of the Charpy test to predict the fracture toughness. For most groove welds, only two  $J_{Ic}$  tests were performed, one precracked in the heat affected zone (HAZ) and one precracked in the weld metal.

The fillet weld specimens are tested for ductility in a break-over bend test and for shear strength in a fillet weld tensile test. Comparisons are made of the shear strength of these fillet welds to the tensile strength obtained from all-weld-metal tensile specimens prepared from the same filler metal at the same depth.

Section 3.2 presents a discussion of findings from the experimental program, excluding the statistical analysis which is presented in Section 4.0. Detailed descriptions of the test procedures and results are presented in Appendix A.

### 3.2 Discussion of Test Results

### 3.2.1 Visual and Radiographic Examination

Wet-welded plates were generally found to have two parallel grooves along each fusion line at the weld root (inadequate joint penetration). Radiography revealed the porosity in the wet-welds, and slag inclusions in a few plates. A crack was found in the 12.7 mm (1/2 in.) ferritic wet-backed weld 11B-2. The ferritic wet backed welds were purposefully made with a poor choice of electrode for wet-backed welding. Wet-backed welds are usually made with an E7018 electrode. However, the same E6013 electrode that was used for the wet welds was also used for these wet-backed welds in order to have consistency in the test matrix. Results from these ferritic wet-backed welds cannot be thought of as typical for wet or wet-backed welds. Note that it is possible the poor results obtained for the wet-backed weld could possibly be affected by the waterproof coating used on the E6013 electrode, which was not intended to be used in the dry.

The order and/or spacing of the specimens was in four cases rearranged to avoid defects detected from radiography. Since there is an extra bend specimen provided, the defect was generally isolated in a single bend specimen. The following plates were the only plates purposefully rearranged to avoid defects:

11B-1 tensile and bend specimens were rearranged to get tensile specimens away from a large crack.

11-1 tensile and bend specimens were rearranged to isolate a slag inclusion approximately 12.7 mm (1/2 in.) long slag in several bend specimens.

20-2 tensile and bend specimens were rearranged to isolate a slag inclusion approximately 9.5 mm (3/8 in.) long in a bend specimen.

21-T-2 all-weld-metal tensile specimen location was chosen to avoid two slag inclusions in the gage length.

In all other plates, it was not deemed advantageous to rearrange specimens, i.e. either the discontinuities were small and would be typical of Type B welds or they were prevalent throughout the weld, e.g. porosity. The significance of the limited rearranging that was done is not thought to be great, since many discontinuities were discovered in test specimens after sawing or testing which were not evident from the NDE. Note also that 1) plate 11B is a wet-backed weld made with an improper electrode, and the results of these wet-backed welds are of questionable use anyway, 2) plate 20 is a dry weld, and 3) plate 21-T is used only for the all-weld-metal specimen. Therefore, only one wet welded plate was rearranged for test specimens and this could not significantly bias the test results of this program.

Normally a plate would be rejected on the basis of the radiographic indication. In view of the use of this data for application in design rules, it was decided to proceed with testing of these plates. Once a welding procedure is qualified under the AWS D3.6 specification for Type B welds, subsequent production underwater welds prepared with this qualified procedure would probably be subjected to less scrutiny than the welds used in these tests. Hence, the number and size of these defects in the test welds are probably less than those of actual service welds.

### 3.2.2 Side Bend Tests

Side bend tests were performed as part of the typical weld qualification tests as outlined in AWS D3.6 Specification. The test gages the ability of the weld to deform plastically as it is bent 180° at a specified radius. The specification requires that for Type B welds, four side bend test specimens be bent to a radius of six times the 9.5 mm (3/8 in.) specimen thickness (6T) or 57.2 mm (2.25 in.). In addition, for the purposes of this project, specimens are bent to selected smaller radii so that it can not only be determined if the weld qualifies as a Type B weld, but also just how much additional ductility is afforded by the welds. Actually, to qualify as a Type A weld, four side bend tests should be bent to a (2T) or 19 mm (3/4 in.) radius. We have indicated several weldments that appear to be able to meet this requirement of Type A welds, although because of a limited number of specimens, only two or three specimens were bent to the (2T) or 19 mm (3/4 in.) radius.

The results of the bend tests are summarized in Table 3.1 in the form of a relative score based on the best performance being equal to 100. The weld type shown in Table 3.1 indicates that only the results of the bend test satisfy the requirements of that weld type, i.e. other requirements may not be satisfied. In addition, because only a limited number of specimens were available and most were used at larger radii, those welds indicated to have passed the Type A bend test requirements did not always pass four tests.

Strict interpretation of the AWS D3.6 Specification indicated that if any of the first four 6T 57.2 mm (2.25 in.) bend tests fail to meet the requirements (i.e., cracks must be less than 3.3 mm (1/8 in.)), the procedure is not qualified as a Type B weld. By this strict interpretation, the 12.7 mm (1/2 in.)

TABLE 3.1  
SUMMARY OF BEND TEST DATA

A36 Base Metal Ferritic Filler			A516 Base Metal Austenitic Filler		
12.7 mm (1/2 in.)	25.4 mm (1 in.)	25.4 mm (1 in.) Restraint	12.7 mm (1/2 in.)	25.4 mm (1 in.)	Depth
31B	23C	38C			60 m Wet (198 ft)
45B	58B	45B			35 m Wet (115 ft)
	60B				30 m Wet (99 ft)
	60B				20 m Wet (66 ft)
94A	80B+, 20C++, 88A	71B	23C	8C	10 m Wet (33 ft)
8C	63B		88A	88A	10 m Wet -Backed (33 ft)
100A*	94A*		100A*	94A*	Dry

- \* The difference in scores of dry welds is due only to variations in the bend radii chosen for the tests.
- + Plate 21D, double bevel weld preparation.
- ++ Plate 21S, used 4.1 mm (5/32 in.) electrode.

ferritic wet-back weld, a ferritic wet weld prepared at 10 m (33 ft) with a 4.1 mm (5/32 in.) electrode as an intentional procedure variation, both austenitic wet welds, and the 25.4 mm (1 in.) ferritic wet welds from 60 m (198 ft) depth (both with and without restraint) do not qualify as Type B welds. The 25.4 mm (1 in.) ferritic wet welds from 60 m (198 ft) were clearly very close to the borderline of Type C to Type B classification according to bend test criteria. Specifically, four out of five 6T bends for the 25.4 mm (1 in.) unrestrained ferritic wet weld at 60 m (198 ft), (23-3) and six out of seven for the same weld restrained (23R-1) did pass. The results of tests on these ferritic welds from 60 m (198 ft) depth were therefore conservatively considered among the group of Type B welds.

The austenitic wet welds did not qualify as Type B welds according to bend test criteria; e.g., 6 out of 8 6T bends passed for the 12.7 mm (1/2 in.) weld and 4 out of 7 for the 25.4 mm (1 in.) weld. It is interesting to note that although the austenitic wet-welds exhibited poor bend test results, these welds have very good fracture toughness. These bend tests failed because pores opened up to greater than 3.3 mm (1/8 in.) although they were bent fully 180°. The present requirement of AWS D3.6 is a good screening test for weld workmanship, but should not be regarded as indicative of the total ductile capacity to rotate (i.e. only the capacity to rotate up to par elongation is indicated) or toughness.

The failure of the 12.7 mm (1/2 in.) ferritic wet-backed weld must be considered along with the fact that these welds were prepared with an improper electrode, E6013. The 25.4 mm (1 in.) ferritic wet-backed weld passed all the 6T bend tests; however, one of the bend specimens (which remains untested) contains a crack and would obviously fail if tested. A 2T and 2.67T bend also passed for this weld, indicating the ductility is quite good. Therefore,

the 25.4 mm (1 in.) ferritic wet-backed weld was still classed as Type B with respect to bend test criteria, notwithstanding the obvious cracking problem that was caused by intentional use of an improper electrode.

### 3.2.3 Transverse-Weld Tension Test

The transverse-weld reduced-section tensile tests all passed the requirements for Type A welds (identical to the requirements for Type B welds). Most (76 percent) of the specimens fractured in the base metal, with the tendency to fracture in the weld increasing with depth (and porosity). Those specimens which fracture in the weld metal exhibited very little elongation. The transverse weld tension test reveals very little about the performance of the weld other than assuring adequate strength and fusion, which can be assured by the bend test. More useful information can be obtained from an all-weld-metal tension test, e.g. weld metal yield, ultimate, and elongation.

### 3.2.4 Hardness Traverse

Small portions of the heat-affected zone (HAZ), usually found near the weld crown, had Vickers hardness (HV1.0) of up to 334 for the wet ferritic welds and up to 460 HV for the austenitic wet welds. Nearby impressions (within 0.5 mm (.008 in.)) were often 200 HV less hard, indicating the high hardness was a very localized phenomenon. This spatial variability on a single specimen explains the wide scatter in hardness measurements both for a single specimen and between specimens. Dry and wet-backed welds were not nearly as hard. In the statistical analysis in section 4.0 it is shown that hardness is generally independent of depth and cannot be correlated to toughness or performance in the bend test. Because of the absence of cracking or brittle fracture

behavior in all the wet welds, the hardness of the weld seems insignificant.

### 3.2.5 Fillet Weld Tests

Fillet weld break-over bend tests and fillet weld tensile tests were conducted and the results of these tests would qualify these fillet welds as Type B. The fillet weld bend specimens failed before being bent to 45°, but failed in the throat exhibiting good fusion and lack of obvious defects.

The failures of the fillet weld tensile tests were all remarkably ductile, i.e. the plates extended (slid apart) appreciably before breaking. The results from pairs of these tests were as follows:

- 11F: Shear strength = 373 and 337 MPa (54.1 and 48.9 ksi)  
(60 percent AWM tensile strength = 47.6 ksi)
- 12F: Shear strength = 379 and 338 MPa (54.9 and 49.0 ksi)  
(60 percent AWM tensile strength = 281 MPa(40.7 ksi)
- 13F: Shear strength = 322 and 310 MPa (46.7 and 45.0 ksi)  
(60 percent AWM tensile strength = 271 MPa (39.3 ksi)

Sixty percent of the specified minimum tensile strength (400 MPa (58 ksi)) of the A-36 base material is 240 MPa (34.8 ksi), and since the shear strength is larger the welds are qualified as Type B fillet welds. They also meet the more stringent requirements for a Type A fillet weld (60 percent of the average of the all-weld-metal ultimate tensile strength) which is also reported above.

### 3.2.6 All-Weld-Metal Tensile Tests

All-weld-metal tensile tests were conducted on the ferritic

wet-welds although these tests are not required for Type B qualification. The tests revealed the weld metal has the required strength, although elongation was insufficient to qualify the welds as Type A. The results are summarized in Table 3.2.

### 3.2.7 Charpy Tests

Charpy impact tests are often used to indirectly estimate the fracture toughness of metals. This practice is less desirable than direct measurement of toughness with  $K_{Ic}$ ,  $J_{Ic}$  or CTOD tests. However, due to the relative difficulty and expense of the latter, the Charpy test will probably continue to be used. Therefore, as part of our investigation, we will investigate the correlation between Charpy impact toughness and  $J_{Ic}$  or  $K_{Ic}$ , as well as investigate the trends in impact energy and toughness among the variables of this experimental program.

Charpy tests were conducted at -2° and 16°C (28° and 60°F) for all weldments. The impact energy for the ferritic weld metal was low (typically 20~47 J (15~35 ft-lbs)) with the exception of the dry welds. For the 12.7 mm (1/2 in.) ferritic welds, HAZ\* impact energy 54~76 J (40~56 ft-lbs) was higher than the weld metal impact energy. For the 25.4 mm (1 in.) ferritic wet welds, the HAZ impact energy 9~15 J (7~11 ft-lbs) was lower than the weld impact energy. The impact energy for the austenitic welds was much higher, ranging from 45 to 155 J (33 to 114 ft-lbs).

Most of the conditions tested indicate "upper shelf" or full shear behavior at 28°F. Specimens which did not exhibit full shear behavior include both thicknesses of the dry and wet-backed

---

\*The notch for these HAZ Charpy tests was located about 1 mm from the fusion line, see the Appendix Section A.9.

TABLE 3.2  
SUMMARY OF ALL-WELD-METAL TENSILE TESTS  
(25.4 mm (1 in.) Thick A-36 Plate, Ferritic Filler)

	Proportional Limit (MPa)	Yield Point ksi		Tensile Strength (MPa)		Elongation (%)
	ksi	(MPa)	ksi	ksi		
60 m (198 ft)	350 350	50.8 50.8	402 402	58.4 58.4	451 451	65.5 65.5
35 m (115 ft)	384 395	55.8 57.4	437 423	63.5 61.4	475 458	69.0 66.5
10 m (33 ft)	472 464	68.5 67.3	507 493	73.6 71.6	556 539	80.7 78.2

E6013 weld metal, the 25.4 mm (1 in.) ferritic HAZ's, and the 25.4 mm (1 in.) dry austenitic HAZ.

If the Charpy tests exhibit upper shelf behavior at this temperature, then the more slowly loaded  $J_{Ic}$  fracture toughness, and the fracture toughness exhibited by the welds in the structure will also be expected to be upper shelf at this temperature. Therefore ductile tearing rather than brittle fracture would generally be anticipated in structures with underwater welds with the following exception. As pointed out above, the HAZ of 25.4 mm (1 in.) thick and thicker is in the transition or lower shelf region of the Charpy toughness vs temperature curve at 28°. The fracture of structures welded with 1 in. thick and thicker plates with the ferritic electrode cannot be generally assured to be ductile above -2°C (28°F) but may depend on strain rate, temperature and constant. Ductile tearing allows load to redistribute and in a redundant structure, considerable stable tearing can probably be accommodated without complete separation of the component.

Although there was some considerable scatter in the Charpy data, as the ranges above show, the toughness within any category of weld and in a particular location (HAZ or weld) varied in a fairly narrow range. The variance exhibited for austenitic welds is primarily due to several exceptionally tough samples. The Charpy test often exhibits a great deal of scatter even for homogeneous base metals. This scatter is partly due to the fact that the Charpy specimen samples only a small volume of material. This localized variation of material properties, as was noted for the hardness test results, is more apparent in the results of a Charpy test than a tensile test, for example.

### 3.2.8 $J_{Ic}$ Fracture Toughness Tests

Tests were conducted to determine the fracture toughness of the weld and heat affected zone. The test selected for this purpose was ASTM E813 " $J_{Ic}$ , a Measure of Fracture Toughness". This test is more appropriate than ASTM E399 ( $K_{Ic}$ ) "Plane-Strain Fracture Toughness" for ductile materials. The  $K_{Ic}$  toughness can still be determined by  $J_{Ic} = K_{Ic}^2/E$ . For several of the tests, the data was reduced such that the crack tip opening displacement (CTOD) could also be determined.

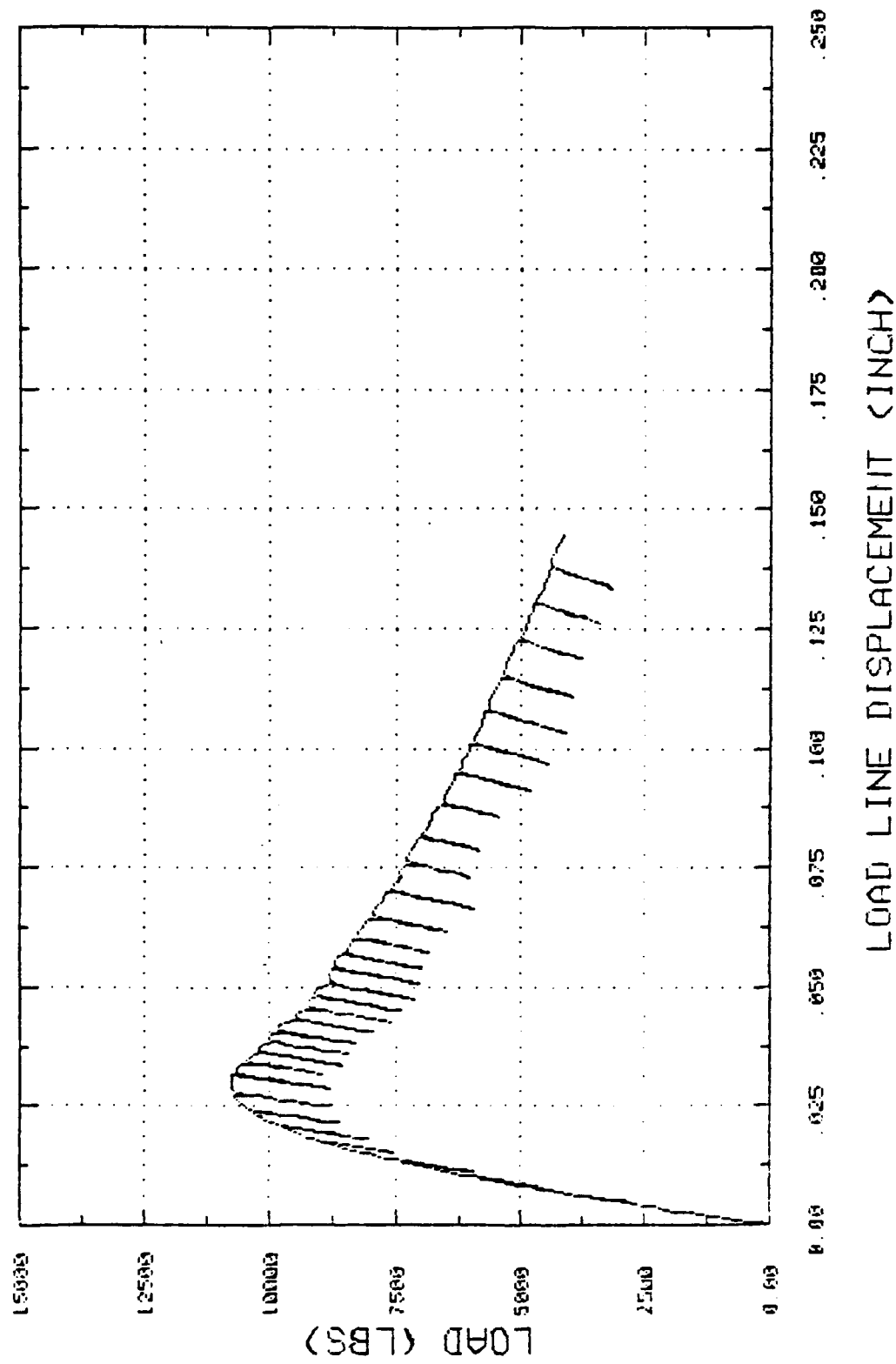
The value of  $K_{Ic}$  determined from this test has been shown to be generally conservative [3.1]. This is chiefly because of the different point of measurement inherent in the test methods E813 ( $J_{Ic}$ ) and E399 ( $K_{Ic}$ ); i.e., the measurement of  $J_{Ic}$  is taken at a point where the R-curve intersects the "blunting line" given by:

$$J = 2 \sigma_{flow} \Delta a.$$

The total crack growth,  $\Delta a$ , at this intersection, theoretically the point of initial actual crack advance, is generally much smaller than the 2 percent offset of the crack length used as a measurement point for  $K_{Ic}$  in ASTM E399. Thus, for steels which fracture by a ductile mode,  $J_{Ic}$  represents a lower bound to  $K_{Ic}$ .

Figure 3.2 shows a typical load vs load line (clip gage) displacement trace for a  $J_{Ic}$ /CTOD test of a 25.4 mm (1 in.) ferritic weld metal mode at 10 m (33 ft). Partial unloadings were performed to obtain the crack length by compliance.  $J$  is calculated from the area under the curve, and CTOD is calculated from the clip gage displacement. Figure 3.3 shows the  $J$ -resistance curve. The line to the left is the blunting line. Note the clear

UNDERWATER WELDS - J<sub>IC</sub>/CTOD TEST  
SPECIMEN 21-3-4W



1.0 in. = 25.4 mm  
1.0 lb. = 4.448N

FIGURE 3.2. EXAMPLE OF LOAD VS LOAD LINE DISPLACEMENT  
FOR J<sub>IC</sub>/CTOD Test

UNDERWATER WELDS - JIC FRACTURE TOUGHNESS PLOT  
SPECIMEN 21-3-4W

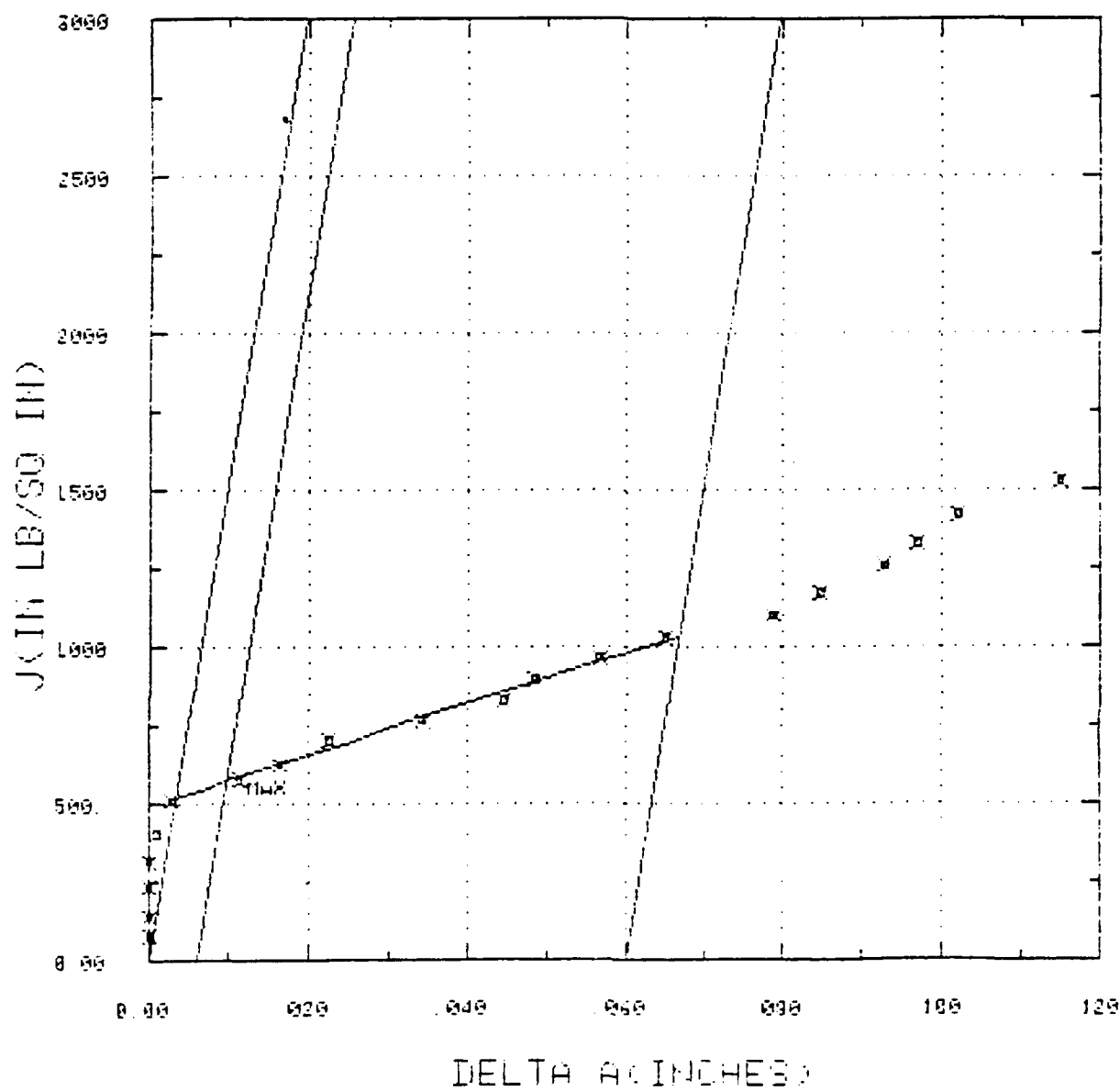


FIGURE 3.3 EXAMPLE OF J RESISTANCE CURVE

$$1.0 \frac{\text{in lb}}{\text{in}^2} = .175 \frac{\text{kJ}}{\text{m}^2}$$

$$1.0 \text{ in.} = 25.4 \text{ mm}$$

break in slope as the initiation of tearing occurs.  $J_{Ic}$  for this specimen was  $91 \text{ kJ/m}^2$  ( $522 \text{ in-lb/in.}^2$ ),  $K_{Ic}$  derived from  $J_{Ic}$  was  $135 \text{ MPa}\sqrt{\text{m}}$  ( $123 \text{ ksi}\sqrt{\text{in.}}$ ).

For failure to occur by ductile tearing in the structure, two criteria must be satisfied: 1) the applied  $J$  (from structural analysis) must exceed  $J_{Ic}$  and 2) the rate of change of the applied  $J$  with respect to crack extension must exceed the rate of change of the  $J$ -resistance curve with respect to crack extension, i.e. the  $J$  applied must remain above the  $J$ -resistance. The slope of the  $J$  resistance curve is therefore also an important material property and has been given the name "tearing modulus" or  $T$ .

$$T = \frac{dJ}{da} \cdot \frac{E}{\sigma_f^2}$$

The slope of the curve is normalized by the modulus over the flow stress squared because it is dimensionless and this is how the term appears in a structural analysis. If, for example, a crack in the structure is loaded such that  $J$  exceeds  $J_{Ic}$  but the applied  $T$  is less than  $T$ -resistance, only a limited amount of tearing will occur (until  $J$ -resistance exceeds  $J$ -applied) and the structure will remain stable. Thus a great deal more resistance to fracture is afforded by these welds than is evident by  $J_{Ic}$  or  $K_{Ic}$  derived from  $J_{Ic}$ .

The CTOD also increases in a stable manner with crack extension. Figure 3.4 shows the CTOD vs. crack extension for this weld and a resistance curve construction similar to that for  $J_{Ic}$  determination. Here the blunting line is given by:

$$\text{CTOD} = 2\Delta a$$

UNDERWATER WELDS - CTOD FRACTURE TOUGHNESS PLOT  
SPECIMEN 21-3-4W

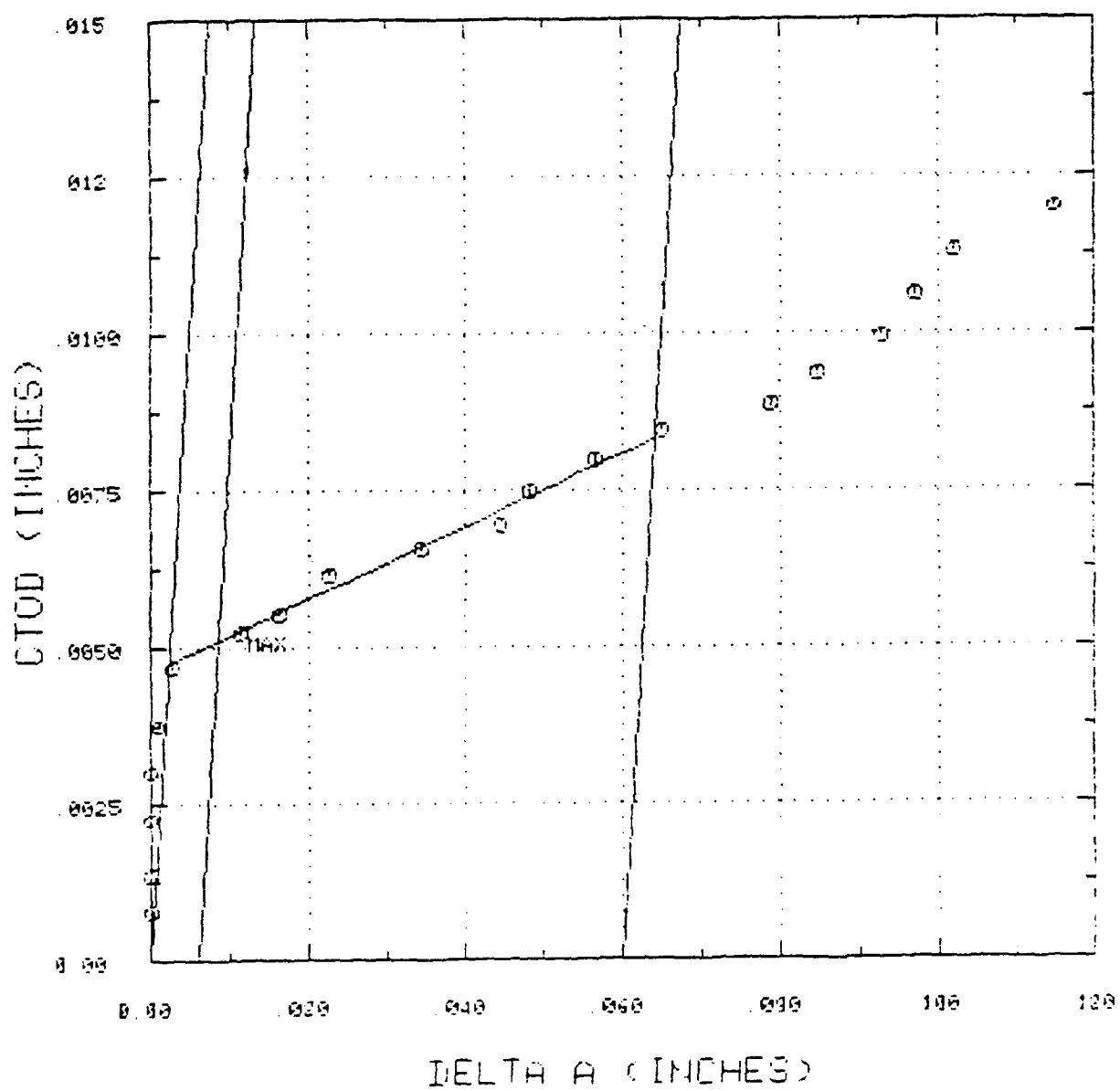


FIGURE 3.4. EXAMPLE OF CTOD RESISTANCE CURVE

1.0 in. = 25.4 mm

Theoretically,  $J$  is equal to the flow stress times CTOD, and the above expression for the blunting line for  $J$  is based on the simple assumption that the apparent crack extension will be one half the CTOD. Again, this analysis works very well for there is a clear break in slope at the initiation of tearing. The point of intersection of the regression line of points between offsets of 0.15 and 1.52 mm (0.006 and 0.06 in.) from the blunting line with the blunting line is designated as the initiation value of CTOD, or  $CTOD_i$ .  $CTOD_i$  for this case was 0.12 mm (0.0048 in.). In the British Standard for CTOD testing, BS 5762 [3.4], there is no definition of  $CTOD_i$ . Rather, to simplify the test and not require compliance crack length measurements, CTOD is taken as the value at maximum load. In Figure 3.4 this point is labelled "max" and has a value of 0.13 mm (.0052 in.). Experience in this type of testing indicates that there is much more scatter in the maximum load value and there is also some thickness and specimen dependence which is not observed for the  $CTOD_i$ . Therefore, the more conservative value of  $CTOD_i$  is recommended.

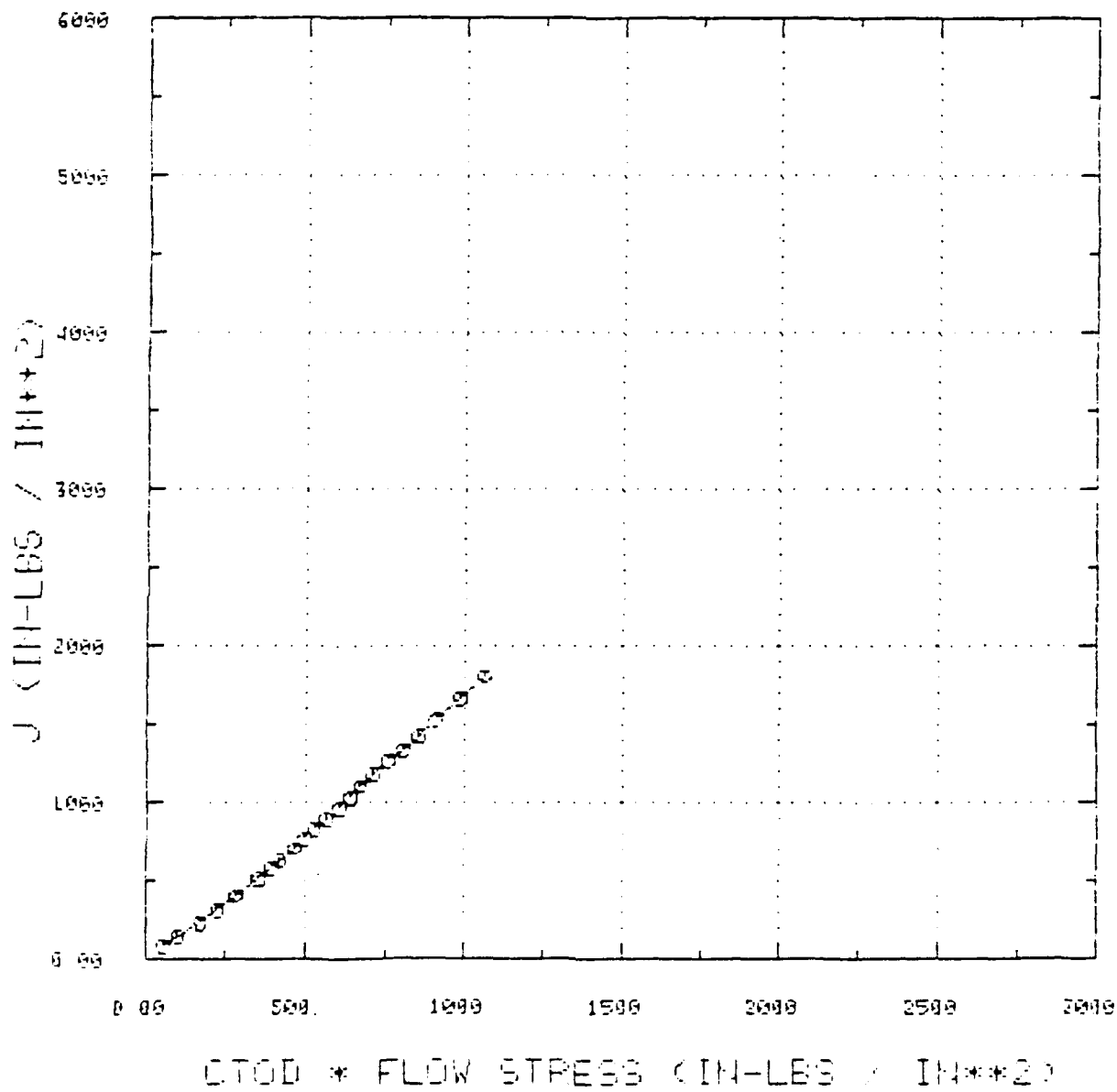
$J$  and CTOD are theoretically related by the expression

$$J = \eta \sigma_f CTOD$$

where  $\eta$  is a factor greater than but nearly equal to 1 and depends on the constraint in the specimen and hardening of the material. Figure 3.5 shows a plot of  $J$  vs CTOD multiplied by flow stress where  $J$  and CTOD were measured independently. From Figure 3.5 it is seen that the value of  $\eta$  is about 1.5 for the 25.4 mm (1 in.) thick specimen. Similar results show  $\eta$  is about 1.7 for the 12.7 mm (1/2 in.) thick specimens.

The bars in Figure 3.6 show  $J_{Ic}$  and are grouped according to the depth of the weld preparation. Figure 3.6 shows the

J(MODIFIED) VS. CTOD\*FLOW STRESS  
SPECIMEN 21-3-4W



$$1.0 \frac{\text{in}-1\text{bs}}{\text{in}^2} = 0.175 \frac{\text{kJ}}{\text{m}^2}$$

FIGURE 3.5 EXAMPLE OF RELATIONSHIP BETWEEN J AND CTOD

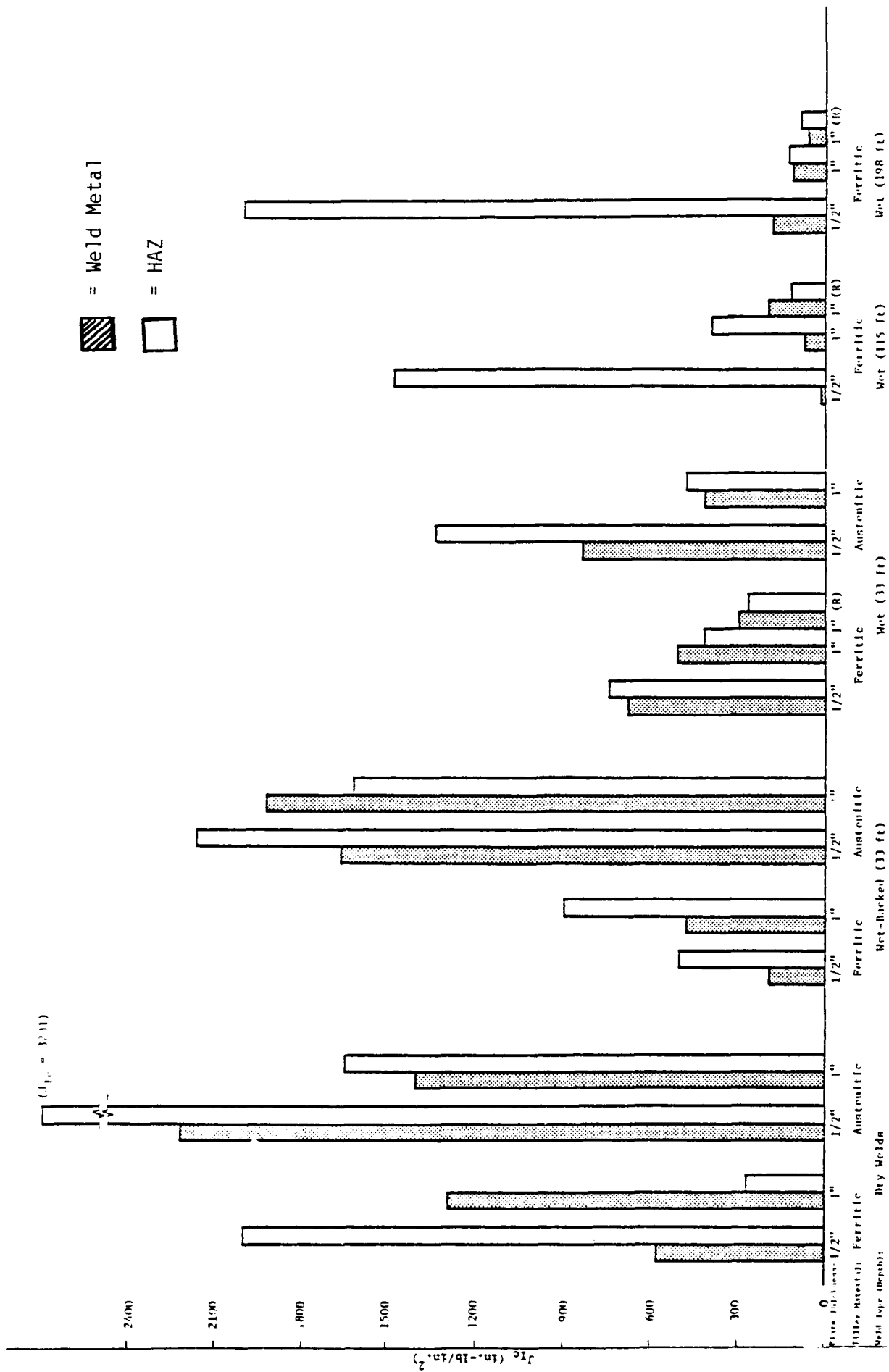


FIGURE 3.6 J<sub>Tc</sub> SHOWN ACCORDING TO WELD TYPE

NOTE:

$$1.0 \frac{\text{in.} - 1\text{b}}{2} = .175 \frac{\text{kJ}}{\text{m}^2}$$

$$\begin{array}{lcl} \frac{1}{2} \text{ in.} & = & 12.7 \text{ mm} \\ 1 \text{ in.} & = & 25.4 \text{ mm} \\ 1.0 \text{ ft} & = & 3048 \text{ mm} \end{array}$$

1/2 in. = 12.7 mm  
1 in. = 25.4 mm

$$\begin{array}{lcl} \frac{1}{2} \text{ in.} & = & 12.7 \text{ mm} \\ 1 \text{ in.} & = & 25.4 \text{ mm} \\ 1.0 \text{ ft} & = & 3048 \text{ mm} \end{array}$$

$$\frac{1}{2} \text{ in.} = 12.7 \text{ mm}$$

relatively high toughness of the wet-backed and dry austenitic welds in both the weld metal and heat-affected zone. The austenitic wet welds at 10 m (33 ft) are not significantly better than their ferritic counterparts.

Restraint does not seem to significantly influence the fracture toughness, although the restrained welds consistently performed slightly worse than the unrestrained equivalent welds in both weld metal and heat-affected zone.

With two significant exceptions 25.4 mm (1 in.) ferritic air weld and 25.4 mm (1 in.) austenitic wet-back weld, the heat-affected zone toughness was generally greater than or about the same as the weld-metal toughness. This may simplify any application of this study to design guidelines.

Figure 3.7 shows the value obtained for  $K_{Ic}$  plotted with the upper shelf Charpy impact energy. Also shown on the figure is the Rolfe-Novak correlation for upper shelf  $K_{Ic}$  and CVN [3.3]:

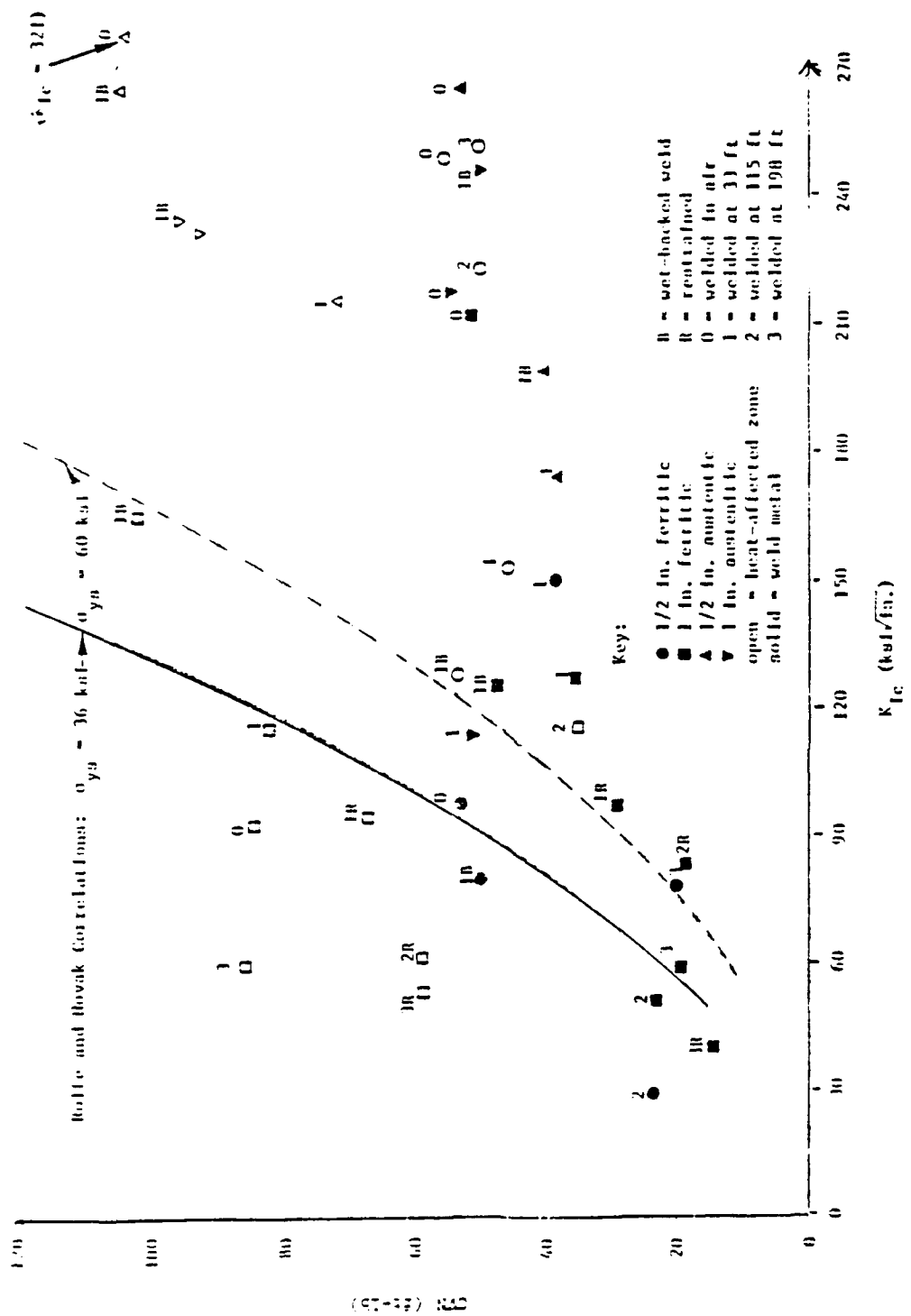
$$\frac{K_{Ic}}{\sigma_{ys}}^2 = \frac{5}{\sigma_{ys}} (CVN - \frac{\sigma_{ys}}{20})$$

Here  $\sigma_{ys}$  is the yield stress in ksi\* and the two lines correspond to  $\sigma_{ys} = 36$  (base-metal yield strength) and  $\sigma_{ys} = 60$  (average yield strength of the weld metals).  $K_{Ic}$  in this relation is in ksi/in. and CVN is the upper shelf Charpy impact energy in ft-lbs.\*

Note that for some HAZ specimens of the 25.4 mm (1 in.) thick ferritic weldments the Rolfe-Novak correlation would yield

---

\*1.0 ksi=6.895 MPa, 1.0 ksi $\sqrt{\text{in.}}$ =1.1 MPa $\sqrt{\text{m}}$ , 1.0 ft-lb=1.356 J



1.0 ksi/in. = 1.1 MPa/in., 1.0 ft-lb = 1.356 J, 1.0 in. = 25.4 mm, 1.0 ft = .3048 m

FIGURE 3.7  $K_{Ic}$  ESTIMATED FROM  $J_{Ic}$  VS UPPER SHELF CHARPY IMPACT ENERGY

unconservative estimates of  $K_{Ic}$ . However, for these 25.4 mm (1 in.) thick ferritic HAZ specimens, the Charpy test did not exhibit upper shelf results at -2°C (28°F), and the  $J_{Ic}$  results could also be "non-upper-shelf". Therefore, the Rolfe-Novak correlation is not applicable to these points. The points with very high  $K_{Ic}$  for which the Rolfe-Novak correlation is overly conservative are for the most part austenitic welds, for which the correlation, which was developed for ferritic materials, is also not applicable. Finally, the one result at 30 J (22 ft-lbs) for which  $K_{Ic}$  is only 33 MPa $\sqrt{m}$  (30 ksi $\sqrt{in.}$ ) is probably a special case. The  $J_{Ic}$  curve for this case exhibited virtually no blunting and was probably in the vicinity of a gross defect. The tearing modulus for this specimen (12-2-1W) was about the same as the tearing modulus for the weld metal specimen at 60 m (198 ft) (13-3-1W). Yet  $K_{Ic}$  for the ferritic weld metal at 60 m (198 ft) was much higher, i.e. 85 MPa $\sqrt{m}$  (77 ksi $\sqrt{in.}$ ). Because the trend is decreasing toughness with increasing depth, one would expect the toughness at 35 m (115 ft) to exceed 85 MPa $\sqrt{m}$  (77 ksi $\sqrt{in.}$ ).

There appears to be less scatter among the weld-metal results than among the heat-affected zone specimens. Therefore, there may be a better correlation for the weld-metal toughness.

$J_{Ic}$  tests indicated great variability in toughness among the welds tested.  $J_{Ic}$  ranged from 4.9 to 565 kJ/m<sup>2</sup> (28 to 3231 in.-lb/in.<sup>2</sup>) and corresponding  $K_{Ic}$  (calculated from  $J_{Ic}$ ) ranged from 33 to 353 MPa $\sqrt{m}$  (30 to 321 ksi $\sqrt{in.}$ ). Austenitic welds were generally tougher than the ferritic welds and the minimum  $K_{Ic}$  was 45 MPa $\sqrt{m}$  (41 ksi $\sqrt{in.}$ ). Excluding the special case discussed above, the minimum  $J_{Ic}$  was 9.5 kJ/m<sup>2</sup> (54 in-lb/in<sup>2</sup>). The HAZ toughness was generally greater than the weld metal toughness. Toughness seemed to decrease with depth, with the exception of the 12.7 mm (1/2 in.) ferritic HAZ specimens.

### 3.2.9 Chemical Analyses

Chemical analysis was performed on both thicknesses of the base metals, a sample of the ferritic weld metal made at 60 m (198 ft), and a sample of the austenitic weld metal made in a wet-backed weld. At the time, it wasn't realized that the weld metals chemistry might change with depth. In retrospect, it would better to have samples of the weld metal from all depths, dry, and wet-backed welds.

Table 3.3 shows the results of these chemical analyses. Note the particularly low manganese in the ferritic weld at 60 m (198 ft). This percentage is probably much lower than would be obtained in a dry weld and is consistent with the results of Ibarra and Olson discussed in Section 2.

TABLE 3.3

CHEMICAL ANALYSIS  
(percent by weight)

Plate Sample	C	MN	Si	P	S	Ni	Cr	Mo	Cu	V	CE
(13) 1/2 in. A-36 (12.7 mm)	.17	.87	.26	.014	.016	.01*	.01*	.01*	.01	.01*	.32
(26) 1 in. A-36 (25.4 mm)	.14	.86	.23	.033	.023	.09	.02	.01*	.04	.01	.30
(23) E6013 welded at 198 ft (60 m)	.09	.32	.22	.020	.010	.02	.01*	.01*	.01	.01	
(31) 1/2 in. A-516 (12.7 mm)	.22	1.04	.20	.018	.015	.01*	.02	.01*	.01	.01*	.40
(41B) 1 in. A-516 (25.4 mm)	.22	1.07	.21	.024	.011	.01	.02	.01*	.01	.01*	.41
(41B) Austenitic Wet-Backed	.05	2.03	.34	.008	.012	62.72	12.52	5.61	.02		

\*Less than or equal to

3.3      References

- 3.1.    Landes, J.D., and Begley, J.A., "Recent Development in  $J_{Ic}$  Testing," Development in Fracture Mechanics Test Methods Standardization, ASTM STP 632, 1977, pp. 57-81.
- 3.2.    Landes, J.D., and Begley, J.A., in Fracture Analysis, ASTM STP 560, 1974, pp. 170-186.
- 3.3.    Rolfe, S.T., and Novak, S.R., "Slow-Bend  $K_{Ic}$  Testing of Medium Strength High-Toughness Steels," ASTM STP 463, 1970, pp. 124-159.
- 3.4.    British Standards Institute BS5762 "Methods for Crack Opening Displacement (COD) Testing".

## 4.0 STATISTICAL ANALYSIS OF TEST DATA

### 4.1.1 Decomposition of The Test Matrix

Statistical analysis was performed for the overall test matrix shown in Figure 4.1 which identifies the test welds from which specimens for bend tests, transverse weld tension tests, Charpy impact tests, hardness traverse, and  $J_{Ic}$  fracture toughness tests have been taken. Not shown in this test matrix are the fillet weld tests and all-weld-metal tension tests, which are analyzed separately.

The test matrix can be considered in total and as the combination of three separate subgroups within which some of the test variables are removed. These subgroups are shown in Figure 4.2.

The Restraint Subgroup allows a one-to-one comparison of 25.4 mm (1 in.) A36 base plate welded with and without restraint of the plates during welding and cooling. Since restraint can cause cracking from the shrinkage strains, it is of interest to see if this restraint influences the test results as well. Since this subgroup includes only one plate thickness and one base metal filler metal combination, conclusions based on analysis of this subgroup are limited to these conditions.

The two variations of the Wet Ferritic Subgroup contain only wet ferritic welds. The first variation (named Wet Ferritic A) is a balanced matrix and includes only those welds prepared without restraint. The second variation (named Wet Ferritic B) includes the restraint welds. Based on analysis of the Restraint Subgroup the restraint variable could not be shown to have a

A36 Base Plate 0.36CE  
E6013 Ferritic Filler

A516 Gr. 70 Base Plate 0.46CE  
Austenitic Filler

Depth Weld-Type	Restrained 1 in. (25.4 mm)	A36 Plate 1 in. (25.4 mm)	A36 Plate 1/2 in. (12.7 mm)	A516 Plate 1 in. (25.4 mm)	A516 Plate 1/2 in. (12.7 mm)
198 ft Wet (60 m)	23R	23	13		
115 ft Wet (35 m)	22R	22	12		
33 ft Wet (10 m)	21R	21	11	41	31
33 ft Wet-Backed (10 m)		21B	11B	41B	31B
Dry		20	10	40	30

First Digit: 1 = 12.7 mm (1/2 in. A36), 2 = 25.4 mm (1 in.)  
3 = 12.7 mm (1/2 in.) A516, 4 = 25.4 mm (1 in.) A516

Second Digit: 0 = Dry weld, 1 = 10 m (33 ft), 2 = 35 m (115 ft),  
3 = 60 m (198 ft)

Letters: B = Wet Backed, R = Restrained

FIGURE 4.1 TOTAL TEST MATRIX OF GROOVE WELDS

A36 Base Plate 0.36CE E6013 Ferritic Filler	
* Restrained 1 in. A36 Plate	1 in. A36 Plate
23R 193 ft)	21
22R 115 ft)	22
21R 33 ft)	

Restraint Subgroup

A36 Base Plate 0.36CE  
A516 Gr. 70

66

A36 Base Plate 0.36CE E6013 Ferritic Filler	
*1 in. A36 Plate	1/2 in. A36 Plate
23R	23
22R	22
21R	21

Wet Ferritic Subgroup A

A36 Base Plate 0.36CE  
E6013 Ferritic Filler

*1 in. A36 Plate	1/2 in. A36 Plate
23R	23
22R	22
21R	21

\*1.0 in.=25.4 mm

A36 Base Plate 0.36CE A516 Gr. 70	
*1 in. 36 Plate	1/2 in. A36 Plate
21	11
21B	11B
20	10

Weld-Type Subgroup

10 m wet  
(33 ft)  
10 m Wet Backed  
(33 ft)  
dry

FIGURE 4.2 SUBGROUPS WITHIN TOTAL TEST MATRIX

significant effect on test results. Therefore, the restrained welds were included in the Wet Ferritic B Subgroup to strengthen the statistical significance of conclusions about the wet ferritic welds. Subgroup B is unbalanced, i.e., there were a greater number of tests on 25.4 mm (1 in.) plate than 12.7 mm (1/2 in.) plate. These subgroups should provide information on how depth and thickness affect the test results, unperturbed by other weld types (e.g., wet-backed and dry) and by other materials.

The Weld Type Subgroup was assembled to study the effects of weld type (i.e., dry welds, wet-backed, and wet welds) and includes both ferritic and austenitic welds. This is also a balanced subgroup.

Finally, the test data can be examined for the total test matrix of Figure 4.1, which is very unbalanced. It is dominated by ferritic welds and contains more 25.4 mm (1 in.) welds than 12.7 mm (1/2 in.) welds. The usefulness of the total test matrix is mainly to examine how conclusions reached for a particular subgroup apply to the data as a whole.

#### 4.2 Grouping and Analysis of Variance

The test results were analyzed by separating them into categories defined by one or two grouping variables (such as depth or thickness) and comparing the means and variances among the groups. Histograms were constructed for each category. All test variables were compared for each grouping variable and for every combination of two grouping variables. This was done among each of the three subgroups and for the total test matrix. The results of these analyses are presented in detail in Appendix B.

#### 4.3 Results of Regression Analysis

#### 4.3.1 $K_{Ic}$

Regression analyses were performed for variables which may be significant in terms of structural performance, i.e.,  $K_{Ic}$ ,  $J_{Ic}$ , Charpy impact energy (CVN), and the bend test score. Hardness would have been included if it could have correlated with  $K_{Ic}$  or Bendscore, but the correlation coefficient to  $K_{Ic}$  was less than 0.1 and the correlation coefficient to Bendscore was only .234, therefore hardness could not be considered as significant in terms of structural performance.

Rolfe and Novak have suggested the following correlation for mild steel when  $K_{Ic}$  and CVN are "upper-shelf":

$$\frac{K_{Ic}}{\sigma_{ys}}^2 = \frac{5}{\sigma_{ys}} (CVN - \frac{\sigma_{ys}}{20})$$

where

$K_{Ic}$  = fracture toughness ( $\text{ksi}/\sqrt{\text{in.}}$ )\*

$\sigma_{ys}$  = yield stress ( $\text{ksi}$ )\*

CVN = Charpy impact energy ( $\text{ft-lbs}$ )\*

---

\*Throughout this chapter, correlations are stated for the variables in English units because the application of these data in the marine industry mainly uses English units. The SI version of correlations (not shown to avoid confusion) can be obtained by the appropriate conversion factors, e.g.

$$1.0 \text{ ksi in.} = 1.1 \text{ MPa}\sqrt{\text{m}}$$

$$1.0 \text{ ft-lb} = 1.356 \text{ J}$$

$$1.0 \text{ ksi} = 6.895 \text{ MPa.}$$

This correlation can be stated as:

$$K_{Ic}^2 = b_0 + b_1 CVN$$

Recall that  $J_{Ic} \propto K_{Ic}^2/E$ . The Rolfe Novak correlation then amounts to a linear relationship between  $J_{Ic}$  and CVN. However, attempts to correlate  $J_{Ic}$  with CVN and other variables were never much better than the correlations of  $K_{Ic}$  with CVN and other variables. For example, within the Wet Ferritic Subgroup the correlation coefficient of  $J_{Ic}$  to CVN is .726, and the correlation coefficient to  $K_{Ic}$  to CVN is .723. For all data in the whole test matrix, the correlation of  $K_{Ic}$  to CVN is even better, .795. Since  $K_{Ic}$  is more easily applied in a fracture mechanics analysis,  $J_{Ic}$  was dropped and an attempt to find a linear relation between  $K_{Ic}$  and CVN and other variables was continued.

The following relations were obtained for regression of  $K_{Ic}$  on different single variables. The correlation coefficient between the variables is shown in parentheses.

- (a)  $K_{Ic} = 3.19(CVN) + 17.2$  (.723)
- (b)  $K_{Ic} = -135(THICKNESS) + 213$  (-.54)
- (c)  $K_{Ic} = 45(ZONE) + 79$  (.383)
- (d)  $K_{Ic} = -.196(DEPTH) + 124$  (-.225)

where

$K_{Ic}$  = fracture toughness  $\text{ksi}\sqrt{\text{in.}}$  [1.0  $\text{ksi}\sqrt{\text{in.}}$  = 1.1  $\text{MPa}\sqrt{\text{m}}$ ]

CVN = Charpy energy ft-lbs [1.0 ft-lb = 1.356 J]

THICKNESS = base plate thickness (in.) [1.0 in. = 25.4 mm]

ZONE = 0 for weld metal, 1 for HAZ

DEPTH = depth of weld (ft) [1.0 ft = 0.3048 m]

Relationship (b) shows that  $K_{Ic}$  decreases with thickness. The Charpy energy also decreases with thickness,

however, and among regressions with two or more variables (which included CVN), thickness was never a part of the relations, indicating that the thickness effect was taken into account in the value of CVN. (For example,  $K_{Ic}$  and CVN share the same thickness/-zone interaction.) This also shows the thickness independence of  $J_{Ic}$ , i.e. the Charpy specimen shows the same relative change as the  $J_{Ic}$  specimen, therefore the thickness effect is real and cannot be attributed to the difference in constraint.

Relationship (c) shows the increase in  $K_{Ic}$  for HAZ as opposed to weld metal. This increase is shown in all subsequent relations and leads to the conclusion that weld metal toughness tests conservatively estimate the toughness for a crack anywhere in the weld or HAZ.

Relationship (d) shows the general decrease in  $K_{Ic}$  with depth. Depth was also not present in any relations with CVN and other variables, indicating the depth effect is well represented by CVN. The following relation was considered optimum (i.e., improvement by adding more variables was minimal) for the Wet Ferritic Subgroup:

$$(e) \quad K_{Ic} = 2.78 \text{ CVN} + 35.13 \text{ ZONE} + 19.4$$

The square of the multiple correlation coefficient ( $R^2$ ) for this expression is .670, compared to .522 for CVN alone. Note that the coefficients for CVN and ZONE are close to the coefficients in the individual relations (a) and (c).

Figure 4.3 shows a plot of  $K_{Ic}$  versus CVN, the numbers on the plot indicate the number of data points at that location. The three outlying and unconservative points between 47 and 61 J (35 and 45 ft-lbs) and between 38.5 and 77 MPa $\sqrt{\text{m}}$  (35 and 70 ksi $\sqrt{\text{in.}}$ )

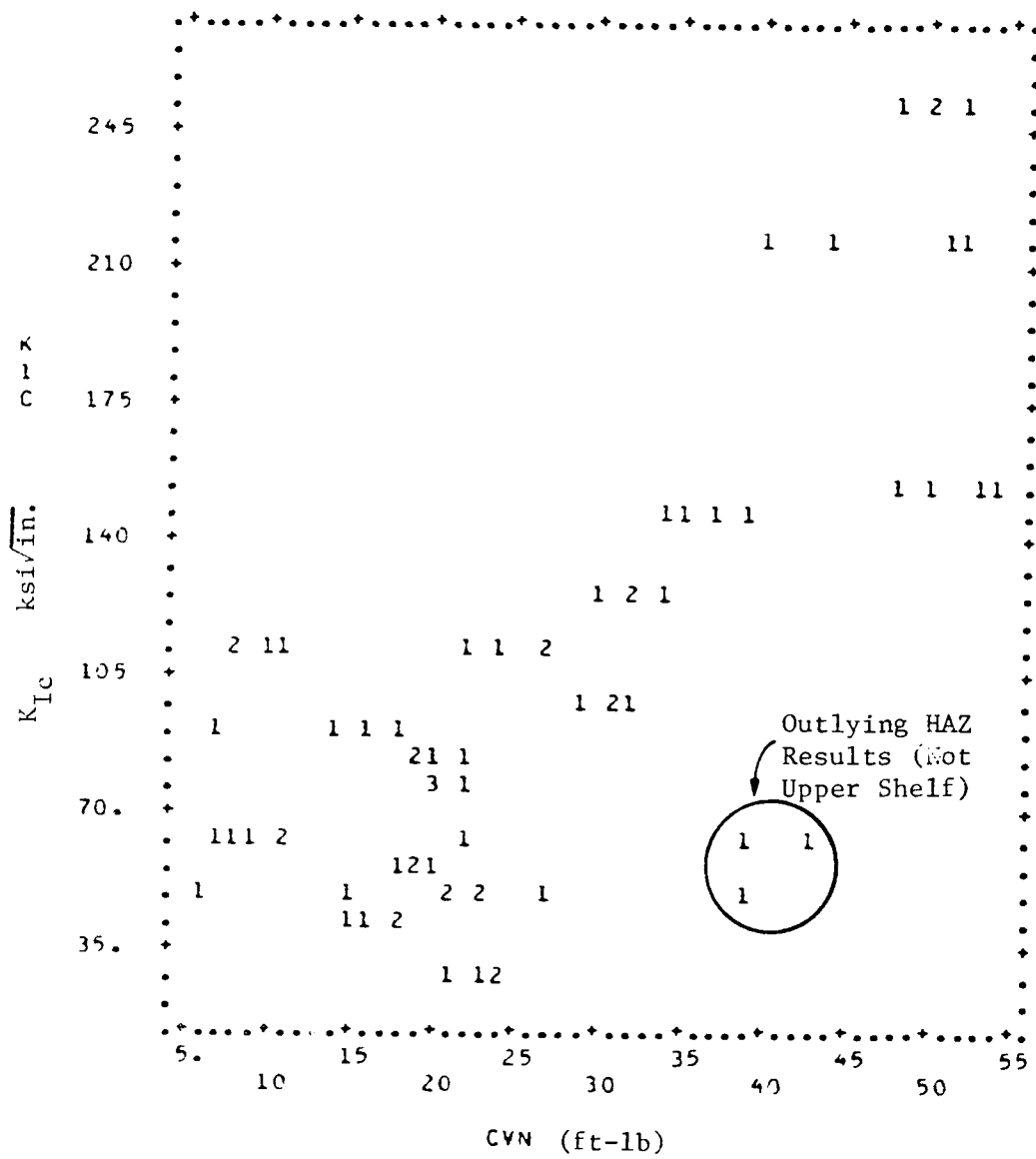


FIGURE 4.3. DISPLAY OF  $K_{Ic}$  VS CVN FOR WET-FERRITIC SUBGROUP OF UNDERWATER WELDS

$$1.0 \text{ ksi}\sqrt{\text{in.}} = 1.1 \text{ MPa}\sqrt{\text{m}}$$

$$1.0 \text{ ft-lb} = 1.356 \text{ J}$$

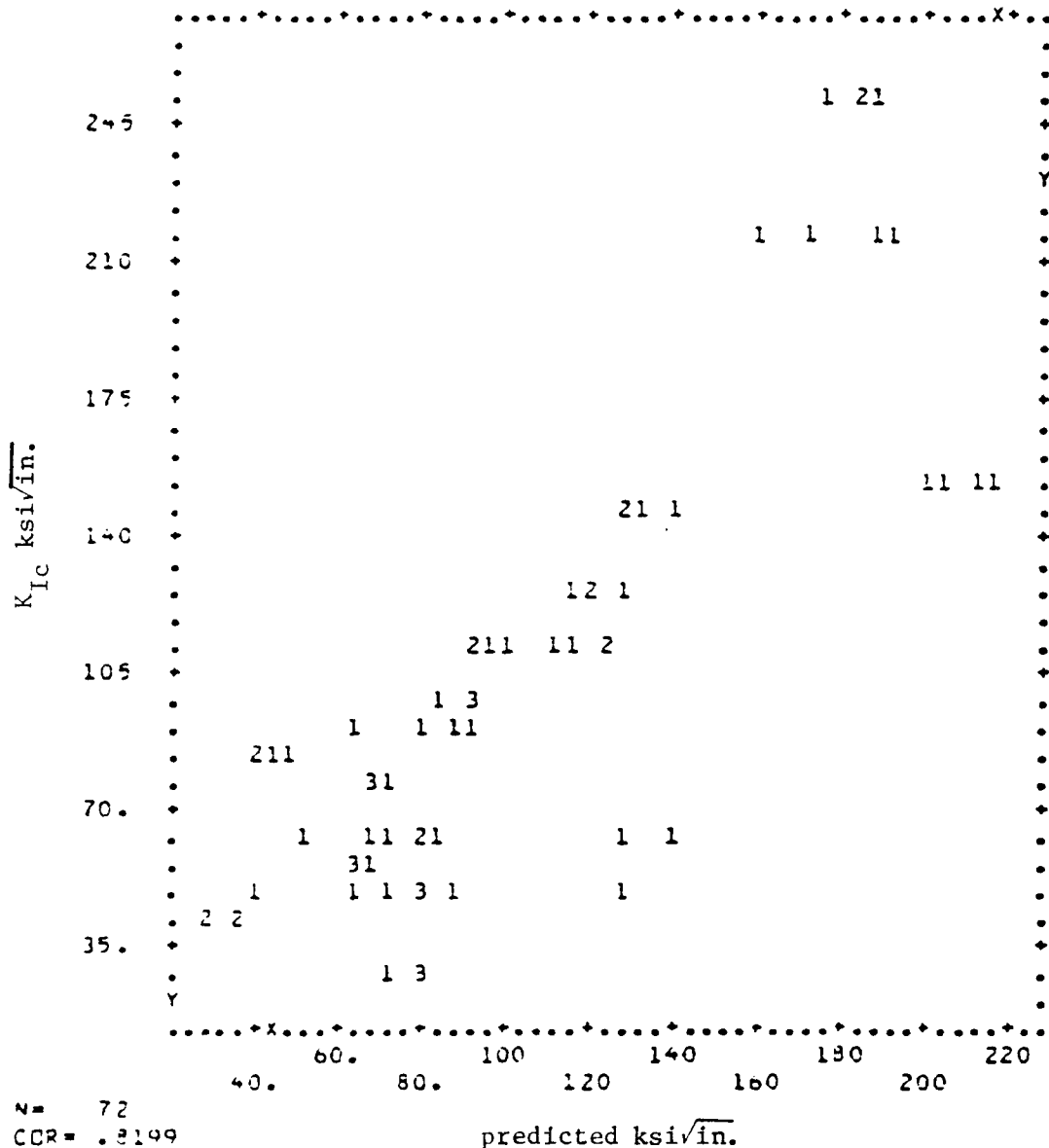
are HAZ results. The HAZ Charpy results were not upper shelf but rather are in the temperature transition region. Because the transition is sensitive to strain-rate, the results cannot be expected to correlate well without a temperature shift. Figure 4.4 shows a plot of  $K_{Ic}$  versus the predicted  $K_{Ic}$  by the above relationship.

The relationship retained an  $R^2$  of .657 when applied to all data, but weld metal/base metal and WETORDRY or DEPTH proved to be significant as well and improved the relationship. WETORDRY (which is equal to 0 for dry welds, 1 for wet-backed welds, and 2 for wet welds at any depth) gave better correlations than depth. Interestingly, it was noted in looking at histograms of the data in groups like Figure 4.5, that the value of many test variables (like  $K_{Ic}$  in Figure 4.5) for wet-backed welds was just between that for dry and wet welds at 10 m (33 ft). Assigning a depth of 4.9 m (16 ft), for the wet-backed welds prepared at 10 m (33 ft) improved the correlation using depth and gave better results than the correlation using WETORDRY.

The strong correlation of  $K_{Ic}$  to CVN is helpful and may be useful in estimating  $K_{Ic}$  from the economical Charpy test. It is informative, however, to look at the regression of  $K_{Ic}$  on grouping variables alone, i.e., exclusive of CVN. The following relation (with an  $R^2$  of .61) was obtained using a depth of 4.9m (16 ft) for the wet-backed welds:

$$(f) \quad K_{Ic} = 75.1(A) - 94.2(THICK) - .321(DEPTH) + 33.9(ZONE) + 201$$

where A = 0 for ferritic welds and A36 base plate  
= 1 for austenitic welds and A516 base plate



	MEAN	ST.DEV.	REGRESSION LINE	RES.S.
X	101.50	46.457	$x = .67223 \times + 33.269$	780.63
Y	101.50	59.101	$y = 1.0000 \times - 146.13$	1161.3

FIGURE 4.4. REGRESSION ANALYSIS:  $K_{Ic}$  VS  $K_{Ic}$  PREDICTED BY  
 RELATION ( $\epsilon$ ) AS A FUNCTION OF CVN AND ZONE  
 FOR UNDERWATER WELDS IN WET FERRITIC SUBGROUP  
 $1.0 \text{ ksi}\sqrt{\text{in.}} \approx 1.1 \text{ MPa}\sqrt{\text{m}}$

HISTOGRAM IF  $K_{Ic}$  (Refer to Appendix B for explanation  
OF TERMS)

CASES DIVIDED INTO GROUPS BASED ON VALUES OF METORDY.

METRACK MFT

MOPHILLS DRY

MOPHILLS MET

MOPHILLS MFT

MOPHILLS DRY

MOPHILLS MET

74

ALL GROUP MEANS ARE DENOTED BY "M'S IF THEY COINCIDE WITH "M'S. "M'S OTHERWISE

	MEAN	214.000	SUM OF SQUARES	184.750	F VALUE	144.250
STDEV.		71.495		67.253		31.513
R.F.S.D.		70.677		74.051		32.136
S.E.M.		25.557		24.025		11.142
MAXIMUM		121.000		263.000		208.000
MINIMUM		93.000		81.000		115.000
SAMPLE SIZE		8		8		8

ALL GROUPS COMBINED

EXCEPT CASES WITH UNUSED VALUES FOR METORDY

MEAN 161.000

STDEV. 64.431

R.F.S.D. 72.015

S.E.M. 13.152

MAXIMUM 171.000

MINIMUM 61.000

SAMPLE SIZE 24

TOTAL 954.60.0000

LVEEN'S TEST FOR EQUAL VARIANCES

DNF - DAY ANALYSIS OF VARIANCE

TEST STATISTICS FOR WITHIN-GROUP

VARIANCES NOT ASSUMED TO BE EQUAL

MELCH

RIGDON-FORSYTHE

$K_{Ic}$  is shown in  $\text{ksiv/in.}$

$1.0 \text{ ksiv/in.} = 1.1 \text{ MPa}\sqrt{\text{m}}$

FIGURE 4.5. HISTOGRAMS OF  $K_{Ic}$  GROUPED BY WELD TYPE FOR WELD TYPE SUBGROUP OF UNDERWATER WELDS

or, including restraint, a slightly better relation ( $R^2 = .62$ ) is obtained:

$$(g) K_{Ic} = 71.9(A) - 81.8(THICK) - .291(DEPTH) + 33.8(ZONE) - 26.0(RESTRAIN) + 195$$

where RESTRAIN = 0 for no restraint  
= 1 for welded with restraint.

Figure 4.6 shows  $K_{Ic}$  versus predicted  $K_{Ic}$  for the above relation.

The best relation including CVN is as follows:

$$(h) K_{Ic} = 1.80(CVN) + 9.63(ZONE) - 30.1(RESTRAIN) + 24.9(A) - .152(DEPTH) + 74.7.$$

The squared multiple correlation coefficient ( $R^2$ ) for this expression was .686, which is not that much greater than the  $R^2$  obtained for Relations (f) or (g) using grouping variables alone. Note that the coefficients for CVN and RESTRAIN have retained their approximate magnitude, compared to the regression coefficients obtained for the Wet Ferritic Subgroup, while the coefficient for ZONE has been reduced but is still positive. Figure 4.7 shows  $K_{Ic}$  versus CVN for all data, and Figure 4.8 shows  $K_{Ic}$  versus  $K_{Ic}$  predicted with the above relationship. A and DEPTH had stronger correlations to  $K_{Ic}$  than ZONE or RESTRAIN. In fact, the following expression had  $R^2$  of .667:

$$(i) K_{Ic} = 2.02(CVN) + 23(A) - .173(DEPTH) + 67.2$$

The coefficient for A implies a bonus of  $25 \text{ MPa} \sqrt{\text{m}}$  ( $23 \text{ ksi}\sqrt{\text{in.}}$ ) as the weld metal changes from ferritic to austenitic. This is important because it implies the results obtained for the

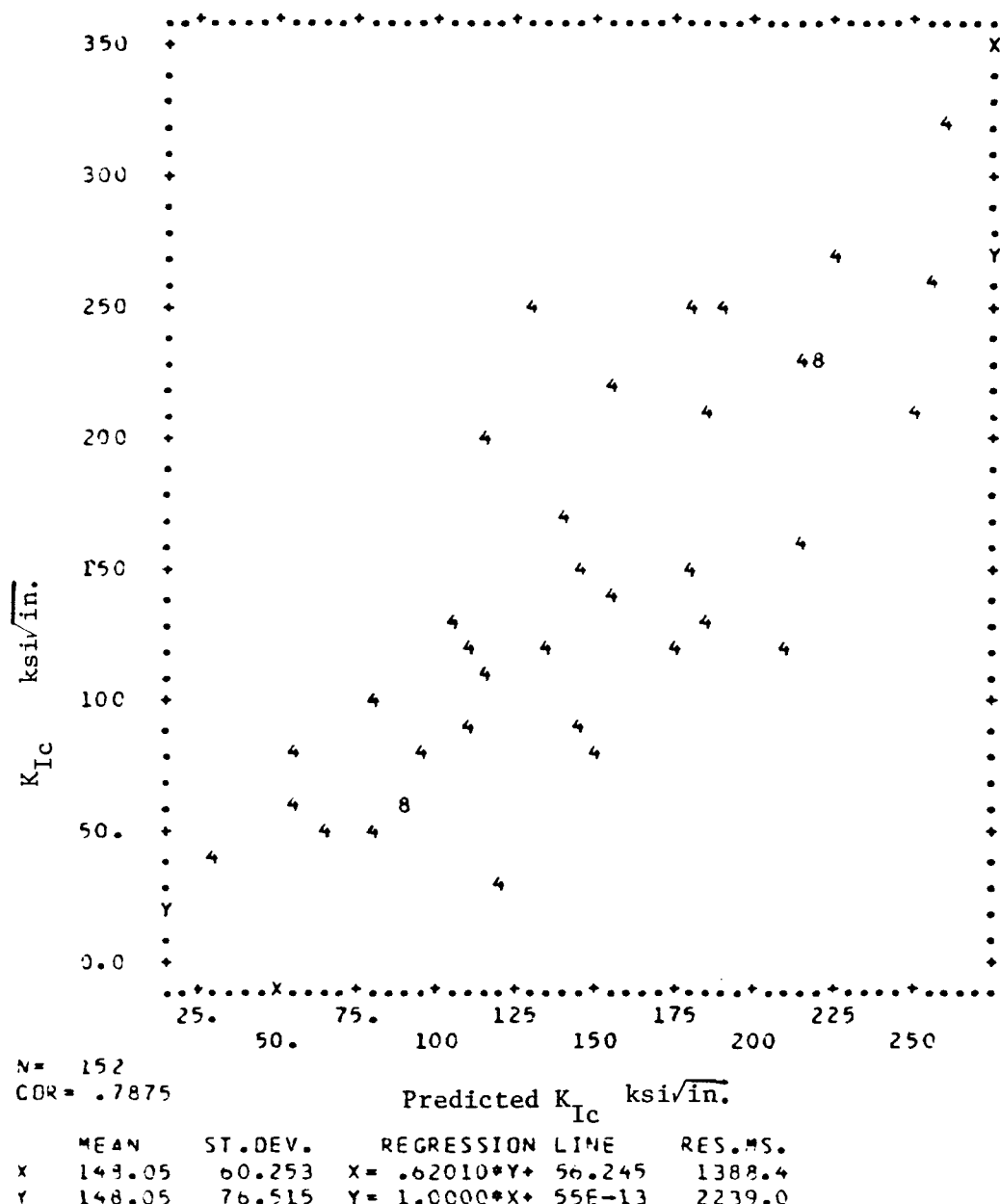


FIGURE 4.6. RESULTS OF REGRESSION ANALYSIS: K<sub>Ic</sub> VS PREDICTED BY RELATION (g) AS A FUNCTION OF MATERIAL, THICKNESS, DEPTH, ZONE, AND RESTRAINT FOR ALL TEST DATA ON UNDERWATER WELDS

$$1.0 \text{ ksi}\sqrt{\text{in.}} = 1.1 \text{ MPa}\sqrt{\text{m}}$$

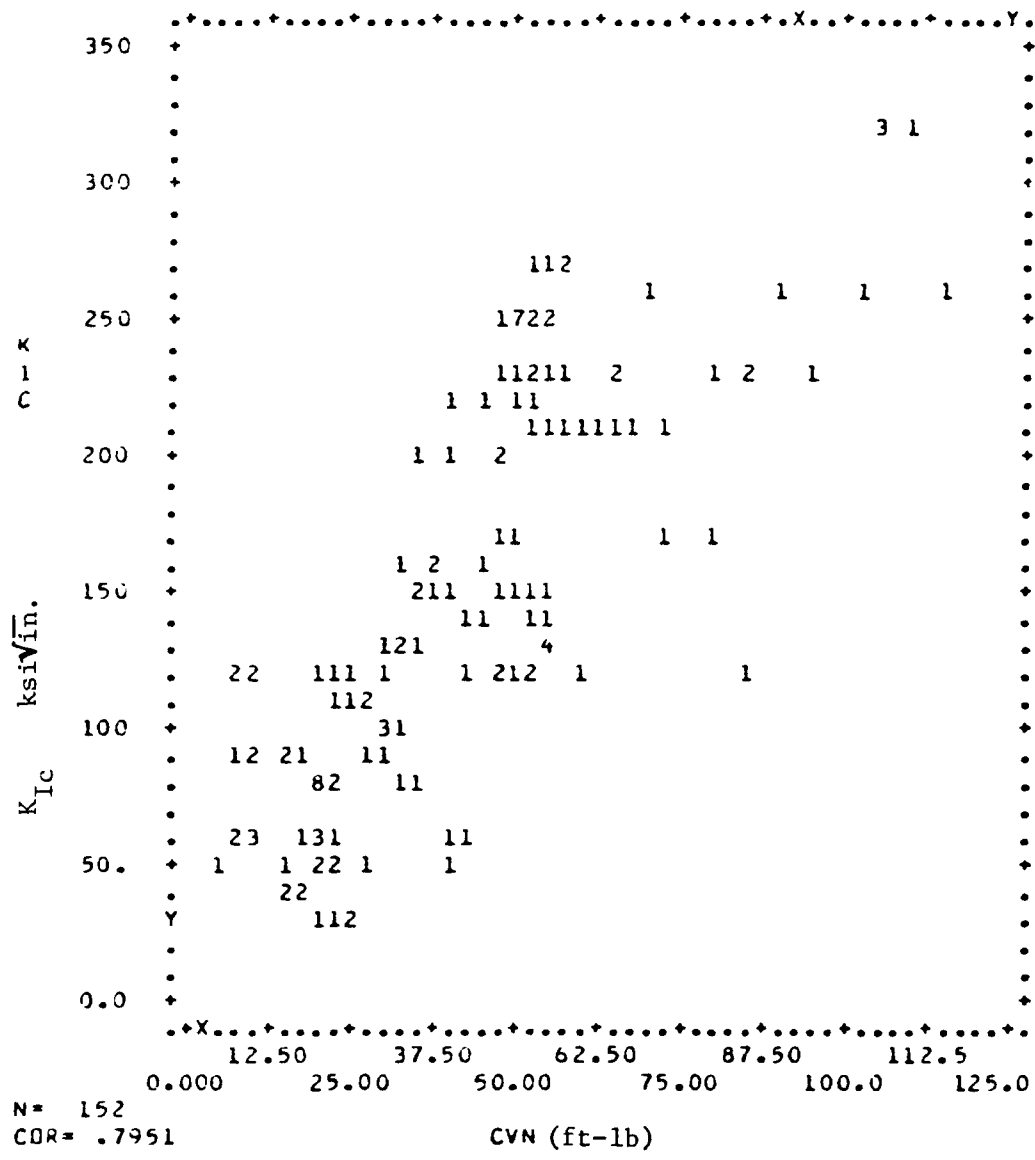
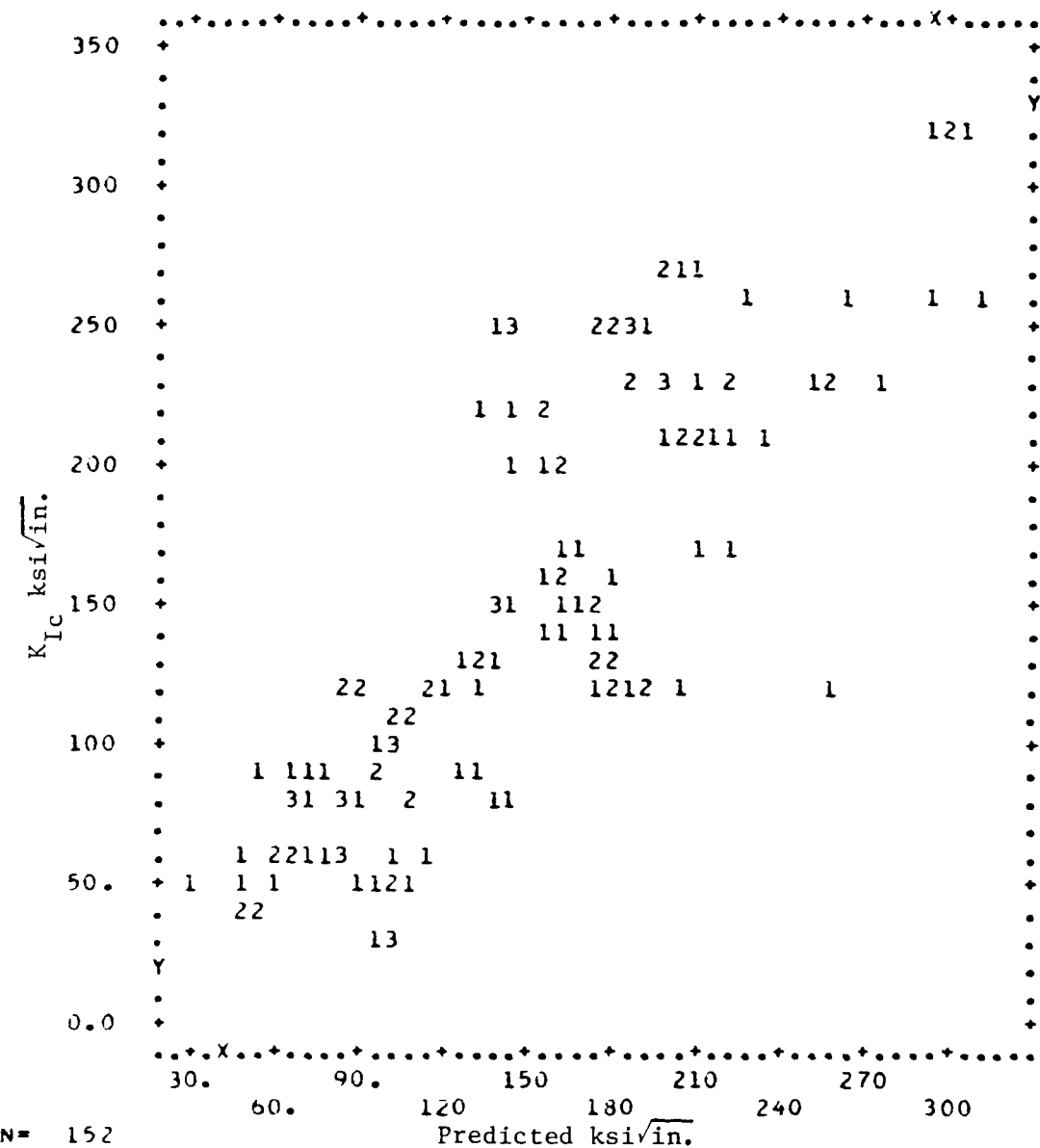


FIGURE 4.7. DISPLAY OF  $K_{Ic}$  VS CVN FOR ALL TEST DATA ON UNDERWATER WELDS

1.0  $\text{ksi}\sqrt{\text{in.}}$  = 1.1 MPa $\sqrt{\text{m}}$ , 1.0 ft-lb = 1.356 J



	MEAN	ST.DEV.	REGRESSION LINE	RES.MS.
X	148.05	3.229	$X = .68287Y + 45.952$	1276.3
Y	148.05	76.515	$Y = 1.0000X + 91E-14$	1862.0

FIGURE 4.8. RESULTS OF REGRESSION ANALYSIS:  $K_{Ic}$  VS  
 $K_{Ic}$  PREDICTED BY RELATION (h) WHICH  
INCLUDES CVN AS WELL AS MATERIAL, DEPTH,  
ZONE, AND RESTRAINT FOR ALL TEST DATA ON  
UNDERWATER WELDS

$$1.0 \text{ ksi} \sqrt{\text{in.}} = 1.1 \text{ MPa} \sqrt{\text{m}}$$

ferritic welds are conservative if applied to austenitic welds as well. Figure 4.9 shows histograms for  $K_{Ic}$  grouped by A. (Refer to Appendix B for definition the terms in Figure 4.9). The mean  $K_{Ic}$  for ferritic welds is  $158 \text{ MPa}\sqrt{\text{m}}$  ( $144 \text{ ksi}\sqrt{\text{in.}}$ ) and for austenitic welds is  $238 \text{ MPa}\sqrt{\text{m}}$  ( $217 \text{ ksi}\sqrt{\text{in.}}$ ), and the minimum is 89 and 126  $\text{MPa}\sqrt{\text{m}}$  (81 and 115  $\text{ksi}\sqrt{\text{in.}}$  for ferritic and austenitic welds, respectively.

The residual mean square, i.e., the sum of the squares of the predicted minus actual  $K_{Ic}$  for the above relation is 1907 in English units. For confidence of 95%, the one-sided value of  $t$  is 1.65. To bound the regression estimate on the intercept only, we should subtract  $79 \text{ MPa}\sqrt{\text{m}}$  ( $1.65\sqrt{1907}=72 \text{ ksi}\sqrt{\text{in.}}$ ) from the regression relationship. This is doubly conservative, owing to the conservative estimate of  $K_{Ic}$  derived from  $J_{Ic}$ . Further, the weld can be assumed to be ferritic since the austenitic welds performed better. The bonus for being in the HAZ can likewise be ignored. Taking all these factors and the confidence limit into account, the following simple conservative relationship is offered:

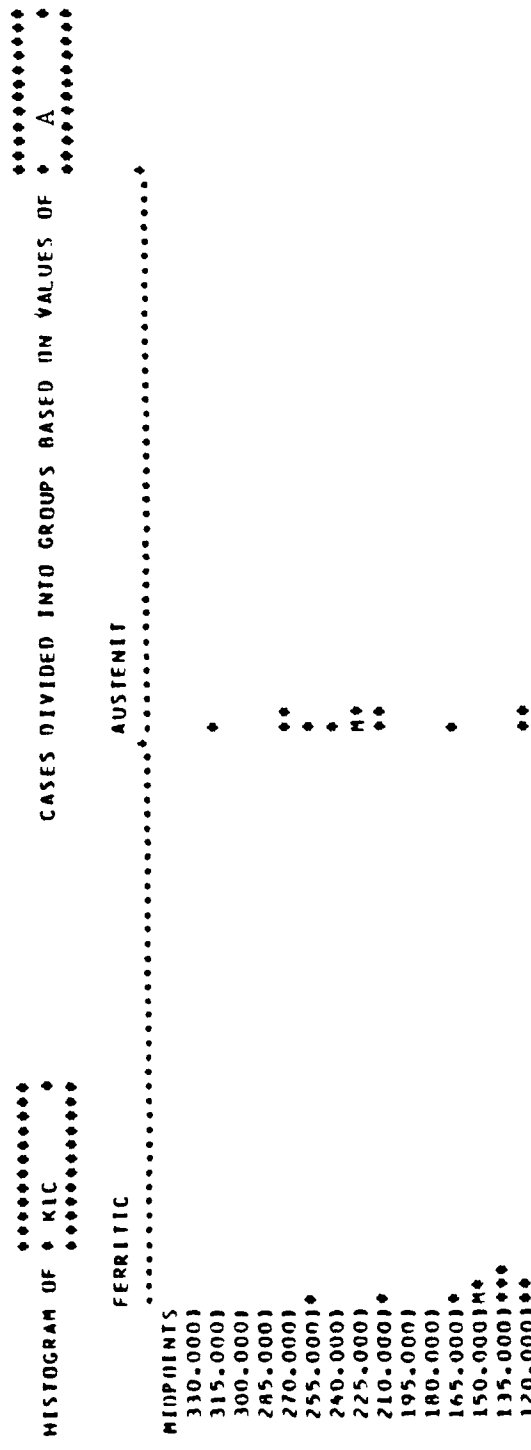
$$(j) \quad K_{Ic} = 2(CVN) - .15(DEPTH) - 8$$

where depth for a wet-backed weld is equal to half the acutal depth.

#### 4.3.2 CVN

Charpy impact energy in itself is useful only as an indicator of material quality; but because of the correlation to  $K_{Ic}$ , it is interesting to look at the regression of CVN on the grouping variables, and compare this to Relations (f) and (g) in the previous section.

WELD-TYPE SUBGROUP



GROUP MEANS ARE DENOTED BY \*'S IF THEY COINCIDE WITH \*\*'S, #'S OTHERWISE

80

ALL GROUPS COMBINED		ANALYSIS OF VARIANCE TABLE				
(EXCEPT CASES WITH UNUSED VALUES FOR CE)		SOURCE	SUM OF SQUARES	DF	MEAN SQUARE	F VALUE
M.FAN	144.333	BETWEEN GROUPS	32266.6667	1	32266.6667	11.23
STD.DEV.	46.775	WITHIN GROUPS	63213.3333	22	2873.3333	.0029
R.F.S.D.	44.362	TOTAL	95480.0000	23		
S.E.M.	13.503	LEVENE'S TEST FOR EQUAL VARIANCES	1.	22	.59	.4519
MAXIMUM	251.000	TEST STATISTICS FOR WITHIN-GROUP				
MINIMUM	81.000	VARIANCES NOT ASSUMED TO BE EQUAL				
SAMPLE SIZE	12	WELCH	1.	21	11.23	.0030
		BROWN-FORSYTHE	1.	21	11.23	.0030

FIGURE 4.9. HISTOGRAMS OF  $K_{IC}$  GROUPED BY MATERIAL COMBINATION FOR ALL DATA IN WELD TYPE SUBGROUP

$K_{IC}$  shown in  $\text{ksiv}_{\text{in}}$ :  $1.0 \text{ ksiv}_{\text{in}} = 1.1 \text{ MPa}\sqrt{\text{m}}$

The following relation is considered optimum and gave an  $R^2$  of .642:

$$CVN = 26.5(A) + 13.5(ZONE) - 25.7(THICK) - .0804(DEPTH) + 51.7$$

This relation contains the same variables and the coefficients have the same sign as Relation (f).

#### 4.3.3 Bendscore

Attempts to correlate bendscore with grouping variables for all data were not very successful. The following relations were obtained:

(a)  $BENDSCORE = -.275(DEPTH) - 9.62(A) + 151$   
 $(R^2 = .31)$

(b)  $BENDSCORE = -.247(DEPTH) + 76.2$   
 $(R^2 = .29)$

Both relationships show the decrease of ductility with increasing depth, and Relation (a) shows that the ferritic welds were generally more ductile than austenitic welds.

If the correlation to all-weld-metal tensile test results were included, excellent relations (valid only for wet ferritic welds) were obtained:

(c)  $BENDSCORE = 3.13(AWMPL) - 128.3$   
 $(R^2 = .90)$

(d)  $BENDSCORE = 3.55(AWMSU) - 197.7$   
 $(R^2 = .86)$

where: AWMPL = all-weld-metal proportional limit in ksi

[1.0 ksi = 6.895 MPa]

AWMSU = all-weld-metal ultimate strength in ksi

[1.0 ksi = 6.895 MPa]

The excellent multiple correlation coefficient ( $R^2$ ) shows how dependent the Bendscore is on the weld metal tensile properties.

#### 4.3.4 All-Weld-Metal Test Results

The all weld metal tensile test results can be related to depth, and the following relationships were obtained.

$$(a) \quad \text{AWMPL} = 70.4 - .104(\text{DEPTH}) \\ (\text{R}^2 = .965)$$

$$(b) \quad \text{AWMSU} = 81.4 - .088(\text{DEPTH}) \\ (\text{R}^2 = .894)$$

These relations are valid only for wet ferritic welds. An attempt was made to relate the percent elongation to depth, but the elongation was lower for 35 m (115 ft) than for 60 m (198 ft) and the regression slope was close to zero. The elongation for pairs of wet ferritic weld metal specimens was:

10 m (33 ft): 12.5 percent, 9.4 percent

35 m (115 ft): 6.3 percent, 6.3 percent

60 m (198 ft): 9.4 percent, 9.4 percent

Like the hardness data which were lower for 35 m (115 ft) than for 10 or 60 m (33 ft or 198 ft), this may be the result of something unique in the welding procedure used at 35 m (115 ft). Recall that the worst fracture toughness  $33 \text{ MPav}\sqrt{\text{m}}$  (30 ksi $\sqrt{\text{in.}}$ ) also occurred for the 25.4 mm (1 in.) thick 35 m (115 ft) weld metal.

#### 4.4 Summary of Statistical Analysis

The results of laboratory tests (bend tests, Charpy tests,  $J_{Ic}$  tests, and all-weld-metal tensile tests) were analyzed with the statistical analysis computer programs BMDP. The results were grouped according to carbon equivalent and electrode, weld type, depth, thickness, weld or HAZ, with or without restraint, and test temperature, and all combinations of two of these grouping variables. Analysis of variance was used to determine the significance of these grouping variables and interactions among the grouping variables. Regression analysis was used to fit linear relations between test results and grouping variables and other test results. In general, the number of tests performed is sufficient to support the conclusions below with good statistical significance.

The following relation for  $K_{Ic}$ , based on weld metal/base metal thickness, depth, and zone (weld or HAZ) was developed:

$$K_{Ic} = 75.1(A) - 94.2(THICK) - .321(DEPTH) + 33.9(ZONE) + 201$$

where: A = 0 for ferritic welds and A-36 base plate,  
          1 for austenitic welds and A516 base plate  
THICK = thickness in inches [1.0 in. = 25.4 mm]  
DEPTH = depth of weld preparation in feet  
          [1.0 ft = 0.3048 m]  
ZONE = 0 for weld metal, 1 for HAZ

A slightly better estimate of  $K_{Ic}$  can be obtained using the following correlation to the Charpy impact energy, CVN, in ft-lb:

$$K_{Ic} = 2.02(CVN) + 23(A) - .173(DEPTH) + 67.2$$

An expression which contains a 95 percent confidence limit on the intercept (lower bound) and which provides a conservative estimate of  $K_{Ic}$  for all test conditions studied (see Section 4.3.1) is:

$$K_{Ic} = 2(CVN) - .15(DEPTH) - 8$$

It is possible that this conservative expression could be implemented in design guidelines to estimate fracture toughness of underwater welds. If the resultant toughness cannot be shown to be adequate,  $J_{Ic}$  or CTOD testing could be required.

Other significant findings of the statistical analysis include:

1) The austenitic welds evaluated have greater  $K_{Ic}$  than the ferritic welds, especially for dry and wet-backed welds, and toughness decreases with increasing depth.

2) The ductility of ferritic wet-backed welds and austenitic wet welds is very poor.

3) Increased thickness had a small deleterious effect on toughness and hardness, but had no effect on ductility.

4) HAZ specimens removed from 12.7 mm (1/2 in.)-thick welds were significantly tougher than the corresponding weld metal specimens. The 25.4 mm (1 in.)-thick specimens had roughly equal HAZ and weld metal toughness.

5) Temperature changes within the service temperature range of marine structures had no significant effect on impact toughness.

6) Restraint had a possible deleterious effect on toughness, but there is approximately 34 percent probability of error in this conclusion. However, it is conservative to accept this chance of error and consider the effect of restraint.

7) Restraint had no significant effect on ductility or hardness.

8) Hardness of austenitic welds was significantly greater than hardness of ferritic welds, and wet welds were much harder than dry or wet-backed welds. Results from the literature and service experience reported in Section 2.2.1 of this report included the following regression relations:

$$HVN = 157 + 566(CE) \text{ for wet-backed welds}$$

$$HVN = 282 + 566(CE) \text{ for wet welds}$$

The relations given above correctly predicted the effect of carbon equivalent and weld type but overestimated the hardness of wet-backed welds by about 150, and the hardness of wet welds by about 230, as shown in the following table.

<u>Weld Type</u>	<u>Predicted Peak HVN</u>	<u>Observed Mean HVN for 33-ft Depth</u>
Wet-backed ferritic	360	230
Wet-backed austenitic	417	246
Wet ferritic	485	236
Wet austenitic	542	329

Since these relations were formulated to predict peak hardness (i.e., HAZ near weld crown) while the observed mean is an average of peak weld-metal-crown hardness and peak midplane HAZ hardness (i.e., the observed hardness excluded HAZ near weld crown) the agreement is considered good.

9) Hardness could not be correlated to either weld metal tensile strength, toughness, or ductility, and therefore is not considered useful in predicting these properties of the welds.

10) The results of bend tests could not be correlated to grouping variables (e.g., depth, CE, thickness, weld type), but the correlation to all-weld-metal tensile properties (proportional limit, yield stress, or ultimate strength) was excellent.

11) The correlation of the weld metal tensile properties to depth was excellent; the following results were obtained:

$$(a) \text{ Proportional limit: } \sigma_{pl} = .104 - 104(\text{DEPTH}), \text{ ksi}^*$$

$$(b) \text{ Ultimate strength: } \sigma_{uts} = 81.4 - .088(\text{DEPTH}), \text{ ksi}^*$$

Section 2.2.2 of this report gave the following relation for  $\sigma_{uts}$ :

$$(c) \sigma_{uts} = 54.2 + 41.9(\text{THICK}) - .037(\text{DEPTH}), \text{ ksi}^*.$$

Since our results were based on all-weld-metal tensile tests from 25.4 mm (1 in.) welds, this expression reduces to the following for 25.4 mm (1 in.) welds:

$$(d) \sigma_{uts} = 96.1 - .037(\text{DEPTH}), \text{ ksi}^*$$

This expression predicts higher strength weld metal than resulted in these test welds as seen by comparing to Expression (b) above.

Transverse-weld tension tests were conducted, but the results were not statistically analyzed because fracture occurred in the base plate for almost all specimens, and the ultimate strength and yield strength of all test specimens fell within a narrow range near the specified base plate material strengths, unaffected by depth, thickness, restraint, or weld type.

---

\* 1.0 ksi = 6.895 MPa, Depth in feet: 1.0 ft = .3048 m

## 5.0 DESIGN GUIDELINES FOR UNDERWATER WET AND WET-BACKED WELDS

### 5.1 Introduction and Overview

Properties and conditions that could influence the performance of underwater wet and wet-backed welds include the state of residual stresses in the weld, yield strength, ductility, ultimate strength, susceptibility to and characteristics of discontinuities, rate of subcritical crack propagation due to fatigue and/or stress corrosion cracking, and fracture toughness.

#### 5.1.1 Residual Stresses

The state of residual stresses is difficult to quantify even for dry welds. Due to lack of information, one must assume that residual stresses of magnitude equal to the yield strength of the base plate or weld material (whichever is lower) may exist locally in underwater wet welds. Higher residual stresses may be present in fillet welds, depending on the configuration. Under applied loads, the strain in the welds may reach up to twice the yield strain of the base plate or weld metal.

#### 5.1.2 Tensile Strength

The weldments tested in this study exhibited excellent yield strength and ultimate strength. Most (76 percent) of the transverse weld tensile specimens failed in the base metal, and even those that failed in the weld (which were only those prepared at greater than 10 m (33 ft) depth) exhibited strengths greater than the minimum specified for the base metal. A rule of thumb widely used in estimating wet weld performance [5.1] suggests that the strength of wet welds is about 80 percent of the strength of

corresponding dry welds. The experimental data suggests that the strength of the wet weld may exceed the strength of the dry weld and are at least as high.

### 5.1.3 Ductility

A rule of thumb [5.1] suggests that wet welds may exhibit only 50 percent of the ductility of corresponding dry welds. In the transverse weld tension tests of this study, the ductility of the weld metal was generally not a problem because the base metal yielded, but the specimens that failed in the weld failed suddenly, and the load-displacement curves exhibited little or no plastic deformation. Fillet weld tensile tests exhibited much better ductility, indicating that the ductility for shear failure (the primary failure mode for the fillet weld tensile specimens) is better than for direct tension.

All-weld-metal tensile tests were conducted using an extensometer to measure elongation of the weld metal. These tests showed the elongation of wet welds ranged from 6.3 percent to 12.5 percent which is about 33 to 66 percent of the 19 percent elongation required by AWS D3.6 Specification for qualification as Type A welds (those suitable for use as structurally critical welds) and about 25 to 50 percent of the 23 percent elongation expected for the base metal.

Bend tests may indicate the ductility of the welds. Side bend tests for groove welds (AWS D3.6 Specification) are required to bend to a radius of 19 mm (3/4 in. or 2T) for Type A welds, but only (57.2 mm (2.25 in. or 6T) for Type B welds. Dry welds, ferritic wet welds at 10 m (33 ft) and austenitic wet-backed welds 10 m (33 ft) passed the bend test requirements for Type A. Ferritic wet-backed welds and austenitic wet welds at 10 m (33 ft) and some

ferritic wet welds at 60 m (198 ft) did not qualify as Type B. (Ferritic wet-backed welds were made with an electrode, E6013, not normally used for wet-backed welds.) It appears that this requirement of AWS D3.6 Specification should assure that qualified Type B welds have at least the ductility observed in these test plates. However, the fact that the austenitic wet welds did not pass the bend tests is misleading. The austenitic wet welds exhibit very good fracture toughness. Most specimens bend to the required radius only they exhibited cracks at pores which opened up greater than 3 mm (1/8 in.) The fact that the weld could tolerate these cracks at such high strains is actually an indication of the good toughness.

Fillet weld break-over bend tests were also performed. The requirements for qualification are not as well defined as the side bend test, and there is essentially no difference in the requirements for Type A and Type B welds. None of the specimens bent 90° but rather fractured at 30° ~ 45°.

Lack of ductility is a serious but not insurmountable problem for wet welds. The existence of residual stresses probably requires that the limited ductility available be used for the shake down (yielding and redistribution) of these residual stresses.

Fortunately, through proper design, underwater wet welded repairs, attachments, and even original fabrication can be made such that the reserve ductility exhibited by dry welds is not required. The principle involves insuring that the structural member remote from the wet weld can become fully plastic before the applied stress (excluding residual stress) in the weld metal exceeds the its yield stress. These design procedures are discussed in the following Section 5.2.

#### 5.1.4 Susceptibility to Cracking and Other Discontinuities

Probably the biggest concern about underwater welds is the susceptibility to cracking and other discontinuities. The weldments for this study were produced in the horizontal flat position in a dive tank without the problems of visibility, access, and diver discomfort attendant to welding underwater in the field. The fabricator inspected the weldments visually, with magnetic particle technique, and with radiography. It must be considered, however, that the only weldments containing cracks were ferritic wet-backed welds made with an electrode not normally used for this purpose. Other discontinuities (within AWS D3.6 Specification requirements) were found and porosity was severe. The susceptibility to discontinuities will largely depend on the experience and skill of the welder/diver.

#### 5.1.5 Resistance to Fracture

In some designs, the problem of fracture occurring because of the presence of cracks may be accommodated by redundancy and interruption in the weld to prevent cracks from propagating into adjacent weld lengths. In other situations, welds may be designed to turn in directions parallel to the direction of applied stresses. If the wet is to be used for a fracture critical member, there must still be considerations of fracture control based on a minimum toughness requirement in the weld qualification procedures and a maximum stress based on this toughness and a maximum credible initial crack size. These restrictions should be more severe for cases where redundancy cannot be accommodated in the design. Fortunately, the weldments tested in this study exhibited a ductile failure mode and sufficient toughness to practically enforce such requirements. Design details to minimize the impact of cracking and fracture control guidelines are discussed in Sections 5.3 and 5.4, respectively.

### 5.1.6 Resistance to Subcritical Crack Growth

Environmentally enhanced subcritical crack propagation under static load or stress corrosion cracking is generally not a problem in mild steels used in offshore and marine construction. Gooch [5.3] found underwater welds to be resistant to stress corrosion cracking (SCC) under normal cathodic protection. However, the effect of sour gas or cathodic overprotection remains to be investigation.

Subcritical crack propagation from corrosion fatigue must be considered. Crack propagation rate data reported by Matlock et al. [5.2] indicates that for range in stress intensity factor ( $\Delta K$ ) less than about  $33 \text{ MPa}\sqrt{\text{m}}$  ( $30 \text{ ksi}\sqrt{\text{in.}}$ ), the crack propagation rate for wet welds is generally lower than that of dry welds or base plate material. However, for higher  $\Delta K$ , the crack propagation rate is high and increases at a much greater exponential rate than dry welds or base plate material. Together with a maximum credible initial crack size dependent on the design configuration, a requirement could be formulated to limit the normally occurring cyclic stress range such that the stress intensity factor range remains well below  $33 \text{ MPa}\sqrt{\text{m}}$  ( $30 \text{ ksi}\sqrt{\text{in.}}$ ). In this manner the underwater weld can be assured to be as resistant to fatigue crack propagation as a dry weld, and normal fatigue design procedures applicable to offshore structures should be applicable. Limitation of cyclic stress from fatigue considerations is discussed in Section 5.5.

### 5.1.7 Statement of Design Guidelines

In summary, assuming that wet welding has been selected as the best approach to the problem, the design guidelines proposed herein consist of a four step procedure as follows:

1) Evaluate the design problem (usually a repair or modification) for the solution which relies most on compressive or shear stresses in the wet or wet-backed welds. The following examples show designs which help limit tensile stress in the welds. These designs may be more complicated and expensive than the designs currently used by underwater welding contractors. Naturally, if the conditions of the repair do not warrant more complicated designs, they would not be required. However, if the use of Type B underwater welds was questionable and the alternative would be a much more expensive dry or hyperbaric repair, then consideration of the following details may be worthwhile. Further, because of extensive redundancy of these designs, NDE requirements may possibly be made less stringent or waived, resulting in additional savings. For example;

- if the chord is too small to allow for a large enough doubler, try to utilize full encirclement split-sleeve doublers when doublers are subject to out of plane loads to distribute the load through compressive contact stresses to the underlying member (as doubler A in Figure 5.1.)
- try to use scalloped doublers (as is currently standard procedure) when doublers are subject to axial load to maximize weld area and make most weld area act in shear rather than tension (as doubler B in Figure 5.1.)

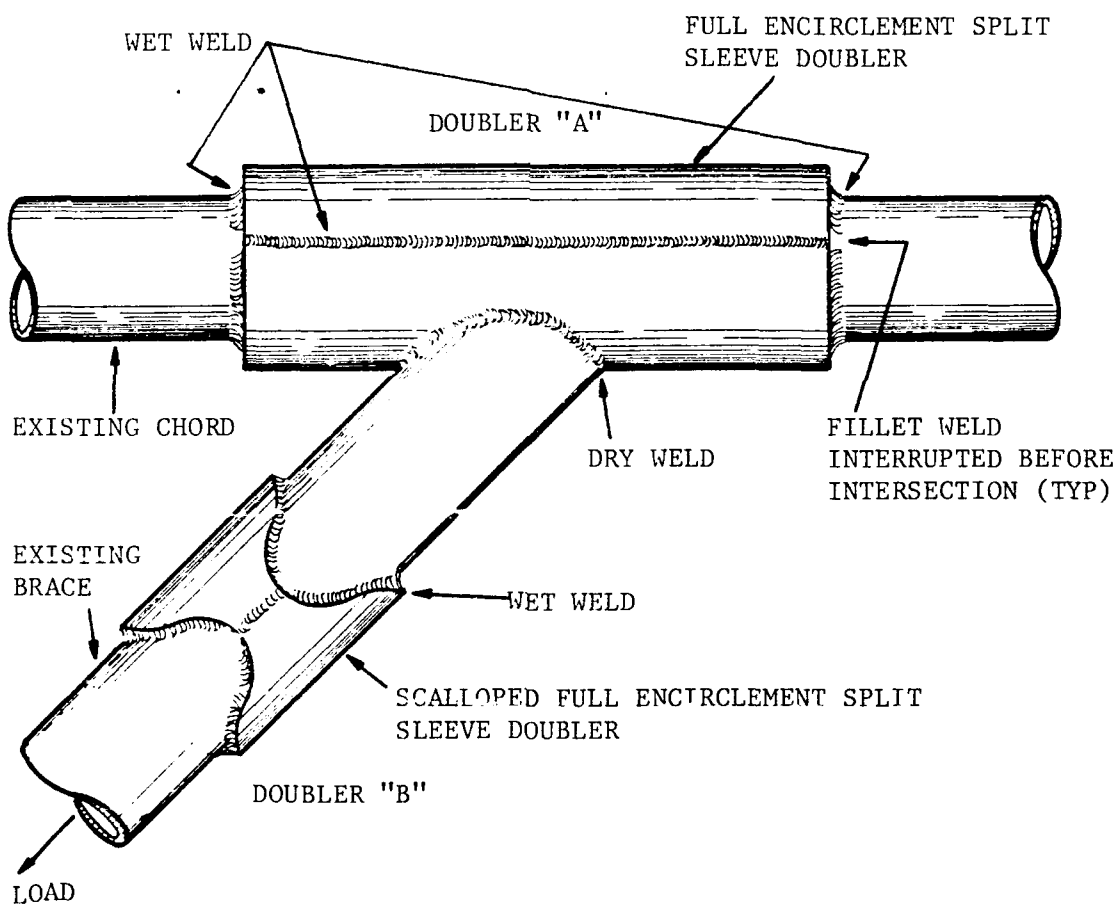


FIGURE 5.1 BRACE REPLACEMENT

- try to use an irregular interlocking connection when groove welds are subject to tension. Note that if the repair was for a pipeline, a leak constitutes a failure and therefore the complicated split sleeve would not be useful. For pipeline repairs, only control of toughness to prevent crack initiation would be useful.
- try to provide as much redundancy as possible. For example, the addition of clip angles to the seam weld as shown in Figure 5.2.
- try to change direction of weld, use discontinuous weld segments, or take other measures which can limit the extent of crack propagation or act as a crack arrestor, as shown in Figure 5.3. Be careful not to create stress concentrations which would be worse than the uninterrupted weld.
- design the repair to minimize restraint and hence reduce the risk of hot cracking.

2) Design the wet weld to be below yield stress when the weakest link remote from the weld is fully yielded from the worst case load combination, as shown in Figure 5.4.

3) Check maximum stress in the weld for fracture based on the fracture toughness, maximum credible crack size, and appropriate stress intensity expression. Alternatively, the CTOD design curve (PD 6493) [5.4] may be used to estimate the maximum flaw size for a

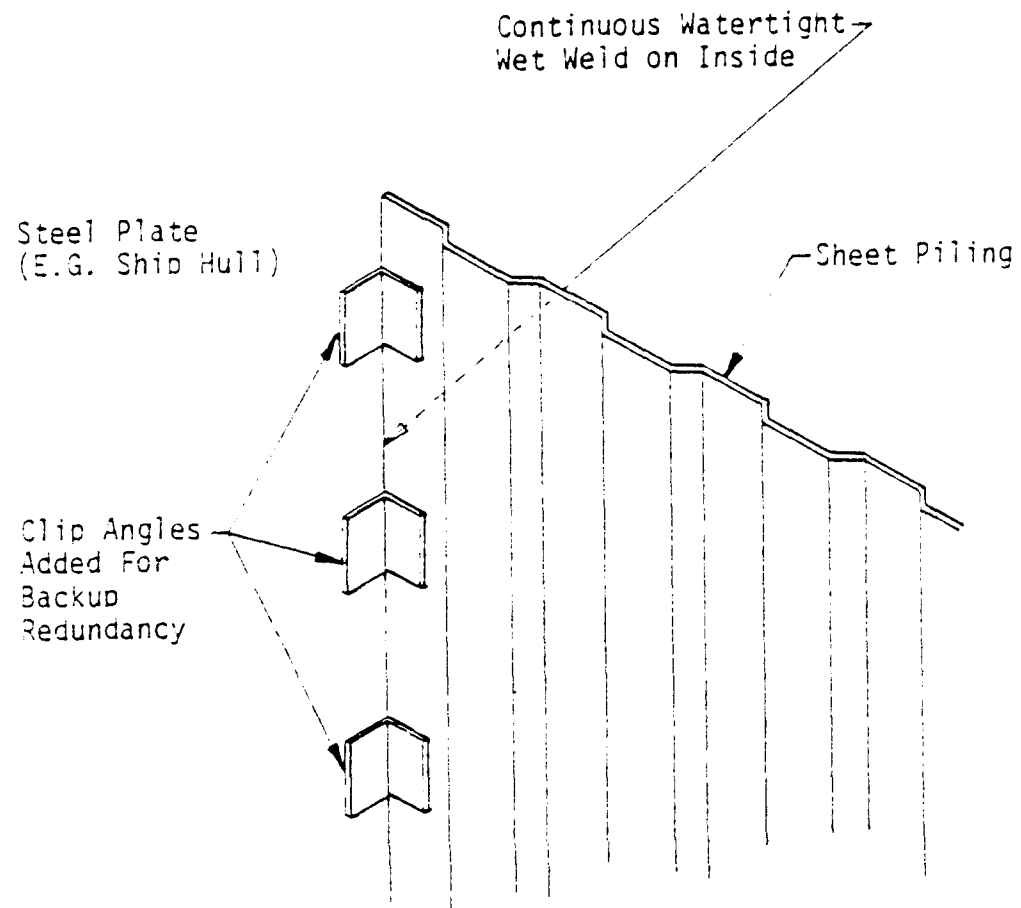
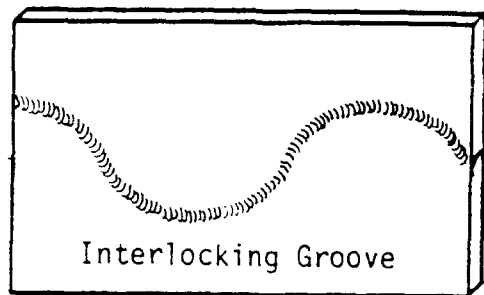
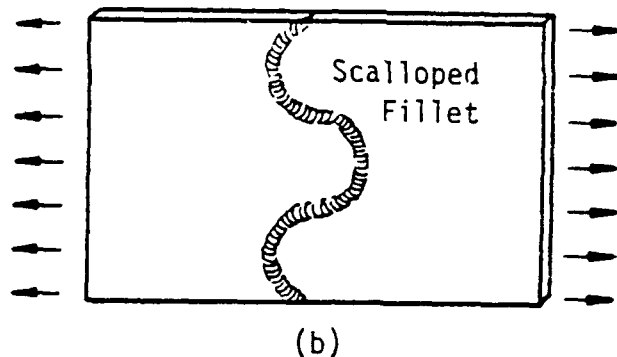


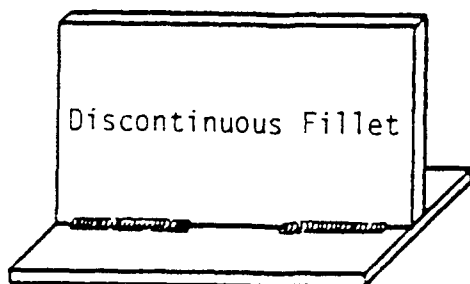
FIGURE 5.2 ATTACHMENT OF COFFERDAM TO STEEL PLATE STRUCTURE



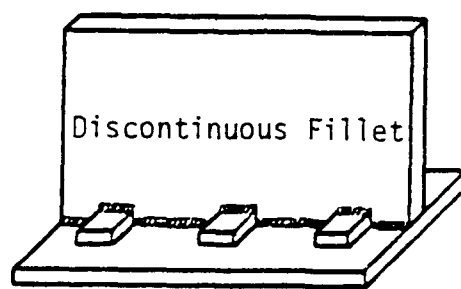
(a)



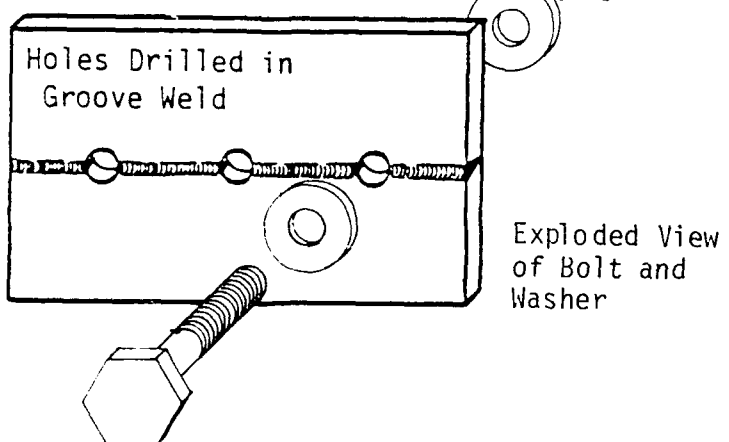
(b)



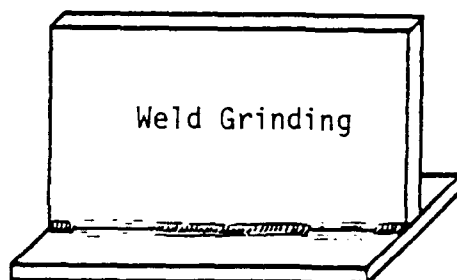
(c)



(d)



(e)



(f)

FIGURE 5.3 DETAILS TO LIMIT CRACK SIZE

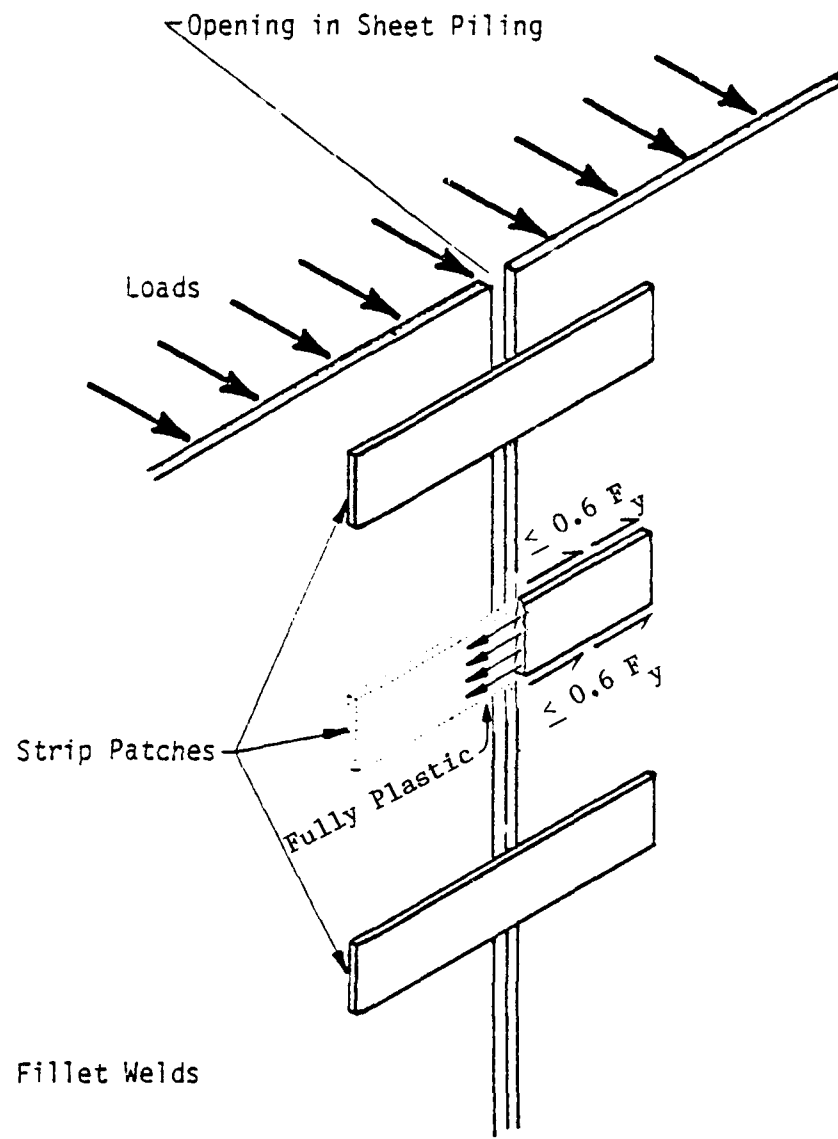


FIGURE 5.4 STRIP PATCH REPAIR OF SHEET PILING

given state of stress. Reduce stress by design change if necessary.

- 4) Check maximum frequently occurring alternating stresses in underwater weld to keep the range in stress intensity factor well below  $33 \text{ MPa}\sqrt{\text{m}}$  ( $30 \text{ ksi}\sqrt{\text{in.}}$ ), i.e., in the regime where the crack would grow faster in the base plate material. Reduce stress by design change if necessary.

## 5.2 Design Procedures to Assure Ductility of Wet and Wet-Backed Welded Connections

The design problem that arises from using underwater wet and wet-backed welds of limited ductility together with members fabricated from ductile mild steel and dry welds is in some ways analogous to the problem of using brittle and crack-prone concrete together with ductile reinforcing steel. The principle involved in the design of reinforced concrete can be applied to the design of wet welded connections, i.e., to provide sufficient material to assure that the weaker material does not reach its limit state before the ductile material has fully yielded, thus avoiding undesirable failure and allowing the redundant structure to redistribute load as the connection yields.

Using such a limit-state procedure is more rational than merely using a reduction factor on allowable stress or additional factor of safety for the weld because it in theory guarantees that overload failure cannot occur in the wet weld, whereas an allowable stress approach could still result in wet weld failure. Further, the limit-state procedure is easier to use because the load used in the analysis will depend only on the plastic capacity of the weakest member in the connection, and not on the external loads

applied to the structure. The assumed external loads may not be known, especially when a repair is made to a structure that was designed many years earlier.

This proposed element of the design procedure can be stated as the following rule:

"The stress in the wet weld should not exceed  $F_y$  (where  $F_y$  is the yield stress of base plate or weld metal, whichever is less) for tensile or compressive stress and 0.6  $F_y$  for shear stress, under loading which would fully yield at least one member of the connection by either axial load, bending or torsional moment, shear or any combination loading, whichever combination creates the highest stress in the wet weld. Critical cross-sections perpendicular to the applied stress should not be composed entirely of wet weld (this precludes girth welds) and shall meet the above requirements."

The procedure is illustrated in Appendix C in several examples corresponding to common usage of underwater wet and wet-backed welding, i.e.,

- 1) A full encirclement split sleeve placed over a hole or crack in a pipeline subject to internal pressure (e.g., for repair of damaged pipeline).
- 2) Strip patches on separating sheet piling subject to tensile hoop stress (e.g., for littoral sheet-pile structures retaining soil as shown in Figure 5.4).
- 3) Attachment of doublers subject to axial load and bending (e.g., for replacement of members in offshore structures as shown in Figure 5.1).

### 5.3 Design Details to Limit Impact of Cracking

Wet welds (as well as dry welds) are susceptible to cracking. Even though no welds prepared properly for this program exhibited cracking, underwater inspection is uncertain and large initial flaw sizes are possible. However, reasonably small initial crack sizes can be achieved using stringent procedure control and quality assurance. If a repair is thought to be so critical that the designer would have difficulty convincing the owner that Type B wet welds can be safely used, it may be reasonable to incorporate in the design some means of limiting the possible initial crack size or otherwise limit the impact of this cracking on overall structural integrity. Design details to limit the impact of cracking on structural integrity will be discussed in the following categories:

- Details to provide redundancy; and
- Details to limit crack size in the wet weld.

#### 5.3.1 Details to Provide Redundancy

Any welds are susceptible to cracking and in the ocean environment these cracks can be expected to propagate and may lead eventually to instability. Therefore, the designs should incorporate as much redundancy as is reasonable.

Sufficient redundancy could possibly be provided by the original structure, if it were highly redundant to begin with.

Redundancy can be inherent in the design system chosen. For example, an underwater lift operation could be conducted with multiple lifting lugs wet welded to the object, and the system capable of safely completing the lift even if one or more of the

lugs were to fail. The design of a repair for a damaged member of an offshore structure might entail the addition of two or more new members to brace the damaged member. The strip patch repair design of Example 2 in Appendix C is inherently redundant, since a number of strips could fail without impairing the performance of the system, and cracks in one strip cannot directly propagate into other strips.

Redundancy could also be provided by an additional and completely independent load transfer system. For example, a cracked plate could be patched inside and out, each patch plate capable of independently carrying the load in the damaged plate. Figure 5.2 shows a continuous seam weld required to provide a watertight seal and capable of carrying the required load. Clip angles are welded on the opposite side (also capable of carrying all the load) to provide a backup against complete collapse if the seam begins to crack.

### 5.3.2 Details to Limit Crack Size

Because the maximum credible initial crack size in a continuous wet weld could be too large with respect to the toughness of the weld and applied stress intensity factor, it may be necessary to limit the maximum credible crack size by having the weld change direction (Figure 5.3a and b), using a discontinuous fillet weld with smooth runout (Figure 5.3c) or using some other feature to get independent discontinuous welds (tabs like those shown in Figure 5.3d, holes (with or without the addition of high strength bolts) like those shown in Figure 5.3e, or grinding as shown in Figure 5.3f).

Such details should be designed with careful consideration of the stress concentration that may be caused by the detail.

These stress concentrations could create a worse situation than the continuous weld. Where weld is interrupted but a watertight seal is required, another material could be used to affect the seal.

#### 5.4 Fracture Control Guidelines

The fracture control requirements should reflect the degree of redundancy and control of maximum crack size incorporated in the design. The fracture toughness may be determined directly through  $J_{IC}$  testing of the weld qualification test plate, through a correlation to Charpy impact energy which has been shown to be conservative for the materials involved such as the correlation developed in this study (see Section 4.3.1), or just estimated from available data on similar weld material. The uncertainty inherent in these estimates of toughness should also be reflected in the guidelines. Alternatively, the CTOD design curve (PD 6493) [5.4] can be used. This empirical design curve is based on much experience and already contains a sufficient margin of safety.

The method of evaluating the weld for possible fracture involves a basic fracture mechanics analysis wherein:

- 1) A critical location and maximum credible critical size of a flaw is identified.
- 2) The maximum credible nominal stress in the weld is calculated, or may be conservatively taken as  $F_y$  (the yield strength of weld metal or base plate whichever is less).
- 3) The maximum credible stress intensity factor ( $K_{max}$ ) is calculated with 1) and 2) and established stress analysis procedures or handbook solutions for  $K$ .

Factors of safety to account for uncertainty should be applied to the crack length and stress. Alternatively, the procedures of PD 6493 may be employed.

- 4) The material toughness ( $K_{Ic}$  or CTOD) is obtained, and reduction factors applied to the toughness.
- 5) If  $K_{Ic} < K_{max}$ , design changes are implemented and the process repeated. For the CTOD curve approach, if  $\bar{a}_{max}$  (the maximum tolerable flaw size) is less than the estimate of the maximum critical flaw size, the design changes are implemented and the process repeated.

Table 5.1 contains suggested factors of safety for use with fracture mechanics analysis which are devised in a way which rationally reflects redundancy, control of crack size, and method of obtaining  $K_{Ic}$ .

The above guidelines are implemented and illustrated in the examples of Appendix C. As a general notion of what size cracks would be allowed according to the toughness data collected in this program, consider the following:

- minimum toughness levels for welds prepared at 10 m (33 ft) depth are about 110 MPa $\sqrt{m}$  (100 ksi $\sqrt{in.}$ );
- a through thickness crack in a wide plate would have a stress intensity factor equal to or less than about  $1.2 \sigma \sqrt{\pi a}$  (where  $\sigma$  = applied stress and  $a$  = half the total crack length);

TABLE 5.1  
SUGGESTED LOAD FACTORS AND STRENGTH REDUCTION FACTORS

Control of Crack Size	Factor on Crack Length	Estimate of Toughness	Reduction Factor on Toughness	Degree of Redundancy	Factor on Applied Stress	Total Effective Factor on Safety $\beta_n$
No control	4.0	Similar Material C	0.5	D E F	1.8G 1.4 1.2	7.2 5.6 4.6
		Charpy Test	0.67	D E F	1.8G 1.4 1.2	5.4 4.4 3.6
		$J_{Ic}$ or CTOD	0.83	D E F	1.8G 1.4 1.2	4.4 3.4 2.8
Changed direction but stresses remain tensile A	2.0	Similar Material C	0.5	D E F	1.8G 1.4 1.2	5.0 3.9 3.4
		Charpy Test	0.67	D E F	1.8G 1.4 1.2	3.8 2.9 2.5
		$J_{Ic}$ or CTOD	0.83	D E F	1.8G 1.4 1.2	3.1 2.4 2.0
B	1.8	Similar Material C	0.5	D E F	1.8G 1.4 1.2	4.8 3.8 3.2
		Charpy Test	0.67	D E F	1.8G 1.4 1.2	3.6 2.8 2.4
		$J_{Ic}$ or CTOD	0.83	D E F	1.8G 1.4 1.2	3.0 2.3 1.9
Changed direction into shear stress A	1.6	Similar Material C	0.5	D E F	1.8G 1.4 1.2	4.6 3.5 3.0
		Charpy Test	0.67	D E F	1.8G 1.4 1.2	2.8 2.7 2.3
		$J_{Ic}$ or CTOD	0.83	D E F	1.8G 1.4 1.2	2.8 2.2 1.8

TABLE 5.1 (Cont'd.)  
SUGGESTED LOAD FACTORS AND STRENGTH REDUCTION FACTORS

Control of Crack Size	Factor on Crack Length	Estimate of Toughness	Reduction Factor on Toughness	Degree of Redundancy	Factor on Applied Stress	Total Effective Factor $\beta_n^{\text{eff}}$
B	1.0	Similar Material <sup>C</sup>	0.5	D	1.8 <sup>G</sup>	3.6
				E	1.4	2.8
				F	1.2	2.4
	1.4	Charpy Test	0.67	D	1.8 <sup>G</sup>	2.7
			E	1.4	2.1	
			F	1.2	1.8	
Discontinuous Weld	J <sub>Ic</sub> or CTOD	Similar Material <sup>C</sup>	0.83	D	1.8 <sup>G</sup>	2.2
				E	1.4	1.7
				F	1.2	1.4
	J <sub>Ic</sub> or CTOD	Similar Material <sup>C</sup>	0.5	D	1.8 <sup>G</sup>	4.3
				E	1.4	3.3
				F	1.2	2.8
B	1.0	Similar Material <sup>C</sup>	0.67	D	1.8 <sup>G</sup>	3.2
				E	1.4	2.5
				F	1.2	2.1
	1.4	Charpy Test	0.83	D	1.8 <sup>G</sup>	2.6
			E	1.4	2.0	
			F	1.2	1.7	
B	J <sub>Ic</sub> or CTOD	Similar Material <sup>C</sup>	0.5	D	1.8 <sup>G</sup>	3.6
				E	1.4	2.8
				F	1.2	2.4
	J <sub>Ic</sub> or CTOD	Similar Material <sup>C</sup>	0.67	D	1.8 <sup>G</sup>	2.7
				E	1.4	2.1
				F	1.2	1.8
B	J <sub>Ic</sub> or CTOD	Similar Material <sup>C</sup>	0.83	D	1.8 <sup>G</sup>	2.2
				E	1.4	1.7
				F	1.2	1.4

A Crack length in analysis is some maximum credible crack length less than the total continuous straight weld length. If when multiplied by the factor, the crack length exceeds that which would be calculated by B below, that procedure can be used.

B Crack length is the total continuous straight weld length.

C Toughness was estimated from available toughness data for a similar material.

D No redundancy.

E Two independent and redundant load transfer systems are used.

F Multiple (greater than E) redundancy is provided.

G Use 1.8 times design maximum stress or 1.0 times yield stress, whichever is less.

H Assumes that the stress intensity factor is proportional to the square root of crack length.

- if stresses about 250 MPa (36 ksi) were applied (yield stress for A-36) the maximum half crack length would be about 43 mm (1.7 in.), or a crack of 86 mm (3.4 in.) total length could be tolerated.

## 5.5 Guidelines For Limiting Cyclic Stress To Control Fatigue Crack Propagation

Obviously, in order to accurately assess the fatigue life of an underwater welded repair subject to cyclic or repeated loads, good crack growth rate data at the appropriate range in stress intensity factor, load ratio, and environment are needed as well as an accurate estimate of future loads and existing flaw size. Only limited crack growth rate data for underwater welds have been generated to date. However, some useful observations may be made from the existing data of Matlock et al. [5.2] (see Figure 2.1).

Specifically, these data suggest that for range in stress intensity factor ( $\Delta K$ ) of about  $33 \text{ MPa}\sqrt{\text{m}}$  ( $30 \text{ ksi}\sqrt{\text{in.}}$ ), the crack growth rates of shallow depth wet welds from several suppliers was generally less than  $2.5 \times 10^{-4} \text{ mm/cycle}$  ( $10^{-5} \text{ in/cycle}$ ). Further, for  $\Delta K$  less than  $33 \text{ MPa}\sqrt{\text{m}}$  ( $30 \text{ ksi}\sqrt{\text{in.}}$ ), the growth rates in underwater wet welds were less than those of surface welds or base metal. This suggests that if the range in stress intensity factor were kept below  $33 \text{ MPa}\sqrt{\text{m}}$  ( $30 \text{ ksi}\sqrt{\text{in.}}$ ), a worst-case fatigue analysis could be performed using data applicable to the base metal, which is more plentiful. Such fatigue analysis methodologies using either fracture mechanics or the Miner's rule (S-N) approach are well established and will not be reviewed herein.

The design guidelines for fatigue amount to a limitation of the range in stress intensity factor and may be stated as follows:

- 1) Calculate the maximum credible nominal stress range that may occur more than 10,000 times in the lifetime of the wet weld. (10,000 is chosen because less frequent stress ranges which may cause a range in stress intensity factor greater than  $33 \text{ MPa}\sqrt{\text{m}}$  ( $30 \text{ ksi}\sqrt{\text{in.}}$ ) will probably still have growth rates much less than  $2.5 \times 10^{-3} \text{ mm/cycle}$  or ( $10^{-4} \text{ in./cycle}$ ), probably resulting in less than 25.4 mm (1 in.) of crack growth over the life of the structure, which seems tolerable for shallow welds with good fracture toughness. Further, occasional overloads act to retard crack growth which is beneficial.)
- 2) Identify the critical location and the maximum credible crack size at the beginning of the lifetime. (This maximum credible initial crack size could rationally be much less than the maximum credible critical crack size used in the fracture control guidelines of the previous section.)
- 3) Maximum credible frequently occurring  $\Delta K_{\max}$  is calculated from 1) and 2) and established stress analysis procedures or handbook solutions for  $K$ .
- 4) If  $\Delta K_{\max} > 33 \text{ MPa}\sqrt{\text{m}}$  ( $30 \text{ ksi}\sqrt{\text{in.}}$ ), design changes are implemented and the process repeated.
- 5) If  $\Delta K_{\max} < 33 \text{ MPa}\sqrt{\text{m}}$  ( $30 \text{ ksi}\sqrt{\text{in.}}$ ), fatigue life calculations are performed according to established procedures using base plate material properties (crack growth rate data or S-N data).

- 6) If fatigue life calculated is not adequate, design changes are implemented and the process repeated.

Note the crack growth rate data which show a growth in wet welds lower than the growth rate for surface welds or base metal (Figure 2.1) are limited to shallow depths only, and this behavior may not be the same for deeper welds. Clearly there is a need for additional crack growth rate data for wet welds.

#### 5.6 References

- 5.1 Grubbs, C.E., and Seth, O.W., "Underwater Wet Welding with Manual Arc Electrodes", Published in Underwater Welding for Offshore Installations, The Welding Institute, Abington Hall, Abington, Cambridge, 1977.
- 5.2 Matlock, D.K., Edwards, G.R., Olson, D.L., and Ibarra, S., "An Evaluation of the Fatigue Behavior in Surface, Habitat, and Underwater Wet Welds", Underwater Welding Soudage Sous L'Eau, Proceedings of the International Conference held at Trondheim, Norway, 27-28 June 1983 under the auspices of the International Institute of Welding, Pergamon Press, Oxford, England, p. 303, 1983.
- 5.3 Gooch, T.G., "Properties of Underwater Welds, Part 1 Procedural Trials and Part 2 Mechanical Properties," Metal Construction, March 1983.
- 5.4 "British Standards Institution, Guidance on Some Methods for the Derivation of Acceptance Levels for Defects in Fusion in Welded Joints," PD6493, London, 1980.

## 6.0 SUMMARY, CONCLUSIONS, AND RECOMMENDATIONS

### 6.1 Use of Wet and Wet-Backed Welds

After an extensive review of the literature, collection of information from contractors and an experimental program; it is concluded that the wet and wet-backed shielded metal arc welding (SMAW) process can produce welds suitable for critical structural applications. However, the limitations of the welds must be considered in the design. The design process should include a thorough consideration of fracture and is therefore inherently more complicated than standard design practice. Material properties may be required that are more expensive to obtain than the results of weld qualification tests. Design details may be required that are more expensive to fabricate than standard weld details. But these expenses should be offset by the savings relative to alternatives of wet and wet-backed welding, e.g., hyperbaric chambers, mini-habitats, or drydocking. Further savings may result from a more efficient plan for quality assurance based on fracture mechanics considerations.

Wet and wet-backed welds can rarely achieve the same quality as dry welds. Wet welds generally have more quality problems than wet-backed welds. Two unique aspects of wet and wet-backed welding are responsible (directly or indirectly) for many of these quality assurance problems: 1) the rapid quench of the weld and 2) evolved gases including dissociation of water.

Wet welds are cooled 10 to 15 times faster than dry welds. Depending on oxygen and manganese content, this cooling may cause martensite and other brittle transformation structures to form in the grain coarsened region of the HAZ. These hard microstructures have limited ductility and are susceptible to

hydrogen damage. Additional variables such as arc energy, weld travel speed, water temperature and water currents make prediction of microstructure difficult.

Evolved gases manifest as porosity which increases with depth. The most troublesome gas is hydrogen, which is available to the weld pool, dissolves into the molten metal and diffuses to the HAZ. The hydrogen may manifest as HAZ cracking as well as porosity. Control of hydrogen cracking is the main consideration in choice of electrode.

It is generally accepted (and supported by this program) that crack-free ferritic wet welds can be made for base metal carbon equivalent (CE) less than 0.4. The electrode which works best seems to be the E6013, an electrode which ironically results in less ductility and lower radiographic quality than low hydrogen electrodes in dry welds. The E6013 electrode has been successfully used in all welding positions. The E7018 electrode is commonly used for wet-backed welds. Base metals with  $0.4 < CE < 0.6$  can be welded with austenitic (high-nickel) electrodes. The commercially used austenitic electrodes are proprietary. Efforts for this program to make austenitic wet welds on A-516 steel (CE = 0.46) deeper than 30 m (100 ft) were not successful.

Another quality problem present in the groove welds prepared for the experimental program was the presence of two parallel grooves (along fusion lines) up to 2.5 mm (0.1 in.) deep due to inadequate joint penetration. It is not known how common this problem is in the general population of wet welds and it has been stated that this problem can be avoided by good workmanship.

The American Welding Society (AWS) has published rules (AWS D3.6, "Specification for Underwater Welding") for qualifying

the welder/diver and welding procedure for underwater welding. AWS D3.6 defines three types of underwater welds according to some mechanical and examination requirements. In descending order of quality level are: Type A, intended for structural applications; Type B, intended for limited structural applications; and Type C, for applications where structural quality is not critical. A fourth type, type O, is intended to have qualities equivalent to those normally specified by the code or standard applicable to the particular type of work (e.g., ANSI/AWS D1.1-82, "Structural Welding Code - Steel").

Data reported in the literature generally conclude that the wet and wet-backed SMAW process can produce the Type B quality level for most structural steels.

Experiments including weld qualification tests per AWS D3.6 specification were performed on a 0.36 CE A-36 steel welded with the E6013 electrode (ferritic) and a 0.46 CE A-516 steel welded with a proprietary nickel-alloy electrode (austenitic). Dry welds, wet-backed welds and wet welds at 10, 20, 30, 35, and 60 m (33, 66, 99, 115, and 198 ft) were tested. The dry welds, ferritic wet welds at 10 m (33 ft), and austenitic wet-backed welds qualified as Type A as far as bend and tensile test requirement. However, since the all-weld metal tensile test was not performed, these welds cannot be qualified as Type A. Most welds qualified as Type B except some ferritic welds at 60 m (198 ft). Austenitic wet welds failed to pass the 6T bend test because pores opened up longer than 3.3 mm (1/8 in.). However, austenitic wet welds had very good toughness. Ferritic wet-backed welds also did not pass as Type B welds. These ferritic wet-backed welds were prepared with the E6013 electrode; had the E7018 electrode been used, they may have been acceptable.

The fact that some welds did not qualify as Type B indicates that the AWS specification is sufficiently discriminatory.

## 6.2 Effect of Variables on Weld Quality

The main variables identified through statistical analysis of data from the literature, from contractors, and from the experimental program are (in descending order of importance):

- Material Composition
- Depth
- Thickness
- Location of Notch in Weld (Weld or HAZ)
- Restraint

Material composition includes base metal and weld metal. The carbon equivalent (CE) of the base metal governs the hardenability of the HAZ (the limits of CE and choice of electrode were discussed previously). Thus, the material composition has a direct effect on ductility, susceptibility to cracking (RT/VT acceptability), and toughness. Bend test results were most dramatically affected; austenitic wet welds exhibited poor bend test ductility attributed to grain boundary segregates. A-36 base metal produces better RT/VT acceptability than low alloy steels, but the austenitic welds were generally tougher than their ferritic counterparts.

Increasing depth usually means poorer RT/VT acceptability, poorer bend test results, and poorer toughness. Possible mechanisms for this degradation with depth include the increase in porosity with depth. The orientation of elongated porosity, which is determined by the welding position, significantly affects the ability of the weld to pass the bend test. Limited crack growth

rate data available for underwater welds shows porosity has a significant effect on fatigue life and actually may retard the crack growth rate in the high cycle regime.

Another mechanism for the degradation of performance with depth is the changes in weld metal chemistry with depth and concomitant changes in microstructure. In the ferritic weld metal, the loss of manganese increases with depth. The loss of manganese with depth and increasing oxygen content with depth both shift the CCT diagram to a shorter time for a given cooling rate, resulting in a lower proportion of fine acicular ferrite. Acicular ferrite gives a higher resistance to cleavage fracture. Note that the loss of manganese can possibly be compensated by additional manganese in the electrodes used for deeper depth.

Thickness has a direct effect on cooling rate (thinner plates give higher cooling rates), since cooling is thought to be controlled primarily by conduction through the base metal rather than heat transfer directly into the water. Thickness has no apparent effect on ductility. Results from the literature show that the tensile strength is greater for thicker specimens, but in this study the welds generally broke in the base metal so this was not observed. Thicker specimens were observed to have a better RT/VT acceptability rate.

There is a significant interaction between thickness and the location of the notch for the fracture toughness. Specifically, the 12.7 mm (1/2 in.) ferritic welds had very tough HAZ relative to the toughness of the weld. The weld and HAZ toughness of the 25.4 mm (1 in.) ferritic welds were comparable to the lower toughness of the weld metal. This result is believed to be due to the observed tendency of the  $J_{Ic}$  and Charpy fractures to deviate from the 12.7 mm (1/2 in.) HAZ into the base metal, which was not observed for

the 25.4 mm (1 in.) welds. Also the 12.7 mm (1/2 in.) base metal may have been tougher than the 25.4 mm (1 in.) base plate. In general, however, the toughness measured from  $J_{Ic}$  and Charpy tests was greater when the notch was located in the HAZ.

Restraint was considered as a possibly important variable. The effect of restraint is to increase the state of residual stress and the possibility of cracking. Restrained welds showed poorer RT/VT acceptability. However, in the experimental program, restraint could not be shown to significantly effect the various test results.

Analysis of the literature and contractor data could not show significance for the effect of polarity, welding position, water temperature and salinity, and rod or wire diameter.

### 6.3 Material Property Data and Correlations

Hardness was measured with Vickers 1 kgf test. Maximum hardness was found in the HAZ in the untempered last passes, 334 HVN1.0 for the ferritic wet welds and 460 HVN1.0 for the austenitic wet welds. The hardness was found to be very localized, impressions 0.5 mm (0.02 in.) from the location of maximum hardness were found to be less hard by as much as 200 HVN. Results in the literature report hardness above 500 HVN. Wet-backed welds had much lower hardness than wet welds. The literature and contractor data suggested the following correlation:

$$\text{HVN} = 157 + 566 (\text{CE}) \text{ for wet-backed welds}$$

$$\text{HVN} = 282 + 566 (\text{CE}) \text{ for wet welds}$$

where: CE = carbon equivalent in percent.

In the experimental program, hardness could not be successfully correlated to the depth or thickness. Interestingly, none of the test results (e.g., bend test,  $J_{Ic}$  test, Charpy test, or tensile test) could be correlated to hardness, indicating hardness is not a factor in weld performance although it may be an indirect indicator for susceptibility to hydrogen cracking in ferritic welds.

Statistical analysis revealed that RT/VT acceptability increased with increasing plate thickness, decreasing water depth and increasing water temperature. RT/VT acceptability for A-36 plates was better than for low-alloy plates.

There was very little toughness, fatigue or Charpy data available from the literature or from contractors. Results from this study (applicable only to the two materials tested) suggest the following correlation of  $K_{Ic}$  to carbon equivalent, thickness, depth, and location of the notch (weld or HAZ):

$$K_{Ic} = 75.1(A) - 94.2(THICK) - .321(DEPTH) + 33.9(ZONE) + 201$$

where:  $K_{Ic}$  = fracture toughness, ksi/in.

[1.0 ksi/in. = 1.1 MPa/m]

A = 0 for A-36/ferritic weld,  
1 for A-516/austenitic weld

THICK = thickness in inches [1.0 in. = 25.4 mm]

DEPTH = depth of weld preparation in feet

[1.0 ft = 0.3048 m]

ZONE = 0 for weld metal, 1 for HAZ

$K_{Ic}$  for wet welds ranged from 33-163 MPa/m (30~148 ksi/in.) for ferritic weld metal and from 126 to 179 MPa/m (115 to 163 ksi/in.) for austenitic weld metal.

The correlation for Charpy impact toughness shows the same trends:

$$CVN = 26.6(A) - 25.7(THICK) - .0804(DEPTH) + 13.5(ZONE) + 52.1$$

where: CVN = impact toughness (ft-lbs). [1.0 ft-lb = 1.356 J]

CVN at -2°C (28°F) for wet welds ranged from 20~48 J (15~35 ft-lbs) for ferritic weld metal, and from 45~117 J (33~86 ft-lbs) for austenitic weld metal.

The apparent detrimental effect of thickness and beneficial effect of having the notch in the HAZ reflect the previously discussed observation that the 12.7 mm (1/2 in.) ferritic wet welds had very tough HAZ, and often the crack deviated into (preferred) the base metal in these tests.

The HAZ was generally tougher in all types of welds, and toughness was generally reduced by increasing depth.

A slightly better estimate of  $K_{Ic}$  can be obtained using the following correlation to the Charpy impact energy, CVN, in ft-lb:

$$K_{Ic} = 2.02(CVN) + 23(A) - .173(DEPTH) + 67.2$$

An expression which contains a 95 percent confidence limit on the intercept (lower bound) and which provides a conservative estimate of  $K_{Ic}$  for all test conditions studied (see Section 4.3.1) is:

$$K_{Ic} = 2(CVN) - .15(DEPTH) - 8$$

It is suggested that this relation be used as part of the design guidelines to estimate toughness from CVN data. The expression will give very low estimates of the toughness for CVN less than 40 J (30 ft-lbs), and if the estimate of toughness is not adequate, the guidelines suggest that the designer go to the expense of obtaining an estimate of  $K_{Ic}$  directly from  $J_{Ic}$  or CTOD type tests.

Bend test results are chiefly influenced by material composition (austenitic wet welds showed poor results) and depth (increasing depth decreased bend test performance, probably due to increased porosity with depth). The literature and contractor data suggested polarity may be significant (DCSP is better). The correlation to the primary variables was poor, but the bend test performance was highly correlated to either weld metal tensile strength or proportional limit, i.e.,

$$\text{BENDSCORE} = 3.13(\text{AWMPL}) - 128.3$$

$$\text{BENDSCORE} = 3.55(\text{AWMSU}) - 197.7$$

where: AWMPL = all-weld-metal proportional limit in ksi\*

AWMSU = all-weld-metal ultimate strength in ksi\*

Fillet weld break-over bend tests were performed on wet ferritic welds at three depths. None of the specimens bent over more than  $45^\circ$  before breaking, but all met the requirements for Type B welds.

All-weld-metal tensile tests were conducted on 25.4 mm (1 in.) thick wet ferritic welds at three depths. The correlation of the weld metal tensile properties (in ksi) to depth (in feet) was

---

\*1.0 ksi = 6.895 MPa

excellent; the following results were obtained:

$$(a) \text{ Proportional limit: } \sigma_{pl} = 70.4 - .104(\text{DEPTH}), \text{ ksi}^*$$

$$(b) \text{ Ultimate strength: } \sigma_{uts} = 81.4 - .088(\text{DEPTH}), \text{ ksi}^*$$

Analysis of the contractor and literature data gave the following relation for  $\sigma_{uts}$  of welds from transverse weld tension tests:

$$(d) \sigma_{uts} = 54.2 + 41.9(\text{THICK}) - .037(\text{DEPTH}), \text{ ksi}^*$$

since our results were based on all-weld-metal tensile tests from 25.4 mm (1 in.) welds, this expression reduces to the following for 25.4 mm (1 in.) welds:

$$(e) \sigma_{uts} = 96.1 - .037(\text{DEPTH}), \text{ ksi}^*$$

This expression predicts higher strength weld metal than resulted in these test welds as seen by comparing to Expression (b) above.

Transverse weld tensile test results from this study showed little variability because 76 percent of these tests fractured in the base metal, yielding identical results. The tendency to fracture in the weld increased with depth (and porosity). The fractures which occurred in the weld exhibited strength comparable to the base metal but failures were abrupt, exhibiting little ductility.

Fillet weld tensile tests were performed and all qualified as Type A welds, i.e., the shear strength exceeded 60 percent of the all-weld-metal tensile strength and 60 percent of the minimum specified base metal tensile strength. Shear strength ranged from

---

\*1.0 ksi = 6.895 MPa

310 to 379 MPa (45 to 55 ksi). The failures were ductile, i.e. considerable extension (sliding apart) took place prior to separation.

#### 6.4 Summary of Design Guidelines

Properties and conditions that could influence the performance of underwater wet and wet-backed welds include the state of residual stresses in the weld, yield strength, ductility, ultimate strength, susceptibility to and characteristics of discontinuities, rate of subcritical crack propagation due to fatigue and/or stress corrosion cracking, and fracture toughness.

The state of residual stresses is difficult to quantify even for dry welds. Due to lack of information, one must assume that residual stresses of magnitude equal to the yield strength of the weld metal may exist locally in underwater wet or wet-backed welds. If the direction of the residual stress under consideration is such that yielding of the base plate would occur prior to yielding of the weld metal, then the residual stresses should be assumed of magnitude equal to the base plate yield strength.

The yield strength of the wet and wet-backed weld metals in this program exceeded base plate yield strength, i.e. the welds were overmatched. Note that this overmatching could not be assured if these weld metals were used with higher strength base plate materials.

Reserve ductility of the wet or wet-backed welds should never be counted upon, i.e., the design should incorporate a "weak-link" that fails before the weld yields. Note that this can be assured by overmatching weld metal and providing weld reinforcement, techniques which are commonly used for dry welds. Thus,

incorporating a "weak-link" is just prudent design, and is not meant to alarm or detract from the usefulness of underwater welding.

The possibility of cracking, subcritical crack growth, and fracture should be dealt with explicitly. Again, this is prudent design procedure and should probably be followed in design of dry welded connections as well.

Assuming that wet welding has been selected as the best approach to the problem, the design guidelines proposed herein consist of a four step procedure as follows:

- 1) Evaluate the design problem (usually a repair or modification) for the solution which relies least on tensile stresses in the wet or wet-backed welds. Try to use as much redundancy as is reasonable, minimize restraint and use details which can limit the size of initial cracks. Examples are provided in Section 5.3.
- 2) Design the wet weld such that applied stress is below yield stress when the weakest link remote from the weld is fully yielded from the worst case load combination.
- 3) Check maximum stress in the weld for fracture based on the fracture toughness, maximum credible crack size, and appropriate stress intensity expression taking into account residual stress distribution in the weld. Alternatively the empirically based CTOD design curve could be used. Reduce stress by design change if necessary.

4) Check maximum frequently occurring alternating stresses in underwater weld to keep the range in stress intensity factor well below  $33 \text{ MPa}\sqrt{\text{m}}$  ( $30 \text{ ksi}\sqrt{\text{in.}}$ ), i.e., in the regime where the crack would grow faster in the base plate material. This assures that standard fatigue design procedures applicable to offshore structures will be satisfactory for the underwater weld. Reduce stress by design change if necessary.

Safety from overload tensile failure is assured by the limit state procedure Step 2. This procedure is more rational than simply specifying a factor of safety on tensile strength.

For the fracture assessment (Step 3) a system of safety factors is developed in Section 5.4. The system includes a factor on crack length (ranging from 1.0 to 4.0) based on how this crack length was estimated and design details (if any) to limit crack size. There is a reduction factor on toughness (ranging from 0.83 to 0.5) based on how the toughness was estimated (e.g., a  $J_{Ic}$  test could be performed (0.83), or the toughness could be assumed to be equal to the toughness of a similar material welded under similar conditions (0.5)). Finally, there is a factor on applied nominal stress (ranging from 1.2 to 1.8) based on the degree of redundancy. (The CTOD design curve has a sufficient margin of safety built into it and such factors are not applicable for the CTOD approach.)

The total effect of these factors when implemented in a fracture mechanics assessment can be equated to a total factor of safety. For example, consider the largest and smallest possible safety factors:

- Total factor of safety of 7.2 - no control of initial crack size, toughness estimated from a similar material, and no redundancy.
- Total factor of safety of 1.4 - crack control is provided by using discontinuous lengths of weld, toughness is estimated by performing a  $J_{Ic}$  test, and multiple redundancy is provided by the design.

Fatigue life calculations should be performed using realistic (unfactored) stresses, crack growth rate data, and crack lengths. The reduction in toughness described above should be used; this will provide a sufficient margin of safety on life.

#### 6.5 Conclusions

1. The data gathered from industry sources and from the literature, and the experimental data obtained provide a basis for the use of the wet and wet-backed SMAW process for critical structural applications provided the limitations of the welds are considered in the design.
2. Despite severe porosity which significantly reduces the net area, the tensile strength of the welds exceeds the rated strength of the ferritic electrode 414 MPa (60 ksi) and exceeds 552 MPa (80 ksi) for the austenitic welds. The shear strength of fillet welds exceeds both 60 percent of the base metal minimum tensile strength and 60 percent of the all-weld-metal tensile strength.

3. Ductility of these welds is limited. Maximum bend test radius for the deeper ferritic welds is 6T or 57.2 mm (2.25 in.). The austenitic wet welds could not bend to this radius without opening up pores greater than 3.3 mm (1/8 in.) and therefore did not qualify as Type B welds. Because these austenitic welds are very tough and strong and otherwise appear to be suitable for use as structurally critical welds, perhaps this requirement of AWS D3.6 Specification should be reconsidered for austenitic welds. The elongation for the ferritic all-weld-metal tests ranged from 6.3 percent to 12.5 percent.
4. The fracture toughness of the welds is sufficient to tolerate flaws (without initiating tearing) larger than those allowed under AWS D3.6 Specification 3.3 mm (1/8 in.) in the presence of stresses as high as the minimum strength of the weld metal 414 MPa (60 ksi). Wet-backed welds and wet welds made at 10 m (33 ft) have fracture toughness ( $K_{Ic}$ , derived from  $J_{Ic}$ ) greater than  $102 \text{ MPa}\sqrt{\text{m}}$  (93 ksi $\sqrt{\text{in.}}$ ). Initiation values of CTOD were greater than 0.09 mm (0.0034 in.). Simple fracture mechanics analysis yield a tolerable defect size of about 25.4 mm (1 in.) in the presence of stress as high as the strength of the weld metal, or about 6.4 mm (1/4 in.) in the presence of twice the minimum yield stress. The CTOD design curve procedure requires consideration of residual stress. The stress considered in a fracture assessment by the CTOD approach can be as high as twice the yield stress, and more conservative results are obtained. For CTOD of 0.09 mm (0.0034 in.), a tolerable defect size just greater than 3.3 mm (1/8 in.) is obtained.

5. The HAZ is as tough as the weld metal for 25.4 mm (1 in.) welds and tougher than the weld metal for 12.7 mm (1/2 in.) welds. Austenitic welds were much tougher than ferritic welds. Toughness decreases significantly with depth, probably due to chemical and microstructural changes as well as increasing porosity.
6. All fracture toughness tests failed in a ductile tearing mode. Four of 19  $J_{Ic}$ /CTOD tests with the crack in the HAZ exhibited a pop-in after some stable tearing. (None of the 29 tests of weld metal popped in.) The four plates were all 25.4 mm (1 in.) thick including a dry ferritic weld  $102 \text{ MPa}\sqrt{\text{m}}$  ( $K_{Ic} = 93 \text{ ksi}\sqrt{\text{in.}}$ ), a wet-backed austenitic weld  $256 \text{ MPa}\sqrt{\text{m}}$  ( $K_{Ic} = 233 \text{ ksi}\sqrt{\text{in.}}$ ), and a wet austenitic weld  $135 \text{ MPa}\sqrt{\text{m}}$  ( $K_{Ic} = 123 \text{ ksi}\sqrt{\text{in.}}$ ). All of the pop-ins arrested and stable tearing was resumed as the failure mode. The maximum crack jump was about 5.1 mm (0.2 in.).
7. The austenitic weld and HAZ Charpy specimens exhibited fully-shear, upper-shelf fracture at  $-2^\circ\text{C}$  ( $28^\circ\text{F}$ ). The wet ferritic weld metal was also upper-shelf at  $-2^\circ\text{C}$  ( $28^\circ\text{F}$ ). Dry and wet-backed ferritic welds and the HAZ of the wet ferritic welds were tougher than the wet ferritic weld metal but were generally not upper-shelf.
8. No cracks were observed either in NDE or in cutting up specimens except the ferritic wet-backed welds which were intentionally made with an improper electrode.

9. Porosity was excessive in the wet welds and increased with depth. Slag inclusions and lack of penetration were found. These discontinuities were acceptable within AWS D3.6 Specification.
10. Peak hardness in the last passes of the welds, particularly in the HAZ, was high. Ferritic welds exceeded 300 HV1.0 and austenitic welds exceeded 400 HV1.0. Since 1) no cracking was observed in the welds, 2) no brittle behavior was exhibited, and 3) hardness could not be correlated to bend test, toughness, or strength performance; it is concluded that the hardness is not a meaningful indicator of weld quality or performance.
11. Bend test performance correlates well with all-weld-metal yield and ultimate stress.
12. All-weld-metal yield and ultimate stress correlate very well (decreasing) with depth.
13. CTOD was shown experimentally to be linearly proportional to  $J$ . Since  $J$  and  $K$  are analytically related, all these toughness parameters are related.  $K_{Ic}$  (from  $J_{Ic}$ ) was correlated to CVN.
14. Design guidelines were formulated which focus on design to add redundancy, limit crack size, minimize restraint, and reduce stress in the weld. The design guidelines give a procedure for fracture analysis. An alternative procedure using the British CTOD design curve would also be applicable. Guidance on fatigue is also offered, but this is based on limited data. Example problems illustrate the applicability and workability of these design procedures.

Recommendations

1. Underwater wet and wet-backed welding should be allowed on marine structures where presently prohibited by companies or regulatory agencies. Underwater welding should be used carefully and limitations of the welds should be considered in the design.
2. More experimental data should be obtained on the fatigue crack growth rate, SCC susceptibility, and fracture toughness of these welds. There is presently enough material left over from the experiments to extract two compact specimens from each plate in the test matrix. In view of the expense of producing these plates, good use could be made of these specimens for the needed tests at a relatively small cost.
3. Testing should also be conducted on welds prepared in poor visibility and in other than the flat horizontal position.
4. Transverse weld tension testing could be eliminated from the AWS D3.6 Specification requirements for procedure qualification provided adequate bend test performance has been demonstrated. All-weld-metal tension tests are useful and should be considered in requirement for Type B welds. Hardness does not seem to indicate weld quality or performance, and maximum hardness requirements could possibly be raised. The allowable size of opened-up pores in the bend test could be increased for austenitic welds. Shear strength requirements of 60 percent of all weld metal strength can easily be obtained for Type B welds.

5. More research should be done on the chemical and concomitant microstructural changes that occur with depth. Weld chemistries and microstructures could be obtained on the scraps of underwater welds from this project. Porosity should also be quantified for the welds used in this project.
6. Research should be performed to document and demonstrate by example the design of underwater welded repairs in handbook form. The repairs should be analyzed by finite element methods to obtain hot spot stresses.
7. There is still a need for continued electrode development, particularly for an electrode to weld higher CE materials at depths greater than 10 m (33 ft).
8. Design guidelines, using those proposed herein as a starting point, should be examined and debated by a committee and eventually published in the form of recommended practice.

## APPENDIX A

### A.1 Documentation of Welding Parameters

Underwater electrodes were transported to the working depth using Sea-Con's patented "Electrode Transfer Device" which was pressurized to the approximate ambient pressure at the working depth. Waterproofing of the electrodes is very important but the techniques and coating are proprietary.

All plate surfaces and edges that were joined by welding were either sandblasted or ground to clean, sound base metal, removing all mill scale or rust that was present.

Plates were welded with the stringer bead technique using Sea-Con's proprietary electrodes. The E6013 electrode used has also been modified by Sea-Con.

Table A.1 shows relevant welding parameters including the initials of the diver, the amperage and voltage range, weld travel speed, and number of passes. This welding data was incomplete for the welds 266, 299, 21S and 21D.

### A.2 Visual and Radiographic Examination

All welds were visually inspected upon receipt at SwRI for the following defects:

- cracks
- surface porosity
- entrapped slag
- incomplete fusion (both at crown and at root after removal of backing bar)

Table A.1

Plate	Welder	Amp	Volts	Travel Speed (in/min)*	Passes
10-1	GLH	150	26	6 ~ 8	21
10-2	GLH	150	26	6 ~ 8	21
10-3	GLH	150	26	6 ~ 8	20
11-1	GLH	175	26	7.7	22
11-2	CAK	170	28	10	20
11-3	CAK	170	28	9.1	20
11F-1	GLH	150	28	5.6	3
11F-2	GLH	150	28	6	3
11F-1T	GLH	150	28	5.6	4
11F-2T	GLH	150	28	5.8	4
11B-1	CAK	170 ~ 165	25	10.6	20
11B-2	CAK	170 ~ 165	25	10.6	26
11B-3	CAK	175	30	11.1 ~ 6.6	24
12-1	CAK	180 ~ 150	24 ~ 18	9.1	25
12-2	CAK	150	22	8.1 ~ 7.9	25
12-3	CAK	170	28	9.1 ~ 12	27
12F-1	CAK	170	24	8.8	3
12F-2	CAK	170	24	10	3
12F-1T	CAK	175 ~ 170	24 ~ 28	7	6
12F-2T	CAK	175	22	6	6
13-1	CAK	165	28	11 ~ 12	34
13-2	CAK	165	28 ~ 30	10 ~ 12	27
13-3	CAK	165 ~ 160	24 ~ 30	12 ~ 13.3	33
13F-1	CAK	165	26	9	3
13F-2	CAK	165	28	6.5	3
13F-1T	CAK	165	28	3.5	5
13F-2T	CAK	165	28	5.8	5.
20-1	GLH	160	25	6	40
20-2	GLH	160	25	6 ~ 8	41
20-3	GLH	160	25	6 ~ 8	43
21T-1	CAK	170	28	10	45
21T-2	CAK	170	28	10	49
21-1	CAK	170	28	9.1	62
21-2	CAK	170	28	8.3	56
21-3	CAK	160 ~ 170	26 ~ 28	8.7	83
21R-1	CAK	170	28	9.1	57
21R-2	CAK	170	28	9.1	59
21R-3	CAK	170	28	10	70
21B-1	CAK	175	28	9 ~ 12	43
21B-2	CAK	170	28	10	44
21B-3	CAK	160	30	11.2 ~ 13.3	59
21S-1	(5/32 in.)	-	-	-	-
21S-2	(5/32 in.)	-	-	-	-

\*1.0 in. = 25.4 mm

Table A.1 (Continued)

Plate	Welder	Amp	Volts	Travel Speed (in/min)*	Passes
21D-1	-	-	-	-	-
21D-2	-	-	-	-	-
266-1	-	-	-	-	-
266-2	-	-	-	-	-
299-1	-	-	-	-	-
299-2	-	-	-	-	-
22-1	CAK	170 ~ 140	25 ~ 26	9.1 ~ 12	49
22-2	CAK	185 ~ 160	30 ~ 24	7 ~ 12	54
22-3	CAK	165	26 ~ 28	10 ~ 13.3	48
22R-1	CAK	180 ~ 150	28 ~ 30	10 ~ 12	56
22R-2	CAK	165 ~ 150	24 ~ 30	8.3 ~ 13.3	66
22R-3	CAK	165 ~ 155	26 ~ 30	9.1 ~ 14.1	62
22T-2	CAK	140	22	10 ~ 11	65
22T-2	CAK	160	20	10.9	42
23-1	CAK	165	26	12	73
23-2	CAK	165	26	12	77
23-3	CAK	170 ~ 155	24 ~ 30	12	82
23R-1	CAK	165 ~ 155	24 ~ 30	12	86
23R-2	CAK	165	24	12	79
23R-3	CAK	165 ~ 155	26 ~ 28	12 ~ 11	91
23T-1	CAK	165 ~ 150	26 ~ 28	12 ~ 11	50
23T-2	CAK	165 ~ 160	26 ~ 28	7.2 ~ 8	59
40-1	CAK	165	24	6.4 ~ 8	28
40-3	CAK	165	24	5.8 ~ 6.4	30
40-5	CAK	165	24	5.4 ~ 7.9	26
41-1	CAK	160	30	9	46
41-2	CAK	155 ~ 150	30 ~ 32	10	33
41-3	CAK	155-150	30 ~ 31	9.5	42
41B-1	CAK	140	30	8 ~ 6.3	23
41B-2	CAK	160	30	6.1 ~ 8.8	26
41B-3	CAK	155	30	5 ~ 13.3	24
30-2	CAK	165	24	6.4 ~ 6.7	13
30-4	CAK	165	24	5 ~ 5.6	11
30-6	CAK	165	24	5 ~ 5.6	15
31-1	CAK	155	32	13.3	13
31-2	CAK	155	30	8 ~ 11	14
31-3	CAK	155	30	11 ~ 12.5	14
31B-1	CAK	140 ~ 155	30	5 ~ 8.1	8
31B-2	CAK	140 ~ 55	30	8.5 ~ 10.9	10
31B-3	CAK	155	30	6.3 ~ 6	8

1.0 in. = 25.4 mm

- craters
- undercuts
- unacceptable weld profile or thickness.

Plates were examined with magnetic particle inspection by the contractor that prepared the welds and all pertinent welding data are reported along with the results of this inspection. The contractor prepared the radiographs, which were read and reported by the contractor. These radiographs were reviewed at SWRI and reshot if found to be inadequate. Macroscopic examination was performed on a transverse slice of each weld prepared by polishing and etching. The radiography and macroscopic examination are intended to reveal the extent of the following discontinuities:

- cracks
- porosity
- slag inclusions
- inadequate joint penetration
- incomplete fusion
- concave root surface
- melt-through.

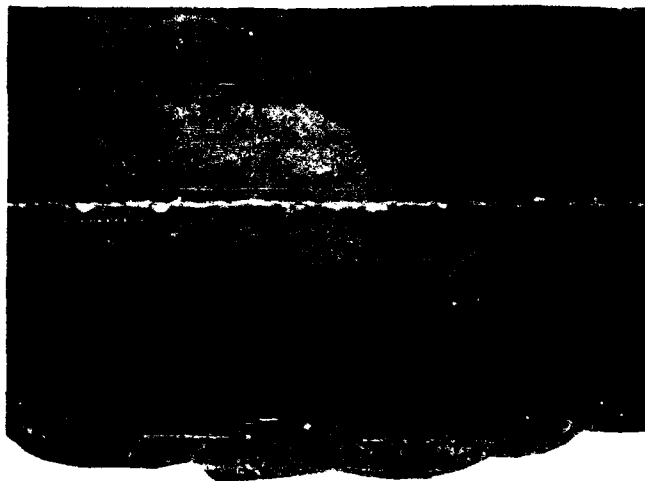
Visual examination indicated all plates were generally free from any obvious visible defects. After the backing bar was removed from the plates, most of the wet welded plates were found to have some inadequate joint penetration at the weld root. This inadequate joint penetration was manifest as two parallel grooves along the fusion lines, ranging up to 2.5 mm (0.1 in.) deep. The extent of this inadequate joint penetration is deemed to be acceptable within the AWS D3.6 Specification for Type B welds. In general, the problem was found to be more severe with welds prepared at deeper depths.

Specimens were generally suitable for testing. Holes, arc-strikes, and surface gouges in the base plate were found, but could be avoided by proper layout of the test specimens. The majority of the plates were winged or misaligned, a condition which results from cooling in the absence of restraint.

Magnetic particle examination reports indicated no detectable defects other than external defects such as poor bead profile, bead overlap, undercut, low weld-metal, surface porosity, and indentations. All of the above were deemed acceptable according to AWS D3.6 Specification for Type A welds.

Radiography and macroscopic examination revealed a variety of discontinuities. Porosity was, of course, prevalent in the underwater welds. In most cases, the extent of this porosity was deemed acceptable within the AWS D3.6 Specification for Type B welds. The density and size of the pores was found to be related to the depth of the weld. As an illustration of this phenomenon, three photographs of 25.4 mm (1 in.) groove weld macroscopic examination specimens prepared at different depths are presented in Figure A-1. Unacceptable slag inclusions were found in a few plates, but in most cases they were avoided during specimen layout. The inadequate joint penetration at the weld root was also detectable with radiography (RT).

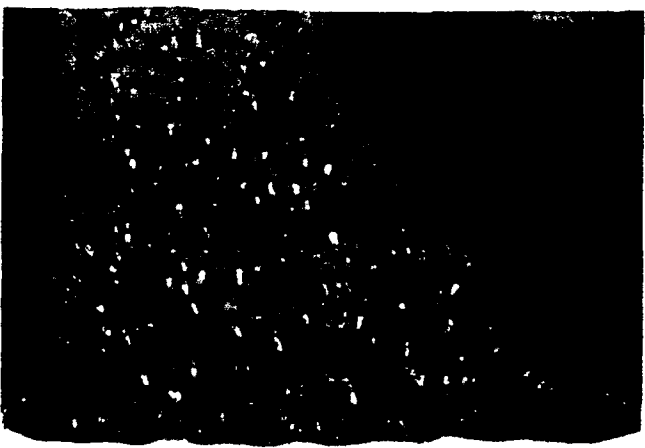
Recall that three groove weld test plates are available for each material/depth combination in the test matrix. One plate was used to extract compact tension specimens for  $J_{IC}$  tests, another plate used for Charpy impact test specimens, and a third for the macroscopic examination specimen, the transverse weld tension specimens, and the side bend test specimens. Plates which contained defects were generally used for the tensile and bend test specimens.



20-2  
Dry Weld



21R-1  
Wet Weld  
at 10 m  
(33 Ft)



23R-1  
Wet Weld  
at 60 m  
(198 Ft)

FIGURE A-1 MACROSCOPIC EXAMINATION SPECIMENS SHOWING INCREASED POROSITY WITH DEPTH

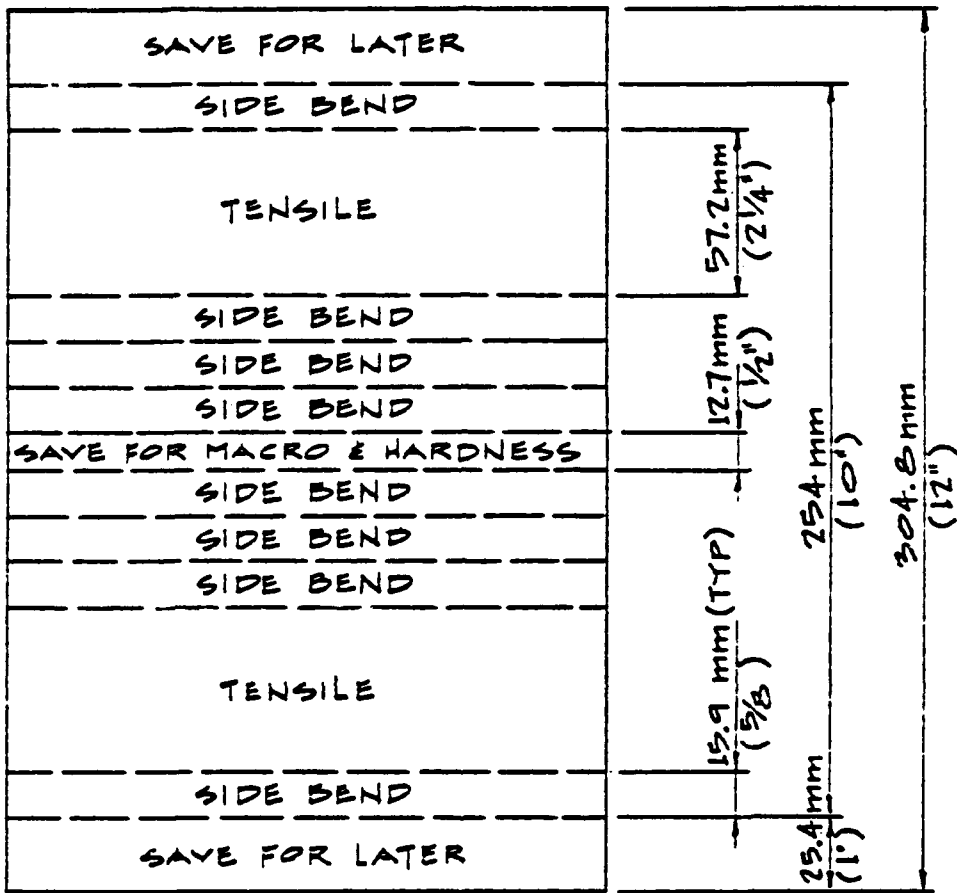
### A.3      Side Bend Tests

Figure A-2 shows the test plate layout and the location of the side bend test specimens. (Also shown is the location of the "macro" or macroscopic examination and hardness test specimen and the tensile specimens.) Note that 25.4 mm (1 in.) of material at the extremities of the plate are discarded.

The side bend test specimen is shown in Figure A-3. Figure A-4 shows the usual logic of the testing procedure. Recall that eight bend test specimens are prepared, but only seven tests are required to be performed. Usually, however, all eight specimens are tested. Four bend tests at 57.2 mm (2.25 in.) radius (6T) are performed on all plates. If none of these fail, remaining specimens are tested at smaller radii as shown in Figure A-4. AWS D3.6 Specification requires four 6T bend tests be performed for qualification as Type B welds. All four of these tests pass (i.e., not fracture or reveal any defects larger than allowed in the specification). Therefore, classification of the welds as Type B depends only on the first four tests. Often, one of the first four 6T bends failed, but further testing showed we could get four or more bends at 6T to eventually pass. These welds are still not classified as Type B.

Table A-2 presents the results obtained (pass or fail) on individual bend specimens. In addition, each weld has been rated as Type A, B, or C, (only insofar as the results of the bend test) and a relative score assigned to each plate according to the following system:

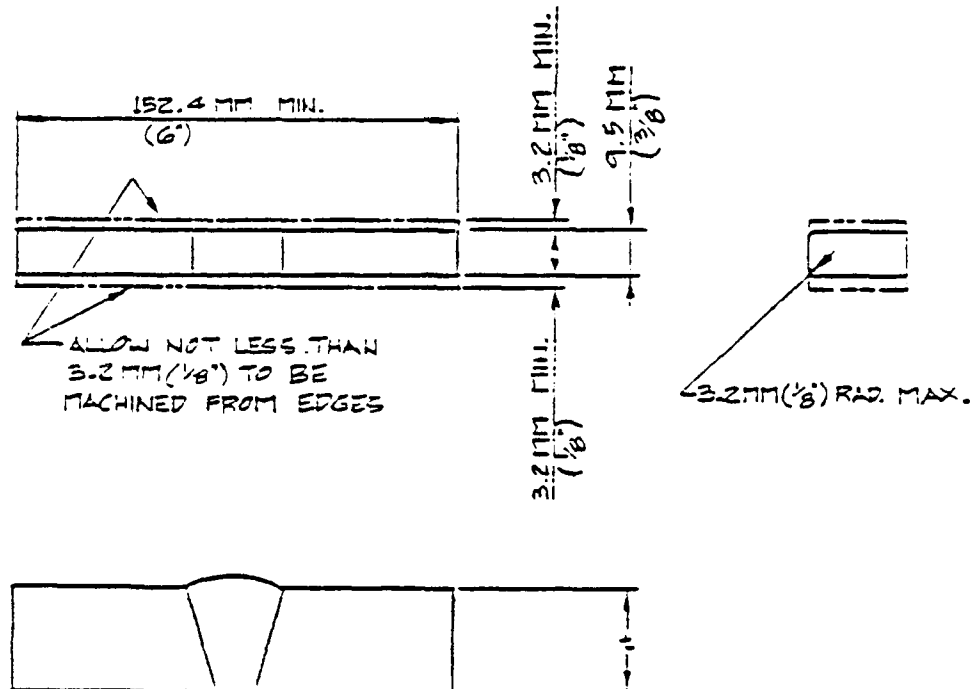
- Since the strain in the bend test is proportional to the radius of curvature, successful completion of a bend test is assigned a number of points inversely



NOTE

1. LEAVE ALL SPECIMENS FULL LENGTH & MACHINE AS SHOWN ON FOLLOWING PAGES
2. ALL SPECIMENS SHOWN 6.4 MM ( $\frac{1}{4}$ ) WIDER THAN REQ'D FINISHED SIZE TO ALLOW STOCK FOR SAW CUTTING

FIGURE A-2 LAYOUT OF TEST PLATE FOR QUALIFICATION TESTS



NOTE:  
1)  $t$  = PLATE THICKNESS

FIGURE A-3 SIDE BEND TEST SPECIMEN

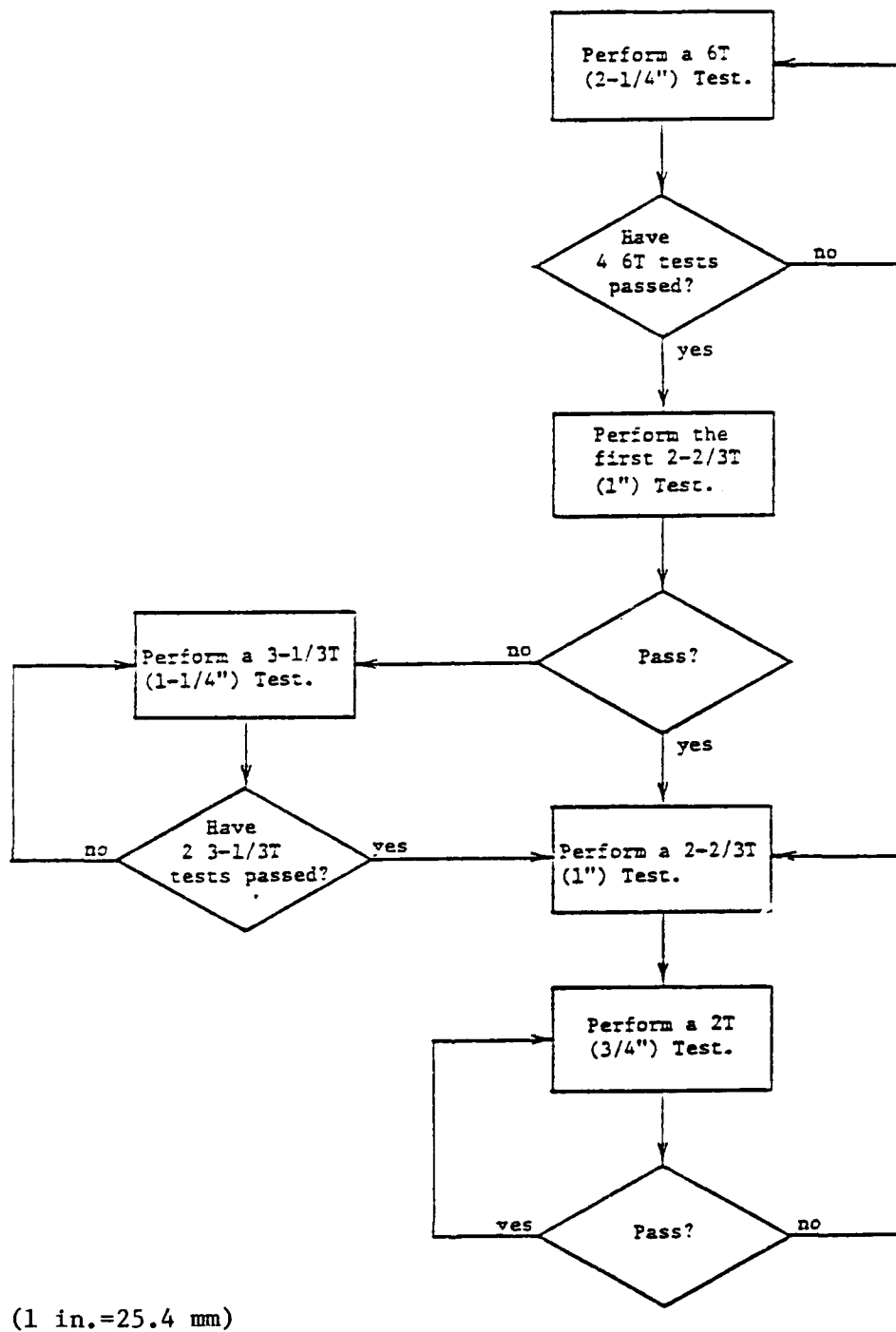


FIGURE A-4 SIDE BEND TEST PROCEDURE

TABLE A-2  
BEND TEST RESULTS

Weld Qualification: Type Specimen	Score	Air Welds			
		A36		A516	
		A 10-3	A 20-2	A 30-2	A 40-3
Bend Radius		100	94	100	94
6T		P	P	P	P
6T		P	P	P	P
6T		P	P	P	P
6T		P	P	P	P
2 2/3T		P	P	P	P
2 2/3T			P		P
2T		P	P	P	P
2T		P	P	P	P
2T		P	P	P	P

Notes:

P = Pass

F = Fail

A Qualifies as Type A as far as the bend test is concerned.

B Qualifies as Type B as far as the bend test is concerned.

C Does not qualify as a structural weld.

TABLE A-2 (Cont'd.)  
BEND TEST RESULTS

Weld Qualification: Specimen	Type	Wet-Backed Welds (33') (10 m)			
		A36		A516	
		C 11B-2	B 21B-3	A 31B-1	A 41B-3
Bend Radius	Score	8	63	88	88
6T		F*+	F+	P	P
6T		F*+	P	P	P
6T		F+	P	P	P
6T		P	P	P	P
6T		P	P		
6T		P			
6T		P			
2 2/3T			P	P	P
2 2/3T				P	P
2T			P	F	F
2T				P	P

Notes:

P = Pass

F = Fail

\* Large visible crack in machined specimen

+ In location of known defect

A Qualifies as Type A as far as the bend test is concerned.

B Qualifies as Type B as far as the bend test is concerned.

C Does not qualify as a structural weld.

TABLE A-2 (Cont'd.)  
BEND TEST RESULTS

Weld Qualification: Specimen	Type	Wet Welds (33') (10 m)							
		A36				A516			
		A 11-2	A 21-1	C 21S-1	B 21D-1	B 21R-1	C 31-3	C 41-3	
Bend Radius	Score	94	88	20*	80+	71	23	8	
6T		P	P	P	P	P	F	F	
6T		P	P	P	P	P	F	F	
6T		P	P	F	P	P	P	F	
6T		P	P	F	P	P	P	P	
6T							P	P	
6T							P	P	
6T							P	P	
6T							P		
2 2/3T		P	P				F	F	
2 2/3T		P	P				P		
2T		P	F				F		
2T		P	P	P			P		

Notes:

P = Pass

F = Fail

\* These scores were estimated since only four tests were conducted.

A Qualifies as Type A as far as the bend test is concerned.

B Qualifies as Type B as far as the bend test is concerned.

C Does not qualify as a structural weld.

TABLE A-2 (Cont'd.)  
BEND TEST RESULTS

Weld Qualification: Specimen	Type	A36 Air Welds 66', 99' and 115'				
		115' (35 m)		99' (30 m)	66' (20 m)	B
		B	B	B	299-2	266-2
Bend Radius	Score	45	58	45	50**	60**
6T		P	P	P	P	P
6T		P	P	P	P	P
6T		P	P	P	P	P
6T		P	P	P	P	P
3 1/3T		F	F	F		
3 1/3T		F	P	F		
3 1/3T		P	P	P		
2 2/3T		F	F	F		

Notes:

P = Pass

F = Fail

+ Large visible crack in machined specimen

\* In location of known defect

\*\* These scores are estimated since only four tests were performed.

A Qualifies as Type A as far as the bend test is concerned.

B Qualifies as Type B as far as the bend test is concerned.

C Does not qualify as a structural weld.

TABLE A-2 (Cont'd.)  
BEND TEST RESULTS

Weld Qualification: Specimen	Type	Wet Welds (198') (60 m)		
		B 13-1	C 23-3	C 23R-1
Bend Radius	Score	31	23	38
6T		P	F	F
6T		P	P	P
6T		P	P	P
6T		P	P	P
6T			P	P
6T				P
6T				P
3 1/3T		F	F	F
3 1/3T		F	F	
3 1/3T		F		
2 2/3T		F	F	
2 2/3T				
2T				
2T				
2T				

Notes:

P = Pass

F = Fail

+ Large visible crack in machined specimen

\* In location of known defect

A Qualifies as Type A as far as the bend test is concerned.

B Qualifies as Type B as far as the bend test is concerned.

C Does not qualify as a structural weld.

proportional to the radius, i.e., 1 point for completion of the 6T bend test, 1.8 points for the 3-1/3T, 2.25 points for the 2-2/3T, and 3 points for the 2T test.

- One point is subtracted for each 6T bend test that fails, since this test is essential for qualification.
- No points are subtracted for failed bend tests at smaller radii.
- The scoring is done on the basis of seven tests, including first all 6T bend tests (all failures plus those that passed, up to seven total). The remainder of the seven tests, if any, are chosen for maximum point value.
- The scores are then normalized by dividing by the highest score (13 points for 10-3 and 30-2) and the percentage is reported in Table A-2.

All the bend tests from the dry welded plates passed, qualifying all the welds as Type A as far as the bend test. It was observed that a very small 0.8 mm (1/32 in.) crack developed in the 12.7 mm (1/2 in.) A-36 plate, and that larger cracks 2.3 mm (3/32 in.) developed in both the A-516 plates. There was no dimpling on the bent surfaces from porosity observed in these specimens, nor was there any evidence of inadequate joint penetration at the root of the welds.

In the wet welds, the extent of inadequate joint penetration on both sides of the root is significant, and often

cracks would form near these discontinuities. Also, there are visible pores in the weld before bending which would open up or dimple on either face (compression or tension).

The ferritic wet-backed welds 11B-2 and 21B-3 both contained cracks which were clearly visible upon sawing the specimen blanks from the plate. Recall that these welds were prepared with the E6013 electrode, when the E7018 electrode is the electrode of choice for wet-backed welds. (The E6013 electrode was used for the dry and wet-backed welds as well as the wet welds to provide consistency in the test matrix.) The crack surfaces contained black and aquamarine (light blue) deposits, indicating the cracks probably occurred while the weld was still hot. These cracks were nearly through the thickness, longitudinal, and parallel to the vertical edge of the welds. As for 21B-3, this crack was isolated to one test specimen, but it eluded the radiographers. Radiographic indications were found for plate 11B-2 and it was called out to be about 38.1 mm (1.5 in.) long. However, this crack was found to extend through one-half of the plate. This plate (11B-2) failed to qualify as a structural weld. (The specimens selected for  $J_{Ic}$  testing from a companion plate, 11B-3, developed cracks along the fusion line when we tested it, the other  $J_{Ic}$  specimen from 11B-3 had a large through thickness crack that prevented precracking.) The performance of all bend test specimens of 21B-3 was good except the cracked specimen which was not tested, and we allowed this plate to qualify as a Type B weld.

All specimens from plate 21-1 passed with the exception of one of the 2T bends which fractured. A large 6.4 mm (1/4 in. dia.) slag deposit was observed at the root of this weld. After testing, upon review of the RT, it was noted that this slag was called out in the RT report by both SwRI and the contractor. It is still felt that this weld should qualify as Type A as far as the bend test.

In the restrained plate 21R-1 all the 6T bends passed. One of the 2-2/3T bends passed, but another developed a 3.3 mm (1/8 in.) crack which was associated with a void in the weld, and is therefore cause for rejection according to AWS D3.6 Specification. Slag was noted in the SwRI RT report in the location of this bend specimen, but was not reported by the contractor. One of the 2T bends passed, although the pores dimpled and some developed cracks up to 2.3 mm (3/32 in.) long. Another of the 2T bends fractured. There was no noticeable defect in this weld except for excessive porosity, and no defects were noted in either of the RT reports in this location. This plate would only qualify as a Type B weld as far as the bend test is concerned.

The austenitic wet welds prepared at 10 m (33 ft) yielded two failed 6T bends in the process of obtaining four 6T bends which passed. Strict interpretation of the AWS D3.6 Specification (on page 26, column 1, item (4) in section 4.5.2) would reject these plates as Type B welds. The austenitic wet-backed welds performed well, and both qualified as Type A welds.

Ferritic welds at 20, 30, and 35 m (66, 99, and 115 ft) all qualified as Type B welds, although 6T was about the limit of the consistently passing bend tests.

The ferritic welds at 60 m (198 ft) suffered generally from extreme porosity. The 6T bends all passed in plate 13-1, but cracks up to 2.3 mm (3/32 in.) long developed about the pores. One bend test was attempted at 2-2/3T or 25.4 mm (1 in. radius), but this specimen fractured. Three tests were then performed at 3-1/3T or 31.8 mm (1.25 in. radius). One of these fractured, and two developed cracks greater than 3.3 mm (1/8 in.) long associated with pores, therefore, all tests at less than 6T failed according to AWS D3.6 Specification. This qualifies this plate only as a Type B

weld as far as the bend test. The 25.4 mm (1 in.) plates from this same depth each failed one of the first four attempted 6T bend tests. Strict interpretation of the AWS D3.6 Specification would disqualify these plates even though four out of five successful 6T bends were obtained and even six out of seven for plate 23R-1. We, therefore, felt that these plates were satisfactory for further testing.

The bend tests seem to uphold the relationship between degradation of ductility in the welds with depth. There might also be preliminary indications that:

- The ferritic wet-backed welds made with the E6013 electrode have problems with cracking. This statement must be tempered with the knowledge that these welds are prepared with other than the ideal electrode (E7018) for wet-backed welds. We used the same ferritic electrode (E6013) as used in the wet welds to promote consistency for comparisons.
- Wet-backed welds made of the A-516 steel material with nickel alloy filler performed quite well, but the wet welds of this material combination could not qualify as Type B welds.
- The thicker plates welded underwater are more susceptible to severe porosity, and therefore, degradation in strength and ductility. This is apparent in comparing plates 11-2 vs. 21-1 and in plates 13-1 vs. 23-3. This is contradicted by the performance of plate 22-1 which performed better than the 12.7 mm (1/2 in.) weld at that depth 35 m (115 ft).

- Restraint may play some additional role in degradation of strength or ductility as evidenced by the poorer performance of plate 21R-1 vs. 21-1, and 22R-3 vs. 22-1. The general performance of 23R-1 was better than 23-3, but neither of these plates qualified as Type B welds.

#### A.4 Transverse-Weld Tension Test

The transverse weld tension test is a qualification test in which the weld is tested in tension perpendicular to the longitudinal axis of the weld. In order to pass, the weld must exhibit tensile strength as great as the minimum specified base metal ultimate tensile strength. The base metals used in the test program were ASTM A-36 structural steel (for specimen numbers with a first digit of 1 or 2) and A-516 pressure vessel plates, carbon steel, for moderate and lower temperature service (for specimen numbers with a first digit of 3 or 4). These specifications require the following tensile properties:

A-36 Steel:	minimum yield point	- 36 ksi
	tensile strength	- 58~80 ksi.

A-516 Steel (grade 70):	minimum yield strength	- 38 ksi
	tensile strength	- 70~90 ksi

The test plate layout showing location of the specimens is given in Figure A-2 and was discussed in the previous section. The test specimen is shown in Figure A-5. Because of the bad alignment of the plate and the inadequate joint penetration at the weld root, it was often necessary to mill the specimens down from full thickness to obtain a flat, unnotched specimen.

Table A-3 shows the ultimate strength, yield strength, and the average of the ultimate strength and yield strength (called

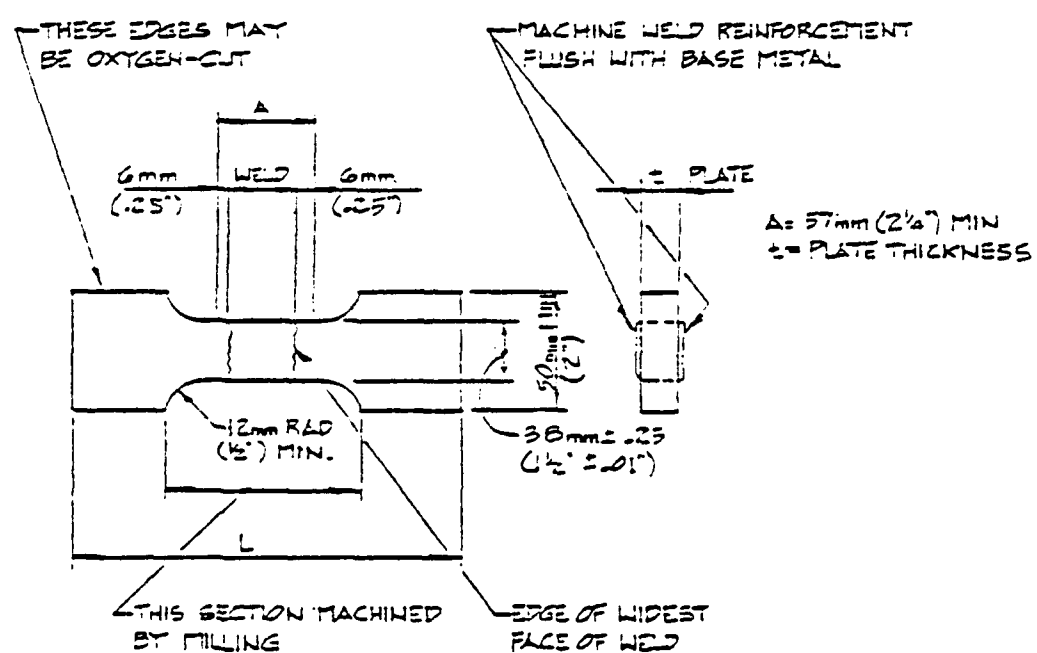


FIGURE A-5 TRANSVERSE-WELD REDUCED-SECTION TENSILE TEST SPECIMEN

TABLE A-3  
TRANSVERSE-WELD TENSILE TEST DATA

A36 Base Metal Ferritic Filler 1/2 in.				A36 Base Metal Ferritic Filler 1 in.				A36 Base Metal Ferritic Filler 1 in.			
			Depth				Depth				Depth
Spec #	13-1-3	13-1-11	23-3-33	23-3-11	23R-1-3	23R-1-11	23R-1-3	299-2-1	299-2-2	299-2-1	299-2-2
$\sigma_u$	73.1*	71.7*	70.5*	70.9*	69.9*	72.2*	70.9*	98.8*	102.0*	98.8*	102.0*
$\sigma_y$	55.6	56.2	46.6	46.0	46.8	49.5	49.5	Wet	Wet	Wet	Wet
$\sigma_f$	64.4	64.0	58.5	58.5	58.3	60.9	60.9	Wet	Wet	Wet	Wet
Spec #	12-3-3	12-3-11	22-1-3	22-1-11	22R-3-3	22R-3-11	22R-3-3	266-2-1	266-2-2	266-2-1	266-2-2
$\sigma_u$	74.4	73.5*	71.6*	67.4*	71.3	71.9	71.9	102.5*	106.0	102.5*	106.0
$\sigma_y$	52.2	58.4	48.8	52.2	47.6	47.5	47.5	Wet	Wet	Wet	Wet
$\sigma_f$	63.3	66.0	60.2	59.8	59.5	59.7	59.7	94.8*	75.0*	103.8	95.0*
								A516 Base Metal Austenitic Filler			
Spec #	11-2-3	11-2-11	21-1-3	21-1-11	21R-1-3	21R-1-3	31-3-3	31-3-11	41-3-3	41-3-11	41-3-11
$\sigma_u$	73.8	73.9	74.3	73.4	73.5	73.2	85.7	83.4	85.0	85.7	85.7
$\sigma_y$	57.2	56.1	51.5	51.3	46.5	46.0	69.9	64.0	55.5	49.9	33'
$\sigma_f$	65.5	65.0	62.9	62.3	60.0	59.6	77.8	73.7	70.2	67.8	Wet
Spec #	11B-2-3	11B-2-11	21B-3-11	21B-1-11			31B-1-3	31B-1-11	41B-3-3	41B-3-3	41B-3-3
$\sigma_u$	77.6	76.6	73.1	73.2			85.6	85.7	83.5	84.7	84.7
$\sigma_y$	68.7	61.1	45.0	46.5			70.0	72.0	49.7	54.8	54.8
$\sigma_f$	73.2	68.9	59.0	60.0			77.8	78.8	66.6	69.8	69.8
Spec #	10-2-2	10-3-11	20-2-7	20-2-11			30-2-3	30-2-11	40-3-3	40-3-11	40-3-11
$\sigma_u$	73.3	72.6	73.0	72.6			81.7	82.8	83.7	82.8	82.8
$\sigma_y$	49.0	50.8	47.6	47.6			57.2	57.7	54.9	54.5	54.5
$\sigma_f$	61.1	61.7	60.3	60.1			69.4	70.2	69.3	68.6	68.6
											Dry

$\sigma_u$  = ultimate tensile strength (ksi)

$\sigma_y$  = 0.2 percent offset yield strength (ksi)

$\sigma_f$  = flow stress =  $\frac{\sigma_y + \sigma_u}{2}$  (ksi)

\* = indicates fracture in weld metal

1.0 ksi = 6.895 MPa

1.0 in. = 25.4 mm

1.0 ft = 0.3048 m

flow stress) computed from the test data. All of the tests qualified as Type A as far as the tensile test is concerned (the requirements for Type A and Type B are identical with respect to the transverse-weld tension test).

It appears that, in general, the tendency to fracture in the weld metal increases with depth, and that this tendency is shared by both specimens from a given plate. The ultimate strengths of specimens fracturing in the weld metal are comparable to those fracturing in the base metal. However, the yield strength of specimens which fractured in the weld metal is noticeably smaller than the yield strength of similar specimens which fractured in the base metal. The load vs. cross-head displacement was autographically recorded during these tests. These curves reveal that the specimens fracturing in the weld metal failed at their ultimate load, while base metal fractures were much more ductile and continued to elongate.

Ultimate strengths of A-36 steel specimens ranged from 466 to 535 MPa (67.7 to 77.6 ksi). The welds prepared at 20 and 30 m (66 and 99 ft) as well as the weld made with a 4.1 mm (5/32 in.) electrode (21S and the double bevel weld (21D) at 10 m (33 ft) were prepared separately from the other A-36 steel specimens. With the exception of one test, the ultimate strength of these specimens ranged from a 48 to 731 MPa (95 to 106 ksi). Because of the higher strength plate apparently used, all but two of these failed in the weld metal. Note that this does not indicate the welds were any worse, only that the base metal strength was greater. Ultimate strengths of A-516 steel specimens ranged from 563 to 590 MPa (81.7 to 85.7 ksi).

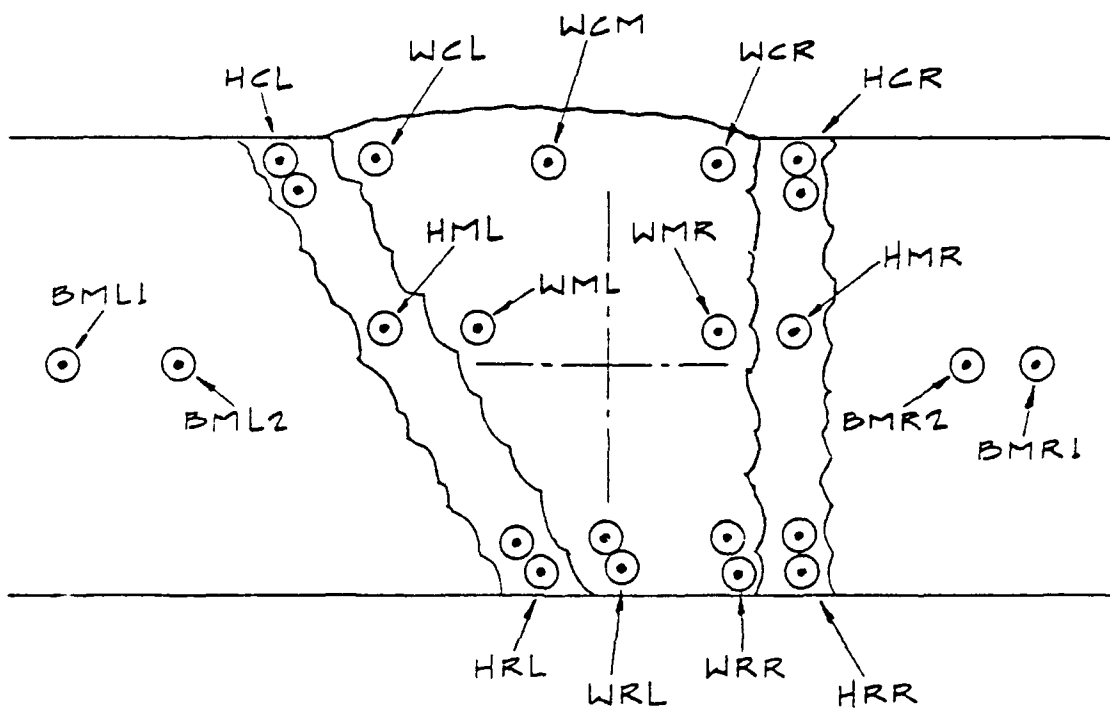
#### A.5 Hardness Traverse

Vickers Hardness Test (ASTM E 92) was performed on transverse sections of the weldments. Impressions were made in the general regions shown in Figure A-6 as well as a hardness traverse across the mid-thickness of the weld as shown in Figure A-7. AWS D3.6 Specification requires that impressions be made with a 10 kgf load. Due to specification limitations, we performed those tests with a 1 kgf load (HV1.0). There is probably not a significant difference in the results for the test, and the hardness data is all consistent for comparisons.

Plots of the hardness (HV vs. distance) were prepared from the hardness traverse across the mid-thickness (Figure A-7). An example of such a plot is given in Figure A-8 for the weld with the highest hardness. In general, the hardest area in this traverse is in the straight (vertical) heat affected zone. This corresponds to the location of the notch in Charpy and  $J_{Ic}$  compact tension specimens.

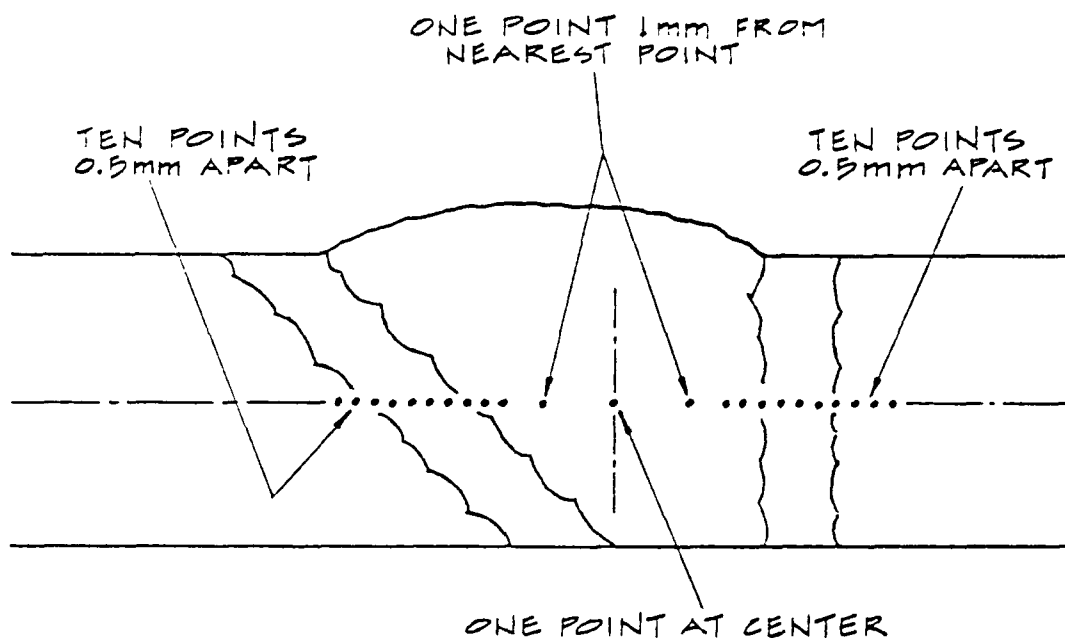
The hardest material (in all welds except the ferritic wet-backed welds) seems to be in the heat affected zone, particularly at the crown of the weld. (The last pass is expected to be the hardest since all previous passes are tempered.) For ferritic wet welds, this material had a Vickers hardness number (HV) of up to 334. (This is roughly equivalent to a Rockwell C Hardness Number of 34.) The HAZ hardness at the weld crown seems to be independent of depth and thickness for wet welds.

For austenitic wet welds, the hardness of the HAZ at the crown was up to 460 HV. Even at mid-thickness, the hardness traverse for 41-3 (shown in Fig. A-8) showed one point at 436 HV. Interestingly, only 0.5 mm (0.02 in.) away the hardness was only



Identify these points by region (ex. BML1 or WCM). Measurement of exact location of these points is not necessary, so long as impression is in the general vicinity indicated in the figure. If a pair of impressions are located in the region (such as HCL), identify the upper impression with a 1 and the lower impression (towards the root) with a 2.

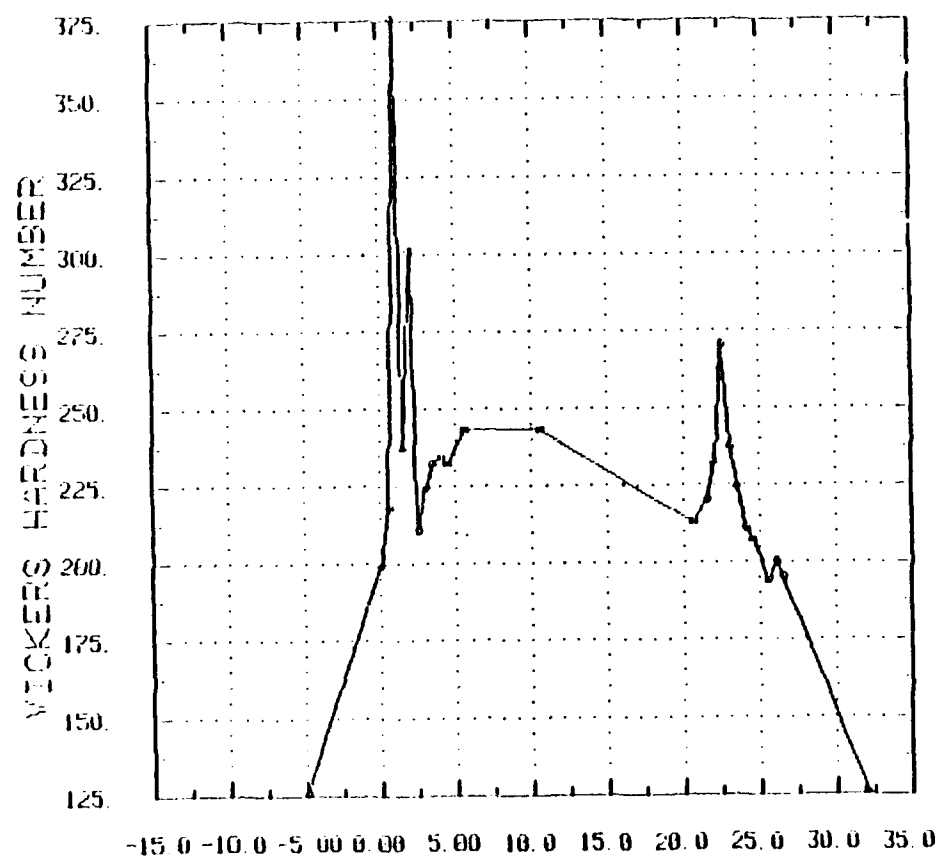
FIGURE A-6 PROCEDURE AND LOCATION OF HARDNESS IMPRESSIONS



A high density of points in a traverse along the mid-thickness of the weld is required. For these points, the distance along the traverse is required. Ten points at about 0.5 mm spacing should be centered on each HAZ such that the first point lies in the base metal and the tenth point lies in the weld metal. If the HAZ is greater than about 4 mm wide, change the spacing on the outermost points to get impressions at least 0.5 mm outside the HAZ. Finally, three points are required in the weld metal, one at the approximate centerline of the weld at mid-thickness and one each about 1 mm from the group of 10 points. Record the hardness from left to right from 1 to 23 along with the distance from point 1 in mm.

FIGURE A-7 PROCEDURE AND LOCATION OF HARDNESS TRAVERSE

VICKERS HARDNESS TRAVERSE - 1 KGF LOAD  
SPECIMEN 41-3 WET WELD(33 FT) 1 INCH THICK 6516



DISTANCE ALONG TRAVERSE (MM)

1 in. = 25.4 mm

1 ft = .3048 m

FIGURE A-8 HARDNESS TRAVERSE: SPECIMEN 41-3

218 and 237 HV on both sides. A point adjacent to where 460 HV was measured at the top (crown) of the HAZ in 41-3 had a hardness of only 260 HV, indicating that this extreme hardness is very localized.

The hardest material in the ferritic wet-backed welds was the weld metal.

Base metal hardness remote from the weld ranged typically from 135 HV to 165 HV for the A-36 material, and from 150 HV to 190 HV for the A-516 material.

Weld metal hardness varied typically from 170 HV to 180 HV at mid-thickness for the ferritic filler when welded wet or dry. The austenitic filler at mid-thickness ranged from 175 to 225 HV. The wet weld 25.4 mm (1 in.) thick at 10 m (33 ft) (as shown in Figure A-8) measured harder at about 250 HV. Ferritic wet-back welds were much harder in the weld metal at mid-thickness than their dry and wet counterparts; 11B-2 was about 225 and 21B-3 was 250 HV. (These plates, welded with an improper electrode, also were found to contain visible cracks and performed poorly in side bend tests.)

Weld crown hardness data are summarized in Table A-4. For the dry welds, the weld crown hardness was typically HV 190 to 215. The ferritic wet welds produced weld crown hardness of HV 180-250. The restrained had a range in weld crown hardness of HV 230 to 285.

#### A.6 Fillet Weld Break-Over Bend Test

The fillet weld break-over bend test is a qualification test for fillet welds designed to determine the ductility and

TABLE A.4  
WELD CROWN HARDNESS RANGE - HV

	12.7 mm (1/2 in.) Thick Ferritic	25.4 mm (1 in.) Thick Ferritic	25.4 mm (1 in.) Thick Restrained Ferritic	12.7 mm (1/2 in.) Thick Austenitic	25.4 mm (1 in.) Thick Austenitic
Dry	208-213	190-201		194-210	197-213
10 m (33 ft)					
Wet-Back	226-232	213-230		141-208	221-227
10 m (33 ft)					
Wet	199-247	203-249	227-283	196-210	193-413
35 m (115 ft)					
Wet	191-211	165-187	172-180		
60 m (198 ft)					
Wet	185-206	180-222	239-285		

fusion of fillet welds, i.e., for much the same purpose as the bend test for groove welds. The test specimen is shown in Figure A-9. The specimen is bent over until it is flat against the base or fractures. If it fractures, it may still be acceptable provided there is complete fusion and the fracture surface reveals no defects unacceptable according to AWS D3.6 Specification.

Six fillet weld break-over tests were conducted, two each for 11F (10 m (33 ft) 12F (115 ft) and 13F (198 ft). All specimens fractured when bent over 30° to 45°. Complete fusion was exhibited; the cracks ran at about 45° through the center or throat of the weld. Porosity was prevalent in the welds, particularly in 13F (the deeper weld). Although it is difficult to determine if 13F was within code requirements for porosity, it is judged that all these tests passed and are qualified as Type B fillet welds.

#### A.7 Fillet Weld Tensile Test

The fillet weld tensile test is a qualification test for fillet welds designed to determine the shear strength of the fillet welds. The test specimen is shown in Figure A-10. All four continuous welds to be sheared are measured with a steel rule, both legs and the throat, and the length of the welds is measured with a micrometer. The specimen is then pulled apart in a tensile machine and the ultimate load reported.

The resultant shear strength is computed. The results were reported in Section 3.2.5. For Type B welds this should be greater than 60 percent of the specified minimum tensile strength of the base metal. For Type A welds, the shear strength of the weld metal should be greater than 60 percent of the tensile strength of the weld metal, measured with an all weld metal tensile test. The results of all-weld-metal tensile tests are reported in Section 3.2.6.

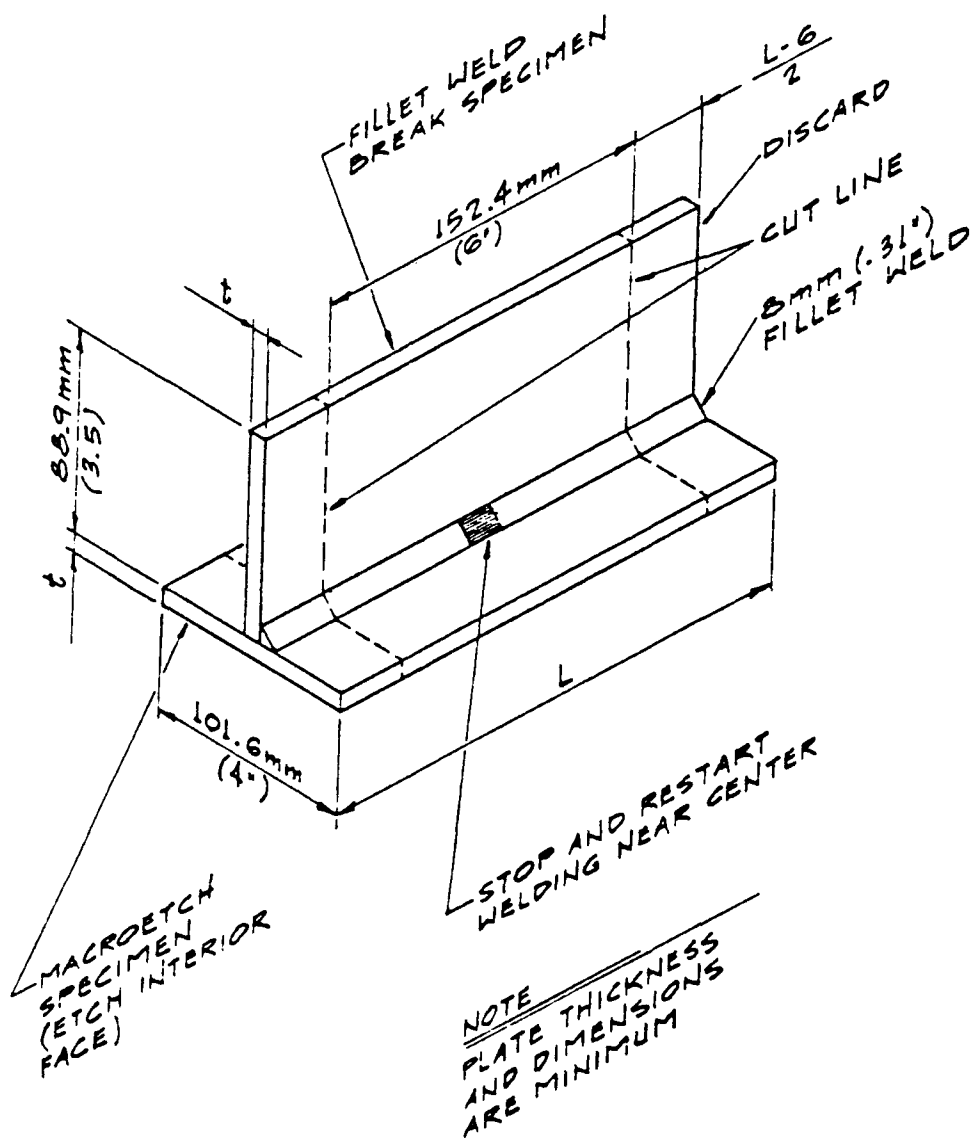


FIGURE A-9 FILLET WELD BREAK-OVER BEND TEST SPECIMEN

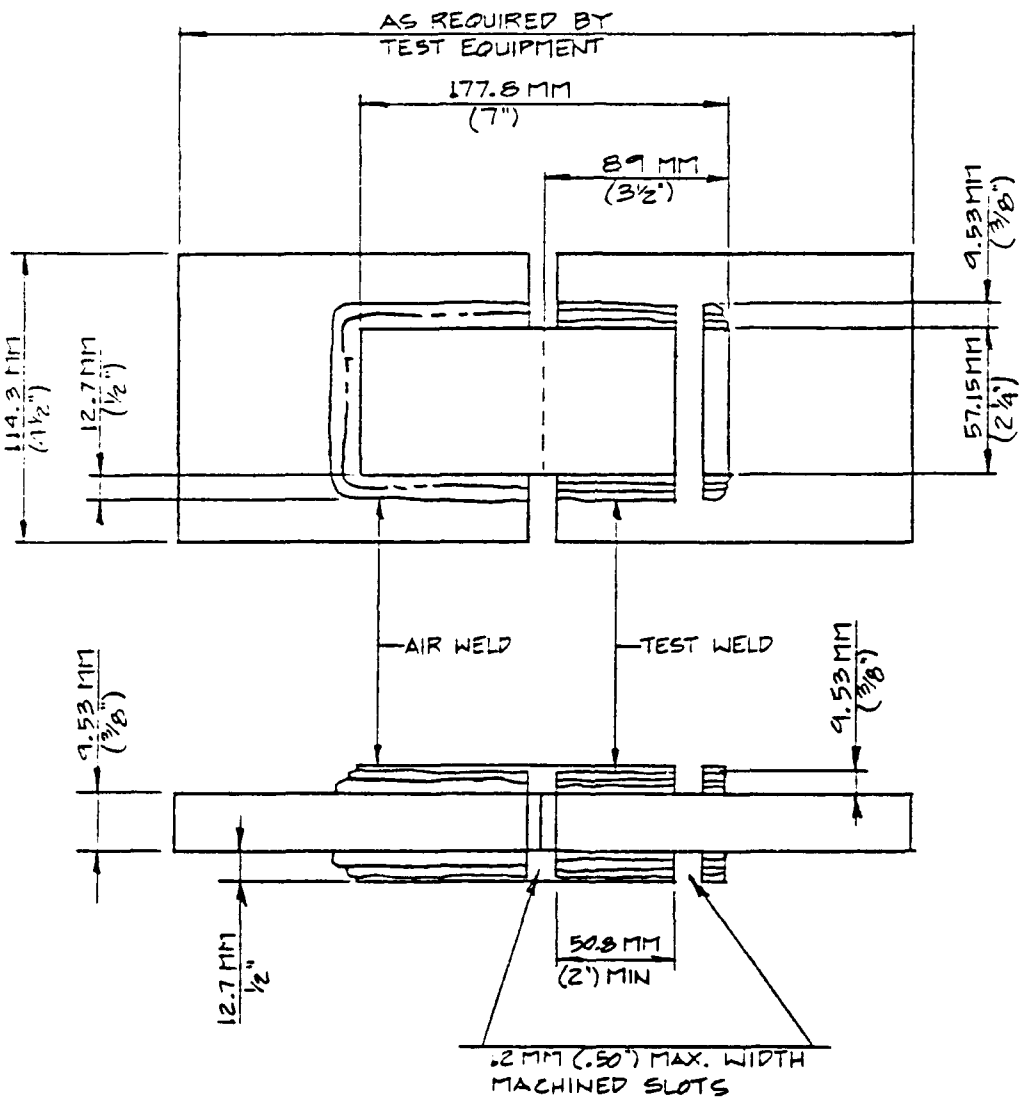


FIGURE A-10 FILLET WELD TENSILE TEST SPECIMEN

Six fillet weld tensile tests were conducted, two from 11F, 12F and 13F. Usually one side would fail first, the specimen would bend due to the eccentric load, then the second side would fail. On specimen 11F-2, after the first side failed the plate broke, but the ultimate strength is considered to be at the first failure. Specimen 13F-1 failed on both sides simultaneously.

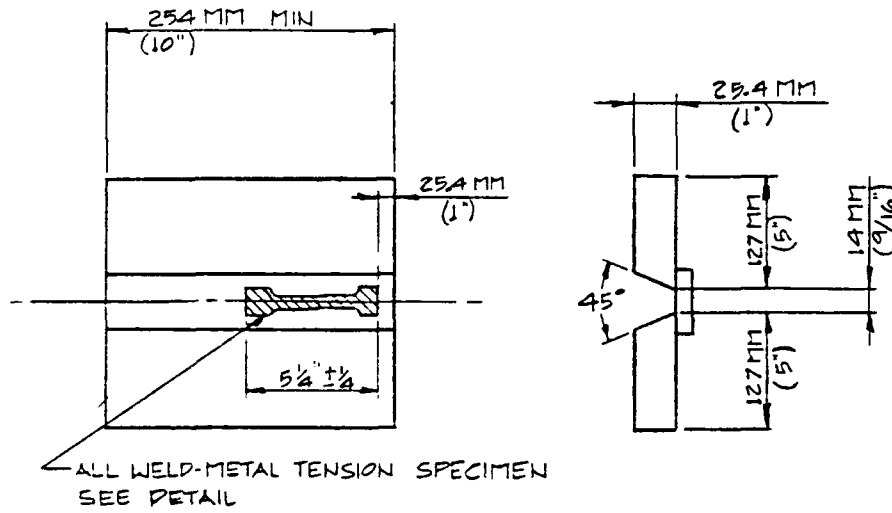
#### A.8 All-Weld-Metal Tension Test

All-weld-metal tension tests were conducted to determine the stress-strain behavior of the ferritic weld metal. Duplicate specimens (Figure A-11) were prepared from pairs of 25.4 mm (1 in.) thick plates welded at 10, 35, and 60 m (33, 115, and 198 ft and tested according to ASTM A 370 specifications. An extensometer was used to measure displacement of the 50.8 mm (2 in.) gage section up to 1.5 percent strain.

The AWS D3.6 Specification requires that for Type A welds, the yield point and ultimate tensile strength should meet or exceed the minimum requirements specified for the base metal. For the A-36 base metal, the required tensile properties are:

- Minimum yield point = 248 MPa (36 ksi)
- Minimum tensile strength = 400 MPa (58 ksi).

In addition, the AWS D3.6 Specification requires minimum elongation of 19 percent for Type A welds. The specification makes no requirements for all-weld-metal tension tests for Type B welds. The results of the six weld metal tests are summarized in Section 3.2.6. All of the tensile strength properties exceed the requirements, but the elongation ranged from only 6.3 to 12.5 percent. Therefore, this test limits all wet ferritic welds to Type B qualification. The stress-strain curves exhibited little work



TEST PLATE SHOWING LOCATION OF TEST SPECIMENS

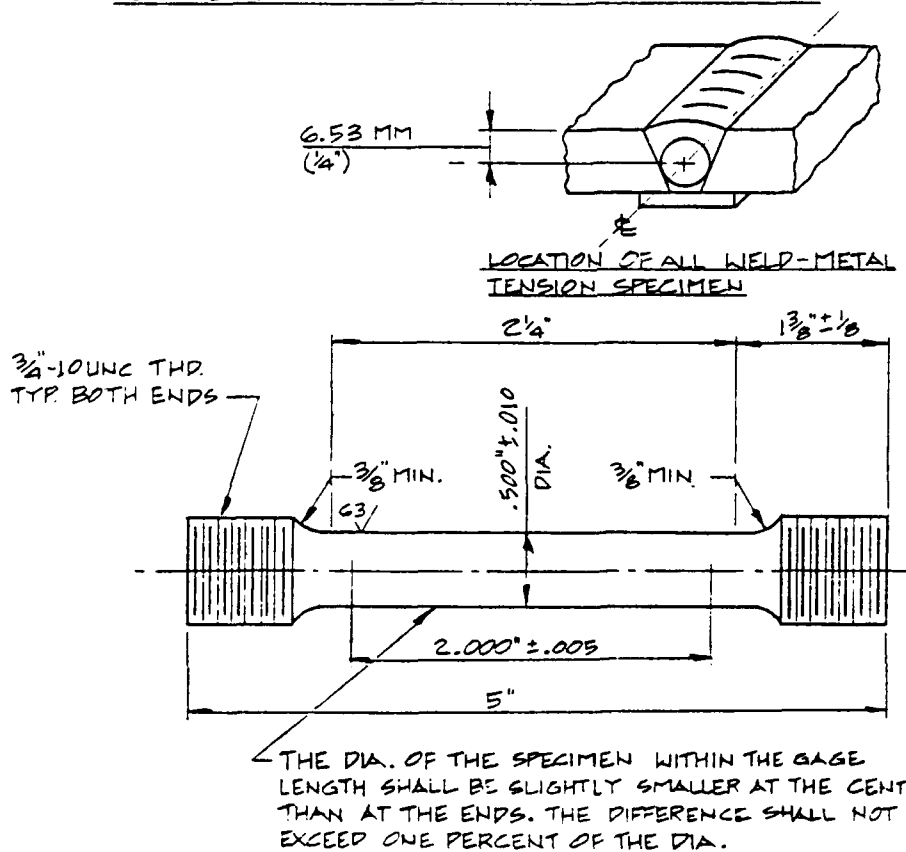


FIGURE A-11 LOCATION AND DRAWING OF ALL-WELD-METAL TENSILE TEST SPECIMEN

hardening. The yield point and tensile strength generally decrease with increasing depth.

#### A.9 Charpy V-Notch Impact Tests

Charpy specimens are taken from a plate according to the layout shown in Figure A-12. Two Charpys are tested at -2°C (28°F), two at 16°C (60°F), then four more are tested at various temperatures to locate the upper shelf of the transition curve. This set of tests is performed for notches located in the weld metal and in the heat affected zone, for a total of 16 tests for each groove weld.

The specimen is machined as shown in Figure A-13. Weld metal Charpys are machined with the notch located in the center of the weld at the elevation of the center of the specimen. The notch in the HAZ Charpy specimens was located in the straight or vertical heat affected zone by scribing a vertical line tangent to the scallops in the weld. Thus, the root of the notch would lie within 25.4 (1 mm) of the fusion line and entirely in the heat affected zone. Refer to Figure A-1 for a macro-etch section to visualize the location of this line.

For weldments not exhibiting full shear fracture appearance at 16°C (60°F), tests were conducted at 54°C and 93°C (130° and 200°F), and depending on these results at some intermediate temperatures. The -2 and 16°C (28° and 60°F) results are presented in Tables A-5 along with a summary of the upper shelf data. A separate page is devoted to each column of the test matrix, i.e. for each material/thickness combination.

Table A-5a shows the Charpy data obtained on the 12.7 mm (1/2 in.) A-36 plates welded with ferritic filler material. The

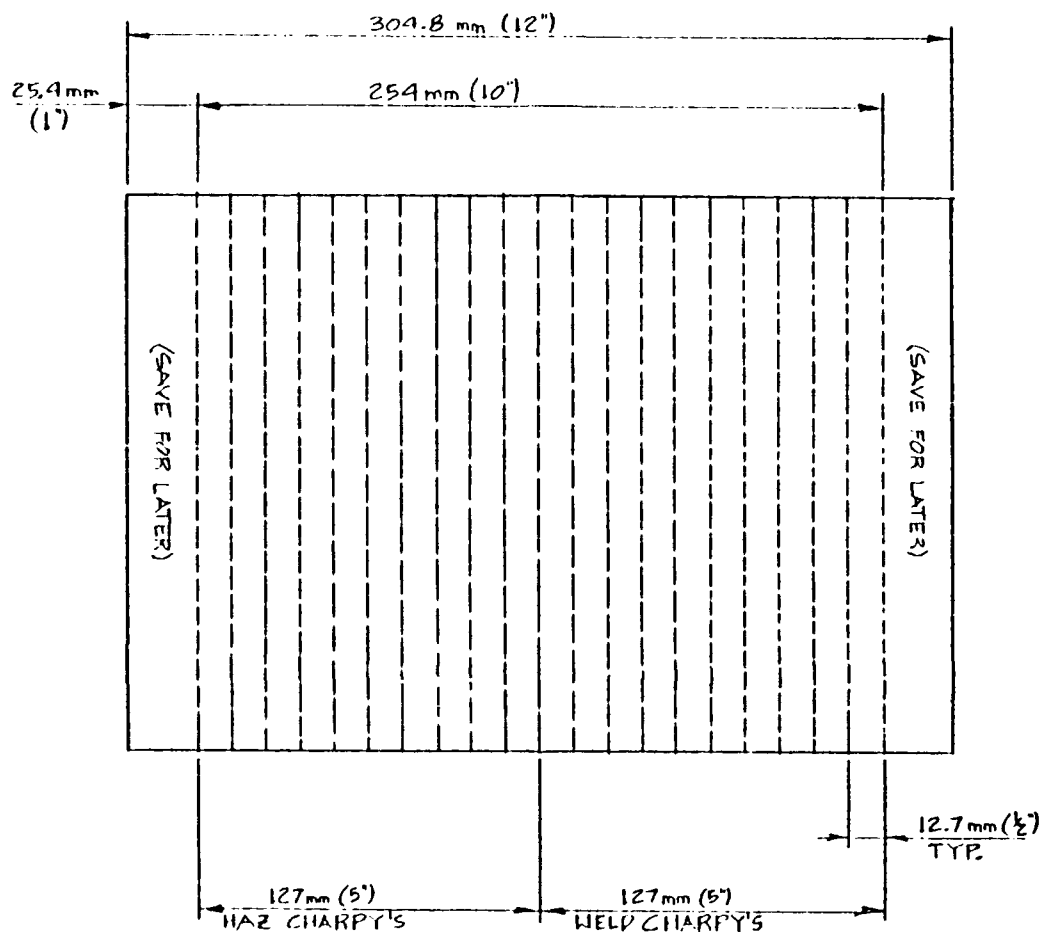


FIGURE A-12 LAYOUT OF TEST PLATE FOR CHARPY IMPACT TEST SPECIMENS

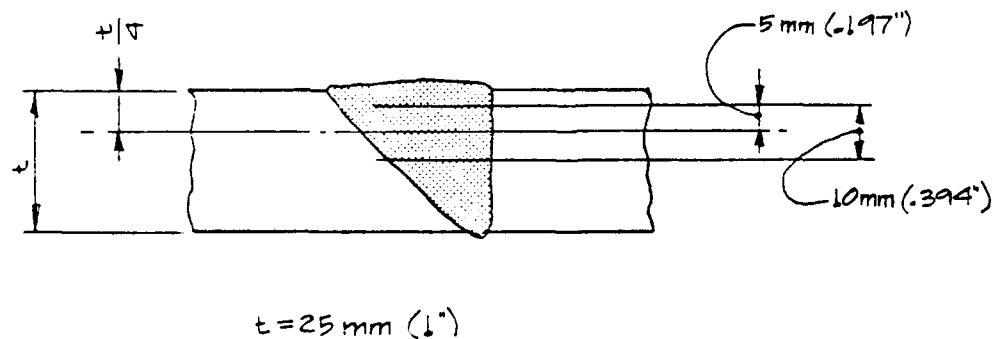
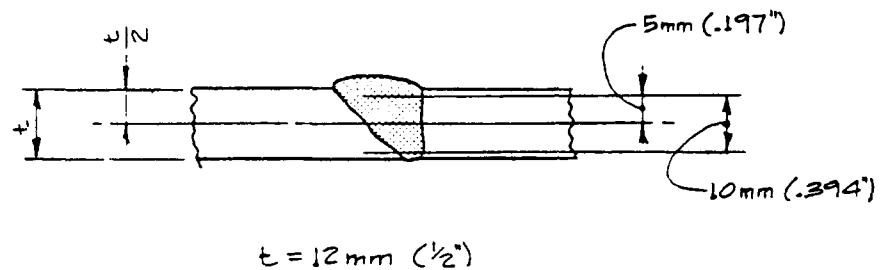
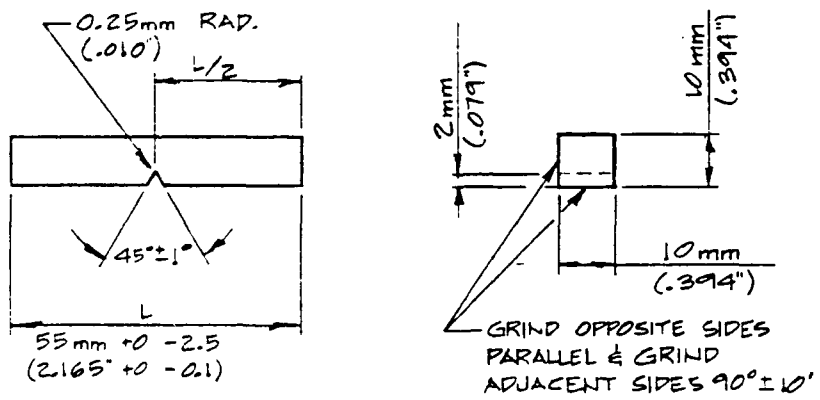


FIGURE A.13. CHARPY V-NOTCH IMPACT TEST SPECIMEN.

TABLE A-5a  
CHARPY DATA FOR 12.7 mm (1/2 in.) THICK 0.36 CE WITH FERRITIC FILLER

Depth	28°F		Weld Metal 60°F		Temp (°F)	Upper Shelf	
	Energy (ft-lbs)	Fracture App. %	Energy (ft-lbs)	Fracture App. %		Energy (ft-lbs)	Fracture App. %
60 m (198 ft)	22	100	20	100	28	20	100
Wet (13-2)	20	100	20	100			
35 m (115 ft)	24	100	27	100	28	24	100
Wet (12-1)	23	100	24	100			
10 m (33 ft)	34	95	39	100	28	37	100
Wet (11-3)	37	100	35	100			
10 m (33 ft)	20	30	36	50	200	47	100
Wet							
Backed (11B-1)	20	40	33	65			
Dry (10-2)	42	75	54	95	95	55	98
	45	80	53				
HAZ							
	28°F		60°F		Upper Shelf		
	50	100	50	100	28	50	100
60 m (198 ft)	48	100	52	100			
Wet (13-2)	8	10	11	20			
35 m (115 ft)	52	100	40	100	28	51	100*
Wet (12-1)	51	100	44	100			
10 m (33 ft)	50	98	54	100	200	83	97
Wet (11-3)	48	98	53	100			
10 m (33 ft)	54	97	56	95	28	55	97
Wet- Backed (11B-1)	55	97	54	95			
Dry (10-2)	51	100	53	28	55	100	
	55	100	54				

ft-lb=1.356 J

°F=1.8°C + 32

TABLE A-5b  
CHARPY DATA FOR 25.4 mm (1 in.) THICK 0.36 CE WITH FERRITIC FILLER

Depth	Weld Metal						Upper Shelf	
	28°		60°		Temp (°F)	Energy (ft-lbs)	Fracture App. %	Upper Shelf
Depth	Energy (ft-lbs)	Fracture App. %	Energy (ft-lbs)	Fracture App. %				
60 m (198 ft)	19	100	20	100	28	19	100	
Wet (23-2)	19	100	18	100				
35 m (115 ft)	23	100	27	100	28	23	100	
Wet (22-3)	21	100	23	100				
20 m (66 ft)	28	100	24	100	28	30	100	
Wet (266-2)	27	100	28	100				
	26	100						
	30	100						
30 m (99 ft)	20	100	22	100	28	21	100	
	18	100	20	100				
Wet (299-2)	21	100						
	18	100						
10 m (33 ft)	34	100	32		28	35	100	
Wet	30	100	41					
21D-2	35		32					
	31		41					
10 m (33 ft)	24	100	25		28	24	100	
Wet	23	100	21					
21S-2	20	100	25	100				
	20	100	21	100				
10 m (33 ft)	32	100	34	100	28	32	100	
Wet (21B-2)	30	98	32	100				
10 m (33 ft)	30	20	21	10				
Wet	26	20	23	15	130	47	100	
Backwd (21B-2)								
Dry (20-3)	41	65	47	95	130	54	78	
	36	65	47	95				

Depth	HAZ						Upper Shelf	
	28°F		60°F		Temp (°F)	Energy (ft-lbs)	Fracture App. %	Upper Shelf
Depth	Energy (ft-lbs)	Fracture App. %	Energy (ft-lbs)	Fracture App. %				
60 m (198 ft)	7	10	11	20	290	86	94	
Wet (23-2)	8	10	11	20				
35 m (115 ft)	24	92*	27	98*	130	37	100*	
Wet (22-3)	22	90*	27	98*				
10 m (33 ft)	8	15	11	25	200	83	97	
Wet (21-2)								
10 m (33 ft)	79	75	50	65	130	103	100	
Wet	48	40	73	65				
Backwd (21B-2)	8	15	10	25				
Dry (20-3)	10	10	30		200	86	100	
	10	10	28	25				

H-1581-356-A      D-1911-32

\* Fracture - compact tension test

TABLE A-5c  
CHARPY DATA FOR 25.4 mm (1 in.) THICK 0.36 CE WITH  
FERRITIC FILLER, RESTRAINED

Depth	With Restraint							
	28°F		Weld Metal		60°F			
	Energy (ft-lbs)	Fracture App. %	Energy (ft-lbs)	Fracture App. %	Temp (°F)	Energy (ft-lbs)	Fracture App. %	
60 m (198 ft)	15	100	18	100				
Wet (22R-2)	16	100	218	100	28	16	100	
35 m (115 ft)	19	100	19	100				
Wet (21R-1)	20	100	22	100	28	20	100	
10 m (33 ft)	31	100	32	100				
Wet (21R-3)	31	100	29	100	28	31	100	

Depth	With Restraint							
	28°F		HAZ		60°F			
	Energy (ft-lbs)	Fracture App. %	Energy (ft-lbs)	Fracture App. %	Temp (°F)	Energy (ft-lbs)	Fracture App. %	
60 m (198 ft)	21	2	6	0				
Wet (23R-3)	39	2	15	0	200	59	100*	
35 m (115 ft)	9	8	39	50				
Wet (22R-1)	22	20	43	20	200	59	100	
10 m (33 ft)	14	10	18	40				
Wet (21R-3)	7	10	16	40	200	69	100	

ft-lb=1.356 J

°F=1.8°C + 32

TABLE A.5d  
CHARPY DATA FOR 25.4 mm (1/2 in.) THICK 0.46 CE WITH AUSTENITIC FILLER

Depth	28°F		Weld Metal 60°F		Temp (°F)	Upper Shelf	
	Energy (ft-lbs)	Fracture App. %	Energy (ft-lbs)	Fracture App. %		Energy (ft-lbs)	Fracture App. %
10 m (33 ft)	37	100	38	100	28	37	100
Wet (31-1)	33	100	45	100			
10 m (33 ft)	47	100	53	100	28	49	100
Wet- Backed (31B-3)	49	100	54	100			
Dry (30-4)	54	100	57	100	28	54	100
	53	100	58	100			

Depth	28°F		HAZ 60°F		Temp (°F)	Upper Shelf	
	Energy (ft-lbs)	Fracture App. %	Energy (ft-lbs)	Fracture App. %		Energy (ft-lbs)	Fracture App. %
10 m (33 ft)	73	75	64	90	28	73	75
Wet (31-1)	63	100*	68	80			
10 m (33 ft)	71	65	103	95	60	103	95
Wet- Backed (31B-3)	89	70	114	95			
Dry (30-4)	106	85	110	100	28	104	85
	104	85	105	100			

\* Fracture jumped into the weld metal

ft-lb=1.356 J      °F=1.8°C + 32

TABLE A-5e  
CHARPY DATA FOR 25.4 mm (1 in.) THICK 0.46 CE WITH AUSTENITIC FILLER

Depth	28°F		Weld Metal 60 °F		Temp (°F)	Upper Shelf	
	Energy (ft-lbs)	Fracture App. %	Energy (ft-lbs)	Fracture App. %		Energy (ft-lbs)	Fracture App. %
10 m (33 ft)	50	100	42	100	28	52	100
Wet (41-2)	52	100	47	100			
10 m (33 ft)	49	100	49	100	28	49	100
Wet- Backed (41B-1)	49	100	50	100			
Dry (40-1)	53	100	55	100	28	57	100
	57	100	59	100			

Depth	28°F		HAZ 60°F		Temp (°F)	Upper Shelf	
	Energy (ft-lbs)	Fracture App. %	Energy (ft-lbs)	Fracture App. %		Energy (ft-lbs)	Fracture App. %
10 m (33 ft)	60	80~	47	100*	28	86	20
Wet (41-2)	86	20	52	100*			
10 m (33 ft)	81	15	85	10	60	96	20
Wet- Backed (41B-1)	85	20	96	20			
Dry (40-1)	53	85	64	100	130	91	100
	58	85	66	98			

~80% of the fracture jumped into the weld metal, the remaining 20% was brittle

\*Fracture jumped into the weld metal

ft-lb=1.356 J      °F=1.8°C + 32

results for the HAZ (full shear fractures, 65~75 J (48~ 55 ft-lbs) do not appear to depend on either depth or test temperature, and these results are similar to the weld metal, tested at 16°C (60°F).

The weld metal, wet-welded, exhibits full shear fractures at both test temperatures, but generally takes less energy to break as the depth (and porosity) increases (e.g. 27 J (20 ft-lbs) at 60 m (198 ft)). The air weld, tested at -2°C (28°F), exhibited some brittle behavior. The wet-backed welds appeared to have 30~40 percent shear at -2°C (28°F) and 50~65 percent shear at 16°C (60°F), and had energies of 27 J (20 ft-lb) for -2°C (28°F) and 45 to 49 J (33 to 36 ft-lbs) for 16°C (60°F), considerably worse than either the dry or wet welds at the same depth. (Recall the poor performance of these ferritic wet-back welds in other tests and the fact that this poor performance is undoubtedly attributable to the purposefully poor choice of electrode for these welds.)

Table A-5b shows the Charpy data for the 25.4 mm (1 in.) thick A-36 plate welded with a ferritic filler. Weld metal impact energies and fracture appearance at each depth are similar to the 12.7 mm (1/2 in.) plate. (Note the poor performance of the weld metal for the wet-backed welds.)

The HAZ fracture energy seems to be affected by the thickness. Where the HAZ fractures were generally full shear in the 12.7 mm (1/2 in.) plate, the wet 25.4 mm (1 in.) plate HAZ fractures were only 10 to 25 percent shear with impact energies from 9.5 to 15 J (7 to 11 ft-lbs). These results seem to be exclusively dependent on plate thickness and temperature as there is no distinguishable trend with depth.

The exception is the plate welded at 35 m (115 ft) where the HAZ had sufficient toughness to force the fracture to jump a

few millimeters away from the notch into the weld metal. The energy and fracture appearance of these specimens was similar to the results for weld metal at this depth.

The HAZ toughness of the air weld in the 25.4 mm (1 in.) plate was also lower than that of the 12.7 mm (1/2 in.) plate with impact energies of only 13.6 J (10 ft-lb) at -2°C (28°F) and 40.7 J (30 ft-lb) at 16°C (60°F). The HAZ performed very well for the wet-backed weld, having more energy but exhibiting a more brittle fracture appearance than the corresponding specimens from the 12.7 mm (1/2 in.) plate.

Table A-5c shows the data from the 25.4 mm (1 in.) A-36 plate with ferritic filler welded under restraint. The HAZ shows an improvement compared to the unrestrained 25.4 mm (1 in.) plate in Table A-5b. The weld metal, exhibiting full shear at all depths, seems to absorb slightly less impact energy than the unrestrained 25.4 mm (1 in.) plate.

Table A-5d and A-5e have the results for the 12.7 mm (1/2 in.) and 25.4 mm (1 in.) A-516 plate welded with an austenitic filler material. The weld metal exhibits a full shear fracture under all conditions, unlike the ferritic weld metal which exhibited brittle fractures in the wet-backed welds and in the dry weld at -2° (28°) only. Impact energies of the weld metal for the wet weld are similar to the ferritic welds at this depth; the dry weld impact energies were about 53 to 58 ft-lbs (10 ft-lbs higher than the corresponding ferritic weld). The 25.4 mm (1 in.) austenitic weld at 10 m (33 ft) (Table A-5d) exhibited higher impact energy at -2°C (28°F) than at 16°C (60°F) (a reversal of the usual trend). The Charpy energy at -2°C (28°F) in the 25.4 mm (1 in.) weld was higher than in the 12.7 mm (1/2 in.) weld.

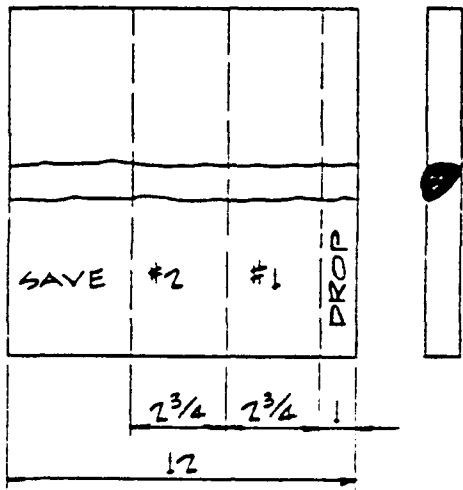
Like the ferritic welds, the HAZ toughness of the austenitic welds is adversely affected by the increase of plate thickness, especially significant in the dry weld. This is especially important since the difference in fracture toughness due to thickness could otherwise be explained away as a difference in constraint.

The 25.4 mm (1 in.) A16 plate HAZ notched specimens seemed to prefer fracturing in the weld metal several millimeters from the notch. Unlike the ferritic welds, which exhibited increased impact energy when this occurred, the austenitic welds exhibited less impact energy when the fracture jumped into the weld metal.

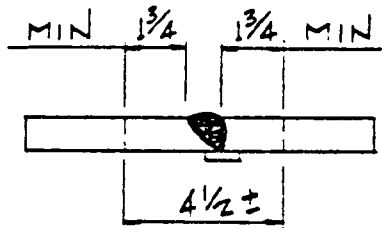
#### A.10 $J_{Ic}$ Tests

The test specimen layout, Figure A-14, allows for four blanks to be extracted, polished and etched. After careful consideration of notch placement, the final specimens were machined as shown in Figure A-15. (The location of the notch for these specimens was selected according to the same criteria for notch placement described for Charpy specimens in the previous section.) Two specimens were tested for each groove weld, one is precracked in the HAZ and another in the weld metal. There is sufficient material still on hand to extract two more compact specimens from each plate.

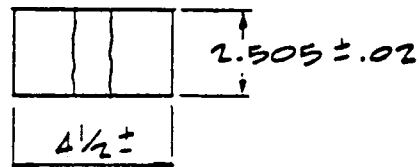
Table A-6 compiles the  $J_{Ic}$  test results. Also shown is the corresponding estimate of  $K_{Ic}$ .  $J_{2c}$  and  $K_{2c}$  represent a  $J$  measurement taken at an offset of 2 percent of the initial precrack length from the blunting line, and presumably  $K_{2c}$  is a closer estimate of the  $K_{Ic}$  that would be obtained from ASTM E 399 because of a similar point of measurement.  $T$  is the dimensionless tearing modulus, related to the slope of the  $J-\Delta a$  resistance curve by:



(A) SAW CUT (NO FLAME) 2 STRIPS APPROX  $2\frac{5}{8}$ " WIDE



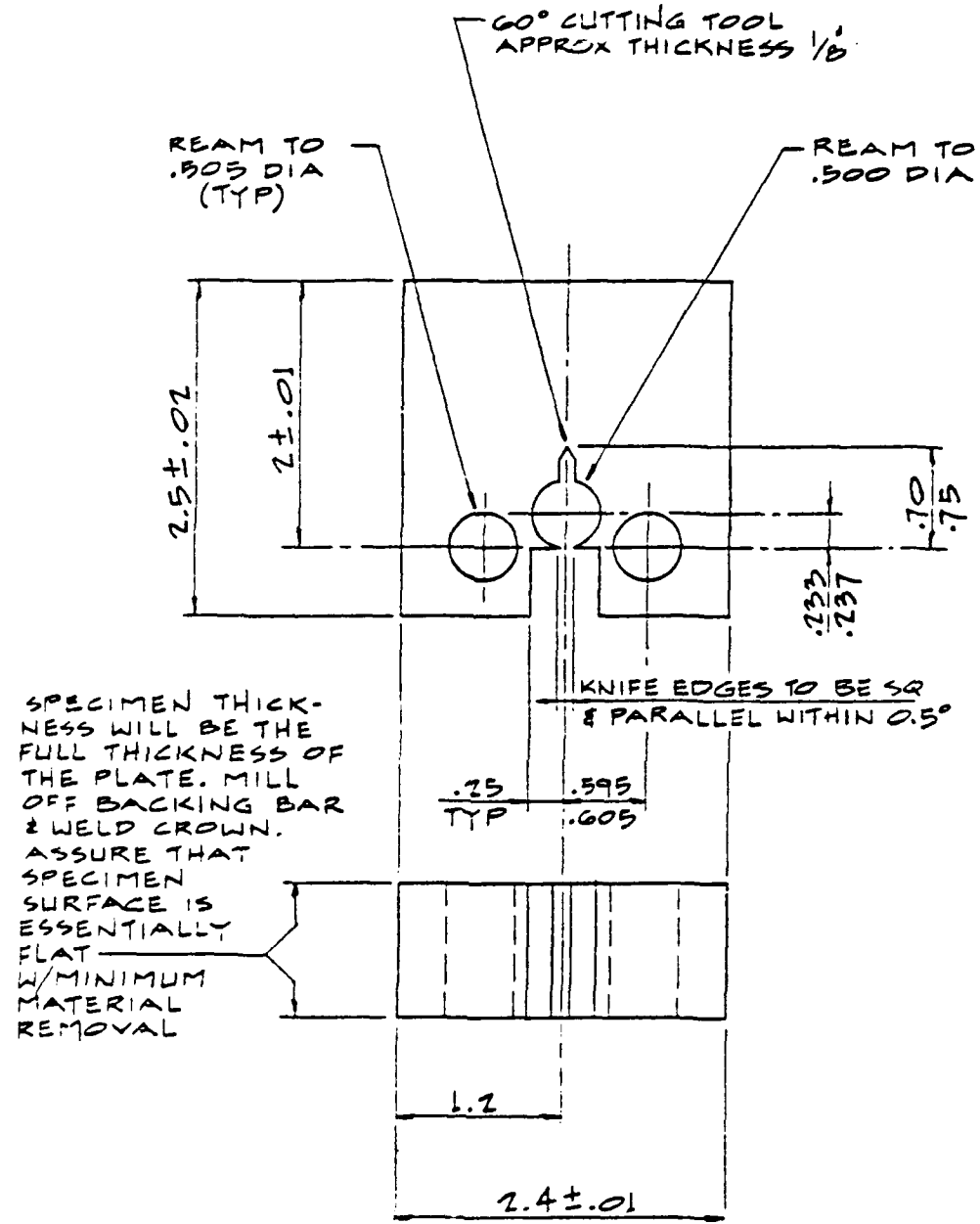
(B) SAW CUT A NOMINAL  $4\frac{1}{2}$ " LENGTH OF THE STRIP W/BOTH CUTS AT LEAST  $1\frac{3}{4}$ " FROM THE WELD CROWN



(C) MILL SIDES OF SPECIMEN BLANK DOWN TO  $2.505 \pm .02$  THEN POLISH & ETCH BOTH SIDES

Note: Dimensions shown in inches, 1 in. = 25.4 mm

FIGURE A.14 LAYOUT AND PRELIMINARY PREPARATION OF  $J_{Ic}$  TEST COMPACT TENSION SPECIMEN



Note: Dimensions shown in inches, 1 in. = 25.4 mm

FIGURE A.15  $J_{Ic}$  COMPACT TENSION SPECIMEN

TABLE A.6 COMPILED RESULTS OF  $J_{Ic}$  TESTS

<u>Specimen</u>	<u><math>J_{Ic}</math> in.-lb/in.<sup>2</sup></u>	<u><math>K_{Ic}</math> (ksi/in.)</u>	<u>2% Offset</u>		<u><math>T</math></u>	<u>Comments</u>
			<u><math>J_{2c}</math> (in.-lb/in.<sup>2</sup>)</u>	<u><math>K_{2c}</math> ksi/in.</u>		
<u>1/2-In. Ferritic Welds</u>						
10-1-2W	582	136	1731	235	259	*
10-1-3H	1981	251	2704	294	188	B
11B-3-3W	206	81	868	166	134	
11B-3-2H	526	130	1310	204	152	
11-1-1W	689	148	1405	212	166	
11-1-2H	748	154	1483	217	163	
12-2-1W	28	30	284	95	69	
12-2-2H	1478	217	2300	271	183	B
13-3-1W	185	77	422	116	60	
13-3-2H	1996	252	3164	318	237	BM, B
<u>1-In. Ferritic Welds</u>						
20-1-2W	1302	204	1841	242	152	
20-1-1H	273	93	487	125	68	NSP, P
21B-1-1W	480	124	1049	183	161	
21B-1-2H	890	168	1290	203	118	BM
21-3-1W	511	128	770	157	71	
21-3-2H	418	115	946	174	136	
21-3-3W	624	135	805	153	42	
21-3-4W	522	123	718	144	44	
21S-1-1W	435	112	637	136	46	
21S-1-2W	432	112	599	132	39	
21D-1-1W	833	160	1150	182	59	
21D-1-2W	308	95	469	117	37	
266-1-1W	358	102	543	125	47	
266-1-2W	397	107	602	132	53	
299-1-1W	416	110	589	131	49	
299-1-2W	309	95	48;	118	50	
21R-2-1W	298	97	644	143	105	
21R-2-2H	273	93	380	110	35	P

1.0 ksi/in.<sup>2</sup> = 0.175 kJ/m<sup>2</sup>      1.0 ksi/in.=1.1 MPa/ $\sqrt{m}$

TABLE A.6 COMPILED RESULTS OF  $J_{Ic}$  TESTS (Cont'd.)

Specimen	$J_{Ic}$ in.-lb/in. <sup>2</sup>	$K_{Ic}$ (ksi/ $\sqrt{\text{in.}}$ )	$J_{2c}$ (in.-lb/in. <sup>2</sup> )	$2\% \text{ Offset}$		$K_{2c}$ (ksi/ $\sqrt{\text{in.}}$ )	Comments
				1-In. Ferritic Welds	2-In. Ferritic Welds		
22-2-1W	78	50	262	96	67		
22-2-2H	390	111	544	132	49		
22R-2-3W	208	81	438	118	73		
22R-2-2H	121	62	341	104	67		
23-1-2W	111	59	302	98	64		
23-1-1H	121	62	281	95	53		
23R-2-2W	54	41	157	71	34		
23R-2-1H	80	50	554	133	133		
30-6-2W	2227	266	3468	332	211	B	
30-6-3H	3231	321	4596	383	241	B	
31B-2-1W	1668	231	2492	282	132	B*	
31B-2-2H	2176	263	3623	340	204	B, BM	
31-2-1W	830	163	1207	196	71		
31-2-2H	1359	208	2000	252	112		
40-5-2W	1414	212	3225	321	277		
40-5-1H	1647	229	2649	291	194		
41B-2-1W	1936	248	2992	309	211		
41B-2-2H	1706	233	2219	266	114	P	
41-1-1W	414	115	643	143	55		
41-1-2H	473	123	473	123	0	NSP, P	
1.0 in-lb/in <sup>2</sup> =0.175 kJ/m <sup>2</sup> 1.0 ksi/ $\sqrt{\text{in.}}$ =1.1 MPa/ $\sqrt{\text{m}}$							

TABLE A-6 COMPILED RESULTS OF  $J_{Ic}$  TESTS (Cont'd.)

Key to Comments

W	= Weld metal
H	= Heat-affected zone
*	= As explained in text, a better estimate of $J_{Ic}$ was obtained by including "invalid" points
BM	= Crack may have deviated from HAZ into basemetall
B	= Thickness requirement of ASSTM E 813 not satisfied
NSP	= Not sufficient points within bounds to satisfy ASTM E 813
P	= Pop-in or sudden large crack advance occurred

$$T = \frac{dJ}{da} \cdot \frac{E}{\sigma_f^2}$$

The tearing modulus is of interest regarding instability of the crack. While  $J_{Ic}$  is a measure of the resistance to slow stable crack advance, the criteria for instability in the structure include an applied  $J$  greater than  $J_{Ic}$  along with an applied  $T$  greater than the tearing modulus.

In a few of the cases the specimen thickness was insufficient to satisfy the requirements of ASTM E813 that this thickness be greater than  $25 J_{Ic}/\sigma_f$ . This was the case for only seven of the tests, namely Specimens 10-1-3H, 12-2-2H, 13-3-2H, 30-6-2W, 30-6-3H, 31B-2-1W, and 31B-2-2H, all 12.7 mm (1/2 in.) thick with  $J_{Ic}$  greater than  $263 \text{ kJ/m}^2$  ( $1500 \text{ in.-lb/in.}^2$ ). Previous testing [1] indicates that the value of  $J_Q$  probably overestimates  $J_{Ic}$  for these cases.

Other tests which do not meet the specifications of ASTM E813 include 20-1-1H, 23-1-1H, 23R-2-2W, and 41-1-2H. The problem with all of these tests was the existence of only two or three valid points between the limits of acceptable crack growth (the bounded region in the  $J$ -resistance curves). These points are used to perform the regression analysis to fit a straight line to the curve between the bounds. ASTM E813 requires at least four valid points, but by judging from nearby points slightly outside the bounded region, a good fit was obtained in all cases except 41-1-2H and the reported  $J_{Ic}$  is considered acceptable for these cases. The exception, 41-1-2H, experienced "pop-in" or a sudden large increment of crack growth early in the test and only four test points were obtained, all close to the blunting line. Actually, other points were obtained, as shown in Figure A-16 only  $\Delta a$  for these points was outside the bounded region of Figure A-17. However, since  $J_{Ic}$  is intended to measure the initiation toughness,

UNDERWATER WELDS - J1C FRACTURE TOUGHNESS PLOT  
SPECIMEN 41-1-2H

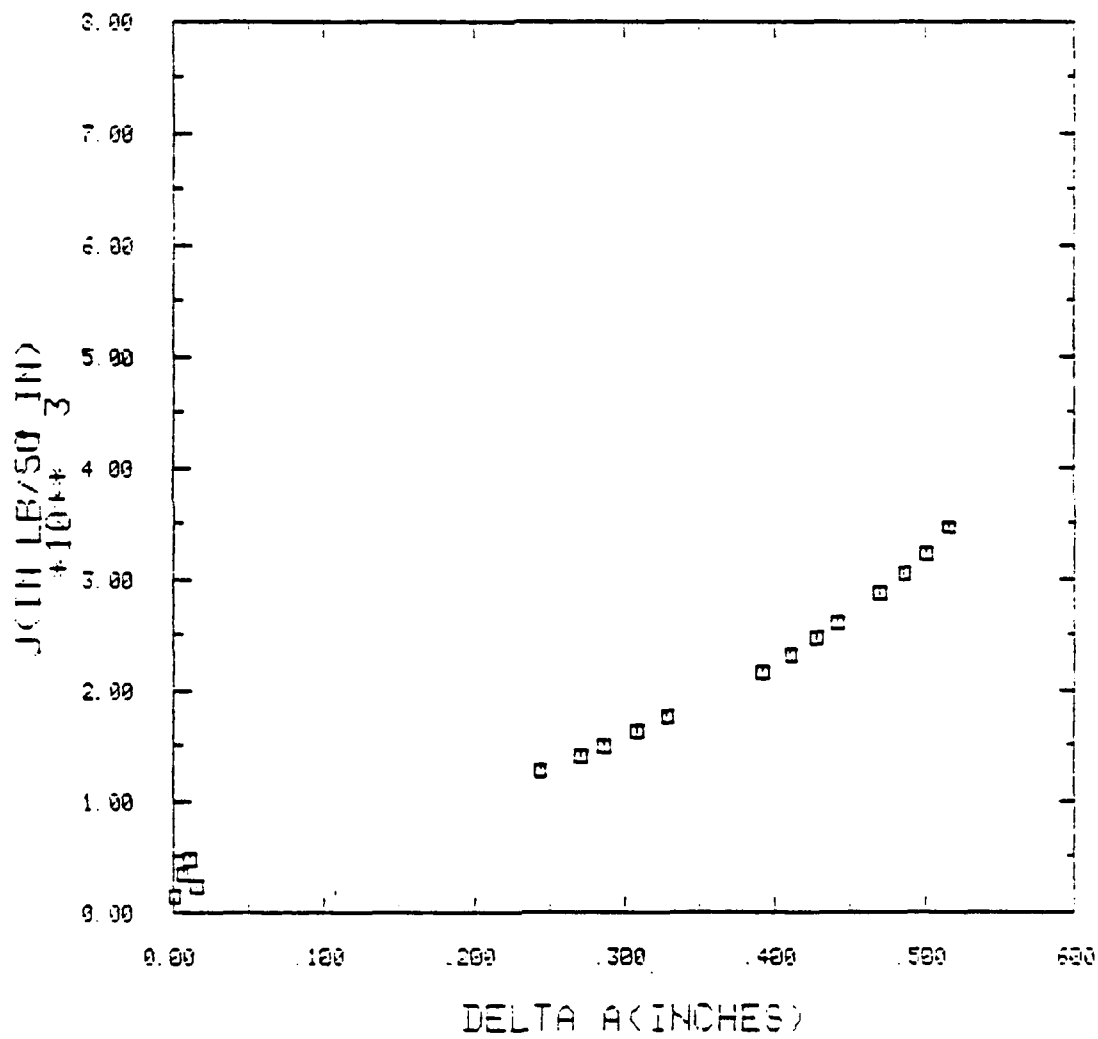


FIGURE A-16 FULL RANGE J-RESISTANCE CURVE: SPECIMEN 41-1-2H

Note: 1.0 in. = 25.4 mm  
 $1.0 \text{ in-lb/in}^2 = 0.175 \frac{\text{kJ}}{\text{m}^2}$

UNDERWATER WELDS - JIC FRACTURE TOUGHNESS PLOT  
SPECIMEN 41-1-2H

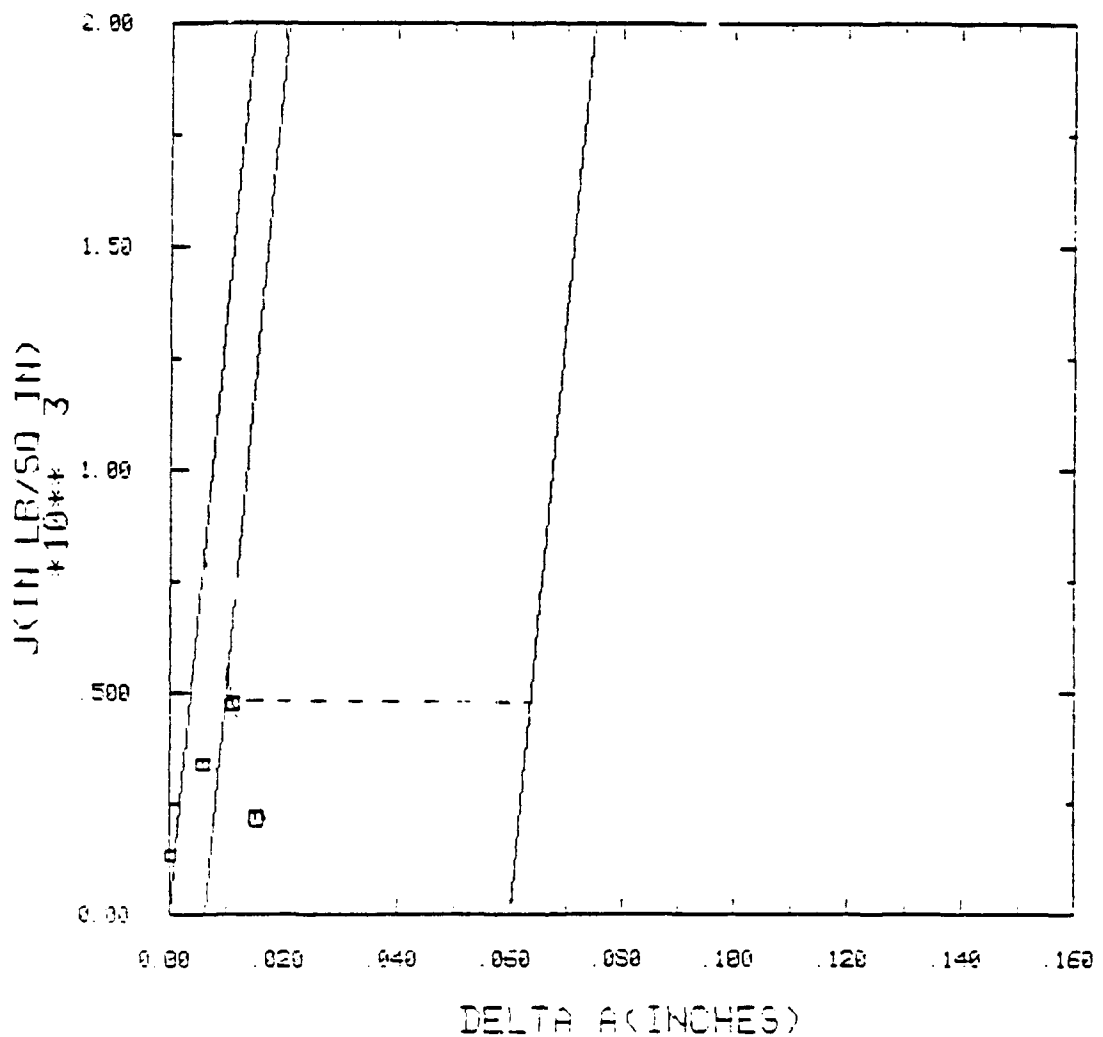


FIGURE A-17 J-RESISTANCE CURVE: SPECIMEN 41-1-2H

Note: 1.0 in. = 25.4 mm

$$1.0 \text{ in-lb/in}^2 = 0.175 \frac{\text{kJ}}{\text{m}^2}$$

the highest  $J$  reached before the "pop-in" is a conservative estimate of  $J_{Ic}$ . The tearing modulus for this case is estimated to 0.0, i.e., instability would occur whenever  $J$  exceeds  $J_{Ic}$ .

## APPENDIX B

### B.1. Variables in the Analysis

#### b.1.1 Grouping Variables

The grouping variables are the materials and conditions which define the test matrix. The following grouping variables were used in the analysis.

- WETORDRY

This variable was used in analysis of the total test matrix and the Weld Type Subgroup. It is arbitrarily assigned a value of 0 for dry welds, 1 for wet-backed welds, and 2 for wet welds.

- DEPTH

This variable is used in all analyses except the Weld Type Subgroup. It is assigned a value equal to the depth (in feet) at which the weld was prepared. Because many tests indicated the wet-backed welds gave results halfway between the dry and 10 m (33 ft) wet welds, it was convenient to assign to the wet-backed welds a depth of 5 m (16 ft) (half the 10 m (33 ft) depth at which they were prepared).

- THICK

This variable is used in all analyses but the Restraint Subgroup, and is assigned a value equal to

the plate thickness in inches (i.e., either 12.7 mm (1/2) or 25.4 mm (1.0)).

- RESTRAIN

This variable was used for analysis of the Restraint Subgroup only. It was arbitrarily assigned a value of 0 for welds prepared without restraint and 1 for welds prepared with restraint.

- CE

This variable is used in the analysis of the total test matrix and of the Weld Type Subgroup. It is equal to the carbon equivalent expressed in percent (i.e., either 0.36 or 0.46). Some confusion regarding the influence of CE could arise because the 0.46 CE plate was welded with an austenitic electrode. Thus another variable is used which is called "A" and is 0 for the A-36/ferritic welds and 1 for the A-516/austenitic welds.

- ZONE

This variable was used to distinguish between Charpy and  $J_{Ic}$  tests for which the notch or crack was located in either the HAZ or the weld metal. It was also used to distinguish between peak midplane HAZ hardness and weld crown hardness. It is assigned a value of 0 for weld metal and 1 for HAZ. Obviously, ZONE is not applied to group test results like bend test data, because there is no relation to HAZ or

weld metal. The ZONE variable was used in all analyses.

- TEMP

This variable, used in all analyses, is applied to results of the Charpy impact tests, which were performed at -2°C (28°F) and 16°C (60°F), plus many temperatures above 16°C (60°F) selected to determine the temperature at which full-shear upper shelf behavior occurred. The value assigned to the variable is the test temperature in degrees Fahrenheit.

#### B.1.2 Results of Tests

The results of tests were separated into groups defined by the above variables and were statistically analyzed to determine the effect of the grouping variables. These effects were subsequently quantified with regression analysis. Regression analysis was also used to try to predict test results that are expensive to obtain (e.g.,  $K_{Ic}$ ) from test results more easily obtained (e.g., Charpy impact energy).

Not all test data were useful in the statistical analysis. For example, results from the transverse weld tension tests (which mostly failed in the base metal) could not be used because they exhibit little variability and seem to only indicate base metal strength, which of course is fairly constant. The following dependent variables were used to evaluate weld performance.

- BENDSCORE

The bend test data could be examined on a pass/fail basis for each test, or on a number of pass/number of failure basis for each bend radius. However, these results are not as useful as the Bendscore, which seems to provide a good indication of the overall performance of each weld in the test matrix. The Bendscore concept is explained in the previous Section 3.4.

The Bendscore is a relative index which could range from 0-100. To generalize results to tests not yet performed, the Bendscore could be converted back to the unnormalized point value by multiplying by 13/100.

- HVN

Many hardness impressions were taken on the weld specimens, both in general areas of the weld cross section and on a traverse across the weld midplane. The hardest material was generally located in the HAZ at the crown of the weld. However, this hardness was relatively independent of depth and thickness among the wet weld population and was not thought to be very useful. Therefore, the peak HAZ hardness at midplane (which showed more variation) was chosen for analysis. This is simply the highest Vickers Hardness Number near the HAZ from the midplane hardness traverse (HVN).

Hardness of the weld metal at midplane was also relatively independent of depth and weld type (wet, wet-backed, or dry). Therefore, peak weld crown hardness was chosen as a significant test result.

These two values of hardness are distinguished by the grouping variable, ZONE.

- CVN

The Charpy impact energy expressed in ft-lb is used as a test result variable. Only those values at -2°C (28°F) and 16°C (60°F) were included because this essentially covers the range of application temperatures (the temperature of seawater). Two identical tests were performed for each temperature. There are thus four values of CVN for the HAZ and four for the weld metal.

- PCTSHEAR

This variable is the observed percentage of the Charpy impact specimen fracture surface which appears to be ductile. The usefulness of this variable is not great, but it is interesting to look at the histograms of PCTSHEAR defined by different groupings. There is a value of PCTSHEAR for each value of CVN.

- TEMPUS

This is the "upper-shelf" temperature in degrees Fahrenheit at which onset of full shear fracture

appearance was obtained. There is just one TEMPUS for the HAZ and for the weld metal for each square in the test matrix. The usefulness of this variable is limited.

- $J_{Ic}$

This variable is the value of  $J_{Ic}$  in inch-pounds per square inch determined from the  $J_{Ic}$  tests as prescribed in ASTM E813. There is one  $J_{Ic}$  value for the weld metal and one for the HAZ for each square in the test matrix. The value of  $J_{Ic}$  and the tearing modulus  $T$ , described below, are useful in an elasto-plastic analysis of crack stability.

- $T$

This is the tearing modulus in dimensionless units. The tearing modulus is the slope of the J-resistance curve normalized by  $E/\sigma_{flow}^2$ . There is one tearing modulus for each value of  $J_{Ic}$ .

- $K_{Ic}$

This variable is a conservative estimate of the plain strain fracture toughness  $K_{Ic}$  expressed in  $\text{ksi}/\sqrt{\text{in}}$ .  $K_{Ic}$  is determined from  $J_{Ic}$  by the relation:

$$K_{Ic} = \sqrt{J_{Ic} \cdot E}$$

In addition to  $J_{Ic}$  and  $K_{Ic}$ , the variables  $J_{2C}$  and the corresponding  $K_{2C}$  were also examined, but no better correlations could be obtained. For a complete

explanation of the variables  $J_{Ic}$ ,  $T$ ,  $K_{Ic}$ ,  $J_{2c}$ , and  $K_{2c}$ , refer to Section 3.2.8.

- ALLWELDMETAL

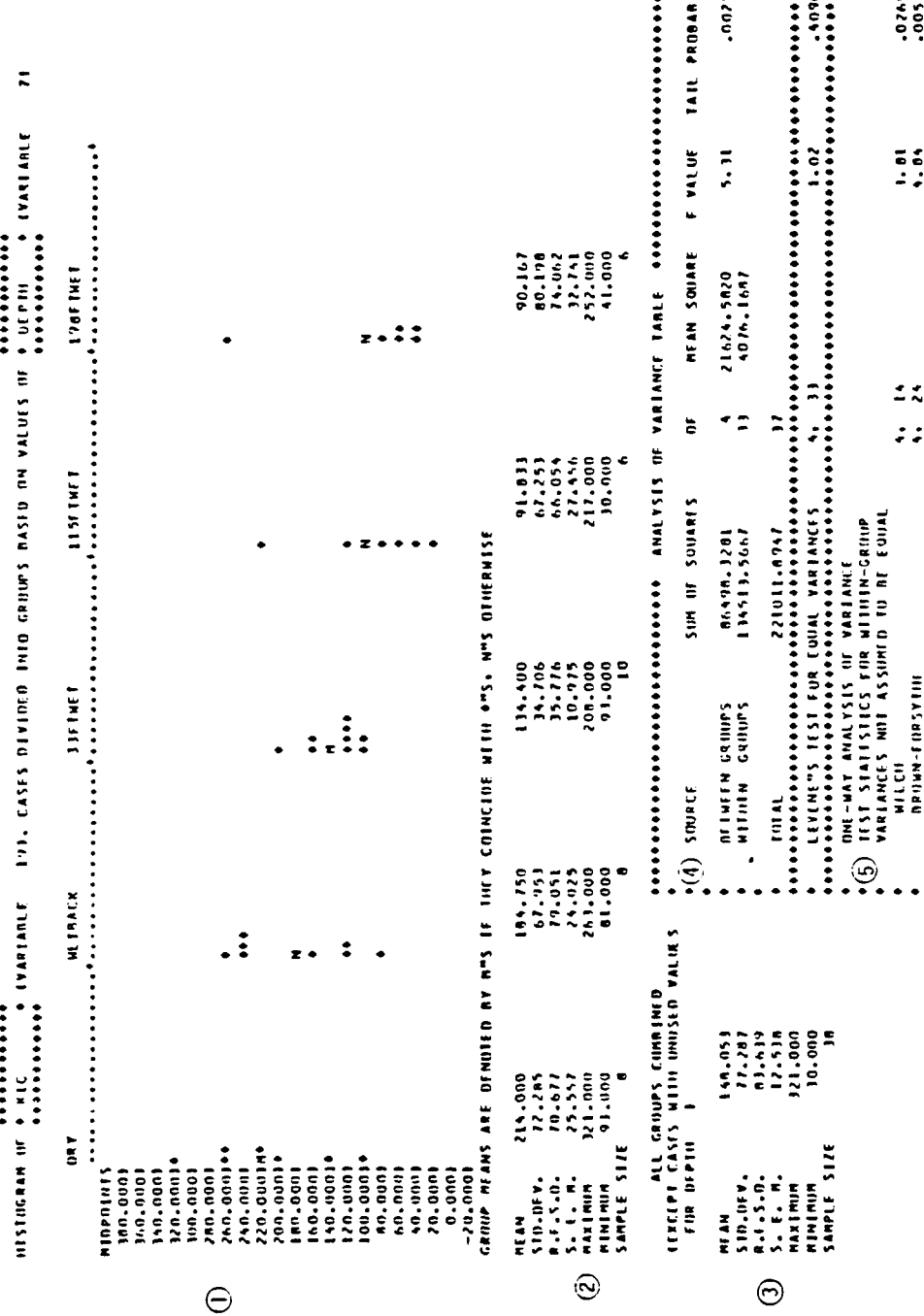
Results of all-weld-metal tension tests (proportional limit, yield stress, ultimate stress, modulus of elasticity, and percent elongation) were used in regression analysis only. These tests could only be grouped by depth.

#### B.2 Results of Grouping and Analysis of Variance

Extensive reference will be made to the histograms and analysis of variance tables produced by the computer program BMDP7D. An explanation of these tables follows. Items in Figure B-1 with a circled number correspond to the explanations below.

1. Side by side histograms of the data in each group. The base of each histogram is the vertical axis. The frequencies are plotted horizontally with the groups offset from one another. Each asterisk represents an observation. When there are too many observations to be plotted in the available space, the number of observations are printed at the right end of the line of asterisks. The M in the histogram represents the group mean; when the group mean does not coincide with an observation, an N is plotted instead of an M.

The midpoint for each interval is printed to the left of the histograms. Each interval includes its upper limit.



$K_{Ic}$  is shown in  $\text{ksi/in.} = 1.0 \text{ MPa}/\text{m}$ , 1 ft = .3048 m

FIGURE B.1.

2. For each group, the program prints
  - mean:  $\bar{x}$
  - standard deviation: s
  - standard error of the mean (S.E.M.)
  - maximum observed value
  - minimum observed value
  - sample size (frequency: N)
  
3. For all groups combined, BMDP7D prints the mean, standard deviation, standard error of the mean, maximum, minimum, and frequency. The standard deviation is computed from the overall mean for the variable (not from the group means).
  
4. A one-way or two-way analysis of variance (ANOVA) that tests the equality of group means.

Let  $x_{ij}$  represent the jth observation in the ith group and  $-\bar{x}_i$  the mean and  $N_i$  the number of observations in the ith group. Then

$$- \text{ between sum of squares: } BSS = \sum_i N_i (\bar{x}_i - \bar{x})^2$$

$$\text{where } \bar{x} = \frac{\sum_i N_i \bar{x}_i}{\sum N_i}$$

$$- \text{ between degrees of freedom} = g-1 \\ \text{where } g \text{ is the number of groups}$$

$$- \text{ between mean square} = BSS/(g-1) \\ - \text{ within sum of squares: } WSS = \sum_i \sum_j (x_{ij} - \bar{x}_i)^2$$

$$- \text{ within degrees of freedom} = \sum_i (n_i - 1)$$

- within mean square =  $WSS/\sum_i (N_i - 1)$
- F value = (between mean square)/within mean square)
- tail probability is the probability of exceeding the F ratio when the group means are equal. (The probability reported is appropriate when the data are sampled from normal populations with equal population variances; however, the distribution of the F ratio is sensitive to the assumption of equal population variances.)

5. Two additional one-way analysis of variance statistics are computed. Neither statistic assumes the equality of variances in each group. The two are:

Welch statistic:

$$W = \frac{\sum_i w_i (\bar{x}_i - \tilde{x})^2 / (g - 1)}{1 + \frac{2(g - 2)}{(g^2 - 1)} \sum_i (1 - w_i/u)^2 / (N_i - 1)}$$

where

$$w_i = N_i/s_i^2, u = \sum_i w_i, \text{ and } \tilde{x} = \sum w_i \bar{x}_i / u$$

When all population means are equal (even if the variances are unequal), W is approximately distributed as an F statistic with g-1 and f degrees of freedom, where f is implicitly defined as

$$1/f = (3/(g^2 - 1)) \sum_i (1 - w_i/u)^2 / (N_i - 1)$$

Brown-Forsythe statistic:

$$F^* = \sum_i N_i (\bar{x}_i - \bar{\bar{x}})^2 / \sum_i (1 - N_i/N) s_i^2$$

Critical values are obtained from the F distribution with  $g-1$  and  $f$  degrees of freedom where  $f$  is implicitly defined by the Satterthwaite approximation

$$\frac{1}{f} = \sum_i c_i^2 / (N_i - 1)$$

and

$$c_i = (1 - N_i/N) s_i^2 / [\sum_i (1 - N_i/N) s_i^2].$$

When there are only two groups, both  $F^*$  and  $W$  reduce to the separate variance t test.  $W$  and  $F^*$  weight the sums of squares in the numerator differently. The two statistics are described by Brown and Forsythe (1974).

A robust test of the equality of variances is provided by a one-way analysis of variance computed on the absolute values of the deviations from the group means (Brown and Forsythe, 1974). This test, named after Levene, is included in the results printed.

#### B.2.1 Results Within the Weld Type Subgroup

The variable WETORDRY, which groups the data according to whether it was a surface weld (dry), wet-backed, or a wet weld prepared at 10 m (33 ft) depth, was shown to be a significant

variable for all test results except upper shelf temperature. Figures B-2 through B-6 show test results grouped by weld type (WETORDRY) and CE. The data in each group include both 12.7 mm (1/2 in.) and 25.4 mm (1 in.) and, except for Bendscore, both weld metal and HAZ.

- $K_{IC}$

Austenitic welds have greater  $K_{IC}$ , but as shown in Figure B-2, the effect of base metal and filler metal is more pronounced in dry and wet-backed welds. The analysis of variance tables calculate the F statistic for the effect of weld type, base plate/filler metal, and the interaction effect. The tail probability is the level of significance of the effect, or the probability that the conclusion that there is an effect is incorrect. The weld-type effect and CE effect are significant at less than 1 percent, and the interaction effect is significant at 7.5 percent. The meaning of the interaction effect is evident in the histograms of Figure B-2, i.e., the effect of CE is not consistent for each weld type.

- CVN

As shown in Figure B-3, the CVN energy decreases from dry to wet-backed to wet welds, and increases for austenitic welds compared to ferritic welds, but there is no interaction.

HIGHWAY 100.0000 \* VARIANT 193. CASES DIVIDED INTO GROUPS BASED ON VALUES OF  
WELD 100.0000 \* VARIANT 69  
\* CF 49  
\* TENSILE F

TYPE OF FREQUENCIES  
FREQUENCY AUSTINIA WILMINGTON WELD  
AUSTINIA FLORIDA AUSTINIA FLORIDA  
WELD AUSTINIA

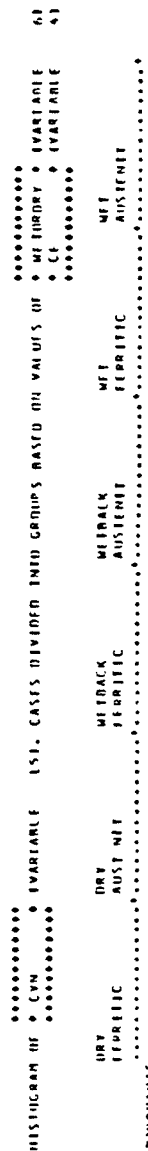
FREQUENCIES ARE DEFINED AS THOSE IF THEY COINCIDE WITH ONE, NOT OTHERWISE

	MEAN	ST. DEV.	N	MEAN	ST. DEV.	N	MEAN	ST. DEV.	N
S.E. M.	10.21	46.76	125.750	243.750	14.108	116.250	152.250	14.688	10.000
S.E. D.	81.767	57.323	115.47	17.005	21.146	48.170	48.170	48.170	48.170
S.E. H.	15.116	24.124	17.916	7.554	9.000	21.344	21.344	21.344	21.344
MAXIMUM	251.000	321.000	168.000	263.000	154.000	208.000	208.000	208.000	208.000
MINIMUM	91.000	212.000	91.000	231.000	115.000	115.000	115.000	115.000	115.000
SAMPLE SIZE	4	4	4	4	4	4	4	4	4

ANALYSIS OF VARIANCE TABLE											
	SUM OF SQUARES	DF	MEAN SQUARE	F VALUE	FAIL PROBABILITY		SUM OF SQUARES	DF	MEAN SQUARE	F VALUE	FAIL PROBABILITY
WELD	19629.0000	2	9814.5000	5.40	.0145		322.66.6667	1	322.66.6667	1.16	.1005
CF	12	1					5442.6667	1	5442.6667	1.00	.0751
INTERACTION	1085.113	2	542.5567				16.16.6667	1	16.16.6667		
EROD	1209.0000	16	1.06.6667								
LEVIN'S TEST FOR TOTAL VARIANCE											
ONE-WAY ANALYSIS OF VARIANCE											
TEST STATISTICS FOR WITHIN-GRUPP VARIANCE NOT ASSUMED TO BE EQUAL											
MILCH	5.	5	1.0.75								
BRIAN-FORSYTHE	5.	5	1.0.75								

$K_{Ic}$  is shown in  $\text{ksi}/\sqrt{\text{in.}}$ :  $1.0 \text{ ksi}/\sqrt{\text{in.}} = 1.1 \text{ MPa}/\sqrt{\text{m}}$

FIGURE B.2.



GROUP MEANS ARE INDICATED BY \*'S IF THEY COINCIDE WITH ONE OR MORE OTHERWISE

MEAN	SD.D.V.	N.F.S.D.	S.E. N.	MAXIMUM	MINIMUM	SAMPLE SIZE
41.000	14.715	14.724	15.014	62.500	42.375	16
51.000	14.724	23.095	21.034	22.241	16.917	16
52.000	14.724	5.560	4.229	55.000	49.000	16
55.000	14.724	16.000	16.000	55.000	47.500	16
55.000	14.724	16.000	16.000	55.000	47.500	16

ALL GROUPS COMBINED  
EXCEPT CASES WITH UNUSUAL VALUES  
FOR WET DRY AND CE

MEAN	SD.D.V.	N.F.S.D.	S.E. N.	MAXIMUM	MINIMUM	SAMPLE SIZE
51.479	21.094	20.696	7.157	114.000	8.000	96

ANALYSIS OF VARIANCE TABLE						
	SUM OF SQUARES	DF	MEAN SQUARE	F	VALUF	F VALUF
WET DRY	1571.5811	2	1785.7917	5.23	.0071	
CE	16120.1667	1	16120.1667	47.74	.0000	
INTERACTION	749.0833	2	374.5417	.16	.6952	
ERROR	30111.1250	70	3151.2347			
LSD'S TEST FOR TOTAL VARIANCES						
WET DRY	5.70					
CE	2.70					
INTERACTION	.0257					
ONE WAY ANALYSIS OF VARIANCE TEST STATISTICS FOR WET DRY GROUP VARIANCES NOT ASSUMED TO BE EQUAL						
WELCH	.0000					
MORRISON-FORSYTHE	.11.67					

FIGURE B.3.

CVN is shown in ft-lb: 1.0 ft-lb = 1.356 J

- BENDSCORE

As shown in Figure B-4, the Bendscore for both types of dry welds, wet-backed austenitic, and wet ferritic welds is good. The wet-backed ferritic welds and the austenitic wet welds had poor scores and hence poor ductility.

- HVN

As shown in Figure B-5, the hardness of ferritic welds and dry austenitic welds is relatively low compared to the austenitic wet-backed welds and especially the austenitic wet welds.

- Tearing Modulus

The tearing modulus decreases from dry to wet-backed to wet welds. The effect of CE is not consistent, for dry and wet-backed welds the austenitic welds had a higher T, but for wet welds, the austenitic welds had a lower T, as shown in Figure B-6.

- Thickness Effect

The 25.4 (1 in.) thick specimens had lower  $K_{Ic}$ , CVN, percent shear, and T, and higher HVN, but the differences were small and generally statistically insignificant.

- Zone Effect

The HAZ specimens had greater  $K_{Ic}$  and CVN, and, as





HISTOGRAM OF VARIABLE 221. CASTS DIVIDED INTO GROUPS BASED ON VALUES OF CT VARIABLE

WELD-AUSTENITE

WELD-FERRITIC

MEAN STD. DEV. S.E. F. N. MAXIMUM MINIMUM SAMPLE SIZE

16.6 7.50 210.710 36.445 10.138 4.7-419 6.1-164 4.4-111 4.5-517 4.6-311 2.1-162 2.1-017 112.000 112.000 4

77.417 50.864 22.070 6.1-164 2.4-210 2.4-210 16.000 116.000 116.000 116.000 116.000 116.000 4

8.1-127 15.719 18.221 9.567 2.4-210 2.4-210 161.000 114.000 114.000 114.000 114.000 114.000 4

15.59 10.000 277.000 114.000 114.000 114.000 114.000 114.000 114.000 114.000 114.000 114.000 4

6.1-164 11.866 11.866 11.866 11.866 11.866 11.866 11.866 11.866 11.866 11.866 11.866 4

277.000 0.000 0.000 0.000 0.000 0.000 0.000 0.000 0.000 0.000 0.000 0.000 4

0.000 0.000 0.000 0.000 0.000 0.000 0.000 0.000 0.000 0.000 0.000 0.000 4

-20.0000 0.0000 0.0000 0.0000 0.0000 0.0000 0.0000 0.0000 0.0000 0.0000 0.0000 0.0000 4

&gt;40.0000

GROUP MEANS AND STANDARD ERRORS FOR CLINIC WITH 95% MHS ELSEWHERE

MEAN STD. DEV. S.E. F. N. MAXIMUM MINIMUM SAMPLE SIZE

16.6 7.50 210.710 36.445 10.138 4.7-419 6.1-164 4.4-111 4.5-517 4.6-311 2.1-162 2.1-017 112.000 112.000 4

77.417 50.864 22.070 6.1-164 2.4-210 2.4-210 161.000 114.000 114.000 114.000 114.000 114.000 4

8.1-127 15.719 18.221 9.567 2.4-210 2.4-210 161.000 114.000 114.000 114.000 114.000 114.000 4

15.59 10.000 277.000 114.000 114.000 114.000 114.000 114.000 114.000 114.000 114.000 114.000 4

6.1-164 11.866 11.866 11.866 11.866 11.866 11.866 11.866 11.866 11.866 11.866 11.866 4

277.000 0.000 0.000 0.000 0.000 0.000 0.000 0.000 0.000 0.000 0.000 0.000 4

0.000 0.000 0.000 0.000 0.000 0.000 0.000 0.000 0.000 0.000 0.000 0.000 4

-20.0000 0.0000 0.0000 0.0000 0.0000 0.0000 0.0000 0.0000 0.0000 0.0000 0.0000 0.0000 4

ALL GROUPS CHARTED EXCEPT CLS WITH UNLISTED VALUES

FOR WELD-FERRITIC AND CT

MEAN STD. DEV. S.E. F. N. MAXIMUM MINIMUM SAMPLE SIZE

16.6 5.503 67.839 67.665 5.5. N. 11.866 277.000 0.000 28

77.417 50.864 22.070 6.1-164 2.4-210 2.4-210 161.000 114.000 114.000 114.000

8.1-127 15.719 18.221 9.567 2.4-210 2.4-210 161.000 114.000 114.000 114.000

15.59 10.000 277.000 114.000 114.000 114.000 114.000 114.000 114.000 114.000

6.1-164 11.866 11.866 11.866 11.866 11.866 11.866 11.866 11.866 11.866

277.000 0.000 0.000 0.000 0.000 0.000 0.000 0.000 0.000 0.000

0.000 0.000 0.000 0.000 0.000 0.000 0.000 0.000 0.000 0.000

-20.0000 0.0000 0.0000 0.0000 0.0000 0.0000 0.0000 0.0000 0.0000 0.0000

ANALYSIS OF VARIANCE TABLE

SUM OF SQUARES DF MEAN SQUARE F VALUE P-VALUE

115.000 1 59.500 4.6-311

59.500 1 46.500 4.6-311

4.6-311 1 4.6-311

2.1-162 1 2.1-162

2.1-017 1 2.1-017

112.000 1 112.000

0.000 4 0.000 4

TESTS FOR EQUAL VARIANCES

LEVELONE'S TEST FOR EQUAL VARIANCES

LEVENE'S TEST FOR EQUAL VARIANCES

BROWNE-FORSYTHE

ONE-WAY ANALYSIS OF VARIANCE

TEST STATISTICS FOR WITHIN-GROUP VARIANCES NOT ASSUMED TO EQUAL WHICH HAD BEEN FORWARDED

S. 0.51 0.016

S. 0.11 0.011

FIGURE B.6.

shown in Figure B-7 there is an interaction effect on CVN with weld type and zone; i.e., the increase in toughness for the HAZ is more pronounced in wet-backed welds. This interaction was not observed for  $K_{Ic}$ .

- Temperature Effect

Temperature did not have a significant effect on CVN or percent shear, even when separated by other grouping variables.

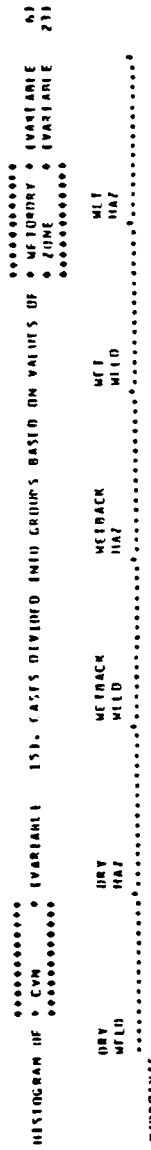
#### B.2.2 Results Within the Restraint Subgroup

Generally, restraint had no significant effect on the test variables. Figure B-8 shows the results for  $K_{Ic}$  divided by ZONE and RESTRAIN. Although the results are not statistically significant, there appears to be an interaction in that the greater toughness in the HAZ compared to weld metal appears to diminish for the restraint case. This effect is not apparent for CVN, for which the HAZ CVN appears to be larger for restrained welds, as shown in Figure B-9.

No interaction effects were observed for depth and restraint or thickness and restraint. As for CVN and percent shear, no temperature effect or interaction of temperature with restraint was evident.

#### B.2.3 Results Within the Wet-Ferritic Subgroup

The wet ferritic subgroup can be considered exclusive of the 25.4 mm (1 in.)-thick restrained welds (referred to as Wet Ferritic A) or including these restrained welds (Wet Ferritic B).



ALL GROUPS COMBINED		ANALYSIS OF VARIANCE TABLE			
SOURCE	SUM OF SQUARES	DF	MEAN SQUARE	F VALUE	TAIL PROBABILITY
METHOD	152.543	2	76.271	4.57	.019
TIME	184.167	1	184.167	20.07	.000
INTERACTION	40.719	2	20.359	5.71	.007
Error	351.611	1250	.281		
LEVENE'S TEST FOR EQUAL VARIANCES					
	5.70	1	5.70	7.00	.000
ONE-WAY ANALYSIS OF VARIANCE					
TEST STATISTICS FOR WITHIN GROUP VARIANCES NOT ASSUMED TO BE EQUAL					
WELCH	5.49	49	11.00	12.57	.000
ARMSTRONG					

PAGE 108 SIMILARITIES - OTHER VARIANTS IN HISTORICAL SINGHUS

110. CASES DIVIDED INTO GROUPS BASED ON VALUES OF  
EVAPORATION AND RAINFALL

WITH RES.  
WITH RES.  
WITH RES.  
WITH RES.

• 0000-0000-0000-0000  
• 0000-0000-0000-0000  
• 0000-0000-0000-0000  
• 0000-0000-0000-0000  
• 0000-0000-0000-0000

189,000  
182,000  
175,000  
168,000

卷之三

6.3.0001  
6.3.0002  
5.6.0001  
4.9.0001  
4.9.0002  
2.2.0001

卷之三

### ANALYSIS OF VARIANCE TABLE

NAME	FIN LINE AND RESTRAIN	STRECH	SUM OF SQUARES	DF	MEN SCAFF	F VAL
WALL	79,010.3	79,010.3	114,001.9	1	114,001.9	-
STRETCH-OF V.	29,185.3	29,185.3	650,001.3	1	650,001.3	-
STRETCH-OF W.	15,000.0	15,000.0	11,000.0	1	11,000.0	-

FIGURE B.8.

$K_{Ic}$  is shown in ksi/in.:  $1.0 \text{ ksi/in.} = 1.1 \text{ MPa}\sqrt{\text{m}}$

PAGE 13		INITIAL WELDS - CVN AND PLATEAQ FOR RESTRAINT STUDY			
		TESTS FOR HYPOTHESIS OF CVN = 0 VARIANCE IS IN CASES DIVIDED INTO GROUPS BASED ON VALUES OF TIME, RESTRAIN, F-TEST, AND VARIANCE			
		WITH RESTRAINTS			
		WITH RESTRAINTS			
		WITH RESTRAINTS	WITHOUT RESTRAINTS		
MEAN	28.033	22.500	18.500		
S.D. OF CVN	5.059	6.179	7.972		
R.F. S.D.	6.277	7.200	9.463		
S.E. M.	1.593	1.840	2.301		
HARMS	18.000	12.000	27.000		
MINIMUM	18.000	15.000	7.000		
SAMPLE SIZE	47	12	12		
LEVINSON'S TEST FOR HOMOGENEITY OF VARIANCE WITH RESTRAINTS					
MEAN	28.033	22.500	18.500		
S.D. OF CVN	5.059	6.179	7.972		
R.F. S.D.	6.277	7.200	9.463		
S.E. M.	1.593	1.840	2.301		
HARMS	18.000	12.000	27.000		
MINIMUM	18.000	15.000	7.000		
SAMPLE SIZE	47	12	12		
ALL GROUPS COMBINED					
TESTS FOR HYPOTHESIS OF EQUAL VARIANCES					
TEST FOR EQUAL VARIANCE WITH RESTRAINTS					
MEAN	29.646	TIME	4.36-0.020		
S.D. OF CVN	9.277	RESTRAIN	4.46-0.020		
R.F. S.D.	9.330	INTERACTION	2.21-0.020		
S.E. M.	1.339	FACTOR	3.39-0.017		
HARMS	43.000	LEVINSON'S TEST FOR EQUAL VARIANCES	7.5-0.012		
MINIMUM	6.000				
SAMPLE SIZE	46				
ONE-WAY ANALYSIS OF VARIANCE					
TEST STATISTICS FOR MAIN EFFECTS					
VARIANCE NOT ASSUMED IN THE EQUAL					
ANCOVA					
REGRESSION					
TEST STATISTICS FOR MAIN EFFECTS					
VARIANCE NOT ASSUMED IN THE EQUAL					
ANCOVA					
REGRESSION					
ANALYSIS OF VARIANCE TABLE					
	SUM OF SQUARES	D.F.	MEAN SQUARE	F-VALUE	F-TEST P-VALUE
TIME	4.36-0.020	1	4.36-0.020	5.77	.0206
RESTRAIN	4.46-0.020	1	4.46-0.020	5.61	.0206
INTERACTION	2.21-0.020	1	2.21-0.020	7.91	.0050
FACTOR	3.39-0.017	1	3.39-0.017	7.5-0.012	.0050
LEVINSON'S TEST FOR EQUAL VARIANCES	7.5-0.012				

FIGURE B.9.

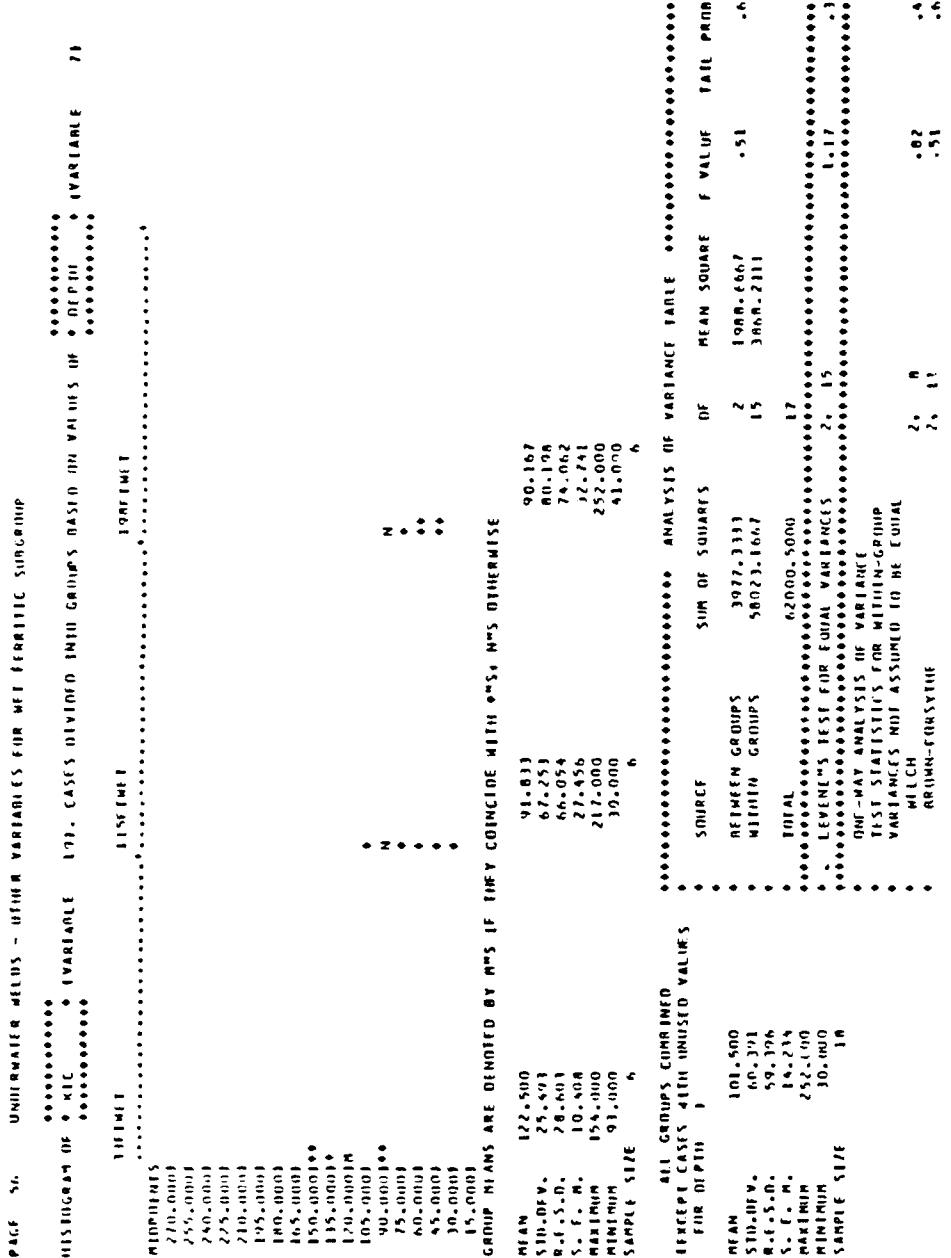
CVN is shown in ft-lb: 1.0 ft-lb = 1.356 J

Both cases were analyzed, and the conclusions are indistinguishable, further supporting the apparent insignificance of restraint. The Wet Ferritic B Subgroup has a larger sample size and this strengthens the statistical significance of the conclusions. Therefore, this discussion is confined to the Wet Ferritic B Subgroup.

- $K_{IC}$

Figure B-10 shows  $K_{IC}$  grouped by depth for the Restraint Subgroup, i.e., for all 25.4 mm (1 in.) welds. Both the mean and the minimum  $K_{IC}$  appear to monotonically decrease with depth, and this conclusion is significant at less than 1 percent. When the 12.7 mm (1/2 in.) welds are added, as in Figure B-11, these trends are confounded. In order to fully understand what is happening to  $K_{IC}$ , it is necessary to look at Figures B-12, B-13, and B-14. Figure B-12 shows  $K_{IC}$  grouped by depth and thickness. The 25.4 mm (1 in.) columns are the same as the columns in Figure B-10, but the 12.7 mm (1/2 in.)  $K_{IC}$  is both extremely high and low. Figure B-13 shows  $K_{IC}$  grouped by thickness and zone, from which it is clear that the apparent greater toughness for the HAZ is a phenomenon common only to the 12.7 mm (1/2 in.) welds. Finally, Figure B-14, which has  $K_{IC}$  grouped by depth and zone, shows that the apparent greater toughness of the HAZ occurs only for the 35 and 60 m (115 and 198 ft) depths. The highest values of HAZ toughness are the 12.7 mm (1/2 in.) welds. These 12.7 mm (1/2 in.) HAZ  $J_{IC}$  tests are suspicious, but the validity of these results is supported by the results of the Charpy tests, as explained below.





$K_{Ic}$  is shown in ksi/in.:  $1.0 \text{ ksi}/\sqrt{\text{in.}} = 1.1 \text{ MPa}/\sqrt{\text{m}}$ , 1 ft = .3048 m

FIGURE B.11.

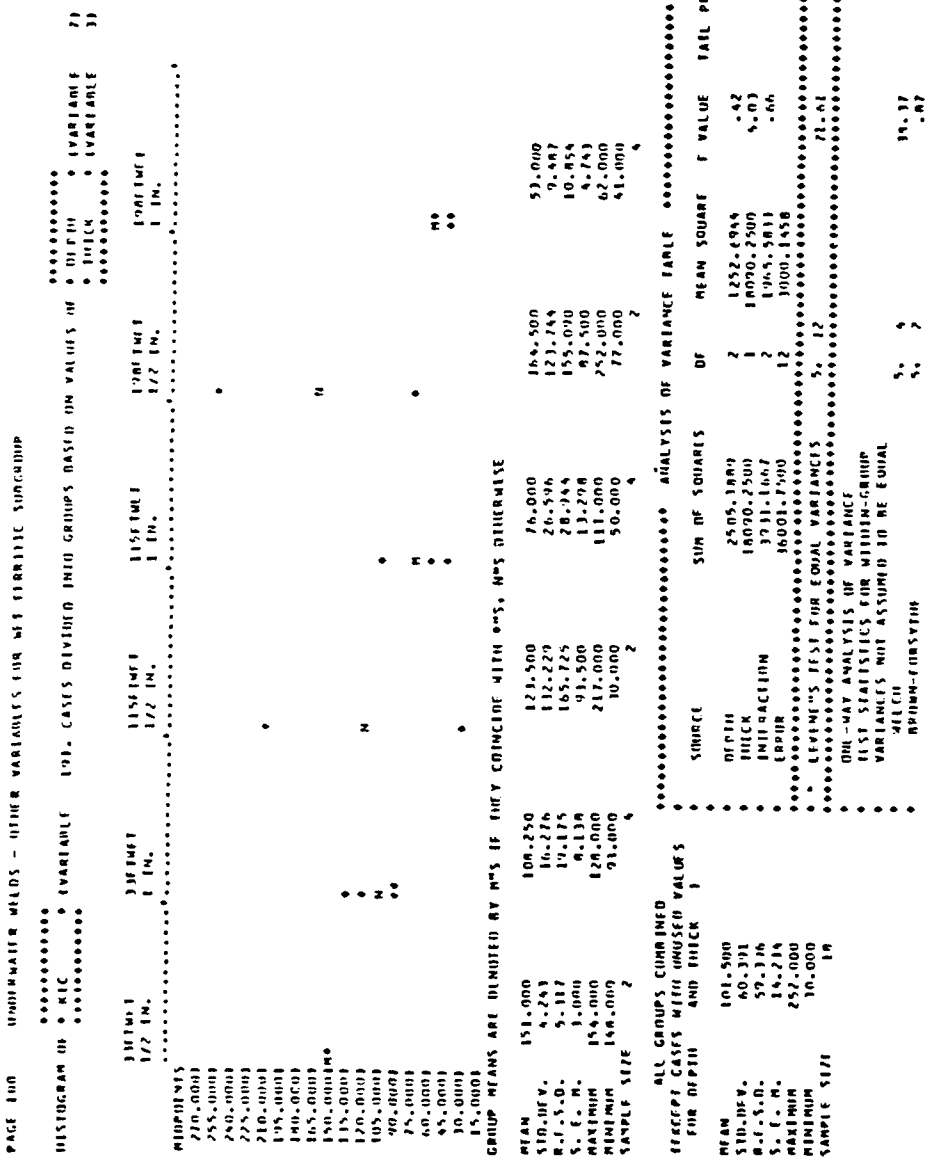
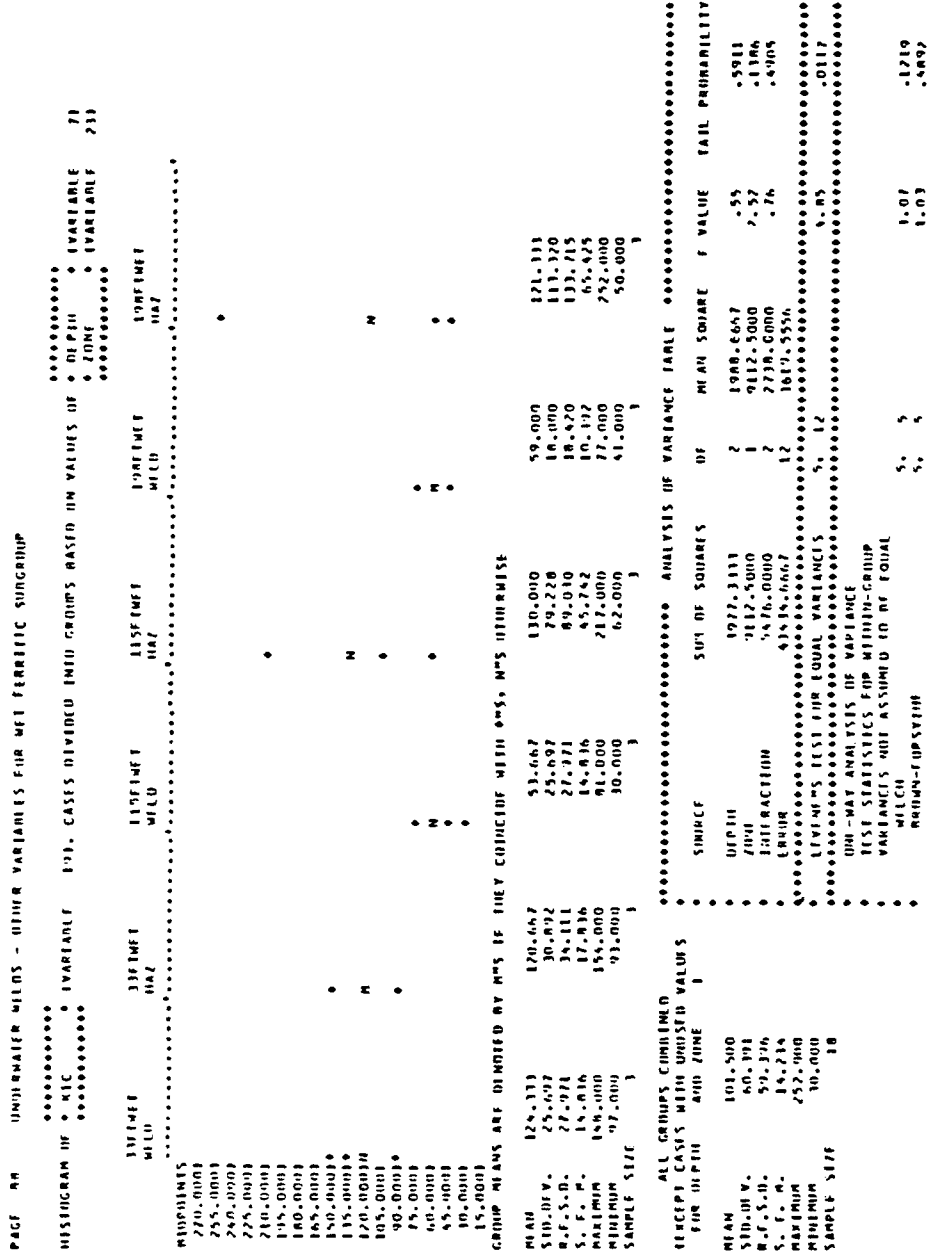


FIGURE B.12.  
 $K_{Ic}$  is shown in ksi/in.: 1.0 ksi/in. = 1.1 MPa/m, 1 ft = .3048 m, 1 in. = 25.4 mm

PAGE 110 MEASURED WINDS - HIGH VARIANCES FROM WEAK PLASTIC SUBGROUP

MEASURED WINDS - HIGH VARIANCES FROM WEAK PLASTIC SUBGROUP  
VARIABLES: 1) CASES DIVIDED INTO GROUPS BASED ON VALUES IN  
THICK, THIN, CRISP, TALL, VARIABLE

THICKNESS	1/2 IN. WILD	1 IN. WILD	1 IN. HAZ
2.0-.0000	*		
2.5-.0000			
3.0-.0000			
3.5-.0000			
4.0-.0000			
4.5-.0000			
5.0-.0000			
5.5-.0000			
6.0-.0000			
6.5-.0000			
7.0-.0000			
7.5-.0000			
8.0-.0000			
8.5-.0000			
9.0-.0000			
9.5-.0000			
10.0-.0000			
10.5-.0000			
11.0-.0000			
11.5-.0000			
12.0-.0000			
12.5-.0000			
13.0-.0000			
13.5-.0000			
14.0-.0000			
14.5-.0000			
15.0-.0000			
15.5-.0000			
16.0-.0000			
16.5-.0000			
17.0-.0000			
17.5-.0000			
18.0-.0000			
18.5-.0000			
19.0-.0000			
19.5-.0000			
20.0-.0000			
20.5-.0000			
21.0-.0000			
21.5-.0000			
22.0-.0000			
22.5-.0000			
23.0-.0000			
23.5-.0000			
24.0-.0000			
24.5-.0000			
25.0-.0000			
25.5-.0000			
26.0-.0000			
26.5-.0000			
27.0-.0000			
27.5-.0000			
28.0-.0000			
28.5-.0000			
29.0-.0000			
29.5-.0000			
30.0-.0000			
30.5-.0000			
31.0-.0000			
31.5-.0000			
32.0-.0000			
32.5-.0000			
33.0-.0000			
33.5-.0000			
34.0-.0000			
34.5-.0000			
35.0-.0000			
35.5-.0000			
36.0-.0000			
36.5-.0000			
37.0-.0000			
37.5-.0000			
38.0-.0000			
38.5-.0000			
39.0-.0000			
39.5-.0000			
40.0-.0000			
40.5-.0000			
41.0-.0000			
41.5-.0000			
42.0-.0000			
42.5-.0000			
43.0-.0000			
43.5-.0000			
44.0-.0000			
44.5-.0000			
45.0-.0000			
45.5-.0000			
46.0-.0000			
46.5-.0000			
47.0-.0000			
47.5-.0000			
48.0-.0000			
48.5-.0000			
49.0-.0000			
49.5-.0000			
50.0-.0000			
50.5-.0000			
51.0-.0000			
51.5-.0000			
52.0-.0000			
52.5-.0000			
53.0-.0000			
53.5-.0000			
54.0-.0000			
54.5-.0000			
55.0-.0000			
55.5-.0000			
56.0-.0000			
56.5-.0000			
57.0-.0000			
57.5-.0000			
58.0-.0000			
58.5-.0000			
59.0-.0000			
59.5-.0000			
60.0-.0000			
60.5-.0000			
61.0-.0000			
61.5-.0000			
62.0-.0000			
62.5-.0000			
63.0-.0000			
63.5-.0000			
64.0-.0000			
64.5-.0000			
65.0-.0000			
65.5-.0000			
66.0-.0000			
66.5-.0000			
67.0-.0000			
67.5-.0000			
68.0-.0000			
68.5-.0000			
69.0-.0000			
69.5-.0000			
70.0-.0000			
70.5-.0000			
71.0-.0000			
71.5-.0000			
72.0-.0000			
72.5-.0000			
73.0-.0000			
73.5-.0000			
74.0-.0000			
74.5-.0000			
75.0-.0000			
75.5-.0000			
76.0-.0000			
76.5-.0000			
77.0-.0000			
77.5-.0000			
78.0-.0000			
78.5-.0000			
79.0-.0000			
79.5-.0000			
80.0-.0000			
80.5-.0000			
81.0-.0000			
81.5-.0000			
82.0-.0000			
82.5-.0000			
83.0-.0000			
83.5-.0000			
84.0-.0000			
84.5-.0000			
85.0-.0000			
85.5-.0000			
86.0-.0000			
86.5-.0000			
87.0-.0000			
87.5-.0000			
88.0-.0000			
88.5-.0000			
89.0-.0000			
89.5-.0000			
90.0-.0000			
90.5-.0000			
91.0-.0000			
91.5-.0000			
92.0-.0000			
92.5-.0000			
93.0-.0000			
93.5-.0000			
94.0-.0000			
94.5-.0000			
95.0-.0000			
95.5-.0000			
96.0-.0000			
96.5-.0000			
97.0-.0000			
97.5-.0000			
98.0-.0000			
98.5-.0000			
99.0-.0000			
99.5-.0000			
100.0-.0000			
100.5-.0000			
101.0-.0000			
101.5-.0000			
102.0-.0000			
102.5-.0000			
103.0-.0000			
103.5-.0000			
104.0-.0000			
104.5-.0000			
105.0-.0000			
105.5-.0000			
106.0-.0000			
106.5-.0000			
107.0-.0000			
107.5-.0000			
108.0-.0000			
108.5-.0000			
109.0-.0000			
109.5-.0000			
110.0-.0000			
110.5-.0000			
111.0-.0000			
111.5-.0000			
112.0-.0000			
112.5-.0000			
113.0-.0000			
113.5-.0000			
114.0-.0000			
114.5-.0000			
115.0-.0000			
115.5-.0000			
116.0-.0000			
116.5-.0000			
117.0-.0000			
117.5-.0000			
118.0-.0000			
118.5-.0000			
119.0-.0000			
119.5-.0000			
120.0-.0000			
120.5-.0000			
121.0-.0000			
121.5-.0000			
122.0-.0000			
122.5-.0000			
123.0-.0000			
123.5-.0000			
124.0-.0000			
124.5-.0000			
125.0-.0000			
125.5-.0000			
126.0-.0000			
126.5-.0000			
127.0-.0000			
127.5-.0000			
128.0-.0000			
128.5-.0000			
129.0-.0000			
129.5-.0000			
130.0-.0000			
130.5-.0000			
131.0-.0000			
131.5-.0000			
132.0-.0000			
132.5-.0000			
133.0-.0000			
133.5-.0000			
134.0-.0000			
134.5-.0000			
135.0-.0000			
135.5-.0000			
136.0-.0000			
136.5-.0000			
137.0-.0000			
137.5-.0000			
138.0-.0000			
138.5-.0000			
139.0-.0000			
139.5-.0000			
140.0-.0000			
140.5-.0000			
141.0-.0000			
141.5-.0000			
142.0-.0000			
142.5-.0000			
143.0-.0000			
143.5-.0000			
144.0-.0000			
144.5-.0000			
145.0-.0000			
145.5-.0000			
146.0-.0000			
146.5-.0000			
147.0-.0000			
147.5-.0000			
148.0-.0000			
148.5-.0000			
149.0-.0000			
149.5-.0000			
150.0-.0000			
150.5-.0000			
151.0-.0000			
151.5-.0000			
152.0-.0000			
152.5-.0000			
153.0-.0000			
153.5-.0000			
154.0-.0000			
154.5-.0000			
155.0-.0000			
155.5-.0000			
156.0-.0000			
156.5-.0000			
157.0-.0000			
157.5-.0000			
158.0-.0000			
158.5-.0000			
159.0-.0000			
159.5-.0000			
160.0-.0000			
160.5-.0000			
161.0-.0000			
161.5-.0000			
162.0-.0000			
162.5-.0000			
163.0-.0000			
163.5-.0000			
164.0-.0000			
164.5-.0000			
165.0-.0000			
165.5-.0000			
166.0-.0000			
166.5-.0000			
167.0-.0000			
167.5-.0000			
168.0-.0000			
168.5-.0000			
169.0-.0000			
169.5-.0000			
170.0-.0000			
170.5-.0000			
171.0-.0000			
171.5-.0000			
172.0-.0000			
172.5-.0000			
173.0-.0000			
173.5-.0000			
174.0-.0000			
174.5-.0000			
175.0-.0000			
175.5-.0000			
176.0-.0000			
176.5-.0000			
177.0-.0000			
177.5-.0000			
178.0-.0000			
178.5-.0000			
179.0-.0000			
179.5-.0000			
180.0-.0000			
180.5-.0000			
181.0-.0000			
181.5-.0000			
182.0-.0000			
182.5-.0000			
183.0-.0000</td			



$K_{Ic}$  is shown in ksi/in.: 1.0 ksi/in. = 1.1 MPa/m, 1 in. = 25.4 mm

FIGURE B.14.

- CVN

When CVN and percent shear are grouped by depth, there is no apparent effect. CVN showed no apparent effect for zone, although there was greater variance among the HAZ results. The 25.4 (1 in.)-thick welds appeared to have lower CVN and percent shear, and this effect was consistent at all depths. All of the above conclusions are only half true, however.

Figure B-15 shows CVN grouped by depth and zone. As was the case for  $K_{Ic}$  (Figure B-14), the weld metal toughness decreases with depth and exhibits little variance, while the HAZ toughness is extremely high and low with great variance and an apparently constant mean with depth. Figure B-16 shows the fracture appearance (percent shear) for the same groups. Note that all the weld metal specimens were full shear, and the HAZ specimens had mixed fracture appearances.

The thickness effect is also influenced by zone, as shown in Figure B-17. Among the weld metal specimens, thickness has very little effect. The 12.7 mm (1/2 in.) HAZ specimens are much tougher than all the rest, but for specimens taken from 25.4 mm (1 in.) welds, the HAZ toughness is much lower, lower even than the corresponding 25.4 mm (1 in.) weld metal specimens. Hence, the thickness effect is a manifestation of a change in HAZ toughness with thickness. This is important because it confirms the suspicious phenomenon observed in the  $J_{Ic}$  tests, and the number of Charpy specimens is sufficient to







assure statistical significance at less than .01 percent (as given in the analysis of variance table in Figure B-17).

Figure B-18 shows that the "thickness effect in the HAZ" is associated with brittle fracture in the 25.4 mm (1 in.) HAZ specimens. These 25.4 mm (1-in.) HAZ specimens are the only specimens with a fracture appearance less than full shear, with a mean percent shear of 30 percent.

As was the case for the other subgroups, there was no temperature effect on the Charpy results.

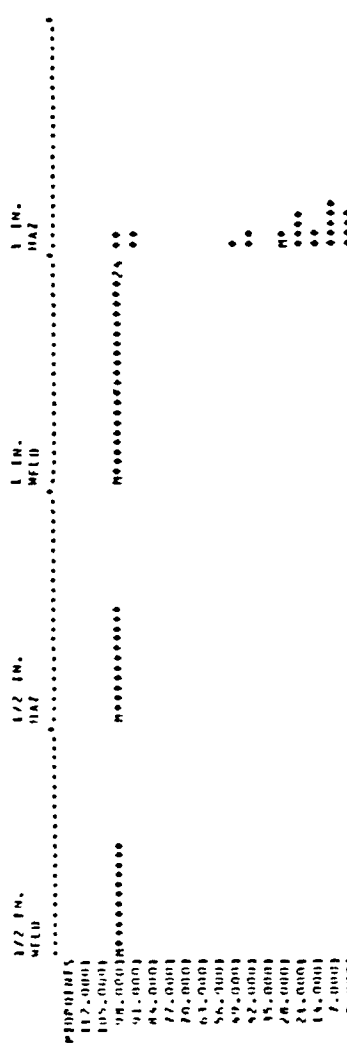
- Tearing Modulus

The tearing modulus was fairly constant with depth, but like  $K_{Ic}$  and CVN, exhibited interactions with thickness and zone. Figure B-19 resembles Figures B-13 and B-17, i.e., the 12.7 mm (1/2 in.) HAZ exhibited very high tearing modulus, nearly twice as high as the weld metal, while the tearing modulus for 25.4 mm (1 in.) welds was independent of zone and of the same order as the 12.7 mm (1/2 in.) weld metal.

- Bendscore

The ductility of the welds is measured with the Bendscore, which decreased monotonically with depth, as shown in Figure B-20. Thickness had no effect on the Bendscore.

PAGE 15 UNDERWATER WILDS - L.VN AND FRESHWATER FIRK WFT STERILE GROUP  
 MEAN STD. DEV. S.E. OF MEAN S.E. OF VARIANCE TEST CASES DIVIDED INTO GROUPS BASED ON VALUES OF TIME & VARIANCE TEST



GROUP MEANS ARE COMPUTED BY PCT'S OF FIRK CONNECTIVE WITH 485. RMS OTHERWISE

	MEAN	STD. DEV.	S.E. S.E.	S.E. S.E.	MAXIMUM	MINIMUM	SAMPLE SIZE
	99.58	1.43	1.000	.417	100.000	95.000	12
							12
							12
							12

ALL GROUPS COMBINED

TEST CASES WITH UNITS VARIANCE

FIR THICK AND TIME

	SOURCE	SUM OF SQUARES	DF	MEAN SQUARE	F VALUE	TAIL PRIMALITY
	THICK	19226.444	1	19226.444	55.22	<.0001
	TIME	19506.778	1	19506.778	56.02	<.0001
	INTERACTION	12000.000	1	12000.000	51.29	<.0001
	ERROR	21677.417	66	325.717		
	LIVETIN'S F TEST FOR EQUAL VARIANCES	1	69	24.91		

ONE-WAY ANALYSIS OF VARIANCE

TEST STATISTICS FOR WITHIN-GROUP

VARIANCES NOT ASSUMED IN THE TOTAL

MILCH-QUADRATIC

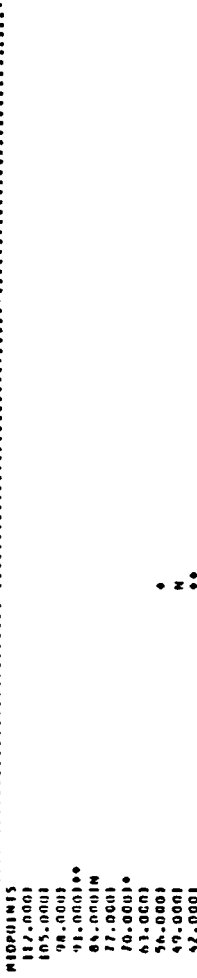
GRUEN-FORSYTHE

CVN is shown in in.: 1 in. = 25.4 mm

FIGURE B.18.



HISTOGRAM OF DEPTH IN FEET FOR 61 CASES DIVIDED INTO GROUPS BASED ON VALUES OF DEPTH VARIABLE  
1986 TWENTY-FIVE



GROUP MEANS ARE DENOTED BY M'S IF THEY COINCIDE WITH O'S. O'S OTHERWISE  
MEAN 8.4333 49.333  
ST.DEV. 11.910 7.566  
R.F.S.O. 13.644 6.867  
S.E.M. 6.888 4.133  
MAXIMUM 94.0000 18.000  
MINIMUM 71.000 15.000  
SAMPLE SIZE 1 3

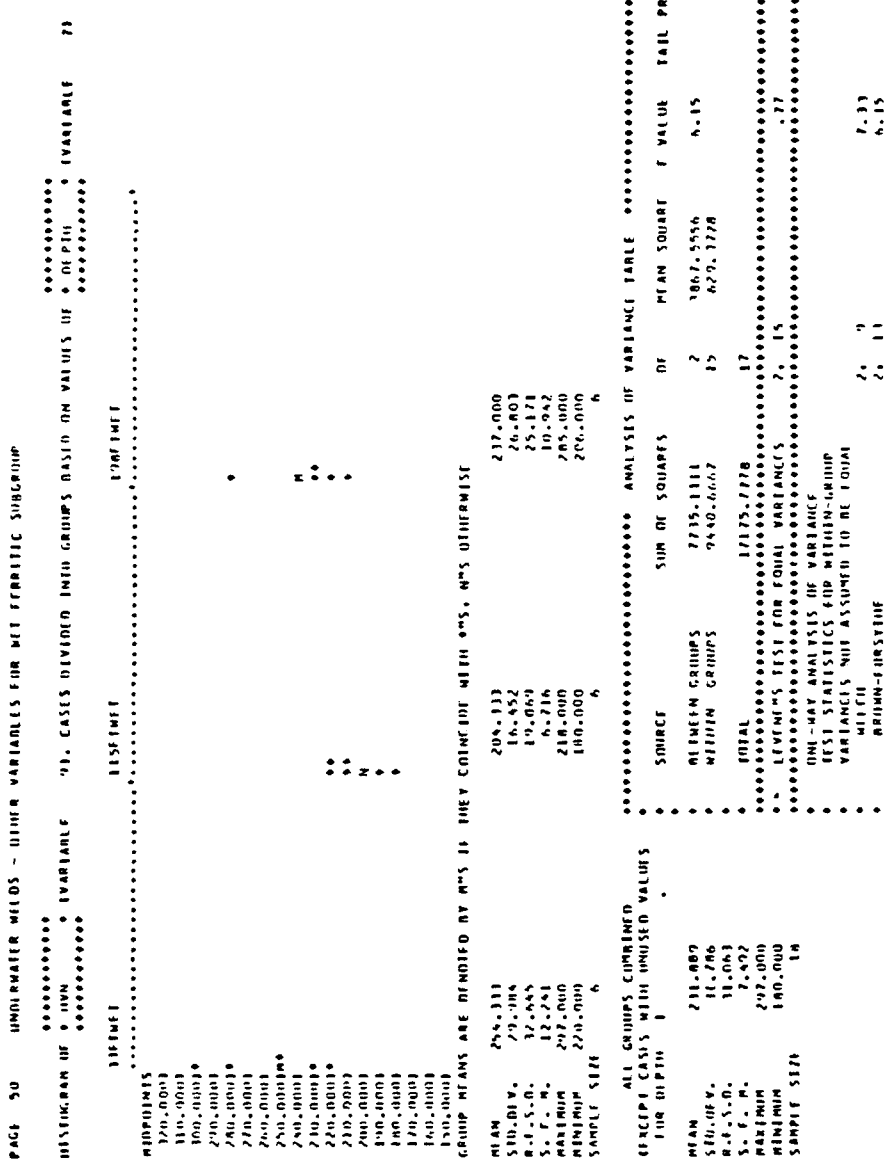
## ALL GROUPS COMBINED

(EXCEPT CASES WITH UNRECD VALUES  
FOR DEPTH)  
MEAN 50.778  
ST.DEV. 24.709  
R.F.S.O. 27.145  
S.E.M. 6.303  
MAXIMUM 94.0000  
MINIMUM 21.000  
SAMPLE SIZE 9

ANALYSIS OF VARIANCE TABLE						
	SOURCE	SUM OF SQUARES	D.F.	MEAN SQUARE	F VALUE	TAIL PROBABILITY
	BETWEEN GROUPS	4451.5516	2	2226.7778	26.70	.0011
	WITHIN GROUPS	510.0000	6	85.0000		
	TOTAL	4963.5516	8			
	LEMMERT'S TEST FOR EQUAL VARIANCES					
	ONE-WAY ANALYSIS OF VARIANCE					
	TEST STATISTICS FOR WITHIN GROUP VARIANCES NOT ASSUMED TO BE EQUAL					
	WELCH					
	BRIGHAM-UR SYME					
			2	4	16.71	.0091
			2	5	26.20	.0022

FIGURE B.20.

CVN is shown in ft.: 1 ft = .3048 m



CVN is shown in ft: 1 ft = .3048 m

- HVN

As shown in Figure B-21, hardness exhibited a peculiar behavior. The hardness for 35 m (115 ft) deep welds was lower than that of the 10 m (33 ft)-deep welds and 60 m (198 ft) welds, which were approximately equal. This effect is significant at about 1 percent and was independent of thickness and zone; the latter is surprising considering that the weld metal hardness was measured at the weld crown, while the HAZ hardness was measured at the midplane. This reduction of hardness at 35 m (115 ft) may be due to something unique about the welding procedure at that depth.

#### B.2.4 Results for All Data

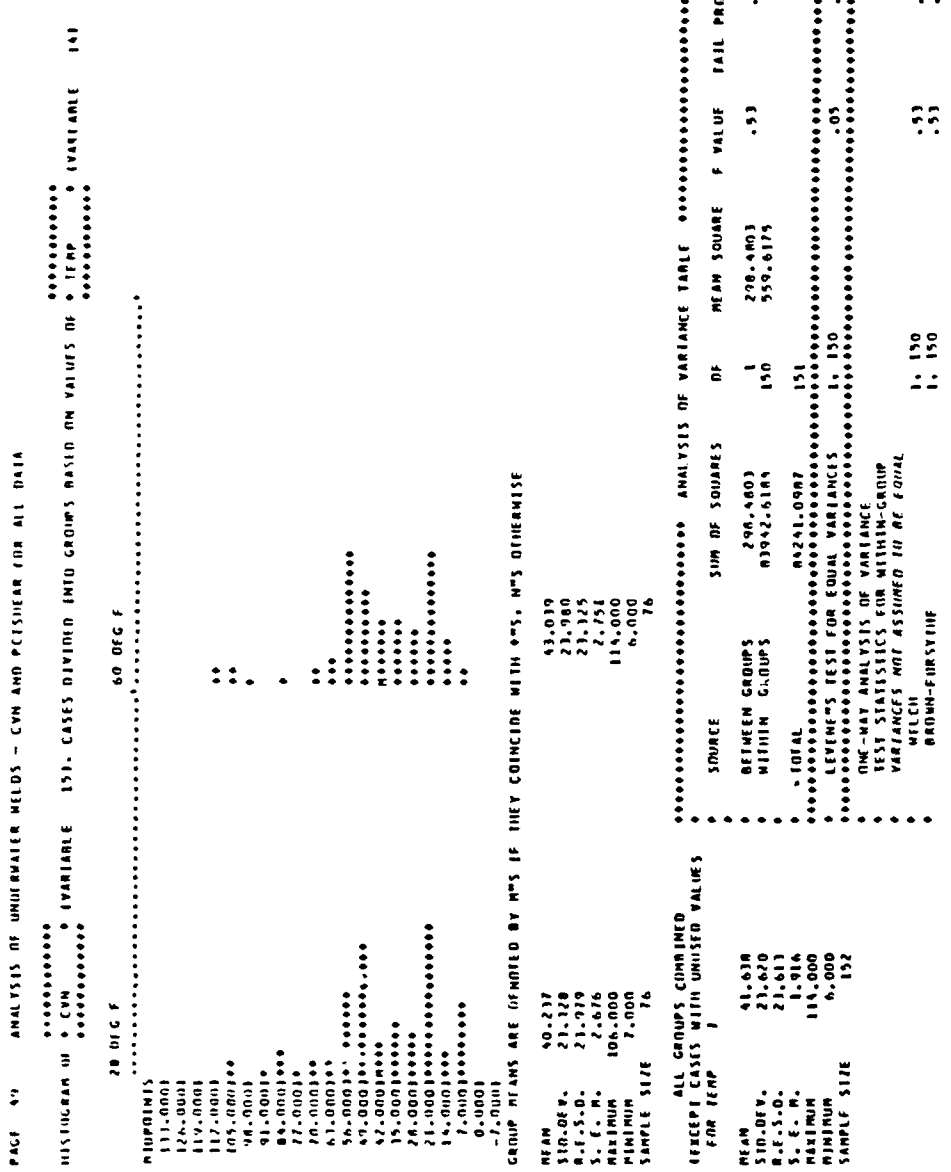
The usefulness of looking at all the data together includes verifying the applicability of trends observed in the subgroups.

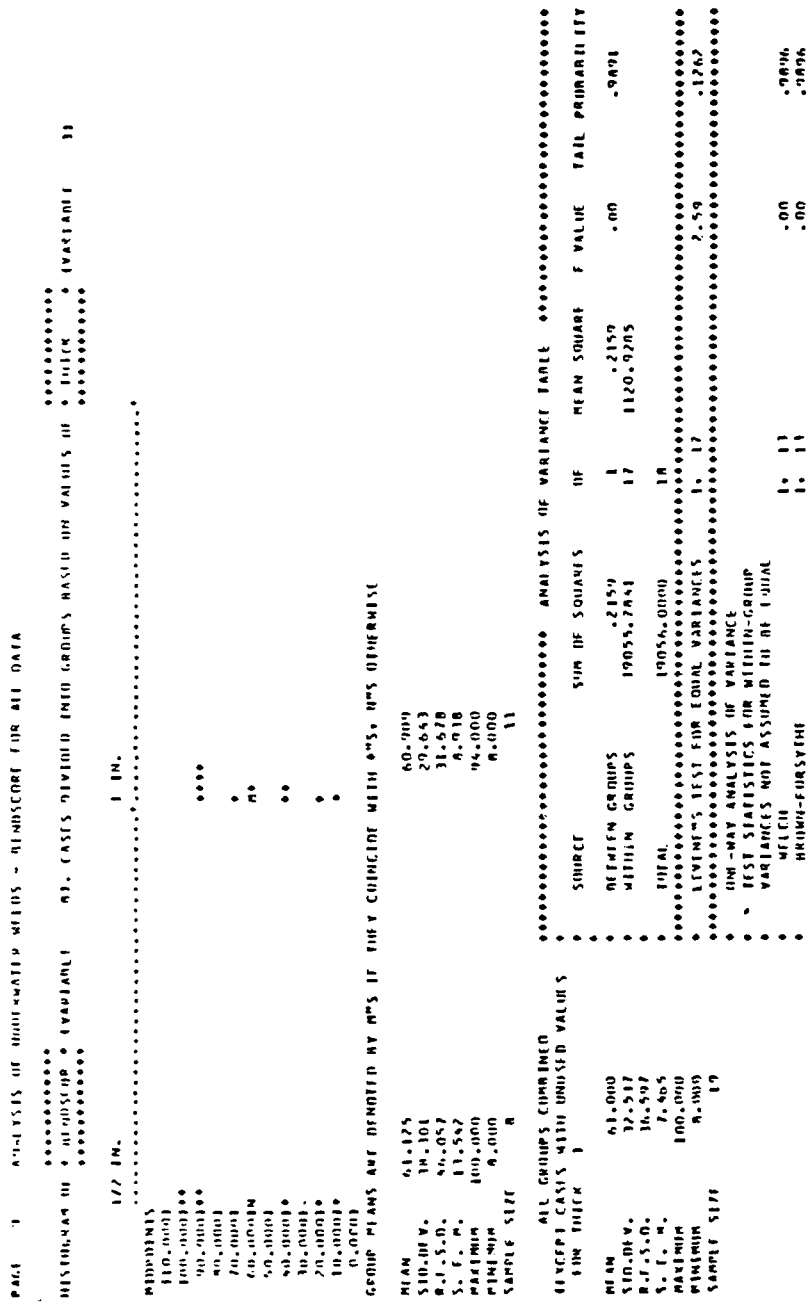
- Temperature Effect

Figure B-22 confirms the independence of toughness from temperature.

- Thickness Effect on Ductility

Figure B-23 confirms the independence of Bendscore from thickness and also shows how the scores tend to cluster in groups. Figure B-24 shows the trend of Bendscore with depth. The mean Bendscore decreases from 97 for dry welds, to 61 for wet-backed welds, to





CVN is shown in in. = 1 in. = 25.4 mm

PAGE 5 - AQUA LIVES IN THE BOTTLED WATER - MINISCRIPT FROM ALL DATA

INTERACTION OF READING & INVESTIGATIVE		NO. CASES INVOLVED IN THE GROUPS DASHED LINE VALUES ARE		INTERACTION OF READING & INVESTIGATIVE	
ITEM	MEAN TRACK	MEAN	MEAN	MEAN	MEAN
MEAN	97.000	91.750	96.800	97.313	101.667
STD. DEP.	1.616	1.722	1.706	1.506	1.506
S.E.D.	.542	.594	.597	.544	.544
S.E.P.	.712	.712	.740	.611	.611
MINIMUM	90.000	86.000	91.000	91.000	94.000
MAXIMUM	98.000	96.000	98.000	98.000	103.000
SAMPLE SIZE	4	4	4	4	4
ALL GROUPS COMBINED					
EXCEPT CASES WITH UNKNOWN VALUES					
ITEM	MEAN	91.000	94.333	91.000	91.000
STD. DEP.	1.717	1.722	1.706	1.506	1.506
S.E.D.	.650	.594	.597	.544	.544
S.E.P.	.745	.712	.740	.611	.611
MINIMUM	86.000	86.000	91.000	91.000	91.000
MAXIMUM	98.000	96.000	98.000	98.000	103.000
SAMPLE SIZE	10	4	4	4	4
ANALYSIS OF VARIANCE TABLE					
SUM OF SQUARES DF MEAN SQUARE F VALUE P VALUE					
SOURCE					
MEAN GROUPS	8443.1167	4	2110.7792	2.76	.
WITHIN GROUPS	1042.8811	16	65.1801		
RESIDUAL	17075.0000	16			
FRACTION'S TEST FOR EQUAL VARIANCES					
ONE-WAY ANALYSIS OF VARIANCE					
TEST STATISTICS FOR WITHIN-CELL VARIANCES					
WITHIN-CELLS ASSUMED TO EQUAL					
WITHIN-CELLS	1.60	7	1.60	1.60	1.60

FIGURE B.24.

CVN is shown in ft: 1 ft = .3048 m

56, 49, and 30 for wet welds at 10, 35, and 60 m (33, 115, and 198 ft), respectively. The minimum for wet-backed welds is the 12.7 mm (1/2 in.) ferritic, and the two smallest for the 10 m (33 ft) depth were both austenitic. Obviously, these welds were not suitable and they can be considered misapplications. Disregarding these three, the minimum Bendscore decreases from 94 for dry welds, to 65 for wet-backed welds, 70, 45, and 23 for wet welds at 10, 35, and 60 m (33, 115, and 198 ft), respectively.

### $K_{IC}$

Figure B-25 shows  $K_{IC}$  grouped by depth and zone. The zone grouping was used to eliminate the extraordinarily high 12.7 mm (1/2 in.) HAZ values. Focusing on weld metal  $K_{IC}$ , the mean decreases from 220 MPa $\sqrt{m}$  (200 ksi $\sqrt{in.}$ ) for dry welds, to 187 MPa $\sqrt{m}$  (170 ksi $\sqrt{in.}$ ) for wet-backed welds, and to 143, 58, 54 MPa $\sqrt{m}$ , (130, 53, and 49 ksi $\sqrt{in.}$ ) for wet welds at 10, 35 and 60 m (33, 115, and 198 ft), respectively. The minimum  $K_{IC}$  decreases from 149 MPa $\sqrt{m}$  (136 ksi $\sqrt{in.}$ ) for dry welds, to 89 MPa $\sqrt{m}$  (81 ksi $\sqrt{in.}$ ) for wet-backed welds, and to 107, 33, and 45 MPa $\sqrt{m}$  (97, 30, and 41 ksi $\sqrt{in.}$ ) for wet welds at 10, 35, and 60 m (33, 115, and 198 ft), respectively.

- Thickness/Zone Interaction for Toughness

Figures B-26 and B-27 show the thickness/zone interaction for CVN and  $K_{IC}$ , and the results for all data are consistent with those observed for other

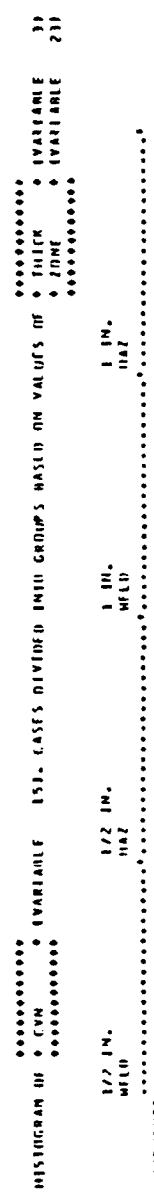
PAGE 147 ANALYSIS OF INFORMATION WILDS - FISHER VARIANCE SUR ALL DATA

CATEGORICAL MEANS ARE INFLUENCED BY %'S OF RAY CHINCAINE WITH ONE, %'S OTHERWISE		ANALYSIS OF VARIANCE TABLE					
		SUM OF SQUARES	D.F.	MEAN SQUARE	F VALUE	TAIL PROBABILITY	
MEAN	221.500	198.300	130.200	130.600	91.667	.000	
S.E.M.	.95.435	.61.318	.60.479	.26.129	.55.514	.25.617	
S.E.D. <sup>a</sup>	.49.979	.49.419	.49.133	.28.361	.47.510	.27.721	
S.E.M.D. <sup>b</sup>	.26.461	.26.239	.40.659	.11.685	.87.116	.49.300	
MAXIMUM	266.000	248.000	261.000	163.000	708.000	10.112	
MINIMUM	116.000	93.000	81.000	97.000	91.000	10.112	
SAMPLE SIZE	4	4	4	4	4	1.000	
ALL CATEGORIES EXAMINED							
INDEPENDENT CASES WITH IMPOSED VALUES		ANALYSIS OF VARIANCE TABLE					
		SUM OF SQUARES	D.F.	MEAN SQUARE	F VALUE	TAIL PROBABILITY	
MEAN	168.051	96.679	32.061	4	21624.5877	.000	
S.E.M.	.77.247	.43.717	.42.446	4	137.024	.000	
S.E.D. <sup>a</sup>	.61.619						
S.E.M.D. <sup>b</sup>	.42.518						
S.E.M.	122.000	121.000	119.000	119.000	1516.3820	.000	
MAXIMUM	180.000	178.000	177.000	177.000	4197.654	.000	
MINIMUM	101.000	100.000	99.000	99.000	1.78	.178	
SAMPLE SIZE	18	18	18	18	1.78	.178	
ONE-WAY ANALYSIS OF VARIANCE							
TEST STATISTICS FOR WITHIN-GROUP VARIANCES AND ASSUMED TDF OF FISHES							
MILCH							
ARMSTRONG & COLE							

FIGURE B-25.

$K_{Ic}$  is shown in ksi/in.:  $1.0 \text{ ksi/in.} = 1.1 \text{ MPa}\sqrt{\text{m}}$ . 1 ft = .3049 m

PAGE 111 ANALYSIS OF UNIFORMITY MILDS - CVN AND PERSIFER FOR ALL DATA



GROUP MEANS ARE DEFINED BY #S IF THEY COINCIDE WITH #S, #S OTHERWISE

	MEAN	ST.D.EV.	S.E.S.D.	MAXIMUM	MINIMUM	SAMPLE SIZE
THICK	17.500	65.436	65.436	12.977	36.000	151
ZINE	31.169	22.310	22.310	13.578	27.365	151
WFID	14.206	22.370	22.370	14.775	29.766	151
S. E. M.	2.128	3.747	3.747	2.035	4.125	151
		114.000	114.000	59.000	96.000	
		40.000	40.000	15.000	6.000	
		12	12	44	44	

	ALL CASES COMBINED			ALL CASES WITH UNIRED VALUES		
	THICK	ZINE	WFID	THICK	ZINE	WFID
MEAN	41.638	23.670	21.613	41.638	23.670	21.613
ST.D.EV.	64.000	64.000	64.000	64.000	64.000	64.000
S.E.M.	10.638	10.638	10.638	10.638	10.638	10.638
S. E. M.	10.638	10.638	10.638	10.638	10.638	10.638
MAXIMUM	114.000	114.000	114.000	114.000	114.000	114.000
MINIMUM	6.000	6.000	6.000	6.000	6.000	6.000
SAMPLE SIZE	152	152	152	152	152	152

LEVENE'S TEST FOR EQUAL VARIANCES

	MEAN SQUARE	DF	MEAN SQUARE	DF	MEAN SQUARE	DF	F VALUE	TABL. F VALUE
THICK	10681.125	1	10681.125	1	10681.125	1	25.98	.000
ZINE	8879.0573	1	8879.0573	1	8879.0573	1	21.59	.000
WFID	5750.0713	1	5750.0713	1	5750.0713	1	11.98	.000
INTERACTION	60865.5223	148	60865.5223	148	60865.5223	148	411.2760	
ERROR								

LEVENE'S TEST FOR EQUAL VARIANCES

ONE-WAY ANALYSIS OF VARIANCE

TEST STATISTICS FOR WITHIN-GROUP

VARIANCES NOT ASSUMED TO BE EQUAL

MILICH

ARMY-FIRSYTHE

FIGURE B.26.

CVN is shown in ft-lb: 1.0 ft-lb = 1.356 J, 1 in. = 25.4 mm

HIGHLY UNBALANCED WEIGHTS - HIGHER VARIANCE  
191. CASES DIVIDED INTO GROUPS BASED ON VALUES IN  
THICK & FINN & VARIANCE TESTS

GROUP	MEAN	ST.D.E.V.	S.E. S.D.	S.E. F.	MAXIMUM	MINIMUM	SAMPLE SIZE
1.00	141.400	79.551	61.507	225.500	225.500	61.300	120.000
1.01-1.02	141.501	61.061	61.100	21.746	21.746	1.100	20.000
1.03-1.04	140.000	79.600	51.100	110.000	110.000	1.100	10.000
1.05-1.06	140.000	79.600	51.100	110.000	110.000	1.100	10.000
1.07-1.08	140.000	79.600	51.100	110.000	110.000	1.100	10.000
1.09-1.10	140.000	79.600	51.100	110.000	110.000	1.100	10.000
1.11-1.12	140.000	79.600	51.100	110.000	110.000	1.100	10.000
1.13-1.14	140.000	79.600	51.100	110.000	110.000	1.100	10.000
1.15-1.16	140.000	79.600	51.100	110.000	110.000	1.100	10.000
1.17-1.18	140.000	79.600	51.100	110.000	110.000	1.100	10.000
1.19-1.20	140.000	79.600	51.100	110.000	110.000	1.100	10.000
1.21-1.22	140.000	79.600	51.100	110.000	110.000	1.100	10.000
1.23-1.24	140.000	79.600	51.100	110.000	110.000	1.100	10.000
1.25-1.26	140.000	79.600	51.100	110.000	110.000	1.100	10.000
1.27-1.28	140.000	79.600	51.100	110.000	110.000	1.100	10.000
1.29-1.30	140.000	79.600	51.100	110.000	110.000	1.100	10.000
1.31-1.32	140.000	79.600	51.100	110.000	110.000	1.100	10.000
1.33-1.34	140.000	79.600	51.100	110.000	110.000	1.100	10.000
1.35-1.36	140.000	79.600	51.100	110.000	110.000	1.100	10.000
1.37-1.38	140.000	79.600	51.100	110.000	110.000	1.100	10.000
1.39-1.40	140.000	79.600	51.100	110.000	110.000	1.100	10.000
1.41-1.42	140.000	79.600	51.100	110.000	110.000	1.100	10.000
1.43-1.44	140.000	79.600	51.100	110.000	110.000	1.100	10.000
1.45-1.46	140.000	79.600	51.100	110.000	110.000	1.100	10.000
1.47-1.48	140.000	79.600	51.100	110.000	110.000	1.100	10.000
1.49-1.50	140.000	79.600	51.100	110.000	110.000	1.100	10.000
1.51-1.52	140.000	79.600	51.100	110.000	110.000	1.100	10.000
1.53-1.54	140.000	79.600	51.100	110.000	110.000	1.100	10.000
1.55-1.56	140.000	79.600	51.100	110.000	110.000	1.100	10.000
1.57-1.58	140.000	79.600	51.100	110.000	110.000	1.100	10.000
1.59-1.60	140.000	79.600	51.100	110.000	110.000	1.100	10.000
1.61-1.62	140.000	79.600	51.100	110.000	110.000	1.100	10.000
1.63-1.64	140.000	79.600	51.100	110.000	110.000	1.100	10.000
1.65-1.66	140.000	79.600	51.100	110.000	110.000	1.100	10.000
1.67-1.68	140.000	79.600	51.100	110.000	110.000	1.100	10.000
1.69-1.70	140.000	79.600	51.100	110.000	110.000	1.100	10.000
1.71-1.72	140.000	79.600	51.100	110.000	110.000	1.100	10.000
1.73-1.74	140.000	79.600	51.100	110.000	110.000	1.100	10.000
1.75-1.76	140.000	79.600	51.100	110.000	110.000	1.100	10.000
1.77-1.78	140.000	79.600	51.100	110.000	110.000	1.100	10.000
1.79-1.80	140.000	79.600	51.100	110.000	110.000	1.100	10.000
1.81-1.82	140.000	79.600	51.100	110.000	110.000	1.100	10.000
1.83-1.84	140.000	79.600	51.100	110.000	110.000	1.100	10.000
1.85-1.86	140.000	79.600	51.100	110.000	110.000	1.100	10.000
1.87-1.88	140.000	79.600	51.100	110.000	110.000	1.100	10.000
1.89-1.90	140.000	79.600	51.100	110.000	110.000	1.100	10.000
1.91-1.92	140.000	79.600	51.100	110.000	110.000	1.100	10.000
1.93-1.94	140.000	79.600	51.100	110.000	110.000	1.100	10.000
1.95-1.96	140.000	79.600	51.100	110.000	110.000	1.100	10.000
1.97-1.98	140.000	79.600	51.100	110.000	110.000	1.100	10.000
1.99-2.00	140.000	79.600	51.100	110.000	110.000	1.100	10.000
2.01-2.02	140.000	79.600	51.100	110.000	110.000	1.100	10.000
2.03-2.04	140.000	79.600	51.100	110.000	110.000	1.100	10.000
2.05-2.06	140.000	79.600	51.100	110.000	110.000	1.100	10.000
2.07-2.08	140.000	79.600	51.100	110.000	110.000	1.100	10.000
2.09-2.10	140.000	79.600	51.100	110.000	110.000	1.100	10.000
2.11-2.12	140.000	79.600	51.100	110.000	110.000	1.100	10.000
2.13-2.14	140.000	79.600	51.100	110.000	110.000	1.100	10.000
2.15-2.16	140.000	79.600	51.100	110.000	110.000	1.100	10.000
2.17-2.18	140.000	79.600	51.100	110.000	110.000	1.100	10.000
2.19-2.20	140.000	79.600	51.100	110.000	110.000	1.100	10.000
2.21-2.22	140.000	79.600	51.100	110.000	110.000	1.100	10.000
2.23-2.24	140.000	79.600	51.100	110.000	110.000	1.100	10.000
2.25-2.26	140.000	79.600	51.100	110.000	110.000	1.100	10.000
2.27-2.28	140.000	79.600	51.100	110.000	110.000	1.100	10.000
2.29-2.30	140.000	79.600	51.100	110.000	110.000	1.100	10.000
2.31-2.32	140.000	79.600	51.100	110.000	110.000	1.100	10.000
2.33-2.34	140.000	79.600	51.100	110.000	110.000	1.100	10.000
2.35-2.36	140.000	79.600	51.100	110.000	110.000	1.100	10.000
2.37-2.38	140.000	79.600	51.100	110.000	110.000	1.100	10.000
2.39-2.40	140.000	79.600	51.100	110.000	110.000	1.100	10.000
2.41-2.42	140.000	79.600	51.100	110.000	110.000	1.100	10.000
2.43-2.44	140.000	79.600	51.100	110.000	110.000	1.100	10.000
2.45-2.46	140.000	79.600	51.100	110.000	110.000	1.100	10.000
2.47-2.48	140.000	79.600	51.100	110.000	110.000	1.100	10.000
2.49-2.50	140.000	79.600	51.100	110.000	110.000	1.100	10.000
2.51-2.52	140.000	79.600	51.100	110.000	110.000	1.100	10.000
2.53-2.54	140.000	79.600	51.100	110.000	110.000	1.100	10.000
2.55-2.56	140.000	79.600	51.100	110.000	110.000	1.100	10.000
2.57-2.58	140.000	79.600	51.100	110.000	110.000	1.100	10.000
2.59-2.60	140.000	79.600	51.100	110.000	110.000	1.100	10.000
2.61-2.62	140.000	79.600	51.100	110.000	110.000	1.100	10.000
2.63-2.64	140.000	79.600	51.100	110.000	110.000	1.100	10.000
2.65-2.66	140.000	79.600	51.100	110.000	110.000	1.100	10.000
2.67-2.68	140.000	79.600	51.100	110.000	110.000	1.100	10.000
2.69-2.70	140.000	79.600	51.100	110.000	110.000	1.100	10.000
2.71-2.72	140.000	79.600	51.100	110.000	110.000	1.100	10.000
2.73-2.74	140.000	79.600	51.100	110.000	110.000	1.100	10.000
2.75-2.76	140.000	79.600	51.100	110.000	110.000	1.100	10.000
2.77-2.78	140.000	79.600	51.100	110.000	110.000	1.100	10.000
2.79-2.80	140.000	79.600	51.100	110.000	110.000	1.100	10.000
2.81-2.82	140.000	79.600	51.100	110.000	110.000	1.100	10.000
2.83-2.84	140.000	79.600	51.100	110.000	110.000	1.100	10.000
2.85-2.86	140.000	79.600	51.100	110.000	110.000	1.100	10.000
2.87-2.88	140.000	79.600	51.100	110.000	110.000	1.100	10.000
2.89-2.90	140.000	79.600	51.100	110.000	110.000	1.100	10.000
2.91-2.92	140.000	79.600	51.100	110.000	110.000	1.100	10.000
2.93-2.94	140.000	79.600	51.100	110.000	110.000	1.100	10.000
2.95-2.96	140.000	79.600	51.100	110.000	110.000	1.100	10.000
2.97-2.98	140.000	79.600	51.100	110.000	110.000	1.100	10.000
2.99-2.100	140.000	79.600	51.100	110.000	110.000	1.100	10.000

SOURCE	SUM OF SQUARES	D.F.	MEAN SQUARE	F VALUE	TAIL PROBABILITY
THICK	11752.808	1	11752.808	7.49	.0112
FINN	15262.161	1	15262.161	3.25	.0613
RELATIONSHIP	15.600	1	15.600	1.55	.2047
FEWIN	1.960	1	1.960	.4159	.6159
LAWNI'S TEST FOR EQUAL VARIANCES	1.1	1	1.1	.70	.4969
ONE-WAY ANALYSIS OF VARIANCE FOR WITHIN-GROUP VARIANCES WHICH ASSUMED TO BE EQUAL	1.1	10	.11	.6113	.6122
ONE-WAY ANALYSIS OF VARIANCE FOR WITHIN-GROUP VARIANCES WHICH ASSUMED TO BE EQUAL	1.1	10	.11	.6124	.6124

FIGURE B.27.

$K_{IC}$  is shown in  $\text{ks/in.} = 1.0 \text{ ksi/in.} = 1.1 \text{ MPa}/\sqrt{\text{in.}}$ , 1 in. = 25.4 mm

groups, i.e., the 12.7 mm (1/2 in.) HAZ specimens show higher toughness than both the HAZ and weld metal 25.4 mm (1 in.) specimens and the 12.7 mm (1/2 in.) weld metal specimens.

## APPENDIX C

### Example 1: Design of a Pipeline Repair

**Problem:** A 305 mm (12 in.) diameter 6.4 mm (1/4 in.) thick pipeline riser requires a wet-welded sleeve to cover and seal a hole about 76 mm (3 in.) long. The yield strength of the pipe is 345 MPa (50 ksi).

**Considerations:** The repair must be leak proof, therefore details to limit crack size are unnecessary because "failure" or leaking will occur upon crack initiation. Therefore a more conservative approach than usual will be adopted when designing against crack initiation. The "second line of defense"; i.e. crack arrest and/or redundancy, which may preclude instability or collapse, does not preclude leaking.

**Solution:** A simple full encirclement split sleeve is chosen. The sleeve requires two longitudinal groove welds and a circumferential fillet weld to close each end.

1. The thickness of the sleeve is chosen to ensure full section yielding of the pipeline before yielding of the weld. A-36 plate is chosen for the sleeve. Conservatively assuming a yield strength of 248 MPa (36 ksi) for the sleeve and uniform stress through the thickness

$$t_{\text{sleeve}} = \frac{F_y \text{ (pipeline)}}{F_y \text{ (sleeve)}} t_{\text{pipeline}}$$

$$= \frac{50 \text{ ksi}}{36 \text{ ksi}} (0.25 \text{ in}) = .35 \text{ in.}$$

use 9.7 mm (3/8 in.) thick sleeve.

2. Because the wet weld metal can be counted on to have a strength greater than 345 MPa (50 ksi), the weld can be detailed normally, i.e. per governing code such as AWS rules.
  
3. Check maximum stress in the weld for fracture. The critical location is the longitudinal weld. Assume the load is high enough to yield the pipeline, therefore the stress in the groove weld is about 248 MPa (36 ksi) not considering the weld reinforcement. The critical crack size is less than 9.7 mm (3/8 in.) since any through crack would constitute failure by leaking. From Table 5.1:
  - a. The repair will be subject to a 4 hour hydro test at greater than operating pressure. This proof test will screen out cracks larger than a given size that would cause failure. However, to prevent failure in the proof test, assume no control of crack size: factor on crack length = 4.0

b.  $K_{Ic}$  is 110 MPa $\sqrt{m}$  (100 ksi $\sqrt{in.}$ ) and was obtained from  $J_{Ic}$  for a test plate using the approved welding procedure: factor on toughness = .83

c. There is no redundancy so 1.8 times maximum stress or 1.0 times yield stress. Since the yield stress of the parent plate is being used there is no factor for the stress.

Therefore, assuming a through crack of 4.0 x 9.7 mm (3/8 in.) and taking  $K=1.2\sigma\sqrt{\pi a}$

$$K_{Ic} \text{ req'd} = \frac{36 \text{ ksi}\sqrt{\pi 1.5 \text{ in.}}}{.83} \quad (1.2)$$

$$= 113 \text{ ksi}\sqrt{\text{in.}} \quad K_{Ic} \text{ (no good)}$$

Increase the thickness of the sleeve. The load is still such that yielding will occur in the pipeline, so no factor on the stress is required even though the stress will now be below yield strength in the parent plate. Since  $K$  is directly proportional to the stress and hence the thickness,

$$t_{\text{req'd}} = \frac{113}{100} (3/8 \text{ in.}) = .424 \text{ in.}$$

use 11.1 or 12.7 mm (7/16 or 1/2 in.) sleeve.

4. Check maximum alternating stress intensity factor to assure that standard fatigue design

rules are applicable. Alternating stress arises from being downstream of a compressor and from vortex shedding on the riser. The maximum alternating stress range is 41.4 MPa (6 ksi). The stress intensity range is:

$$\Delta K = 1.2 \sqrt{\pi} (6 \text{ ksi}) / \sqrt{.375} = 7.8 \text{ ksi}\sqrt{\text{in.}}$$

which is well below  $33 \text{ MPa}\sqrt{\text{m}}$  ( $30 \text{ ksi}\sqrt{\text{in.}}$ ) and in the regime where fatigue crack growth would be much slower in the underwater weld than in the base metal.

## Example 2: Design of Strip Patch Repair for Sheet Piling

**Problem:** In order to carry the load across a split in some sheet piling, it has been determined that 12.7 mm (1/2 in.) thick 102 mm (4 in.) wide plates will be welded across the split on 0.61 m (2 ft) centers as shown in Figure 5.4. For the plates,  $F_y$  is 248 MPa (36 ksi).

**Considerations:** The sheet piling is holding wet soil, so the problem is to keep a split on some sheet piling from getting wider and the repair does not have to be water tight.

**Solution:**

1. Use fillet welds along the sides of the plates to rely only on shear stress. The rated strength of the E6013 electrodes is 414 MPa (60 ksi).
2. Determine the length of plates required. The effective throat distance for the fillet welds is:

$$t = (.707) (1/2 \text{ in.} - 1/16 \text{ in.}) = .3 \text{ in.}$$

recognizing some weld throat loss due to "suck up", use  $t=.25$  in.

$$F_v = 0.225 (60 \text{ ksi}) = 13.5 \text{ ksi}$$

The strength of the welds is therefore

$$f = 13.5 \text{ ksi} \cdot .25 \text{ in.} = 3.37 \text{ k/in.}$$

Design the fillet welds so that the plate can be fully yielded before the shear stress in the fillet welds approaches  $F_y$ .

Force in plate at yield = 36 ksi (4 in.) • 0.5 in. = 72 k

$$l_{req'd} = \frac{72 \text{ k}}{3.4 \text{ k/in}} = 21 \text{ in.}$$

Assume the gap is less than 51 mm (2 in.) wide, then use plates 610 mm (24 in.) long with 267 mm (10.5 in.) long fillet welds on each side.

3. Fracture is not a problem because of the reliance solely on shear stresses and the high degree of redundancy (number of patch plates).
4. Fatigue from alternating stress is not a problem.

Example 3: Design of a Replacement of Damaged Tubular Brace  
Subject to Tension

Problem: The brace is cracked at the weld to the spud can. The spud can is not damaged, so the brace will be cut away and a replacement component will be fit and attached to the brace with a doubler. The replacement component will be shop welded in advance to half a sleeve which will be attached to the spud can, see Figure 5.1. The spud can is 305 mm (12 in.) in diameter and 12.7 mm (1/2 in.) thick. The original brace is 254 mm (10 in.) in diameter and 12.7 mm (1/2 in.) thick. Both components have a yield strength of 345 MPa (50 ksi).

Considerations: The brace can be put into significant tension when structure is subject to wave loading. Therefore, the use of details to limit the crack size are warranted since the brace is deemed critical.

Solution:

1. The brace connection should use a scalloped full encirclement split sleeve (Doubler B in Figure 5.1) to maximize weld length and area, and to utilize shear stress as much as possible to transfer the axial load. The connection to the spud can (Doubler A in Figure 5.1) should use an interlocking full encirclement split sleeve doubler to transfer axial load from the brace through contact on the opposite side of the spud can. Since the longitudinal weld of this split sleeve will

still have to support tension, circumferential fillet welds are used on the ends to provide a redundant load path. The weld is to be made in shallow water (depth of 10 m (33 ft)) and since higher carbon equivalent base plate is to be welded, austenitic electrodes are selected. The rated strength of the electrode is 552 MPa (80 ksi), so the allowable stress is .225 the rated strength or 124 MPa (18 ksi). The toughness of the weld is  $253 \text{ MPa}\sqrt{\text{m}}$  (230 ksi $\sqrt{\text{in.}}$ ) which was obtained from a correlation to the Charpy toughness.

2. Size the split sleeves. Use a replacement brace component the same size as the original brace to minimize stiffening of the joint. The shop weld is designed under the governing code, e.g. AWS rules, and is not considered here.

Doubler B:

1. Try a 19 mm (3/4 in.) thick sleeve with  $F_y=248$  MPa (36 ksi). The scalloped sleeve has a total circumference of 838 mm (33 in.) but an arc length of weld of 1575 mm (62 in.) on either end. Take 838 mm (33 in.) as being in tension and 737 mm (29 in.) in shear. The throat for the 19 mm (3/4 in.) leg fillet weld is:

$$.707(.75-.06) - .12 = .37 \text{ in.}$$

accounting for a loss factor.

The stress in each end weld when the brace is fully yielded in tension is then:

$$\begin{aligned}\text{Force in brace} &= \pi \cdot 10 \text{ in.} \cdot 0.5 \text{ in.} \cdot 50 \text{ ksi} \\ &= 785 \text{ k}\end{aligned}$$

$$\begin{aligned}\text{Stress in weld} &= 785 \text{ k}/(62 \text{ in.} \cdot 0.37 \\ &\quad \text{in.}) = 34 \text{ ksi (no good)}\end{aligned}$$

Try increasing the thickness of Doubler B by the ratio of 234 MPa (34 ksi) to the allowable stress in shear, or

$$t_{\text{sleeve}} = \frac{34 \text{ ksi}}{18 \text{ ksi}} (0.75 \text{ in.}) = 1.4 \text{ in.}$$

Since less than half the weld is in shear, using 12.7 mm (1/2 in.) thick looks adequate.

2. Detail the weld with an interruption to avoid an intersection with the axial weld. Changing direction will serve to control crack length.
3. Check maximum stress in the weld for fracture. The critical location is at the apex of the scallop where the weld is in direct tension. When the brace is fully yielded the stress in this part of the weld is 124 MPa (18 ksi). The maximum credible flaw size is 51 mm (2 in.).

From Table 5.1:

- a. Changed direction into shear stress, and maximum flaw size is less than the continuous length of weld. The factor on crack length is therefore 1.6.
- b. The toughness was estimated from a Charpy test, use a factor of 0.67 on the toughness.
- c. The structure is highly redundant, so a factor of 1.2 on the stress is appropriate.

Stress analysis reveals that the stress concentration factor for this geometry is 2.0. The maximum K is then:

$$\begin{aligned}K_{Ic} \text{ req'd} &= (2.0) (1.2) 18 \text{ ksi} \sqrt{\pi(1.6)^2 / .67} \\&= 137 \text{ ksi} \sqrt{.67} = 204 < 236\end{aligned}$$

Doubler A:

The chord is in compression from dead load, so the critical load for fracture of doubler A is the axial tension in the brace. The split sleeve will have two longitudinal groove welds subject to tensile or hoop stress. Since the maximum credible flaw size is the same, i.e. 51 mm (2 in.), try a 19 mm (3/4 in.) doubler sleeve. It is now known that the stress must be kept below 124 MPa (18 ksi) to tolerate

this flaw, so calculate the length of the doubler:

$$l_{\text{req'd}} = \frac{785^k}{18 \text{ ksi } 0.75 \text{ in.}} = 58 \text{ in.}$$

Doubler A should be 1.5 m (5 ft) long.

Since circumferential fillet welds also hold the doubler to the chord, this system is highly redundant. Check maximum alternating stress intensity for fatigue. Maximum alternating load in the brace is estimated to be  $100^k$ . The alternating stress range in either weld (Doubler A or B) is then.

$$\frac{100^k}{785^k} \times 18 \text{ ksi} = 2.3 \text{ ksi}$$

The maximum range in stress intensity factor is then:

$$\Delta K = (2.0) 2.3 \text{ ksi} \sqrt{\frac{1}{2 \text{ in.}}} \\ = 11.5 \text{ ksi} \sqrt{\text{in.}} < 30 \text{ ksi} \sqrt{\text{in.}}$$

Therefore crack growth will be in the regime where the crack would grow faster in the base metal, and standard fatigue design procedures are applicable.

## BIBLIOGRAPHY

1. American Welding Society, "Specification for Underwater Welding--AWS D3.6," 1983, Miami, Fla.
2. Brown, A. J.; Staub, J. A.; and Masubuchi, K., "Fundamental Study of Underwater Welding," 4th Annual Offshore Technology Conference OTC 1621, April 30 - May 3, 1972.
3. Brown, R. T., and Masubuchi, K., "Fundamental Research on Underwater Welding," Welding Journal, Vol. 54, No. 6, June 1975.
4. Burner, W. K., "Generalized Summary of the State-of-the-Art of Underwater Welding," Naval Engineers Journal, April 1978, pp. 68-74.
5. Dadian, M., "Review of Literature on the Weldability Underwater of steels," Welding In The World, Vol. 14, No. 3/4, 1976.
6. Fukushima, T.; Fukushima, S.; Kinugawa, J., "Some Mechanical Properties of Multi-pass Welds by Underwater Wet Plasma Welding," National Research Institute for Metals, Tokyo, Japan, 1979.
7. Grubbs, C. E., and Seth, O. W., "Underwater Wet Welding with Manual Arc Electrodes," Published in Underwater Welding for Offshore Installations, The Welding Institute, Abington Hall, Abington, Cambridge, 1977.

8. Hamasaki, M.; Sakakibara, J.; and Arata, Y., "Underwater Wet Welding and Hydrogen," Metal Construction, December 1981, pp. 755-756.
9. Helburn, S., "Underwater Welders Repair Drilling Rig," Welding Design & Fabrication, July 1979.
10. Madatov, N. M., "Energy Characteristics of the Underwater Welding Arc," Welding Research, Vol. 13, No. 5, May 1967.
11. Masubuchi, K., and Meloney, M. B., "Underwater Welding of Low-Carbon and High-Strength (HY-80) Steel," Offshore Technology Conference, OTC 1951, 1974.
12. Military Standard: Underwater Welding Requirements for Naval Facilities, MIL-STD-1692 (YD) February 1976.
13. Nagarajan, V., and Loper, C. R., "Underwater Welding of mild Steel-A Metallurgical Investigation of Critical Factors," Offshore Technology Conference, Houston, Texas, OTC 2668, 1976.
14. Sadowski, E. P., "Underwater Wet Welding Mild Steel with Nickel Base and Stainless Steel Electrodes," Welding Journal, July 30, 1980, pp. 30-38.
15. Shinada, K.; Nagata, Y.; Wada, H., Tamura, M.; Omae, T.; Manabe, Y.; and Nobushige, T., "Development of Underwater Welding Techniques," Technical Review, Mitsubishi Heavy Industries, Vol. 16, No. 2, Ser. No. 45, June 1979.

16. Stalker, Q. W., "Welding Institute Research on Underwater Welding," Published in Underwater Welding for Offshore Installations, The Welding Institute, Abington Hall, Abington, Cambridge, 1977.
17. Stalker, A. W.; Hart, P. H. M.; and Salter, G. R., "A Preliminary Study of Underwater Manual Arc Welding," The Welding Institute, Abington Hall, Abington, Cambridge, December 1974.
18. Stalker, A. W.; Hart, P. H. M.; and Salter, G. R., "An Assessment of Shielded Metal Arc Electrodes for the Underwater Welding of Carbon Manganese Structural Steels," Offshore Technology Conference, OTC 2301, Houston, Texas, May 5-8, 1975.
19. Tsai, C. L., and Masubuchi, K., "Interpretive Report on Underwater Welding," Welding Research Council, Bulletin No. 224, February 1977.